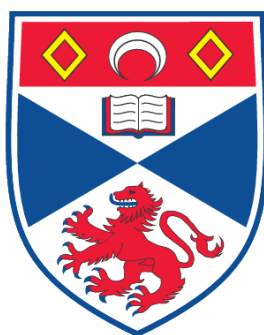


**THE INFLUENCE OF THE C-N<sup>+</sup>----- F-C CHARGE DIPOLE  
INTERACTION IN FLUORO ORGANIC CHEMISTRY**

**Natalie Elizabeth Jane Gooseman**

**A Thesis Submitted for the Degree of PhD  
at the  
University of St. Andrews**



**2008**

**Full metadata for this item is available in the St Andrews  
Digital Research Repository  
at:**

**<https://research-repository.st-andrews.ac.uk/>**

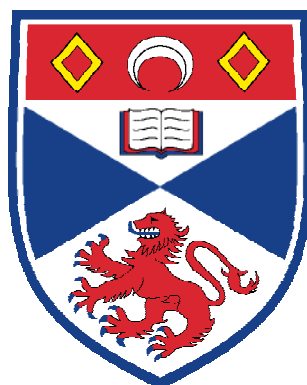
**Please use this identifier to cite or link to this item:**

**<http://hdl.handle.net/10023/695>**

**This item is protected by original copyright**

**This item is licensed under a  
Creative Commons License**

**The influence of the C-N<sup>+</sup>----- F-C  
charge dipole interaction in  
fluoro organic chemistry.**



University  
of  
St Andrews

A thesis presented for the degree of Doctor of Philosophy to  
the School of Chemistry, University of St Andrews

Natalie Elizabeth Jane Gooseman

March 2008

*“Turn everything negative into something positive  
then you’ll never be upset”*

Vanessa’s words of wisdom....

## Copyright

In submitting this thesis to the University of St. Andrews I understand that I am giving permission for it to be made available for use in accordance with the regulations of the University Library for the time being in force, subject to any copyright vested in the work not being affected thereby. I also understand that the title and the abstract will be published, and that a copy of the work may be made and supplied to any *bone fide* library or research worker, that the thesis will be electronically accessible for personal or research use, that my thesis will be electronically accessible for personal or research use, and that the library has the right to migrate my thesis into new electronic forms as required to ensure continued access to the thesis. I have obtained any third-party copyright permissions that may be required in order to allow such access and migration.

Signature of Natalie E-J Gooseman..... Date.....

## Declaration

I, Natalie Elizabeth-Jane Gooseman, hereby certify that this thesis, which is approximately 38,000 words in length, has been written by me, that it is the record of work carried out by me and that it has not been submitted in any previous application for a higher degree.

Signature of Natalie E-J Gooseman..... Date.....

I was admitted as a research student in September 2003 and as a candidate for the degree of Ph.D in September 2003; the higher study for which this is a record was carried out in the University of St. Andrews between September 2003 and March 2008.

Signature of Natalie E-J Gooseman..... Date.....

I hereby certify that the candidate has fulfilled the conditions of the Resolution and Regulations appropriate for the degree of Ph.D in the University of St. Andrews and that the candidate is qualified to submit this thesis in application for that degree.

Signature of Professor David O'Hagan..... Date.....

## Acknowledgements

I have so many people and organisations to sincerely thank for their encouragement, assistance and guidance during my PhD research. Firstly I would like to thank my supervisor, Professor David O'Hagan for taking a good challenge on, showing me direction and offering me sound advice about my research.

Truly believing it is the members of the close knit 'DOH group' that have helped in my personal development as well as keeping my sanity, I wish to thank them with my heart.

Past and present members have not only assisted me with practical and theoretical chemistry problems they have also helped me as a family would do. This 'St Andrews family' is one which I am so lucky to have been born into and I will never forget how the group let me experience a totally different life - which of course has had its ups and downs but mainly consisting of such enjoyable times! I would like to say a special thanks (in the usual manner) to my academic brother Gildas, academic little sister and great friend Mayca, uncles Kenny, Marcello, Cosi and Ryan. I am very appreciative of Lukey Luke for helping me with NMR interpretation and I would like to acknowledge Dr Caroline Briggs for her previous research, which mine follows from.

Both within the chemistry department and the Centre for Bio-molecular Sciences the members of staff are very helpful and the facilities which they run are fantastic. An exceptional thank you goes out to Professor Alexandra Slawin for not only the X-ray crystallography analysis on such a vast number of crystals but for her caring approach to me as an individual. Special thanks must also go to Dr Tomáš Lébl for his considerable help with NMR problems and assistance with analysis. Tomáš and Melanja Smith provide a super NMR service which is hugely appreciated. My gratitude also goes out to Catherine Botting who runs the electrospray facility, Caroline Horsburgh for high resolution analysis and Silvia Williamson for elemental analysis.

As well as the University of St Andrews chemistry department and its staff I would like to thank my industrial supervisor Dr Rob Young at GlaxoSmithKline for his interest and assistance throughout the research program. During my PhD I was fortunate enough to experience a work placement at the company's research facility in Stevenage and I would also like to thank the staff there, in particular Richard Upton for his assistance with NMR studies and for carrying out variable temperature experiments. Dr D. Tozer, Dr Andrew Teale and Michael Peach at the University of Durham carried out the DFT calculations and I wish to thank them tremendously for their collaboration with this project.

This PhD research was funded by the Biotechnology and Biological Sciences Research Council (BBSRC) and GlaxoSmithKline and I am extremely grateful for this.

My parents, family and uncle Iain have always been there to cheer me up and allowed me to explain exactly what step of my synthetic route I was at and how it was going, even though they didn't have the foggiest! Vanessa, my little 'schwester' has been more like a big sister in the last four years, being a massive support both emotionally and financially! Without gushing I want her to know how much I appreciate her kindness and the fact that she was always there for me.

I would also like to thank friends from Grimsby and previous work colleagues at Syngenta for their genuine enthusiasm and backing to start a new adventure in academia. If it was not for the likes of Tina, Greg, Emma, Jo, Nicky, Chris, Jane and so many others like them, I may not have had the courage to embark on this "PhD journey". I must also talk about Ron Aisthorpe at Novartis who took me under his wing when I started at the company at the age of seventeen, he not only supervised me in my early career but with his enthusiasm he introduced synthetic chemistry in an interesting and fun manner which led me to where I am now.

Lastly, Matthieu, I thank you wholeheartedly, for everything. You are my best friend, my love and the best chef around!

# Contents

## Abbreviations and symbols

## Abstract

## Chapter 1: Introduction

<b>1.1</b>	<b>Abundance and occurrence of fluorinated natural products</b>	1
1.1.1	Fluorinated metabolites from plants	2
1.1.2	Fluorinated metabolites from bacteria	2
<b>1.2</b>	<b>Minerals</b>	7
<b>1.3</b>	<b>The discovery of fluorine</b>	8
<b>1.4</b>	<b>Fluorine production today</b>	10
<b>1.5</b>	<b>Chemical synthesis of fluorine</b>	10
<b>1.6</b>	<b>Applications of organic fluorine compounds</b>	11
1.6.1	Pharmaceuticals	11
1.6.2	Anaesthetics	13
1.6.3	Agrochemicals	14
1.6.4	Polymers	18
<b>1.7</b>	<b>Applications of inorganic fluoride</b>	20
1.7.1	Fluoride in water and toothpaste	20
1.7.2	Uranium hexafluoride	22
<b>1.8</b>	<b>General properties of fluorine and the C-F bond</b>	23
1.8.1	Electronegativity	23
1.8.2	Atomic size	24



1.8.3	Steric influence of fluorine	25
1.8.4	The C-F bond	26
1.8.5	Acidity and basicity effects	29
<b>1.9</b>	<b>Fluorine as a hydrogen bonding acceptor</b>	31
<b>1.10</b>	<b>Fluorine as an inductive activator of a hydrogen-bond donor group</b>	34
<b>1.11</b>	<b>The fluorine <i>gauche</i> effect</b>	35
1.11.1	The 1,2-dihaloethanes	35
1.11.2	The origin of the fluorine <i>cis</i> and <i>gauche</i> effects	37
1.11.3	The fluorine <i>gauche</i> effect In 9,10-difluorostearic acid	39
1.11.4	Fluorine in amides	41
1.11.5	Fluorinated collagens	44
1.11.6	Fluorine in esters	47
1.11.7	$\beta$ -Fluoroamines	48
1.11.8	Fluoroethanol	52
<b>1.12</b>	<b>References for chapter one</b>	55

## **Chapter 2: Charged C-N<sup>+</sup> ..... F-C dipole interactions**

<b>2.1</b>	<b>Introduction</b>	61
<b>2.2</b>	<b>Medium sized rings</b>	64
<b>2.3</b>	<b>Nine membered rings in nature and synthetic procedures</b>	66
<b>2.4</b>	<b>Aims and objectives</b>	67
<b>2.5</b>	<b>Synthesis of nine membered <math>\beta</math>-fluoro aza rings :</b>	
	Strategy 1 – cyclisation <i>via</i> putricine	69
	Strategy 2 – ring closing metathesis	72

<b>2.6</b>	<b>Synthesis of eight membered rings</b>	83
2.6.1	Strategy 1 <i>via</i> fluorination of hydroxy-cyclooctane	83
2.6.2	Synthesis of a fluoro diazepine	88
2.6.3	Strategy 2 - eight membered rings <i>via</i> cyclisation with a fluorinated C <sub>3</sub> unit	90
2.6.4	Synthesis of a di-fluoro-diazocane	96
2.6.5	Strategy 3 - eight membered rings <i>via</i> cyclisation of a pyrazolidine ring	103
<b>2.7</b>	<b>Four membered β-fluoro azedinium rings</b>	110
2.7.1	Evaluation of azetidinium hydrobromide by X-ray analysis	112
2.7.2	X-ray analysis of 3-fluoroazetidinium hydrochloride and hydrobromide	113
2.7.3	Theoretical evaluation of the 3-fluoroazetidinium conformation	117
<b>2.8</b>	<b>Conformation of β-fluoro pyrrolidinium rings</b>	119
<b>2.9</b>	<b>An electrostatic <i>gauche</i> effect in β-fluoro- and β-hydroxy- N-ethylpyridinium cations</b>	122
2.9.1	N-Ethylpyridinium targets	125
2.9.2	Synthesis of fluoro N-ethylpyridinium salts	125
2.9.3	Synthesis and evaluation of the hydroxyl pyridinium salt	129
2.9.4	Synthesis of the chloro pyridinium salt	131
2.9.5	Synthesis of the fluoro bis-pyridinium salt	133
<b>2.10</b>	<b>References for chapter two</b>	137

## **Chapter 3: Charged C-O<sup>+</sup> ..... F-C dipole interactions**

<b>3.1</b>	<b>Introduction</b>	<b>141</b>
<b>3.2</b>	<b>A stereoselective study on fluorine, C-F ----<sup>+</sup>O-R</b>	<b>146</b>
<b>3.3</b>	<b>Synthesis of 2-fluoro-4-(1,1-dimethylethyl)cyclohexanone</b>	<b>150</b>
<b>3.4</b>	<b>Grignard reactions</b>	<b>153</b>
<b>3.5</b>	<b>Synthesis of the 3-fluorophenylcyclohexanols with phenyl lithium</b>	<b>160</b>
<b>3.6</b>	<b>Fluoro ketal study</b>	<b>161</b>
<b>3.7</b>	<b>Synthesis of <math>\alpha</math>-fluoro epoxides</b>	<b>165</b>
<b>3.8</b>	<b>References for chapter three</b>	<b>169</b>

## **Chapter 4: Experimental**

<b>4.1</b>	<b>General experimental procedures</b>	<b>171</b>
<b>4.2</b>	<b>Experimental protocols</b>	<b>176</b>
<b>4.3</b>	<b>References for chapter four</b>	<b>254</b>

<b>Appendix 1:</b>	<b>X-ray crystallographic data</b>	<b>256</b>
--------------------	------------------------------------	------------

<b>Appendix 2:</b>	<b>List of publications and conferences attended</b>	<b>300</b>
--------------------	--	------------

<b>Appendix 3:</b>	<b>Publications</b>	<b>302</b>
--------------------	---------------------	------------

## Abbreviations and symbols

$\sigma$	Sigma
$\pi$	Pi
Å	Angstrom
$\alpha$	Alpha
ax	axial
$\beta$	Beta
aq	aqueous
BBSRC	Biotechnology and Biological Sciences Research Council
Bn	benzyl
BOC	<i>t</i> -Butoxycarbonyl
Bp	Boiling point
br	broad
calc.	calculated
CDS	Cambridge Structural Database
CI	Chemical Ionisation
d	doublet
de	diastereoselectivity
D	Deuterium
DAST	(Diethylamino)sulfur trifluoride
DCM	Dichloromethane
dd	doublet of doublet
DFT	Density Functional Theory
DMF	<i>N,N</i> -Dimethylformamide
ees	enantiomeric excesses

EI	Electron Ionisation
ES	Electro Spray
eq	equatorial
5-FDA	5'fluoro-5'-deoxyadenosine
GC-MS	Gas Chromatography-Mass Spectrometry
GSK	GlaxoSmithKline
h	Hours
HOMO	Highest Occupied Molecular Orbital
HRMS	High Resolution Mass Spectroscopy
Hz	Hertz
IR	Infrared spectroscopy
<i>J</i>	coupling constant
Lit.	Literature
LC-MS	Liquid Chromatography-Mass Spectrometry
LUMO	Lowest Unoccupied Molecular Orbital
m	multiplet
M	Molar concentration
MeCN	Acetonitrile
MeOH	Methanol
Mp	Melting point
m/z	molecular mass to charge ratio
NADH	Nicotinamide Adenine Dinucleotide
NMR	Nuclear Magnetic Resonance
nOe	nuclear Overhauser effect
Ph	phenyl
PLP	pyridoxal-5'-phosphate

ppm	parts per million
PTFE	Polytetrafluoroethylene
Py	Pyridine
RT	Room temperature
s	singlet
SAM	<i>S</i> -adenosyl-L-methionine
t	triplet
TBAF	Tetra butyl ammonium fluoride
TFA	Trifluoroacetic acid
THF	Tetrahydrofuran
TMSCl	Trimethylsilyl chloride
Ts	Tosyl
TLC	Thin Layer Chromatography
VT	Variable Temperature
$\delta$	Delta
$\omega$	Omega
$\mu$	Mu
$\Delta G^\circ$	Gibbs free energy difference

## Abstract

**Chapter 1** introduces the discovery of elemental fluorine by H. Moissan and some uses of inorganic fluoride. Organo fluoro compounds and their place in pharmaceuticals and agrochemicals are also introduced. The general properties of fluorine and the C-F bond are discussed as well as conformational influences such as the fluorine *gauche* effect.

**Chapter 2** describes the C-N<sup>+</sup>-----F-C charge dipole interactions within protonated amines and explains the influence of a β fluorine on the conformation on various crystalline structures. A number of systems are synthesised which contain this charge dipole interaction, such as four, five and eight membered aza heterocycles. It was demonstrated that these provided a N<sup>+</sup>-C-C-F *gauche* torsion angle.

This electrostatic effect was also observed in the non-protonated N-ethylpyridinium cations possessing a fluorine β to the charged nitrogen. This clearly showed that hydrogen bonding is not playing a part in the observed N<sup>+</sup>-C-C-F *gauche* interactions and that it is a purely electrostatic effect.

**Chapter 3** discusses the effort to explore the C-O<sup>+</sup>-----F-C charge dipole interaction and the synthetic approaches that were taken towards candidate substances. However in the event a Grignard reaction on a fluoro cyclohexanone was found to provide an unexpected product where rearrangement followed by fluorine elimination had occurred.

**Chapter 4** details the experimental procedures for the compounds synthesised in this thesis and an Appendix outlines the detail of 24 crystal structures that were solved during this research.

# Chapter 1 Introduction

## 1.1 Abundance and occurrence of fluorinated natural products

Fluorine is the most abundant halogen in the earth's continental crust, where it occurs as fluoride in the form of minerals and rocks. In fact fluorine is the 13<sup>th</sup> most abundant element, at 544 ppm in crustal rocks.<sup>1</sup> Despite its relatively high occurrence in the earth's crust, fluoride ion is the least bio-available of the halides. The availability of the halides in surface water differs considerably, with fluoride concentrations of about 1.2 ppm compared to bromide at 65 ppm and chloride at 19,000 ppm.<sup>1</sup> The incorporation of fluoride into bio-molecules appears to be nearly non-existent. This can be explained by its low bio-availability and fluoride ion's high energy of solvation ( $-437 \text{ kJmol}^{-1}$ )<sup>2</sup>, hydrogen bonding to water to generate  $\text{F}^- (\text{H}_2\text{O})_x$  clusters. This solvation renders it unreactive as a nucleophile. It has however been shown that many plants accumulate fluoroacetate and the bacteria *Streptomyces cattleya* and *Streptomyces calvus*<sup>3</sup> are capable of biosynthesising organo-fluorine metabolites. In addition a few other naturally occurring fluorinated organic compounds have been isolated from plants.

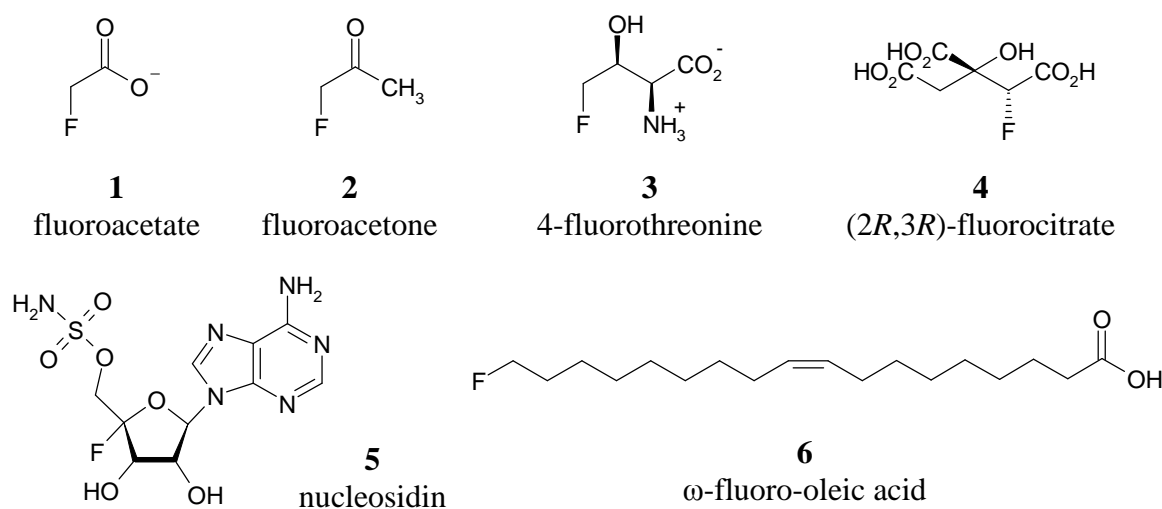


**Figure 1.1** Natural products known to contain fluorine.



### 1.1.1 Fluorinated metabolites from plants

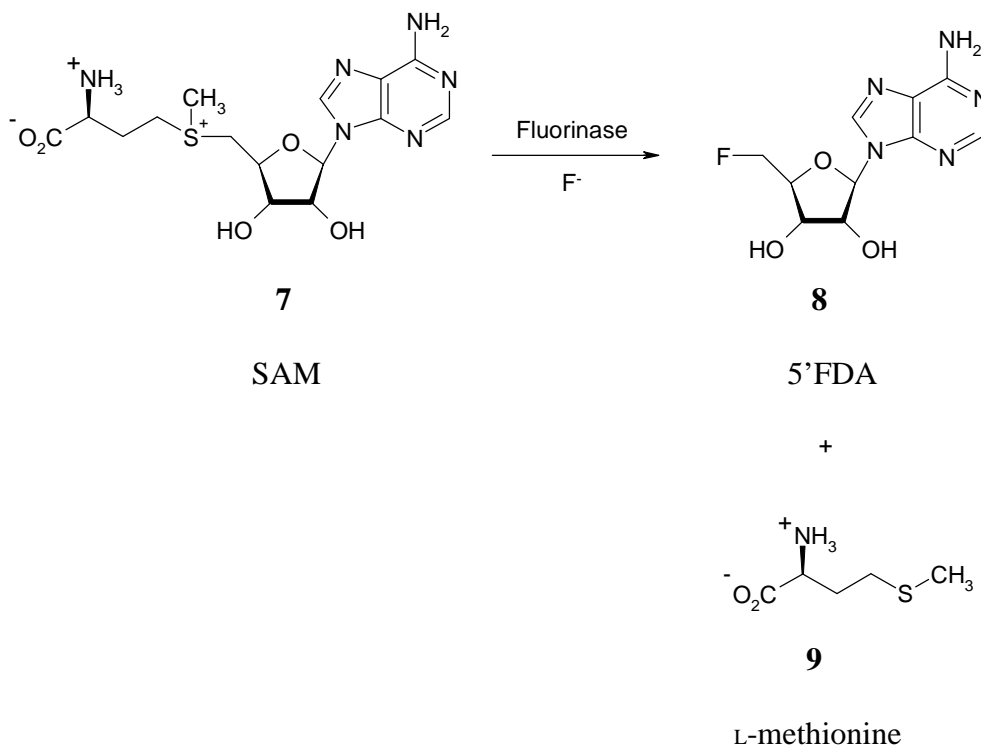
Fluoroacetate **1** has been isolated from various plant species such as *Oxylobium parviform*, also known as box poison (Australia) and *Dichapetalum cymosum* from South Africa.<sup>4</sup> These plants are highly toxic, with the fluoroacetate being converted to (2*R*,3*R*)-fluorocitrate **4**, itself a metabolite which has been found in plants, *via* condensation of fluoroacetyl-CoA with oxaloacetate. Upon digestion grazing animals have been known to die in large numbers. The soya bean plant (*Glycine max*) and a wheat grass (*Agropyron cristatus*) are able to produce fluoroacetate **1** and fluorocitrate **4** when a fluorine rich soil is provided.<sup>5</sup>

Peters and Shorthouse<sup>6,7</sup> reported in 1967 the uptake of inorganic fluoride and the production of fluoroacetone **2** from the plant *Acacia georginae* which is native to Australia.  $\omega$ -Fluoro-oleic acid **6** and other  $\omega$ -fluoro fatty acids have been identified from seeds of the West African shrub *Dichapetalum toxicarium*.<sup>8</sup> The leaves, however, show an accumulation of the only slightly less toxic fluoroacetate **1**.

### 1.1.2 Fluorinated metabolites from bacteria

Nucleocidin **5** was isolated from *Streptomyces calvus*, an organism identified from an Indian soil sample.<sup>9, 10</sup> It has anti-trypanosomal and antibiotic properties. In 1993 a team from the University of Exeter attempted to re-isolate nucleocidin **5** from *Streptomyces calvus* but were unsuccessful. They did however complete a total synthesis to explore its activity against infected HIV cells.<sup>11</sup> Fluoroacetate **1** and 4-fluorothreonine **3** are known to be bio-synthesised by *Streptomyces cattleya* in the presence of fluoride ion.<sup>12</sup> The enzyme responsible for C-F bond formation has been identified as 5'-fluoro-5'-deoxyadenosine synthase, also known as 'the fluorinase'. The fluorinase catalyses the reaction of *S*-

adenosyl-L-methionine (SAM) and inorganic fluoride ion to provide 5'fluoro-5'-deoxyadenosine (5'FDA) and L-methionine.<sup>13, 14</sup>



**Scheme 1.1** Formation of 5'FDA *via* the fluorination enzyme from *S. cattleya*.

The fluorinase has been purified and overexpressed, allowing X-ray structure analysis. The crystal structure of the enzyme as a hexamer is shown in **Figure 1.2**. The trimeric subunit with SAM bound to the enzyme is shown in **Figure 1.3**.<sup>15</sup>

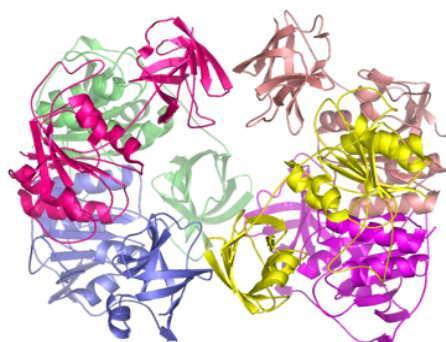


**Figure 1.2** An X-ray structure of the fluorinase, consisting of a hexamer (dimer of trimers).

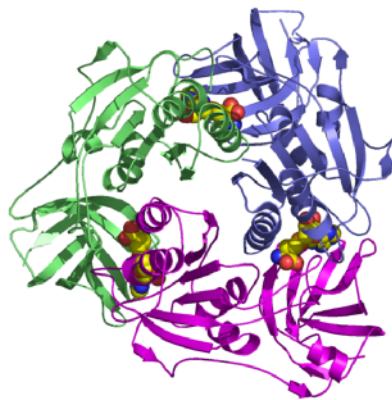
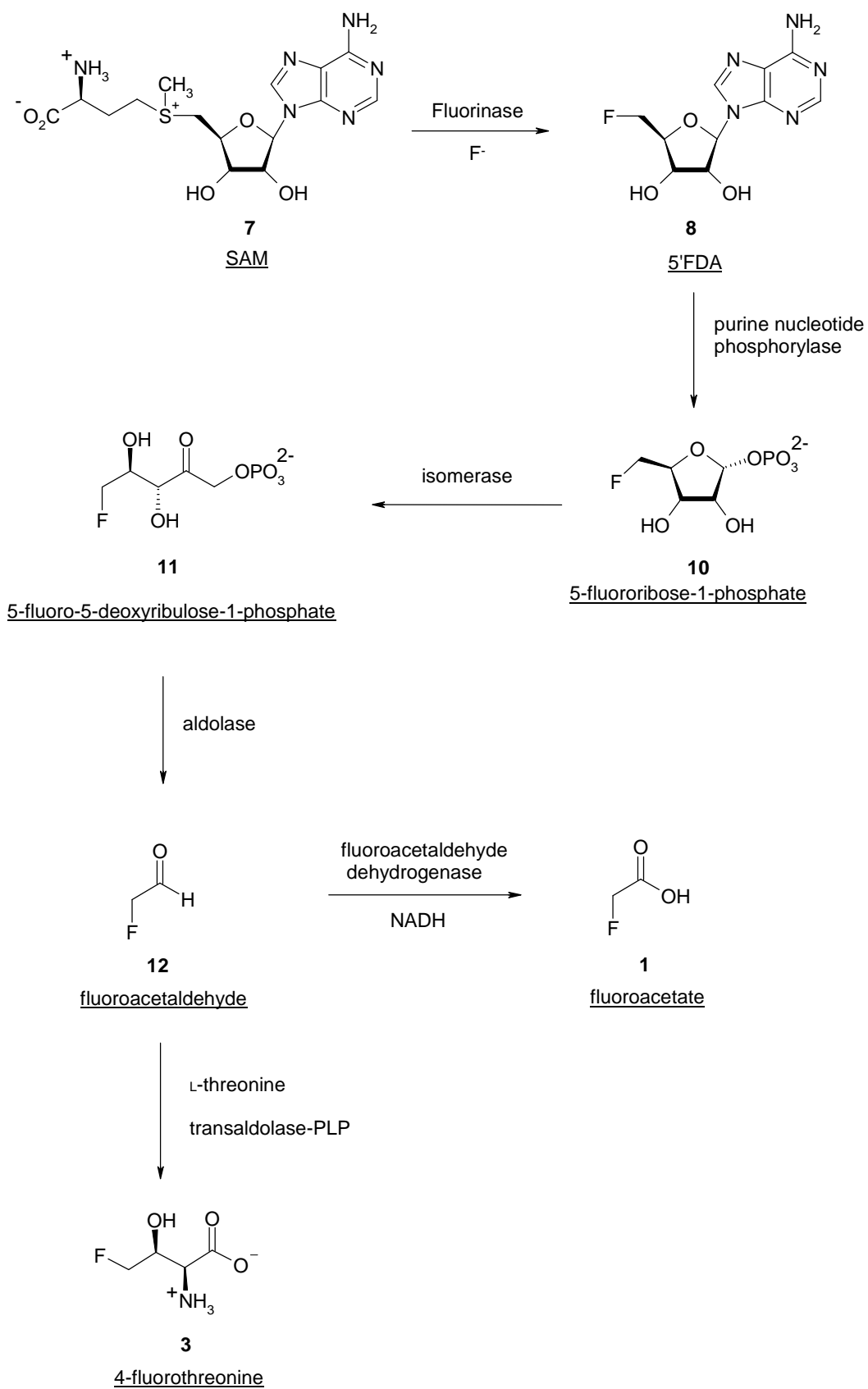


**Figure 1.3** An X-ray structure of the fluorinase with three bound SAM molecules.

The remainder of the biosynthetic pathway, leading to fluoroacetate **1** and 4-fluorothreonine **3** has also been studied.<sup>16-20</sup> The enzymes responsible for the various transformations and intermediates are shown in **Scheme 1.2**. All but one of the enzymes (aldolase) have been isolated and purified.



**Scheme 1.2** The biosynthetic pathway to the metabolites fluoroacetate **1** and 4-fluorothreonine **3**.

The fluorinase has been utilised in C-<sup>18</sup>F bond formation for use in positron emission tomography (PET) for imaging agents. At present this tumour imaging technique requires positron emitting isotopes, where <sup>11</sup>C and <sup>18</sup>F are most commonly in use, with <sup>18</sup>F being the preferred isotope owing to its relatively long half life,  $t_{1/2}$  110 minutes, compared to <sup>13</sup>C at  $t_{1/2}$  20 minutes. Currently <sup>18</sup>F isotope pharmaceuticals are synthesised chemically, taking time and producing side products. Biotransformation methods are attractive owing to selectivity, giving very few side products. The fluorinase enzyme has been utilised to generate <sup>18</sup>F labelled compounds when incubated with [<sup>18</sup>F]-HF, providing radiochemical yields for [<sup>18</sup>F]-5'-FDA up to 95%.<sup>21</sup>

## 1.2 Minerals

Fluorine is present in numerous natural minerals, with over 350 known to contain the element. Fluorite is a well known mineral, with its variety of colours, arising due to the presence of impurities. Some fluorine containing minerals exhibit luminescence, where light is emitted when it is excited by an energy source. The energy source can be provided by various means e.g. light (UV), electrons, X-rays and ions.<sup>22</sup>

Luminescence can be sub-divided: when the energy source is turned off and the mineral ceases to emit light, this is fluorescence; should it continue for more than  $10^{-8}$  seconds then this is phosphorescence.<sup>23</sup> Fluorescence from UV light in fluorite is well known, most commonly due to the presence of yttrium, causing defects in the crystal lattice or because europium or another lanthanide element is present as a trace impurity (activators). The analytical technique, cathodoluminescence microscopy and spectroscopy, where a beam of electrons is directed at the mineral sample is used routinely to analyse crystal defects. Photoluminescence (optical absorption) employing a range of wavelengths is used to detect the presence of rare earth elements. Divalent samarium and ytterbium have been discovered in natural fluorite with use of this technique.<sup>24</sup>

Thermoluminescence is also known to occur, although it is rarer. A variety of natural fluorite – chlorophane (**Figure 1.4**), exhibits a glow upon heating, observed at high temperatures between 119 and 224 °C.<sup>25</sup> Thermoluminescence can be used to determine the age of a mineral.

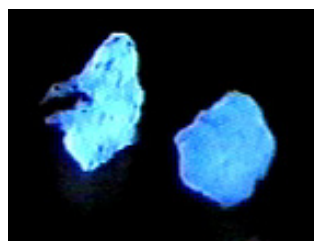


**Figure 1.4** Image of chlorophane.

### 1.3 The discovery of fluorine

Fluorspar (fluorite,  $\text{CaF}_2$ ) was known in the 15<sup>th</sup> century, where it was used as a flux (flußspat) in the German mining industry. It was not until the 1700's that it was used to produce hydrogen fluoride (fluoric acid) upon treatment of fluorspar with sulfuric acid. It was this observation which led to the development of an identification test for the mineral by the Swedish pharmacist, Karl Wilhelm Scheele which was reported in 1771. Later he showed hydrogen fluoride could also be generated by the addition of nitric or phosphoric acids to fluorspar.

Concentrated hydrofluoric acid, prepared by heating fluorspar and sulfuric acid, was reported by J. L. Gay-Lussac and L. J. Thénard in 1809.<sup>26</sup> They also described its strong corrosive activity on the human skin. It was however later, in 1856 when anhydrous hydrofluoric acid was first obtained. Edmond Frémy achieved this by treating crude, wet hydrofluoric acid with potassium fluoride, which precipitated potassium hydrogen fluoride. This was re-crystallised, removing potassium hexafluorosilicate, dried and then heated to give anhydrous hydrogen fluoride, which was condensed at low temperatures.

The isolation of fluorine itself was attempted by Humphry Davy, but alas he did not obtain the unknown element, fluorine. In 1813 he wrote:

*“from the general tenor of results that I have stated, it appears reasonable to conclude that there exists in the fluoric compounds a peculiar substance, possessed of strong attractions for metallic bodies and hydrogen, and which, in consequence of its strong affinities and high decomposing agencies, it will be very difficult to examine in a pure form, and, for the sake of avoiding circumlocution, it may be denominated fluorine, a name suggested to me by M. Ampère.”*

Seventy-three years later, the French chemist Henri Moissan was more successful and in 1886 he prepared gaseous fluorine by electrolyzing potassium hydrogen fluoride in anhydrous liquid hydrogen fluoride. He achieved this with use of platinum and iridium electrodes sealed into a platinum U-tube which was in turn sealed with fluorite tops. The equipment was cooled to  $-50\text{ }^{\circ}\text{C}$  and hydrogen was produced at the anode and fluorine at the cathode. He also reported that the fluorine gas produced caused silicon crystals to burst into flames.<sup>1</sup>

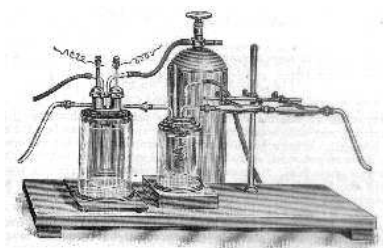


**Figure 1.5** Henri Moissan's equipment, used to obtain gaseous fluorine.

Henri Moissan received various awards such as the Davy medal in 1896, and was awarded Fellowships with the Royal Society and The Chemical Society (London). In 1906 he was honoured with the Nobel Prize in Chemistry. His major works include *Le Fluor et ses Composés* (1900; 'Fluorine and its Compounds') and *Le Four électrique* (1897; 'The Electric Furnace').



**Figure 1.6** A portrait of Henri Moissan and a French stamp commemorating the centenary of  $\text{F}_2$  isolation.

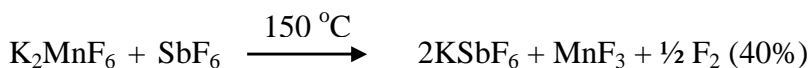
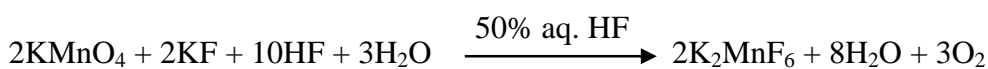


## 1.4 Fluorine production today

Today a similar process is used for the production of gaseous fluorine which is distributed with and without nitrogen dilution. Fluorine is manufactured within a jacketed cell tub, filled with an electrolyte solution of potassium hydrogen difluoride. The temperature must be maintained at 74 °C for efficient F<sub>2</sub> production. Should the temperature rise the corrosion rate increases (damaging the cell) and HF and KF·2HF contaminate the fluorine produced.<sup>27</sup> If lower, the electrolyte solution solidifies, reducing the efficiency of the cell. The gas is removed by a fluorine flow system and delivered to the fluorine compartment which is purged with nitrogen. Hydrogen gas is generated at the cathode.

## 1.5 Chemical synthesis of fluorine

A more recent development in fluorine research, is the production of elemental fluorine *via* synthetic methods. In 1986 Professor Karl O. Christe was preparing for a fluorine chemistry meeting to celebrate the 100<sup>th</sup> anniversary of Moisson's findings. He discovered a reaction to obtain significant amounts of fluorine.<sup>28</sup> Reacting potassium permanganate with fluoride in hydrogen fluoride generated manganese fluoride. Treatment of this with antimony hexafluoride produced elemental fluorine. It is also possible to obtain fluorine at room temperature using MnF<sub>6</sub> in place of SbF<sub>6</sub>.



**Scheme 1.3** The reaction scheme to chemically synthesise elemental fluorine.

## 1.6 Applications of organic fluorine compounds

### 1.6.1 Pharmaceuticals

The incorporation of fluorine into pharmaceuticals has often been found to increase lipid solubility, therefore promoting the rate of adsorption and transportation of drugs. Placing a fluorine atom at a strategic site may contribute to its metabolic stability as well as alter its basicity or acidity, all important properties in pharmaceutical design. Fluorine may also assist in protein binding. Often a fluorinated analogue is found to be more potent than its non-fluorinated counterpart.

Many of today's pharmaceuticals contain fluorine with an estimated 20% having at least one fluorine atom.<sup>29</sup> Some of the best selling prescription drugs are fluorinated (**Figure 1.7**).

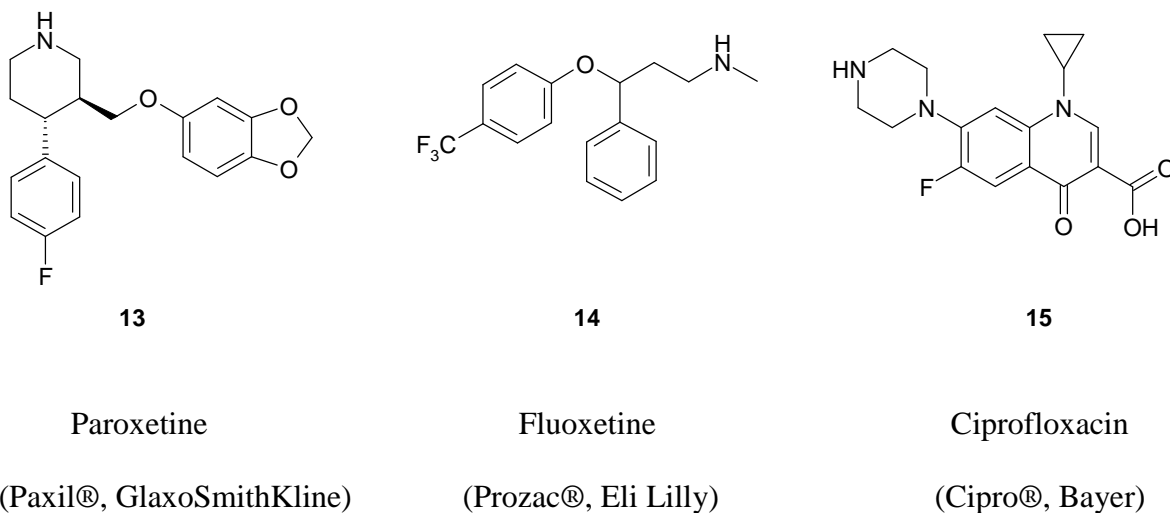


**Figure 1.7** Examples of pharmaceuticals containing fluorine.

An interesting area of pharmaceutical design is that of bio-isosteric mimicking, where some functional groups which are unstable or degrade to undesirable products are substituted using fluorine or fluorinated groups. Here the new group mimics the polarity, electrostatic charge distribution or geometry of the original group.<sup>30</sup> An example of this is diazepam (Valium®) **16** and the analogue (**17**) where the chlorine has been replaced with the trifluoromethoxy group (OCF<sub>3</sub>). The biological activity is unchanged and there is similar electron density through the molecule, the sterics however alter with the larger OCF<sub>3</sub> group.

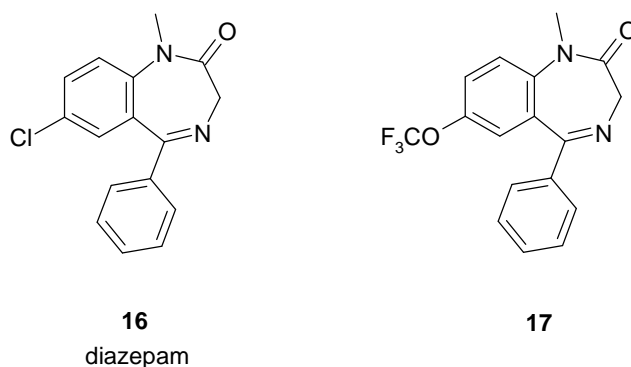


**Figure 1.8** Diazepam and analogue **17**.

Flunitrazepam (Rohypnol®) **18** is a fluorinated analogue of diazepam. This drug is 7 - 10 times more potent than diazepam and as such is used as a strong sedative. It is also well known to be misused as a 'date rape drug'.

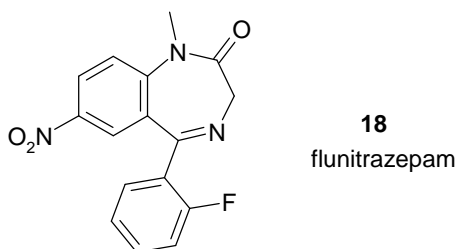


**Figure 1.9** Flunitrazepam is a fluorinated analogue of diazepam.

### 1.6.2 Anaesthetics

Fluorinated compounds have found a central role in the anaesthetic field. Since the 1950's fluorine has been used to develop new materials to replace ether and chloroethane which were in wide use although they are highly flammable. One benefit of using fluorinated anaesthetics is the reduction in flammability, they also were found to have fewer side effects. The first fluorinated anesthetic to be used on patients was Fluoroxene ( $\text{CF}_3\text{CH}_2\text{OCH}=\text{CH}_2$ ) in 1953.<sup>3</sup> It was however Halothane ( $\text{CF}_3\text{CHClBr}$ ), introduced in 1956 that became the most popular anaesthetic to be used with about 70-80% of operations using this anaesthetic in the 1980's.<sup>4</sup> Since then various other substances have come to market, with the key materials being Sevoflurane ( $((\text{CF}_3)_2\text{CHOCH}_2\text{F})$ ) and Desflurane ( $\text{CF}_3\text{CHFOCHF}_2$ ), providing a more efficient delivery having low blood-gas partition coefficients and reduction in side effects and shorter recovery times.

Sevoflurane is the anaesthetic of choice of many anaesthetists as it is non-irritant by inhalation and does not require a vaporiser, whereas Desflurane is less volatile and as such requires a vaporiser and more equipment for its administration. It is also an irritant but has a faster onset.<sup>31</sup> With Desflurane being less soluble in the blood (0.4%) its effects wear off more quickly. Sevoflurane has a blood-gas solubility of 0.6%.<sup>32</sup> A possible explanation for this is that Sevoflurane has one more  $\text{CF}_3$  group than Desflurane, which could make it more lipophilic, hence more soluble in the blood.

### 1.6.3 Agrochemicals

Since the 1950's fluorine has played a significant part within the agrochemical industry. Its presence can affect and also improve the properties of agrochemicals, such as solubility, volatility, penetration and toxicology.<sup>33</sup> Agrochemicals in the form of herbicides, fungicides and insecticides often contain fluorine, with about half of the molecules in field trials containing the element.<sup>34</sup> A number of major products on the market today contain a fluorine atom.

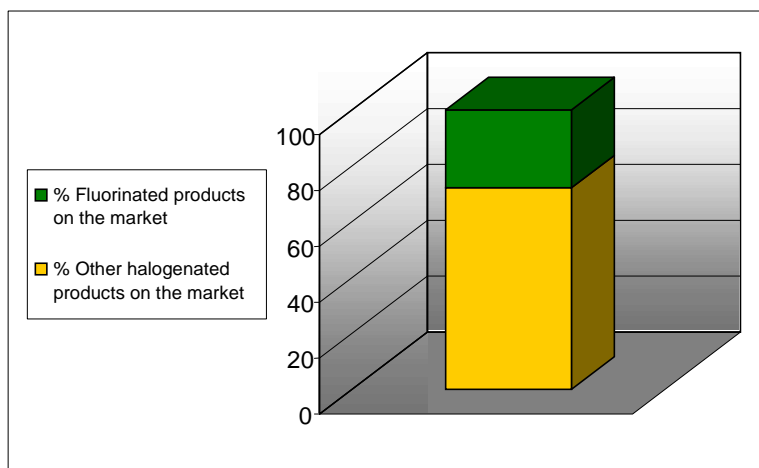


**Figure 1.10** Approximately 30% of the halogenated agrochemicals on the market today contain fluorine.

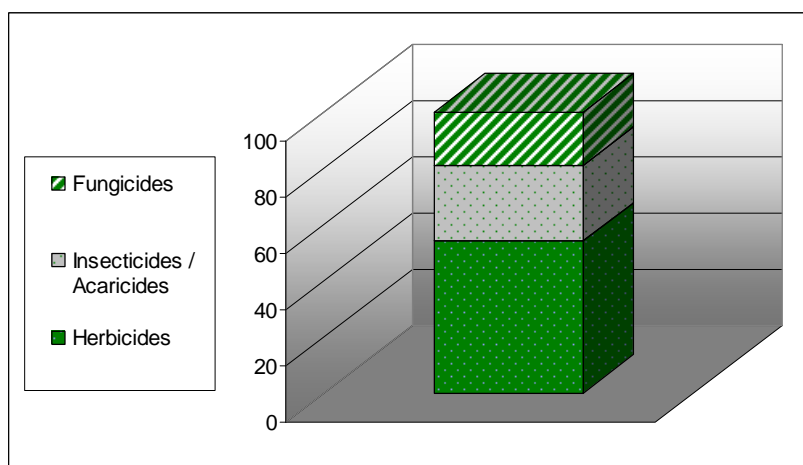


**Figure 1.11** Herbicides represent the largest proportion of this 30% share.

When the author was employed at Syngenta (Grimsby), the site was involved with the synthesis of five active ingredients. Four of these actives contained fluorine, demonstrating the importance of fluorine in today's agrochemical industry. These active ingredients are sold under the names of Clodinafop-propargyl **19**, Flumetralin **20**, Lufenuron **21** and Prodiamine **22**.

### Clodinafop-propargyl

Clodinafop-propargyl **19** is a selective herbicide and plant growth regulator, controlling weeds such as wild oats and black grass in cereal crops. The herbicide works by inhibiting the enzyme, acetyl coenzyme A carboxylase which is involved in fatty acid biosynthesis for cell membrane development. It is sold under the name of various products, but mainly as 'Topik' and 'Horizon'.

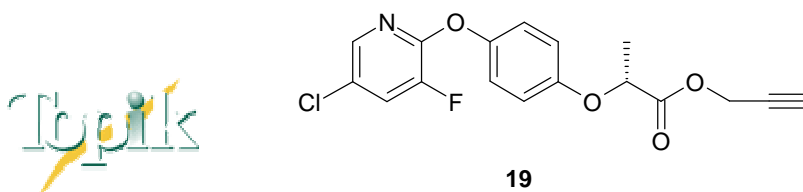


**Figure 1.12** Topik's logo and the structure of its active ingredient – Clodinafop-propargyl.

### Flumetralin

Flumetralin **20** is sold in the USA as 'Prime +', for use on tobacco plants and as a plant growth regulator (it controls bud growth).

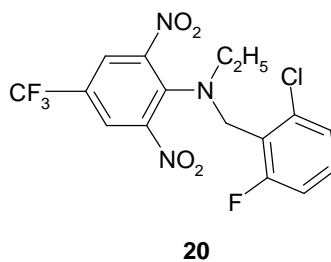


**Figure 1.13** Flumetralin contains both an aromatic fluorine and a  $\text{CF}_3$  group.

### Lufenuron

Lufenuron **21** is a N-benzoyl-N'-phenyl urea, used as an agrochemical insecticide ('Match') as well as a veterinary product, 'Program' for flea treatment of domestic animals. Lufenuron is an insect growth regulator, inhibiting chitin production, preventing eggs from hatching and thus stopping the insect life cycle.

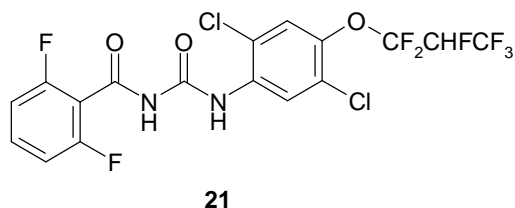


**Figure 1.14** Lufenuron is used both as an insecticide in agrochemicals and in the veterinary field (Program).

The fluorine positioning is important for both chitin synthase inhibition and degradation in the soil. It has been found that fluorine in the 2- and 6- positions are the most beneficial sites for activity against chitin production.<sup>33</sup>

**Prodiamine**

Prodiamine **22** is a herbicide that controls grasses and broad leafed weeds in turfs, ornamental grasses and golf courses. It is marketed as ‘Barricade’.

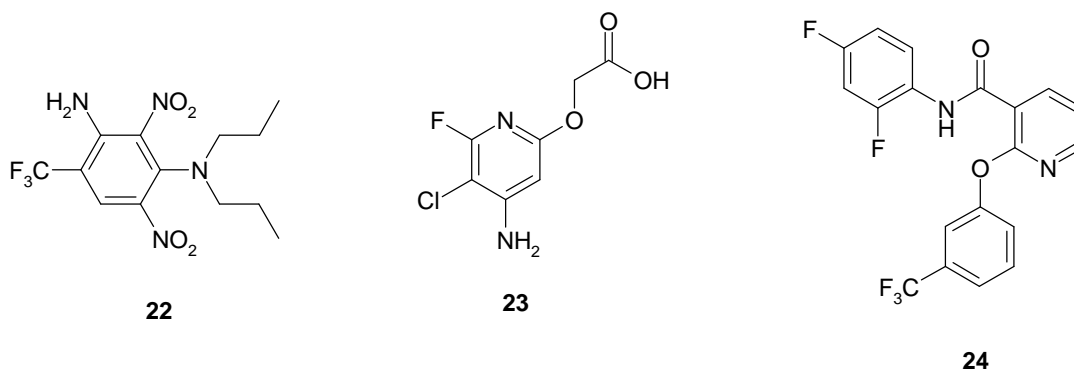


**Figure 1.15** Prodiamine (Syngenta) **22**, fluroxypyr **23** and diflufenican **24**.

Here in St Andrews, a few fluorinated herbicides are in use on the golf links, treating the most famous courses in the world. Fluroxypyr **23** (as a mix in ‘Bastion T’) is used to treat broad leafed weeds and diflufenican **24** is present in ‘Spearhead’, another herbicide.<sup>35</sup>

Fungicides complete the range of agrochemicals containing fluorine. ‘Flutriafol’ **25** (Impact, Syngenta) is a highly active, broad spectrum fungicide used on rice crops. Flutriafol **25** is a triazole fungicide, part of a large group of triazole derivatives acting as an inhibitor of the cytochrome-P<sub>450</sub> dependent demethylation of an intermediate in sterol biosynthesis in fungi.<sup>33</sup> Of the azoles used commercially as fungicides, 19% of these contain fluorine or fluorinated substituents.



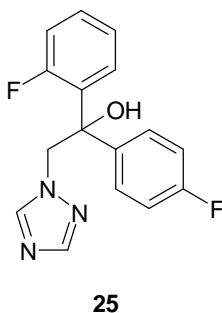
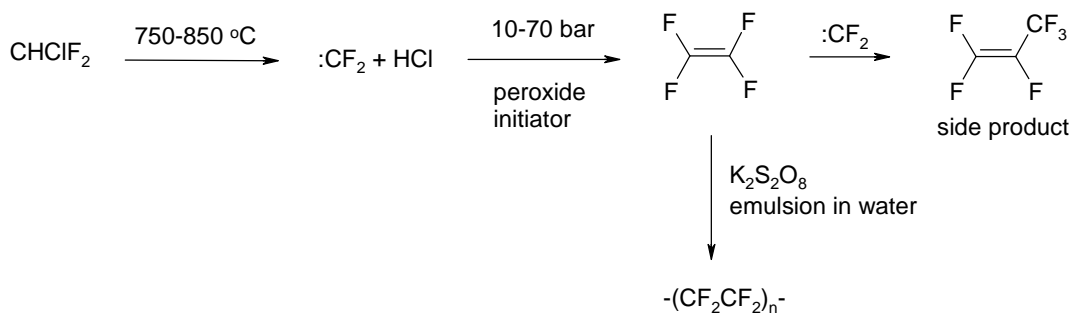


**Figure 1.17** Flutriafol **25** represents one of the fluorinated triazoles used commercially.

### 1.6.4 Polymers

Polytetrafluoroethylene (PTFE) is a widely used polymer, being more chemically and thermally stable than its non-fluorinated counterpart, polyethylene.<sup>36</sup> PTFE and its properties were discovered by Roy Plunkett at DuPont in 1938. The commercial synthesis of PTFE is shown in **Scheme 1.4**. Thermal fragmentation of  $\text{CHClF}_2$  provides difluorocarbene which then couples to generate tetrafluoroethylene. The polymer is obtained by radical-mediated emulsion polymerisation.



**Scheme 1.4** Synthesis of polytetrafluoroethylene (PTFE).

PTFE has a variety of applications, from the well known Teflon® coated cooking equipment to uses within fabric, for example Goretex® outdoor clothing. Teflon® is also used in roofing materials; famously it coated the glass fibre roof of the Millennium Dome, 320 meters in diameter, making it the largest single roofed structure in the world.<sup>37</sup> PTFE coated fabric has also been used to construct the roofing of Edinburgh’s science attraction ‘Our Dynamic Earth’.

Today there are over twenty fluoropolymers which are in use commercially.<sup>38</sup> They are often rather expensive and as such used for specialist applications, for example coating space equipment and cables offering not only durability but resistance to atomic oxygen and fire respectively. Lumiflon (Fluoro Ethylene - Alkyl Vinyl Ether) is one such polymer manufactured by Asahi Glass. Lumiflon based paints are used on buildings, bridges and transportation.

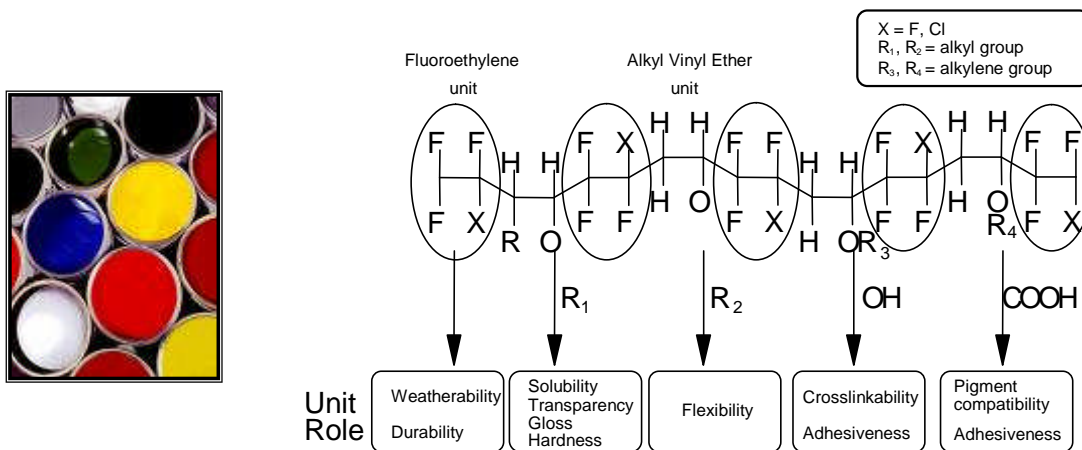


**Figure 1.18** Lumiflon is a fluorinated resin, added to paints and resins for durability.

## 1.7 Applications of inorganic fluoride

### 1.7.1 Fluoride in water and toothpaste

Fluoride occurs naturally in water, at low levels. It has been found that in areas where this fluoride concentration is higher, the incidence of tooth decay in children was lower. During the 1940's a study was conducted on the control of dental caries with fluoridated water within the USA and Canada. Soon after the US Public Health Service recommended that fluoride be added to water supplies, England and Wales followed suit in the 1960's.<sup>39, 40</sup>

In the UK today, some local authorities in England and Wales have chosen to artificially increase the water supply fluoride content to 0.7 - 1 ppm. This distributes to approximately 10% of the population. Birmingham and Newcastle are two major cities which are part of this fluoridation scheme. Scotland is however 'non-fluoridated' with only one public water supply in Morayshire being at a natural concentration of 1ppm<sup>41</sup>, all others are at a much lower level. Here in St Andrews the natural fluoride level was measured in 2006 on average as 0.067 mgF/l (0.067 ppm).<sup>42</sup> In 2004, after a public consultation in 2002, water fluoridation was discussed in the Scottish Parliament and the ex-First Minister – Mr Jack McConnell is quoted as saying

*“I can confirm that, having listened to the views that have been expressed, we will not be changing the current legislation on fluoridation of water supplies in this Parliament”.*<sup>43</sup>

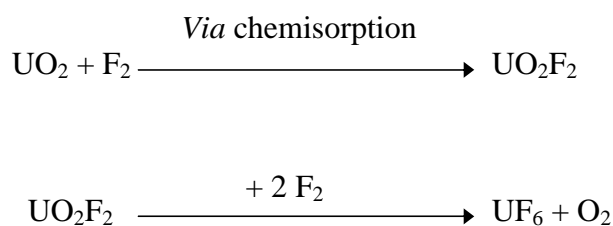
Ireland, on the other hand has mandatory artificial water fluoridation. The case for fluoridated water is controversial, with some governmental bodies, dentists and academics promoting it, while others oppose it. Dental caries are thought to be controlled by fluoride in three ways, by improving the structure of the enamel throughout its development and therefore resisting acid damage, assisting with re-mineralisation, improving enamel crystal properties and reducing the plaque bacteria's (*Streptococcus mutans*) ability to produce

acid. Although there is a lot of evidence to support the benefits of water fluoridation and use of fluorine containing products there may also be negative impacts on health. Dental fluorosis (mottling of teeth) is known to occur with a high intake of fluoride, this may occur from drinking fluoridated water or overexposure from fluoride toothpaste or other dental products. There have been investigations on the possibility of bone defects caused by ingestion of fluoride, with about 50% of injected fluoride being taken up in the bone. Studies have found however that ingestion of fluoridated water does not pose a greater risk to bone fracture / skeletal fluorosis to the general population.<sup>44, 45</sup> Various other health concerns exist over adverse effects such as cancer, birth and renal effects but there is limited evidence of these and in a year 2000 review 'The York Review' it was concluded that apart from dental fluorosis there was no solid evidence to show that water fluoridation caused any other adverse effects.<sup>46</sup>

Fluoride toothpaste was introduced onto the European market in the 1970's, significantly decreasing the incidence of dental decay globally. Typically the fluoride concentration is 1000-1500 ppm and in children's toothpaste it is lower at 500 ppm. Obviously one of the major issues is the swallowing of toothpaste in children or excessive amounts applied, leading to enamel fluorosis.

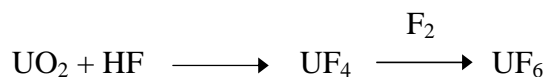
### 1.7.2 Uranium hexafluoride

Naturally occurring uranium is made up from three isotopes:  $^{238}\text{U}$  (99.3%),  $^{235}\text{U}$  (0.7%) and traces of  $^{234}\text{U}$ .<sup>47</sup> Uranium in the form of uranium hexafluoride ( $\text{UF}_6$ ) is used to separate the isotopes of uranium-235 and uranium-238 and various methods such as gas centrifugation<sup>48</sup> and gaseous diffusion are used. Uranium hexafluoride is heated to a gaseous state and with fluorine only having one stable natural isotope the isotopomers of  $\text{UF}_6$  have different molecular weights due to the different uranium isotopes present, enabling easy separation by mass using centrifugion through diffusion membranes. Once these are separated the energy from fission of  $^{235}\text{U}$  can be harvested within a power station. Uranium hexafluoride can be formed *via* uranyl fluoride in a two step process from the reaction of uranium dioxide with fluorine gas (**Scheme 1.5**).<sup>49</sup>



**Scheme 1.5** The process to obtain uranium hexafluoride.

The commercial process used to manufacture  $\text{UF}_6$  at Springfields Fuels in Preston, UK converts uranium ore, yellowcake ( $\text{U}_3\text{O}_8$ ) into uranium dioxide which is fluorinated using hydrogen fluoride to give uranium tetrafluoride. Further fluorination with fluorine gas provides the final product,  $\text{UF}_6$  ready for enrichment (**Scheme 1.6**).<sup>50</sup>



**Scheme 1.6** The chemical process used to manufacture uranium hexafluoride.

## 1.8 General properties of fluorine and the C-F bond

### 1.8.1 Electronegativity

Electronegativity is “*The power of an atom in a molecule to attract electrons to itself.*”<sup>51</sup>

The halogens have high electronegativity values, with fluorine the highest value on the Pauling scale (**Table 1.1**). Fluorine’s high electronegativity influences its polarisation ability, providing a C-F bond with a large dipole moment (**Figure 1.19**). The dipole moment ( $\mu$ ) is calculated from  $\delta$  (electric charge) times distance.

	Pauling electronegativity	Dipole moment C-X $\mu$ <sup>30</sup>
F	3.98	1.41
Cl	3.16	1.46
Br	2.96	1.38
I	2.66	1.19
H	2.20	0.4

**Table 1.1** Fluorine is the most electronegative element in the periodic table.

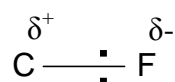


**Figure 1.19** The C-F bond has a large dipole owing to fluorine’s electronegativity.

### 1.8.2 Atomic size

Fluorine has a small size compared to the other halogens, using the Bondi's scale of van der Waals radii as illustrated in **Table 1.2**.<sup>52</sup> Fluorine is of similar size to oxygen and larger than hydrogen. Despite this difference in size, hydrogen is often replaced by fluorine in molecular design and synthesis because it is the next smallest atom to hydrogen and provides minimal steric change.<sup>53</sup>

	<b>Atomic radii (Å)</b>
H	1.20
O	1.52
F	1.47
Cl	1.75
Br	1.85
I	1.98

**Table 1.2** Van der Waals radii according to the Bondi scale.<sup>52</sup>

Williams and Houpt also reported a van der Waals radii scale (**Table 1.3**).<sup>54</sup> This shows that fluorine and oxygen are of an identical size and that hydrogen is smaller. It is clearly more accurate to compare fluorine's size to that of oxygen rather than to that of hydrogen.

	<b>Ionic radius X<sup>-</sup> (Å)</b>
H	1.15
O	1.44
F	1.44

**Table 1.3** Williams and Houpt scale.<sup>54</sup>

### 1.8.3 Steric influence of fluorine

Fluorinated substituents often change the geometric size of a molecule compared to its non-fluorinated counterpart. For example a  $\text{CF}_3$  group appears to occupy a much larger volume than  $\text{CH}_3$  as shown in **Figure 1.20**.<sup>55</sup>

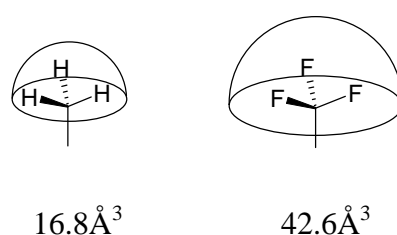


**Figure 1.20** The van der Waals volumes of  $\text{CH}_3$  and  $\text{CF}_3$ .<sup>55</sup>

The steric size can also have an effect on conformational equilibrium. The energy difference between axial and equatorial substituents on cyclohexane reports steric influence, (A value). It is found that a single fluorine atom has little effect on the energy difference, whereas a  $\text{CF}_3$  group is much larger than a  $\text{CH}_3$  group.<sup>56</sup> This is explained by the increased energy of the 1,3-di-axial interactions with  $\text{CF}_3$ .

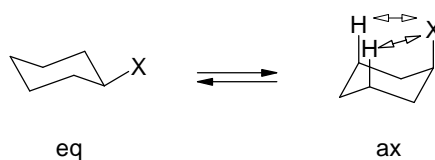


**Figure 1.21** Cyclohexane with substituent X changes the free energy difference ( $\Delta G^\circ \text{ ax / eq}$ ).



X	$\Delta G^\circ$ ax/eq (kcalmol <sup>-1</sup> )
H	0.00
F	0.15
OCH <sub>3</sub>	0.65
CH <sub>3</sub>	1.7
CH(CH <sub>3</sub> ) <sub>2</sub>	2.1
CF <sub>3</sub>	2.4

**Table 1.4** A values. Free energy differences ( $\Delta G^\circ$ ) for ax / eq interconversion.

#### 1.8.4 The C-F bond

The C-F bond is the strongest covalent bond in organic chemistry as indicated by comparison of bond dissociation energies as shown in **Table 1.5** and **Figure 1.22**.<sup>57</sup>

C-X bond	Bond Dissociation Energy (kJmol <sup>-1</sup> )
C-H	439
C-F	472
C-Cl	350
C-Br	293
C-I	239

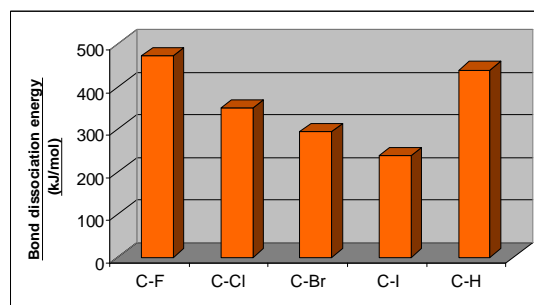


**Table 1.5** and **Figure 1.22** C-F bond dissociation energies.

If we compare the bond dissociation energy of methane to those from halogenated methanes, it is evident that  $\text{CF}_4$  has the strongest C-X bonds.

C-X bond in the methane series	Bond Dissociation Energy ( $\text{kJmol}^{-1}$ )
$\text{CH}_4$	435
$\text{CF}_4$	515
$\text{CCl}_4$	295
$\text{CBr}_4$	235

C-X bond	Bond dissociation energy ( $\text{kJ/mol}$ )
C-F	515
C-Cl	295
C-Br	235
C-H	435

**Table 1.6** and **Figure 1.23** Bond dissociation energies in halogenated methanes.<sup>1</sup>

The C-F bond is similar in length to that of C-H, and C-F often replaces C-H in, for example, drug design.

C-X bond	Length ( $\text{\AA}$ )
C-H	1.09
C-C	1.54
C-O	1.43
C-F	1.38
C-Cl	1.77
C-Br	1.94
C-I	2.13

**Table 1.7** Bond lengths of selected C-X species.<sup>30, 58</sup>

Fluorine substitution of a hydrogen in HC-C to a FC-C is known to affect the C-C bond length, making it shorter (**Table 1.8**). Further substitution of fluorine onto the C-C bond results in a further shortening.<sup>56</sup>

C-C bond	Length (Å)
CH <sub>3</sub> -CH <sub>3</sub>	1.513
CH <sub>3</sub> -CH <sub>2</sub> F	1.504
CH <sub>3</sub> -CHF <sub>2</sub>	1.498
CH <sub>3</sub> -CF <sub>3</sub>	1.494

**Table 1.8** Substituting hydrogen for a fluorine **decreases** C-C bond length.

However adding fluorine to trifluoromethylethane results in a gradual increase in bond length as the fluorines are pulling electron density to each end of the molecule.

C-C bond	Length (Å)
CF <sub>3</sub> -CH <sub>3</sub>	1.494
CF <sub>3</sub> -CH <sub>2</sub> F	1.501
CF <sub>3</sub> -CHF <sub>2</sub>	1.524
CF <sub>3</sub> -CF <sub>3</sub>	1.545

**Table 1.9** Further substituting hydrogen for fluorine **increases** FC-C bond length.

The C-H bond length is short at 1.09Å, compared to C-F at 1.38Å. In a sterically hindered system this may influence the mobility of a substituent. For example in **Figure 1.24**, rotation of the phenyl ring is restricted when X = F, owing to the longer bond length and larger atomic size.<sup>59</sup>

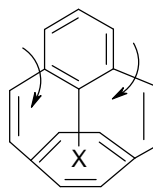


**Figure 1.24** When X = F, the phenyl ring rotation is restricted relative to X = H.

### 1.8.5 Acidity and basicity effects

The effect of introducing fluorine into a carboxylic acid is illustrated by the change in  $pK_a$ s of the acetic acids in **Table 1.10**. The electronegativity of fluorine increases the acidity of the carboxylic acid because of the negative inductive effect. Acidity increases with increasing fluorine substitution. The opposite is true for amine bases. Here fluorine's high electronegativity leads to a decrease in electron density at nitrogen and the basicity is lowered. **Table 1.11** lists some amines and demonstrates the change in  $pK_b$  when fluorine is present. Lipophilicity in turn is also affected by fluorine substitution.

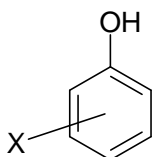
Carboxylic acid	$pK_a$
$CH_3CO_2H$	4.76
$CH_2FCO_2H$	2.59
$CHF_2CO_2H$	1.30
$CF_3CO_2H$	0.50
$CCl_3CO_2H$	0.66

**Table 1.10**  $pK_a$  values of carboxylic acid and its fluorinated analogues.<sup>56</sup>

Amine	pK <sub>b</sub>
CH <sub>3</sub> CH <sub>2</sub> NH <sub>2</sub>	10.6
CF <sub>3</sub> CH <sub>2</sub> NH <sub>2</sub>	5.7
CCl <sub>3</sub> CH <sub>2</sub> NH <sub>2</sub>	5.4
C <sub>6</sub> H <sub>5</sub> NH <sub>2</sub>	4.6
C <sub>6</sub> F <sub>5</sub> NH <sub>2</sub>	-0.36

**Table 1.11** pK<sub>b</sub> values of amines and fluorinated analogues.<sup>4</sup>

Fluorine can affect the acidity of other functional groups e.g. phenols, benzoic acids and anilines. In phenols, fluorine and the other halogens increase the acid strength and the extent is dependent on the position of substitution.<sup>56</sup> Substitution at the *ortho* position has the greatest effect on increasing acidity, followed by *meta* and *para* (*ortho* > *meta* > *para*) as shown in **Table 1.12**. Of the halogenated phenols, fluorine is the least ‘acid enhancing’ despite its high electronegativity presumably owing to lone pairs donating through the  $\pi$ -electron system, thus weakening the acidities.

 <b>X</b>	<b>Ortho</b>	<b>Meta</b>	<b>Para</b>
H	10.00	10.00	10.00
F	8.73	9.29	9.98
Cl	8.56	9.12	9.41
Br	8.45	9.03	9.37
I	8.51	9.03	9.33

**Table 1.12** pK<sub>a</sub> of halogenated phenols.

## 1.9 Fluorine as a hydrogen bonding acceptor

Hydrogen bonding can be described as a weak electrostatic attraction between a lone pair of electrons on a heteroatom, and a covalently bonded hydrogen atom that carries a  $\delta+$  charge. There has been considerable discussion regarding the ability of organic fluorine to enter into X-H $\cdots$ F-C bonding. Fluorine however holds its lone pairs very tightly and this renders it a weak hydrogen bond acceptor. As a result carbon-fluorine to hydrogen bonds are not as strong as those to oxygen and nitrogen, however such bonds have been clearly observed,<sup>54</sup> however they are relatively rare and very much ‘*system dependent*’.<sup>54</sup>

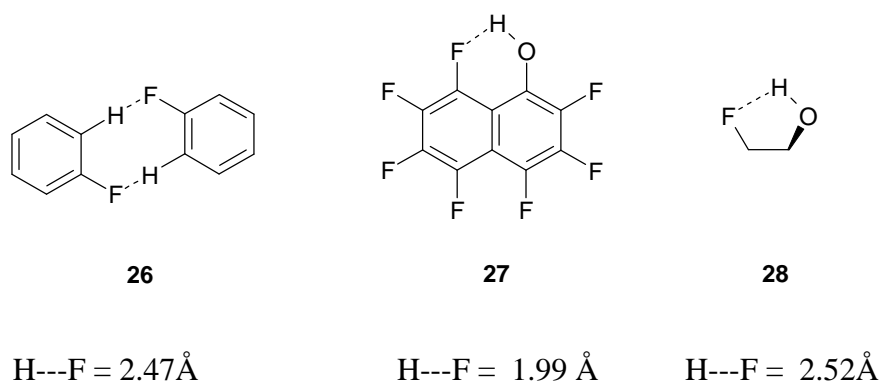
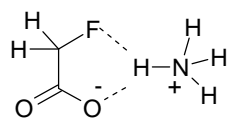


**Figure 1.25** Three examples of fluorine hydrogen bonding **26**<sup>60</sup>, **27**<sup>61</sup>, **28**.<sup>62</sup>

Short non-bonding distances between X-H $\cdots$ F-C is the most obvious indication of such hydrogen bonding. In general XH $\cdots$ F-C systems with a hydrogen-fluorine distance in the range of 2.0 -2.4 $\text{\AA}$  are considered to have a ‘hydrogen bond’. Interactions beyond van der Waals contact (2.7 $\text{\AA}$ ) are very weak.

N-H systems with hydrogen bonding to F-C species have been reported by Dunitz.<sup>63</sup> An example highlighted by Dunitz is shown in **Figure 1.26**.



29

O···H	2.03Å
F···H	2.29Å

**Figure 1.26** Hydrogen bonding is observed between ammonium  $N^+H$  salt and F-C species 29.

Generally the C-F bond acts as a hydrogen bond acceptor when there is no better acceptor, such as oxygen or nitrogen, available. The strength of a  $C-F\cdots H-O$  hydrogen bond is weak and has been measured at  $2.4 \text{ kcal mol}^{-1}$  in the gas phase, half of that of an OH hydrogen bond.<sup>64</sup>

Various studies have been conducted on C-F to H-O and H-C distances, using the Cambridge Structural Database System (CSD). Here the X-ray structures have been evaluated and C-F to H distances measured.<sup>63-65</sup> The general consensus is that fluorine 'hardly ever makes hydrogen bonds',<sup>66</sup> with very few molecules (~40) exhibiting short C-F to H-C, H-N or H-O distances ( $< 2.35\text{\AA}$ ). It must be noted that these distances may not only be caused by hydrogen bonding but also because of crystal packing. The interactions can be considered weak, for example when analysing the molecules showing  $C-H\cdots C-F$  distances up to  $2.9\text{\AA}$ , a wide range of  $C-H\cdots F$  angles, between  $70^\circ$  and  $180^\circ$  is observed. Ideal hydrogen bonds should have an angle of  $180^\circ$ .

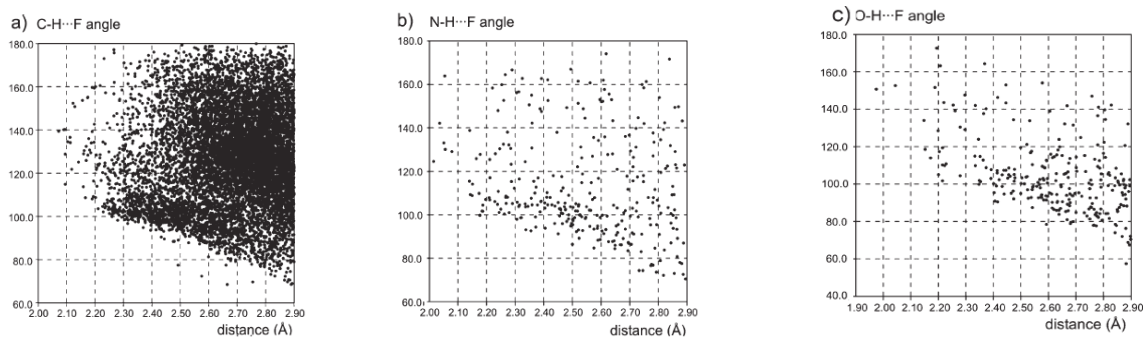


**Figure 1.27** Distances (F...H) and angles (X-H...F) of C-H...F, N-H...F and O-H...F compounds, as found on the CSD, version 5.25, November 2003.<sup>65</sup>



## 1.10 Fluorine as an inductive activator of a hydrogen-bond donor group

Fluorine also has the ability to promote hydrogen bonding to adjacent functional groups. Fluorine as a substituent on for example, aromatic systems enhances the acidity of the hydrogens on the ring. This in turn increases the hydrogen's ability to act as hydrogen bridge donors. In the case of aromatic systems where one aromatic ring is fluorinated, providing acidic hydrogens **30** and the other having an electron rich aromatic  $\pi$  electron system, they can interact with one another as demonstrated in **Figure 1.28**.<sup>30</sup> This is of importance in the drug design and biological activity of fluorinated drugs on proteins and receptors.

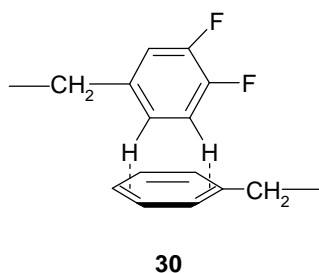


**Figure 1.28** Aromatic C-H--- $\pi$  interactions can be enhanced by fluorination.

Fluorine is also known to decrease the basicity of amines and increase the acidity of alcohols. These in turn, become better hydrogen-bond donors. It is well known that the presence of a halogen can increase a drug's potency / toxicity. In anti-inflammatory steroids, when fluorine is substituted at the C-9 position their potency is often increased<sup>67</sup> owing to the fluorine influencing the acidity of the hydroxyl group at C-11 and its hydrogen bonding ability. Betamethasone **31** is an example where this is observed (**Figure 1.29**).

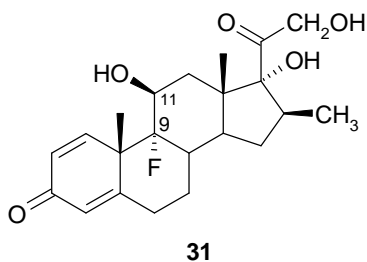


**Figure 1.29** Betamethasone **31**, where the C-9 fluorine increases C-11 OH acidity, improving drug binding.

## 1.11 The fluorine *gauche* effect

### 1.11.1 The 1,2-dihaloethanes

Alkanes, e.g. butane and haloalkanes such as 1,2-dibromoethane **34** in general have lower energy *anti* conformations, with a torsion angle X-C-C-X of  $\sim 180^\circ$ . *Gauche* conformations (X-C-C-X =  $\sim 60^\circ$ ) have a higher energy and are thus less populated. There are however a number of compounds particularly containing fluorine, that exhibit a preference for a *gauche* conformation, and this observation has been coined the “*gauche effect*”<sup>68</sup> by Wolfe. He described this as:

*‘a tendency to adopt that structure which has the maximum number of gauche interactions between the adjacent electron pairs and / or polar bonds’.*

The most common example of the *gauche* effect in fluorinated compounds is that of 1,2-difluoroethane **32** which is often compared to other di-haloethanes such as 1,2-

diiodoethane **35**. More recently the crystal structures of **32** and **35** have been solved and their conformations discussed.<sup>69</sup> Here two different phases of crystalline 1,2-difluoroethane **32** were obtained from cooling the liquid to near its melting point (169K) to 158K. X-ray diffraction of the two crystal phases showed similar *gauche* conformations with torsion angles near to  $68^\circ$ . 1,2-Diiodoethane **35** was also crystallised and an exact *anti* conformation, with a torsion angle of  $180^\circ$  was apparent.

Previously *ab initio* calculations and various techniques such as IR, Raman, microwave and electron diffraction have been used to show this *gauche* preference. The *anti* conformer has been measured to 0.5 – 1.00 kcal/mol higher in energy than the *gauche* conformer in the gas phase.<sup>70</sup>

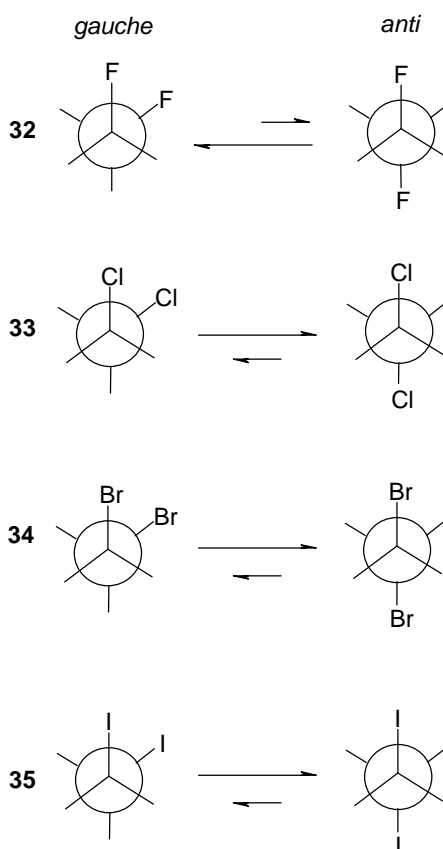


**Figure 1.30** Conformational preferences for 1,2-dihaloethanes.

	% <i>Gauche</i>	% <i>Anti</i>	Energy difference (kcal/mol in the gas phase)
1,2-C <sub>2</sub> H <sub>4</sub> F <sub>2</sub>	96	4.0	0.81
1,2-C <sub>2</sub> H <sub>4</sub> ClF	58	42	
1,2-C <sub>2</sub> H <sub>4</sub> Cl <sub>2</sub>	27	73	1.05
1,2-C <sub>2</sub> H <sub>4</sub> Br <sub>2</sub>	11	89	
1,2-C <sub>2</sub> H <sub>4</sub> I <sub>2</sub>	12	88	2.0

**Table 1.13** Conformational composition and energy differences for 1,2-dihaloethanes as measured by electron diffraction<sup>69</sup> and IR.<sup>71</sup>

### 1.11.2 The origin of the fluorine *cis* and *gauche* effects

Currently there are two reasonable rationalisations for the *gauche* effect in 1,2-difluoroethane **32**. These are the ‘bent bond theory’ of Wiberg<sup>72</sup> and that of hyperconjugative stabilisation as proposed by P. Rablen.<sup>73</sup>

Wiberg examined electron density in the  $\sigma$  bonds of the isomers of 1,2-difluoroethene where it is known that the *cis* isomer is more stable than the *trans* form. It was found by calculation on the *cis* isomer that the electron density in the C-F bond is localised around the fluorine atom, it is a highly polarised bond. However in the C-H bond the electron density is at the centre of the bond. This asymmetry impacts on the degree of overlap in the C-C bond. For the *cis* isomer there is good orbital overlap in a C-C bent bond. Whereas for the *trans* isomer there is poor electron density overlap in the C-C bonding orbital as the trajectory of electron density from each carbon atom is pulled in opposite directions. This leads to destabilisation of the *trans* isomer relative to the *cis*. This observation is known as the ‘*Cis Effect*’.

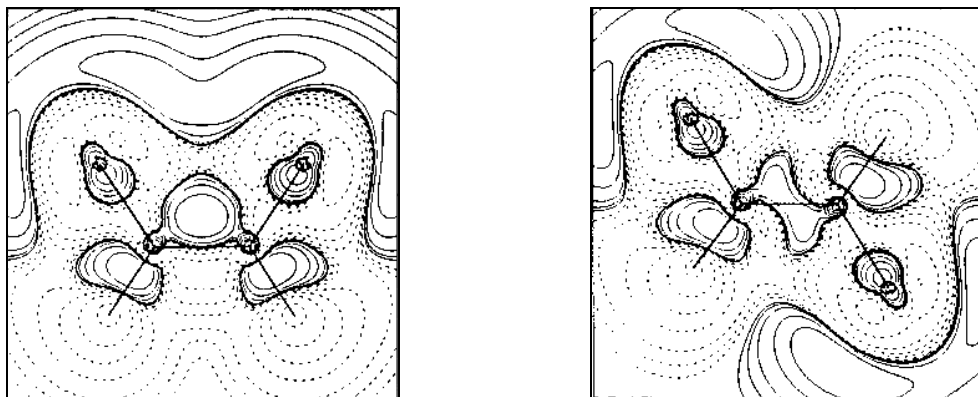


**Figure 1.32** Electron density maps of *cis* (left) and *trans* (right) 1,2-difluoroethene

The preference for a *gauche* vs an *anti* conformation in the case of 1,2-difluoroethane **32** can be also rationalised using this observation. In the *gauche* conformation the electron density arrangement provides good C-C bond overlap, whereas in the *anti* conformer overlap is poorer.

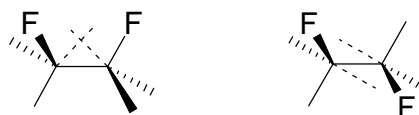


**Figure 1.33** Direction of bond orientation for *gauche* (left) and *anti* (right) conformations of 1,2-difluoroethane **32**.

An alternative and currently prevailing explanation for the *gauche* effect is hyperconjugation.<sup>73</sup> This involves a stabilising interaction between an occupied orbital and a vicinal antibonding / unoccupied orbital. In the *gauche* conformer of 1,2-difluoroethane **32** a C-H bond (HOMO) is stereoelectronically positioned such that it can donate electron density into the  $\sigma^*$  orbital (LUMO) as illustrated in **Figure 1.34**. This occurs twice in 1,2-difluoroethane and again favours a *gauche* conformation.

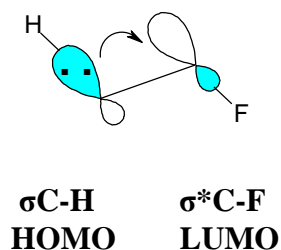


**Figure 1.34** Electron donation from the filled C-H orbital (HOMO) into the un-filled C-F  $\sigma^*$  anti-bonding orbital (LUMO) in 1,2-difluoroethane **32**.

It follows that the *anti* conformer is destabilising because the C-F bonds are antiparallel to each other and the C-F  $\sigma$  bonds cannot behave as electron donors. There are no hyperconjugative stabilising interactions.

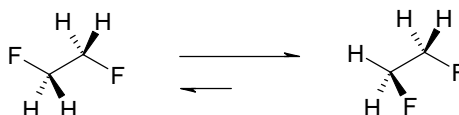
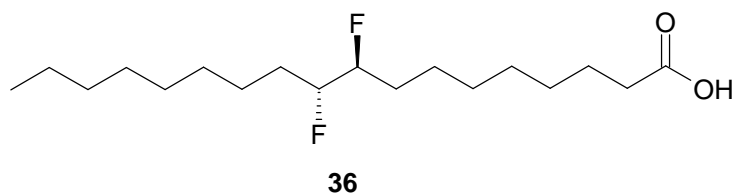


**Figure 1.35** The *gauche* conformation is preferred over the *anti* in 1,2-difluoroethane.

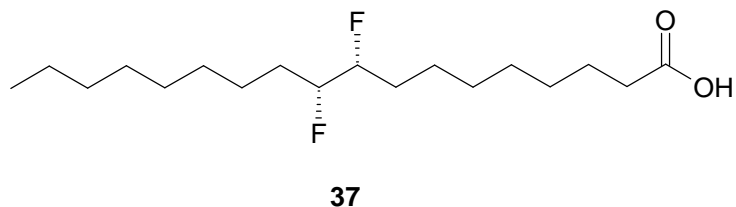
### 1.11.3 The fluorine *gauche* effect in 9,10-difluorostearic acid

The *gauche* effect has been observed in systems other than 1,2-difluoroethane and 2,3-difluorobutane which are usually given as illustrative examples of the effect. *Erythro* **36** and *threo* **37** 9,10-difluorostearic acids have very different physical properties. The *threo* isomer has a melting point of 86-88 °C whereas the *erythro* isomer has a much lower melting point at 67-69 °C.<sup>74</sup> Langmuir isotherm analysis was undertaken to examine more

closely the conformational flexibility of the diastereoisomers. The results indicated that the *erythro* stearic acid has considerable conformational disorder whereas the *threo* isomer was comparable to normal stearic acid. In an extended anti-zig-zag conformation, the *threo* isomer **37** has two vicinal fluorines *gauche* to one another, enabling the fluorine *gauche* effect to stabilise the system. In the *erythro* stearic acid **36** the *gauche* **36b** conformation is in competition with the anti-zig-zag extended conformation, providing a disordered system. This observation that the *gauche* effect can stabilise hydrocarbon chains may have an impact in the design of specialist materials within the liquid crystal industry.



(±)-*erythro*-9,10-difluorostearic acid, mp = 67-69 °C



(±)-*threo*-9,10-difluorostearic acid, mp = 86-88 °C

**Figure 1.36** *Erythro* and *threo* isomers of 9,10-difluorostearic acid. <sup>74</sup>

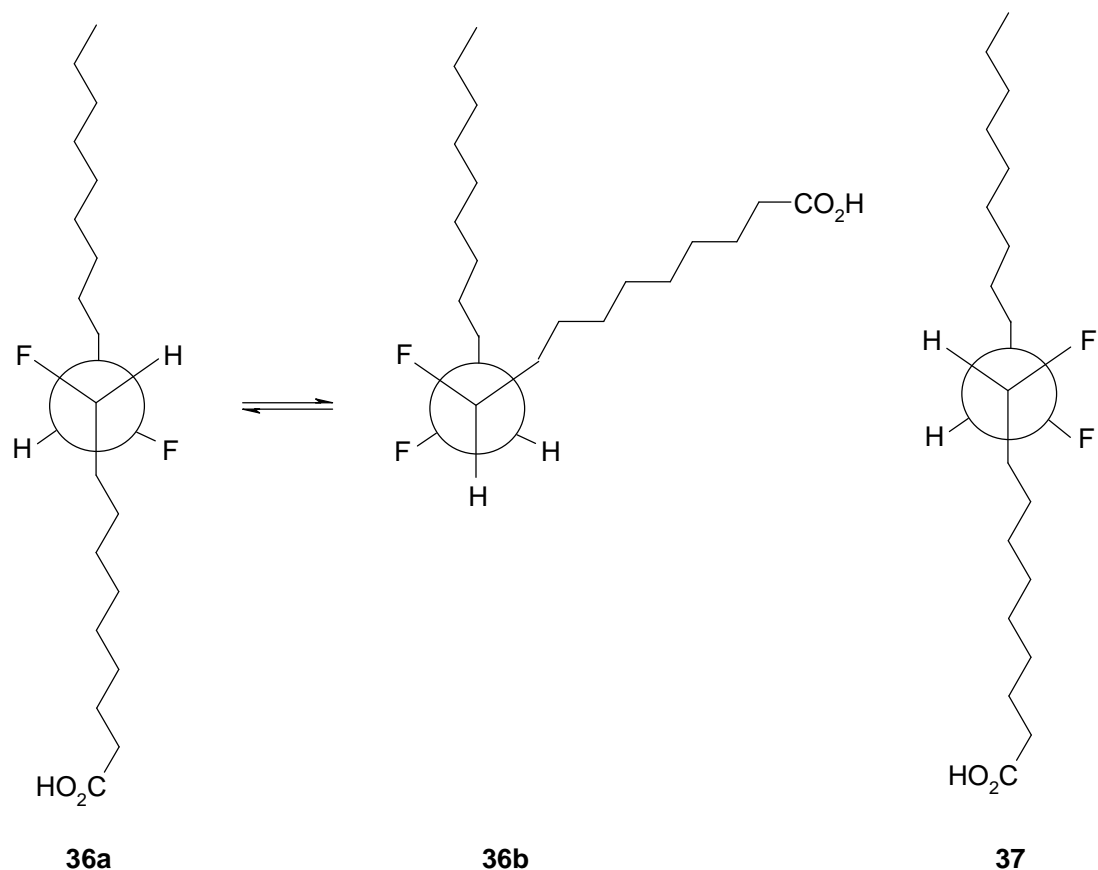
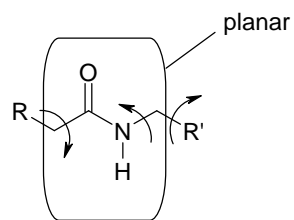


**Figure 1.37** The *erythro* isomer of **36** exhibits disorder owing to competing *anti* and *gauche* conformations.

#### 1.11.4 Fluorine in amides

Amides are an important functional group in pharmaceuticals as well as playing their significant role in peptides and proteins. The amide bond is planar but has rotational freedom around the XC-CO and N-C bonds as shown in **Figure 1.38**, presenting different R and R' orientations.

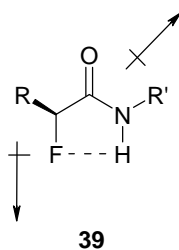




38

**Figure 1.38** The amide bond is planar over six atoms, C-CO-NH-C.

The effect of fluorine on the conformation of  $\alpha$ -fluoroamides **39** has been studied. X-ray crystallography has revealed that F-C-C=O prefers an antiparallel *trans* arrangement, as shown below where the F-C bond is *cis* to the N-H bond and *anti* to the C=O bond (**Figure 1.39**). For fluoroacetamide the energy difference between the *cis* and the *trans* conformers has been calculated to be  $\sim 7$  kcal mol<sup>-1</sup> (**Figure 1.40**).<sup>75</sup> A number of factors contribute to this including dipole relaxation and fluorine-hydrogen bonding.



39

**Figure 1.39** An antiparallel F-C, C=O conformation is observed with  $\alpha$ -fluoroamides.

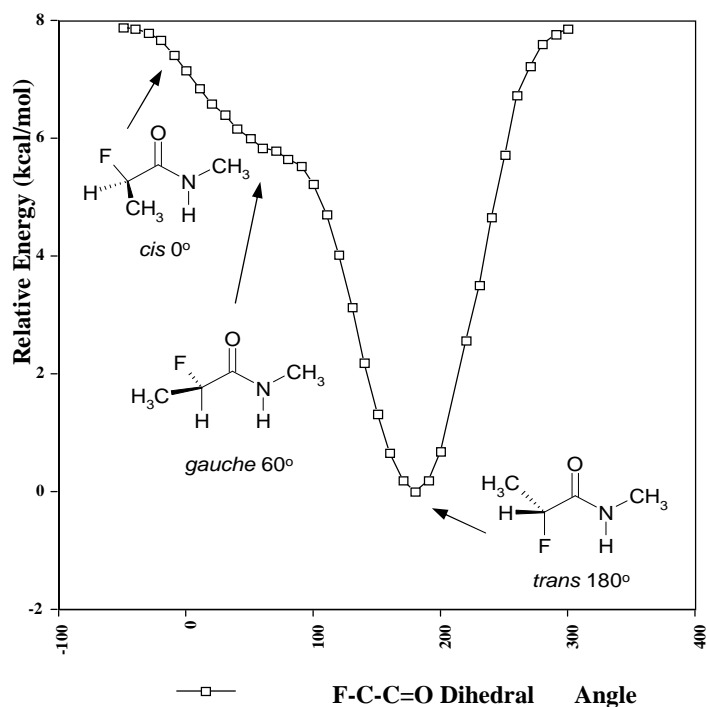


**Figure 1.40** A rotational energy profile of *N*-methyl-2-fluoropropionamide showing the most stable *trans* conformer.<sup>75</sup>

$\beta$ -Fluoroamides have also been explored and it has been found both by X-ray diffraction analysis and theoretical evaluation that such moieties adopt a *gauche* conformation.<sup>76</sup> Density Functional Theory (DFT) calculations on **40** indicate a  $1.8 \text{ kcal mol}^{-1}$  preference for the C-F, C-N *gauche* vs *anti* conformation.

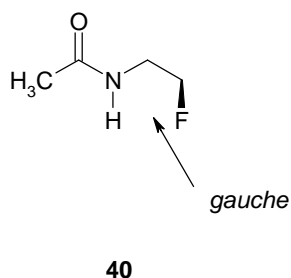


**Figure 1.41** The *N*- $\beta$ -fluoroethylamide motif prefers a *gauche* conformation.

The combination of these two effects, the  $\alpha$ -fluoro *cis* effect and  $\beta$ -fluoro *gauche* effect in amides has been used to influence in a predictive manner the conformation of amide **41**.<sup>77</sup> This was prepared as a liquid, and was subjected to slow cooling to 270K in a glass capillary to obtain a crystal for X-ray analysis. In the resultant structure a torsion angle of  $62.9^\circ$  was measured for N-C-C-F of the  $\beta$ -fluoroamide moiety. With the second fluorine the C-F bond of the  $\alpha$ -fluoroamide moiety was observed to align *cis* to the N-H bond and antiparallel to C=O. These preferences could clearly be utilised in drug design where a particular amide conformation is required and / or restricted rotation within a molecule is desired.

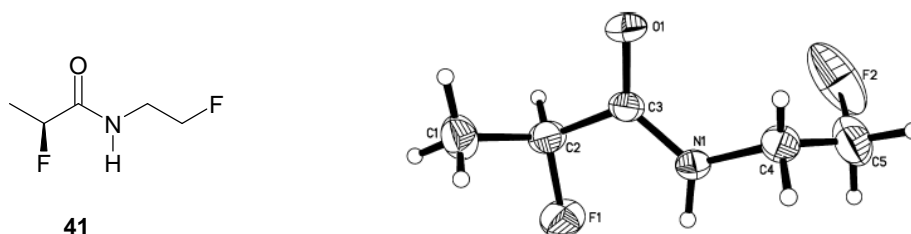


**Figure 1.42** The solid state conformation of **41** shows a planar  $\alpha$ -fluoroamide and a *gauche*  $\beta$ -fluoroamide moiety.

### 1.11.5 Fluorinated collagens

Collagen **42** is a protein, consisting of chains of amino-acids with an X-Y-Gly (glycine) sequence. X and Y are usually proline (Pro) and 4-(*R*)-hydroxyproline (Hyp) respectively. These chains are wound in tight triple helices, providing fibrils of great tensile strength and thermal stability.

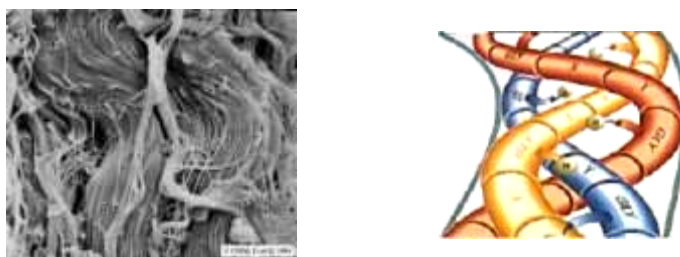
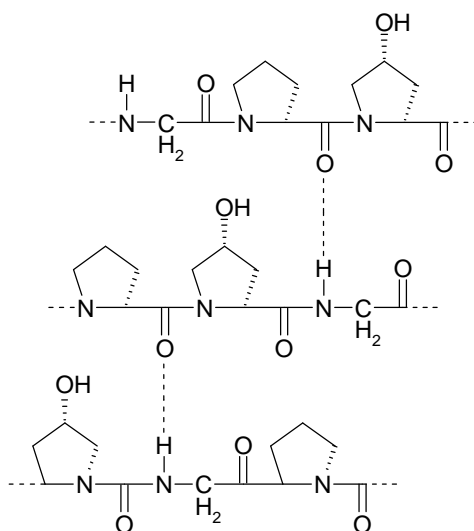


**Figure 1.43** Electron microscope image of collagen fibres and the triple helix consisting of Pro, Hyp and Gly residues.

The collagen triple helix **42** is held together predominantly by  $\text{NH}\cdots\text{O}=\text{C}$  backbone hydrogen bonding. Previously it was thought that additional hydrogen bonding occurred from the unusual 4-hydroxyproline residues, to further stabilise this structure and generate fibres. It was indeed found by X-ray diffraction analysis that bridging water molecules connected Hyp residues on one chain to a carbonyl on an adjacent chain.<sup>78</sup>

However in 1998 Raines reported that the likelihood of bridging water molecules contributing to collagen stability was doubtful owing to the amount of water required, also collagen is quite stable in anhydrous environments. Collagen analogues without hydroxyl groups were prepared by Raines, replacing OH for fluorine. In this case the electron withdrawing C-O bond is substituted for the electronegative fluorine. Fluorine is also of a similar size to oxygen, but does not form hydrogen bonds and so made a reasonable mimic for the hydroxyl replacement.<sup>79, 80</sup>



42

**Figure 1.44** Collagen is stabilised by intermolecular N-H $\cdots$ O=C hydrogen bonding.

Specifically 4-(*R*)-fluoroproline residue (Flp) was used to incorporate fluorine into collagen oligomers and the thermal stabilities of triple helices determined. It emerged that fluorinated collagen triple helices are more stable than the natural collagen at elevated temperatures. The difference in energy between the two was calculated, finding the Hyp collagen less stable by  $\sim 6 \text{ kcal mol}^{-1}$ . The stability increased with no obvious ability to hydrogen bond, indicating that OH hydrogen bonding is not the reason for collagen's strength. They concluded that stereoelectronic inductive effects (*gauche* effect) from the polar C-F / C-O bond contribute to the stability of the triple helix. In the case of the fluorinated analogue the fluorine *gauche* effect can explain the increased stabilisation. The C-F bond aligns *gauche* to the electron-withdrawing C-N amide bond, providing a pyrrolidine ring conformation which stabilises the helix. The inductive effect to fluorine also stabilises the *trans* amide rotamer over the *cis* (**Figure 1.45**).

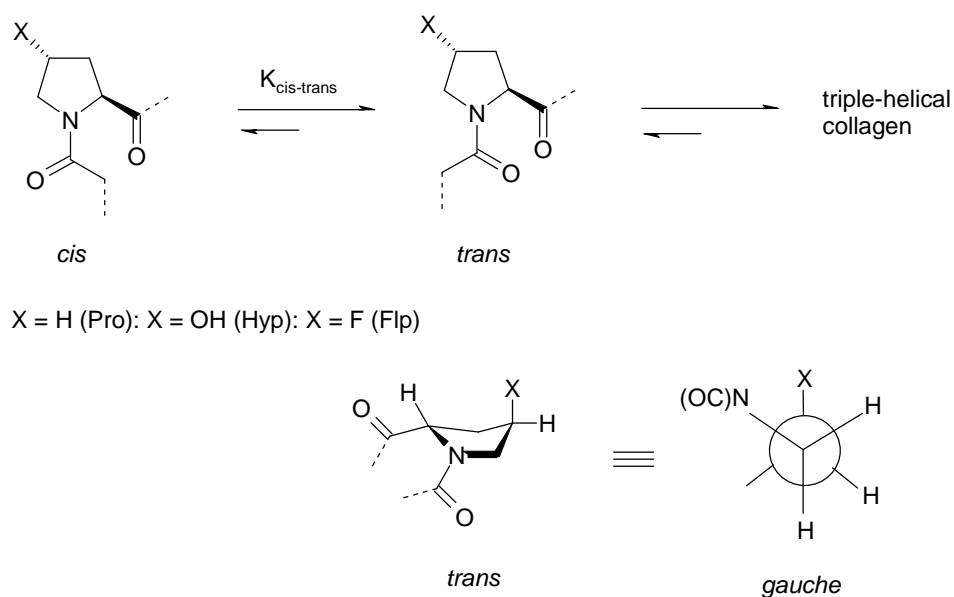


**Figure 1.45** Collagen is stabilised by N-H $\cdots$ O=C bonding and in addition by the *gauche* effect between electronegative OH and the electron withdrawing amide group.

### 1.11.6 Fluorine in esters

2-Fluoroethyl acetate **43** is an example of an *O*- $\beta$ -fluoroethyl ester. The conformation of this molecule has been studied by theoretical calculations. It was found that the lowest energy conformation again has the C-F C=O bonds *gauche* to each other, with a small but measurable energy difference of  $\sim 0.5 \text{ kcal mol}^{-1}$  between the *gauche* and the *anti* compounds. This extends from the  $\beta$ -fluoroamides highlighted above and is another example where an electronegative group (ester-oxygen) becomes involved in a ‘fluorine *gauche* effect’.<sup>81</sup>

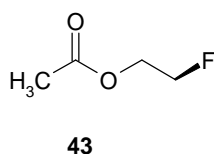


**Figure 1.46** 2-Fluoroethyl acetate **43** has a preference for the *gauche* conformation.

A number of  $\beta$ -fluoroethyl esters **44-46** have been prepared at St Andrews and subjected to X-ray crystallography analysis. The O-C-C-F torsion angles from the crystal structures are shown in **Figure 1.47** and all have values in the 66-70° range.<sup>81</sup>

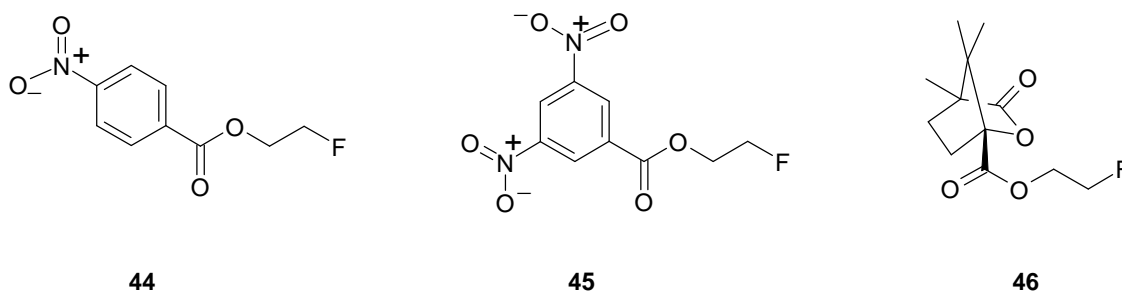


**Figure 1.47** X-ray analysis indicates a *gauche* relationship between C-F and C-O bonds.<sup>81</sup> Torsion angles (F-C-C-O): **44** = 66.7°, **45** = 69.7° / 67.0°, **46** = 69.6°.

### 1.11.7 $\beta$ -Fluoroamines

In each of the cases described above, the substituent vicinal to fluorine has a lone pair conjugated into a carbonyl (e.g. F-C-C-NC=OR, F-C-CO-C=OR). It's interesting to consider the *gauche* effect in fluoroethylamine **47**, **48**, **49** and fluoroethanol **58**, **59**, **60**. 2-Fluoroethylamine has been subjected to Density Functional Theory (DFT) calculations to determine its conformational preference.<sup>82</sup> The energy differences between the *gauche* and *anti* conformers has been explored by varying the trajectory of the nitrogen lone pair. It was found that when the nitrogen lone pair is orientated towards the fluorine **47** there is no apparent *gauche* effect with the *gauche* conformer being higher in energy than the *anti* by +0.9 kcal mol<sup>-1</sup>. The electrostatic repulsion between electronegative fluorine and the nitrogen lone pair appears to counteract any inherent stereoelectronic *gauche* stabilisation. When the nitrogen lone pair is not pointed at the fluorine **48**, **49** the amine hydrogen is now

in a position suitable for intramolecular C-F $\cdots$ H-N bonding. Both of these structures are favoured (-0.9 and -1.0 kcal mol<sup>-1</sup>) over the *anti* conformers, indicating stabilisation but owing to intramolecular H $\cdots$ F bonding.

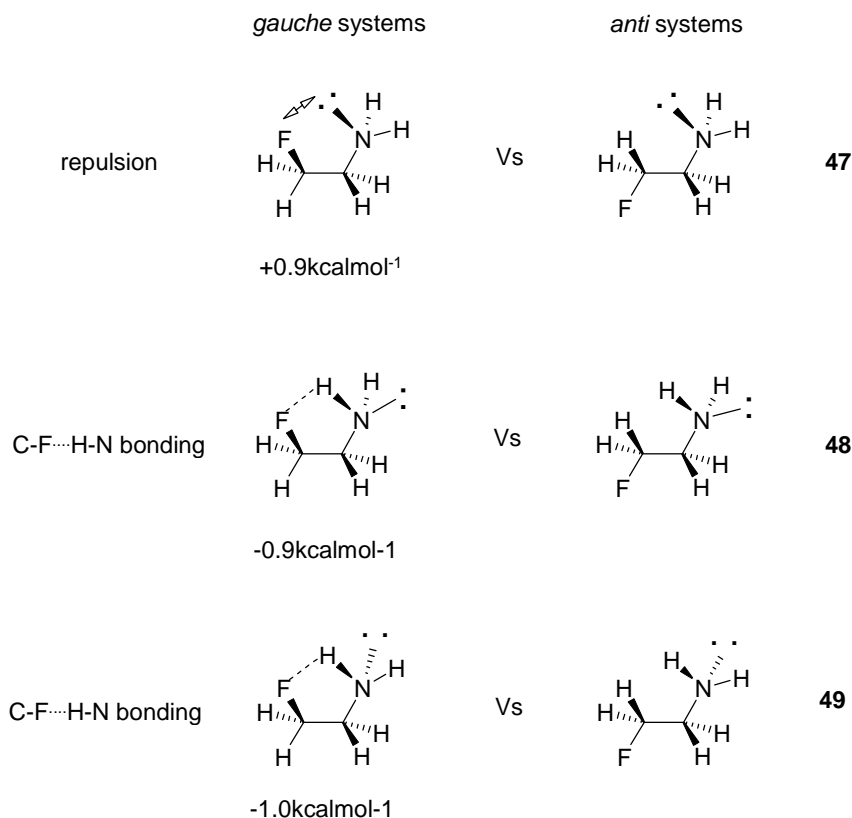


**Figure 1.48** Conformations of 2-fluoroethylamine.

In 2-fluoroethylamine **50**, not only is there the possibility of intramolecular F $\cdots$ H bonding but the C-N bond is much more polarised owing to the positive charge on the nitrogen. This leads to a favourable F $\delta^-$  $\cdots$ N $^+$ H electrostatic interaction. DFT analysis indicated that the *gauche* conformer is more stable than the *anti* by a relatively large 5.8 kcal mol<sup>-1</sup> (**Figure 1.49**).<sup>82</sup>



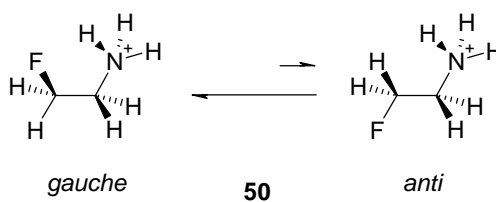


**Figure 1.49** The *gauche* conformer of the 2-fluoroethyl ammonium cation is favoured (5.8 kcal mol<sup>-1</sup>).<sup>82</sup>

X-ray crystallographic studies on the hydrochloride salt of 2-fluoroamine support a *gauche* conformation with the F-C-C-N<sup>+</sup> torsion angle measured at 67.8°. It is of interest to note that the angle was estimated by calculation to be 52.7°, smaller than that actually observed in the structural study. This could be due to weakened (N)H<sup>+</sup>⋯F bonding in the solid state because of the dominating intermolecular interactions between this group and the Cl<sup>-</sup> counter ion. The shortest NH<sup>+</sup>⋯F intramolecular distance was measured at 2.5 Å, indicating that the structure may be further stabilised by a weak hydrogen bond.

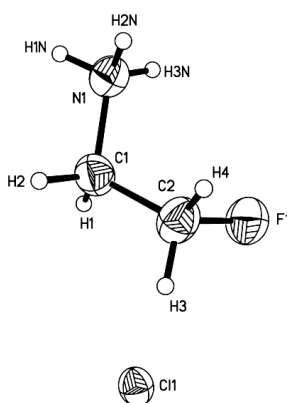


**Figure 1.50** X-ray crystal structure of 2-fluoroethyl ammonium hydrochloride.<sup>82</sup>

Numerous other protonated amines have also been studied both theoretically, by NMR and by X-ray crystallography exploring their conformational preference. Lankin and Snyder have investigated the conformational preferences within protonated 3-fluoropiperidinium

systems.<sup>83-85</sup> In 1993 they proposed a charge-dipole interaction between the charged nitrogen (position 1) and the polarised fluorine (position 3)  $(\text{NH}_2)^+ \cdots \text{F}^{\delta-} - \text{C}^{\delta+}$ . This favoured an axial fluorine **51** with a *gauche* C-F, C-N<sup>+</sup> conformation, despite the 1,3-diaxial interaction with hydrogen which would normally favour an equatorial conformer. This axial preference was observed by <sup>1</sup>H NMR with 3-fluoropiperidine hydrochloride in D<sub>2</sub>O. When dissolved in NaOD / D<sub>2</sub>O the salt was neutralised to give the free base and then the equatorial fluorine **52** was favoured.

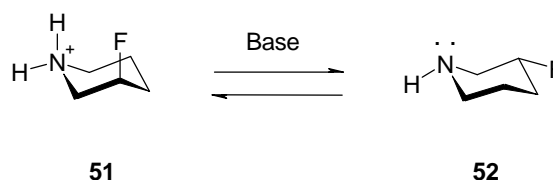


**Figure 1.51** 3-Fluoropiperidine hydrochloride favours an axial fluorine conformer.<sup>83-85</sup>

Lankin and Snyder have investigated the conformations of 3,5-difluoropiperidine hydrochloride, methylated 3-fluoropiperidine salts and 4,4-diphenyl analogues. Their findings will be discussed in **Chapter 2**.

Here at St Andrews various  $\beta$ -fluoro-ammonium systems **53-57** have been synthesised in order to study the X-ray structures and to examine the torsion angles between the charged nitrogen and the fluorine atom. The resultant structures and torsion angles are given in **Figure 1.52**. In every case a *gauche* conformation is observed, supporting an electrostatic interaction. The C-N<sup>+</sup>, C-F torsion angles are, however, larger than that of an 'ideal' *gauche* structure ( $60^\circ$ ), possibly due to (N)H $\cdots$ Cl intermolecular interactions between the amine and the counter ion.

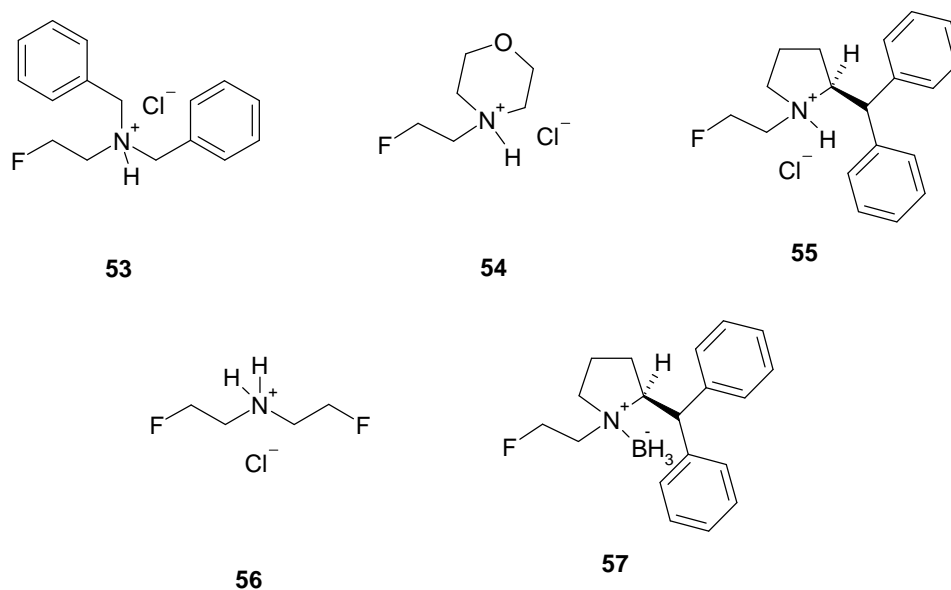


**Figure 1.52** X-ray crystallography analysis has been carried out on these  $\text{NH}^+$  amines. Torsion angles ( $\text{F-C-C-N}^+$ ): **53** =  $81.9^\circ$ , **54** =  $78.8^\circ$ , **55** =  $74.1^\circ$ , **56** =  $74.2^\circ / 75.9^\circ$ , **57** =  $67.1^\circ$ .

### 1.11.8 Fluoroethanol

The halogenated alcohols, 2-chloroethanol, 2-bromoethanol and 2-fluoroethanol **58** are also known to prefer a *gauche* over an *anti* conformation owing to an internal hydrogen bond.<sup>86</sup> 2-Fluoroethanol **58** has also been studied by Dixon and Smart.<sup>62</sup> They found no significant stereoelectronic ‘fluorine *gauche* effect’ but the observed *gauche* preference was due to intramolecular hydrogen bonding. The energy difference between the *gauche* and *anti* systems **59**, **60** with no hydrogen bonding was found to be negligible at  $0.1 \text{ kcal mol}^{-1}$ . It appears that hydrogen bonding with a short hydrogen bond of  $2.25 \text{ \AA}$  alone can account for  $1.9 \text{ kcal mol}^{-1}$  of the difference, rather than a stereoelectronic *gauche* effect.<sup>62</sup>

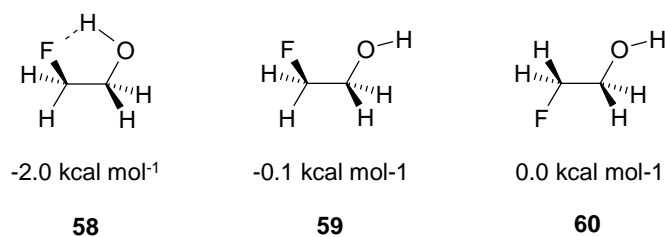


**Figure 1.53** 2-Fluoroethanol and its conformations.

More recently 2-fluoroethanol has been re-evaluated using Density Functional Theory (DFT) calculations, carried out at St Andrews with co-workers at The University of Durham. They found comparable results, favouring the *gauche* conformer **58** with intramolecular hydrogen bonding<sup>82</sup> and without an inherent *gauche* preference.

However the protonated form of 2-fluoroethanol **61**, **62**, **63** was also considered and DFT calculations performed on various conformations (**Figure 1.54**) and a large *gauche* effect was found.<sup>82</sup> The difference in energies are -4.4, -7.0, -7.2 kcalmol<sup>-1</sup> respectively and these observations show that the *gauche* structure is significantly favoured over the *anti* when the lone pair on oxygen is orientated towards fluorine **61**. Here the lone pair appears not to repel the fluorine. The favourable energy difference of 4.4 kcal mol<sup>-1</sup> is apparently provided by an electrostatic interaction as no F<sup>⋯</sup>H hydrogen interaction exists. Two other conformers **62**, **63** were investigated with bridging hydrogen bonding (7.0 and 7.2 kcal mol<sup>-1</sup>), further stabilising the *gauche* conformations.

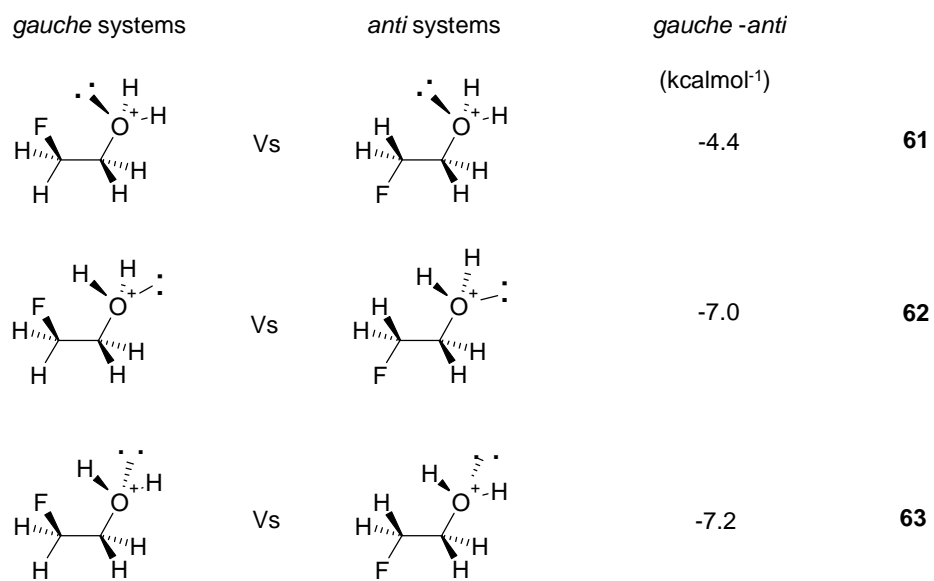


**Figure 1.54** Conformations and relative energies of protonated 2-fluoroethanol studied by DFT. <sup>82</sup>

## 1.12 References for chapter one

1. N. N. Greenwood and A. Earnshaw, *Chemistry of the Elements*, Pergamon Press, Oxford, 1984.
2. C.-G. Zhan and D. A. Dixon, *J. Phys. Chem.*, 2004, **108**, 2020-2029.
3. W. R. Dolbier, Jr., *J. Fluorine Chem.*, 2005, **126**, 157-163.
4. R. D. Chambers, *Fluorine in Organic Chemistry*, Blackwell Publishing, Oxford, 2004.
5. D. B. Harper and D. O'Hagan, *Nat. Prod. Rep.*, 1994, **11**, 123-133.
6. R. A. Peters and M. Shorthouse, *Nature*, 1967, **216**, 80-81.
7. R. A. Peters, *Fluoride*, 1973, **6**, 189-190.
8. R. A. Peters and P. J. Hall, *Biochemical Pharmacology*, 1959, **2**, 25-36.
9. S. O. Thomas, V. L. Singleton, J. A. Lowery, R. W. Sharpe, L. M. Pruess, J. N. Porter, J. H. Mowat and N. Bohonos, *Antibiotics Ann.*, 1957, 716-721.
10. G. O. Morton, J. E. Lancaster, G. E. Van Lear, W. Fulmor and W. E. Meyer, *J. Am. Chem. Soc.*, 1969, **91**, 1535-1537.
11. A. R. Maguire, W. D. Meng, S. M. Roberts and A. J. Willetts, *J. Chem. Soc., Perkin Trans. 1*, 1993, 1795-1808.
12. M. Sanada, T. Miyano, S. Iwadare, J. M. Williamson, B. H. Arison, J. L. Smith, A. W. Douglas, J. M. Liesch and E. Inamine, *J. Antibiot.*, 1986, **39**, 259-265.
13. D. O'Hagan, C. Schaffrath, S. L. Cobb, J. T. G. Hamilton and C. D. Murphy, *Nature*, 2002, **416**, 279.
14. C. Schaffrath, H. Deng and D. O'Hagan, *FEBS Lett.*, 2003, **547**, 111-114.
15. C. Dong, F. Huang, H. Deng, C. Schaffrath, J. B. Spencer, D. O'Hagan and J. H. Naismith, *Nature*, 2004, **427**, 561-565.
16. H. Deng, D. O'Hagan and C. Schaffrath, *Nat. Prod. Rep.*, 2004, **21**, 773-784.

17. S. J. Moss, C. D. Murphy, D. O'Hagan, C. Schaffrath, J. T. G. Hamilton, W. C. McRoberts and D. B. Harper, *Chem. Commun.*, 2000, 2281-2282.
18. S. L. Cobb, H. Deng, J. T. G. Hamilton, R. P. McGlinchey and D. O'Hagan, *Chem. Commun.*, 2004, 592-593.
19. C. D. Murphy, S. J. Moss and D. O'Hagan, *Appl. Environ. Microbiol.*, 2001, **67**, 4919-4921.
20. C. D. Murphy, D. O'Hagan and C. Schaffrath, *Angew. Chem., Int. Ed.*, 2001, **40**, 4479-4481.
21. H. Deng, S. L. Cobb, A. D. Gee, A. Lockhart, L. Martarello, R. P. McGlinchey, D. O'Hagan and M. Onega, *Chem. Commun.*, 2006, 652-654.
22. J. Gotze, *Anal. Bioanal. Chem.*, 2002, **374**, 703-708.
23. *Dictionary of Chemistry*, Oxford University Press, 1996.
24. U. Kempe, M. Ploetze, A. Brachmann and R. Boettcher, *Mineral. Petrol.*, 2002, **76**, 213-234.
25. F. A. Balogun, J. O. Ojo, F. O. Ogundare, M. K. Fasasi and L. A. Hussein, *Radiat. Meas.*, 1999, **30**, 759-763.
26. R. E. Banks, *J. Fluorine Chem.*, 1986, **33**, 3-26.
27. Air Product's West I and II Fluorine Plants Process and Equipment Overview, Identification no. 5019-F2-1200, 2006.
28. K. O. Christe, *Inorg. Chem.*, 1986, **25**, 3721-3722.
29. C. Isanbor and D. O'Hagan, *J. Fluorine Chem.*, 2006, **127**, 303-319.
30. P. Kirsch, *Modern Fluoroorganic Chemistry*, WILEY-VCH, 2004.
31. D. W. Galloway, anaesthetist, Edinburgh, personal communication, 2007.
32. F. J. M. Walters, *Update in Anaesthesia*, **9**, 1998.
33. P. Jeschke, *ChemBioChem*, 2004, **5**, 570-589.
34. G. Sandford, *Phil. Trans. R. Soc. Lond. A*, 2000, **358**, 455-471.

35. Gordon Moir, St Andrews Links greenkeeper, personal communication, 2007.
36. G. Sandford, *Phil. Trans. R. Soc. Lond. A*, 2000, **358**, 455-471.
37. V. Smil, *Nature*, 2000, **408**, 910.
38. D. Brewis and R. Dahm, *Adhesion to Fluoropolymers*, Rapra Technology Ltd, 2006.
39. D. Browne, H. Whelton and D. O'Mullane, *J. Dent.*, 2005, **33**, 177-186.
40. P. T. C. Harrison, *J. Fluorine Chem.*, 2005, **126**, 1448-1456.
41. Scottish Executive, Health consultations document, *Towards Better Oral Health in Children, A Consultation Document on Children's Oral Health in Scotland*, 2002.
42. David Horrocks, Scottish Water, Public Health Team, personal communication, 2007.
43. Scottish Parliament, Official Reports, meeting minutes, Public Water Supplies (Fluoridation), Col 12045, Thursday 18 November 2004.
44. L. S. Kaminsky, M. C. Mahoney, J. Leach, J. Melius and M. J. Miller, *Crit. Rev. Oral Biol. Med.*, 1990, **1**, 261-281.
45. S. Hillier, C. Cooper, S. Kellingray, G. Russell, H. Hughes and D. Coggon, *Lancet*, 2000, **355**, 265-269.
46. M. S. McDonagh, P. F. Whiting, P. M. Wilson, A. J. Sutton, I. Chestnutt, J. Cooper, K. Misso, M. Bradley, E. Treasure and J. Kleijnen, *BMJ*, 2000, **321**, 855-859.
47. J. D. Lee, *Concise Inorganic Chemistry*, Blackwell Science, Oxford, 1998.
48. D. Seed, British Nuclear Fuels, personal communication, 2007.
49. S. S. Sazhin and A. P. Jeapes, *J. Nucl. Mater.*, 1999, **275**, 231-245.
50. S. W. Whitehead, Springfields, personal communication, 2007.
51. L. Pauling, *J. Am. Chem. Soc.*, 1932, **54**, 3570-3582.
52. A. Bondi, *J. Phys. Chem.*, 1964, **68**, 441-451.



53. D. O'Hagan and H. S. Rzepa, *Chem. Commun.*, 1997, 645-652.
54. B. E. Smart, *J. Fluorine Chem.*, 2001, **109**, 3-11
55. D. Seebach, *Angew. Chem., Int. Ed.*, 1990, **29**, 1320.
56. K. Uneyama, *Organofluorine Chemistry*, Blackwell Publishing Ltd, 2006.
57. D. R. Lide, *CRC Handbook of Chemistry and Physics*, 84<sup>th</sup> edition, CRC Press, London, 2003.
58. J. G. Stark and H. G. Wallace, *Chemistry Data Book*, 2nd Edition in SI, John Murray, London, 1997.
59. S. A. Sherrod, R. L. Da Costa, R. A. Barnes and V. Boekelheide, *J. Am. Chem. Soc.*, 1974, **96**, 1565-1577.
60. V. R. Thalladi, H.-C. Weiss, D. Blaeser, R. Boese, A. Nangia and G. R. Desiraju, *J. Am. Chem. Soc.*, 1998, **120**, 8702-8710.
61. F. Lahmani, A. Zehnacker, G. Denisov and G. G. Furin, *J. Phys. Chem.*, 1996, **100**, 8633-8639.
62. D. A. Dixon and B. E. Smart, *J. Phys. Chem.*, 1991, **95**, 1609-1612.
63. J. D. Dunitz and R. Taylor, *Chem. Eur. J.*, 1997, **3**, 89-98.
64. V. J. Hoy, J. A. K. Howard, D. O'Hagan and G. T. Smith, *Tetrahedron*, 1996, **52**, 12613-12622.
65. H. I. Suss, J. Hulliger and K. Reichenbacher, *Chem. Soc. Rev.*, 2005, **34**, 22-30.
66. J. D. Dunitz, *ChemBioChem*, 2004, **5**, 614-621.
67. J. Bikowski, R. Pillai and B. Shroot, *J. Drugs Dermatol.*, 2006, **5**, 125-130.
68. S. Wolfe, *Acc. Chem. Res.*, 1972, **5**, 102-111.
69. F. Akkerman, J. Buschmann, D. Lentz, P. Luger and E. Roedel, *J. Chem. Crystallogr.*, 2003, **33**, 969-975.
70. J. R. Durig, J. Liu, T. S. Little and V. F. Kalasinsky, *J. Phys. Chem.*, 1992, **96**, 8224-8233.

71. K. Tanabe, *Spectrochim. Acta, Part A*, 1972, **28**, 407-424.
72. K. B. Wiberg, *Acc. Chem. Res.*, 1996, **29**, 229-234.
73. P. R. Rablen, R. W. Hoffmann, D. A. Hrovat and W. T. Borden, *J. Chem. Soc., Perkin Trans. 2*, 1999, 1719-1726.
74. M. Tavasli, D. O'Hagan, C. Pearson and M. C. Petty, *Chem. Commun.*, 2002, 1226-1227.
75. J. W. Banks, A. S. Batsanov, J. A. K. Howard, D. O'Hagan, H. S. Rzepa and S. Martin-Santamaria, *J. Chem. Soc., Perkin Trans. 2*, 1999, 2409-2411.
76. D. O'Hagan, C. Bilton, J. A. K. Howard, L. Knight and D. J. Tozer, *J. Chem. Soc., Perkin Trans. 2*, 2000, 605-607.
77. C. R. S. Briggs, D. O'Hagan, J. A. K. Howard and D. S. Yufit, *J. Fluorine Chem.*, 2003, **119**, 9-13.
78. J. Bella, M. Eaton, B. Brodsky and H. M. Berman, *Science*, 1994, **266**, 75-81.
79. S. K. Holmgren, K. M. Taylor, L. E. Bretscher and R. T. Raines, *Nature*, 1998, **392**, 666-667.
80. S. K. Holmgren, L. E. Bretscher, K. M. Taylor and R. T. Raines, *Chem. Biol.*, 1999, **6**, 63-70.
81. C. R. S. Briggs, D. O'Hagan, H. S. Rzepa and A. M. Z. Slawin, *J. Fluorine Chem.*, 2004, **125**, 19-25.
82. C. R. S. Briggs, J. Allen Mark, D. O'Hagan, D. J. Tozer, A. M. Z. Slawin, A. E. Goeta and J. A. K. Howard, *Org. Biomol. Chem.*, 2004, **2**, 732-740.
83. D. C. Lankin, N. S. Chandrakumar, S. N. Rao, D. P. Spangler and J. P. Snyder, *J. Am. Chem. Soc.*, 1993, **115**, 3356-3357.
84. J. P. Snyder, N. S. Chandrakumar, H. Sato and D. C. Lankin, *J. Am. Chem. Soc.*, 2000, **122**, 544-545.

85. A. Sun, D. C. Lankin, K. Hardcastle and J. P. Snyder, *Chem. Eur. J.*, 2005, **11**, 1579-1591.
86. E. Wyn-Jones and W. J. Orville-Thomas, *J. Mol. Struct.*, 1967, **1**, 79-89.
- .

## Chapter 2

# CHARGED C-N<sup>+</sup> ----- F-C DIPOLE INTERACTIONS

### 2.1 Introduction

When a C-F bond replaces a C-H bond it can significantly influence the conformation of organic molecules. This chapter has a particular focus on the influence of a fluorine atom positioned  $\beta$  to a charged nitrogen atom.

Lankin and Snyder<sup>1</sup> have observed the preferred conformations of a number of fluoropiperidinium ring systems. As discussed in **Chapter 1**, protonated 3-fluoropiperidine is found to prefer a conformation with the fluorine axial **51a**, rather than equatorial **51b**. In **51a**, the C-F bond is *gauche* to the C-N<sup>+</sup> bond, and the preference for this conformation can be explained in terms of a C-F  $\cdots$  C-N<sup>+</sup> charge-dipole interaction.

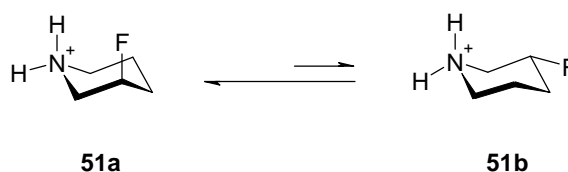


**Figure 2.1** 3-Fluoropiperidinium **51** prefers conformer **a** with the fluorine axial.

The preferred conformation of the di-fluoro piperidinium analogue **64** has also been studied by <sup>1</sup>H NMR.<sup>2</sup> The protonated hydrochloride exists predominantly in the di-axial conformation **64a**, in a ratio of ~ 98 : 2, in water at RT.

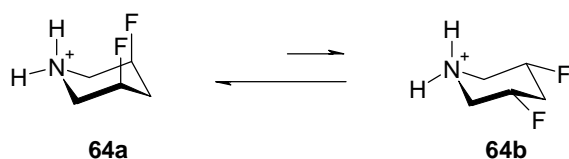


**Figure 2.2** Piperidinium **64** prefers conformation **64a**.

Lankin and Snyder then investigated<sup>3</sup> the effect of quarternary methyl substituents on the conformation of 3-fluoropiperidine salts. They carried out a computational analysis as well as X-ray crystallography and NMR studies on the di-methylated systems **65a** and **65b**. It was found that the fluorine adopts an axial preference, despite the increased steric influence of the methyl substituents. Again it appears that there is a favourable electrostatic interaction between the fluorine and the positively charged dimethylamine group.

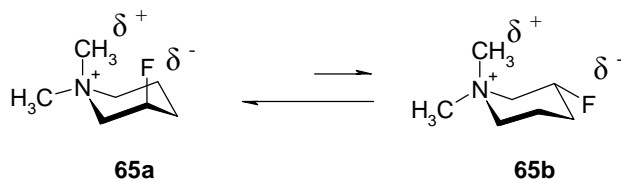


**Figure 2.3** The preferred conformer **65a** has the fluorine axial.

N-Dimethyl-4,4-diphenylpiperidinium **66** has been synthesised and the preferred conformation evaluated. Computational calculations suggest a higher population of the axial fluorine conformer **66a**. X-ray crystallography also showed a clear axial preference and NMR studies in water agree with this.<sup>3</sup>

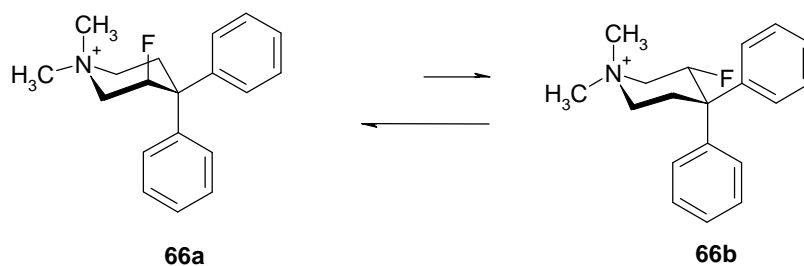


**Figure 2.4** The axial conformer **66a** was found to dominate.

Interestingly the neutral mono-methylated amine **67** shows an axial preference in the solid state as observed from X-ray diffraction studies, whereas computational and NMR studies suggest similar populations of the two conformers at equilibrium. Thus solid state packing effects must influence the ultimate solid state structure.

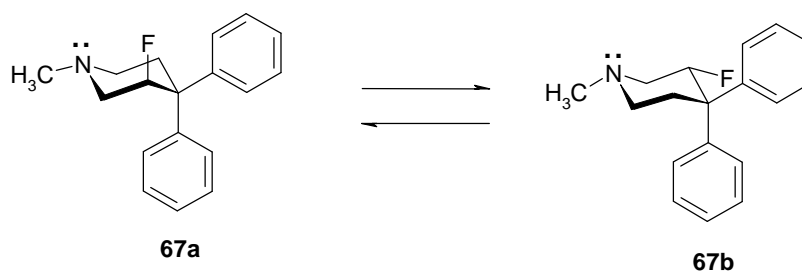
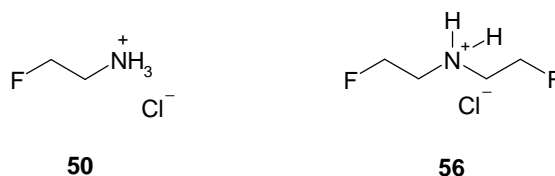


**Figure 2.5** Conformers **67a** and **67b** are similar in energy.

The subsequent research develops from recent work at St Andrews<sup>4</sup> where the *gauche* preference in the hydrochloride salt of 2-fluoroethylamine **50** was explored. That study also extended to various 2-fluoroethylammonium salts such as **56**. As summarised in **Chapter 1**, both DFT and X-ray diffraction studies confirmed that there is a strong *gauche* preference ( $\sim 5.8 \text{ kcal mol}^{-1}$ ) in the 2-fluoroethylammonium cation **50** and the origin is clearly similar to that rationalised by Lankin and Snyder for their piperidinium ring systems.



## 2.2 Medium sized rings

It was interesting to explore if such an effect could influence the conformation of medium sized rings. Medium sized rings have inherent strain due to transannular interactions. These rings are 'conformationally flexible', having no clear minimum energy conformation and thus a lot of conformational mobility.

The heats of combustion of different sized hydrocarbon rings relate directly to their inherent ring strain, thus the rings with high strain energy have high heats of combustion.

The trend is shown in **Figure 2.6**.

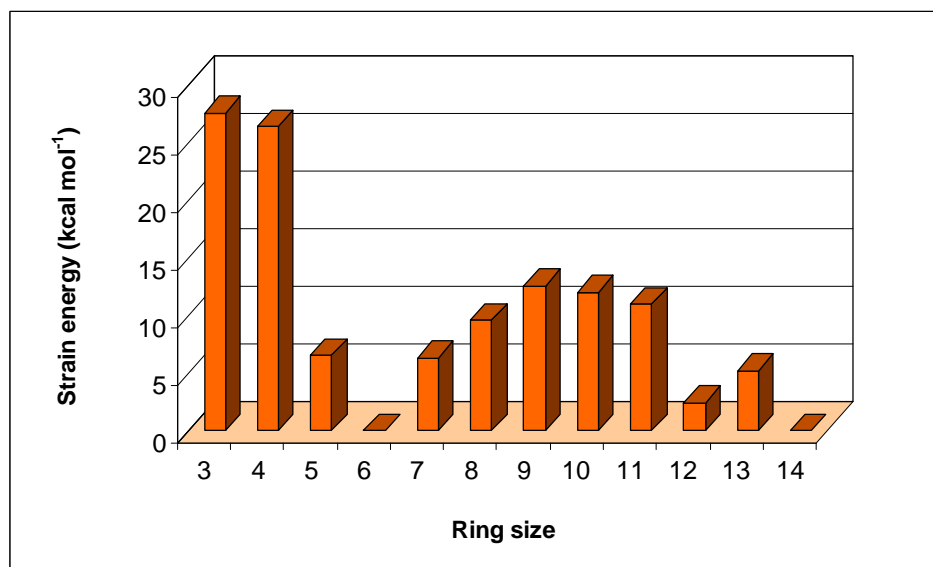


**Figure 2.6** Heats of combustion of C<sub>3</sub> – C<sub>14</sub> hydrocarbon rings.

Cyclooctane is known to have at least 10 different solution conformations (**Figure 2.7**), with the boat-chair and twist-boat-chair (category 1) being the most stable.<sup>5</sup> It has been calculated that ‘crown’ cyclooctane is populated at room temperature, with 6% of cyclooctane being in this conformation at a given time. Category 3 conformations are high in eclipsing strain, thus they hardly populate in solution and category 4 have been calculated to have very high energies and have no significant population.

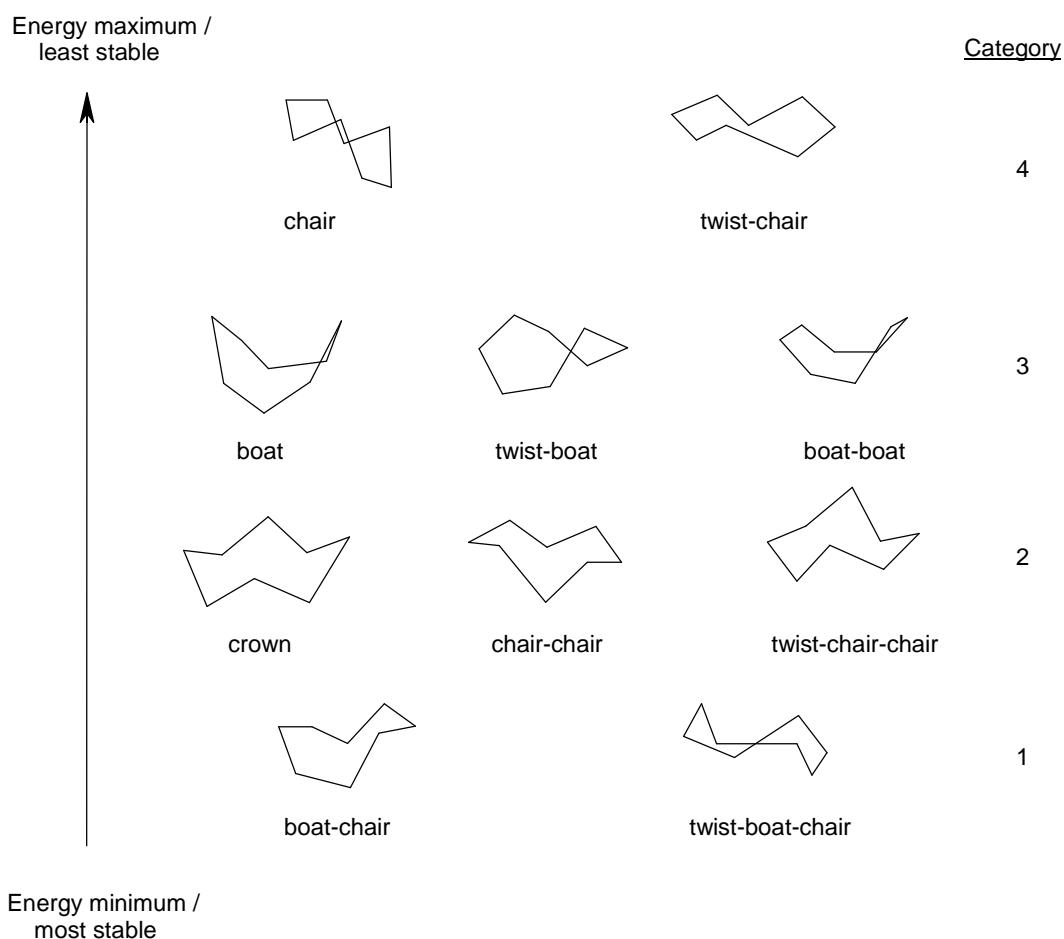


**Figure 2.7** Different energy conformers of cyclooctane.



For nine membered ring systems (cyclononane) there are four minimum-energy conformations, the twist-boat chair, twist-chair-boat, twist-chair-chair and twist-boat-boat. The twist-chair-boat conformation dominates as the lowest energy conformer.

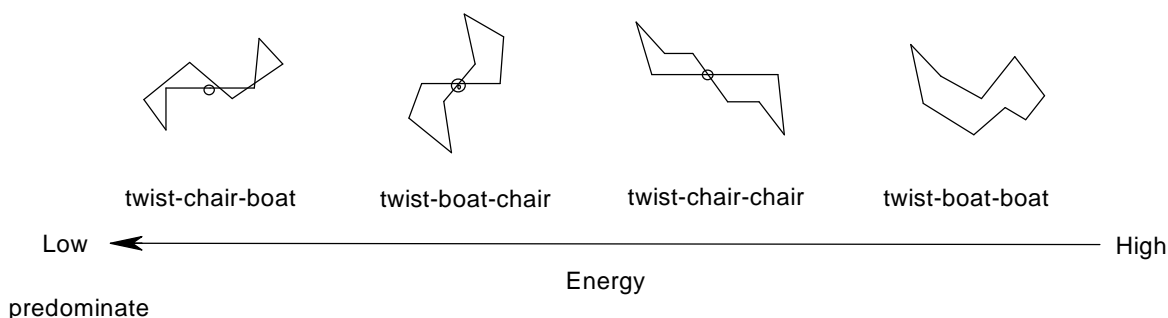
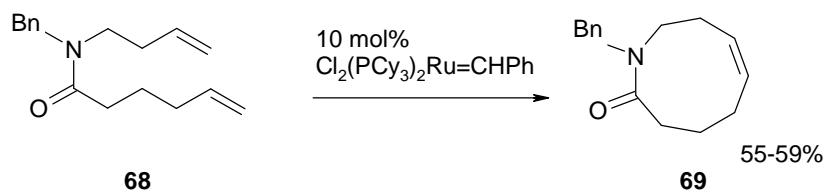


**Figure 2.8** The minimum-energy conformations of cyclononane.

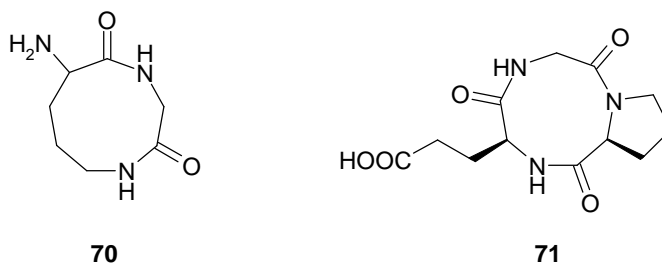
### 2.3 Nine membered rings in nature and synthetic procedures

Unsaturated nine-membered lactams and saturated nine-membered lactams are often used in the chemical preparation of natural products as well as in peptide mimetics and therefore a number of methods have been developed to prepare them. The common methods for their synthesis involve ring expansion and ring closing metathesis (RCM) using Grubbs ruthenium type catalysts.<sup>6,7</sup>



**Scheme 2.1** Synthesis of a nine membered lactam **69** using RCM.<sup>8</sup>

A few diazonanes (saturated nine membered rings with two nitrogens) have been isolated from marine natural products. Cyclic diamide **70**, a secondary metabolite has been isolated from *Streptomyces acrimycin*,<sup>9</sup> and triamide **71** was discovered from the bacterium '*Ruegeria*', found in cell cultures of the sponge '*Suberites domuncula*'.<sup>10, 11</sup>



It is however, the synthesis of nine-membered amines, not amides which was of interest in this program and unfortunately methods for their synthesis are not widely described.

## 2.4 Aims and objectives

This aspect of the research aimed to utilise the known  $\beta$ -fluoro ammonium *gauche* preference to limit the number of accessible conformations of medium sized azetidinium rings. It was anticipated that strategic placement of a fluorine atom within an N-heterocycle would provide a favoured conformation with the fluorine *gauche* to a positively charged  $N^+$ . This is anticipated to result in the fluorine adopting an axial conformation. If the fluorine is positioned  $\beta$  to two charged nitrogens then one would expect again a significant preference for a given conformation.

Synthetic targets included seven, eight and nine membered N-heterocyclic rings **72**, **73** and **74** as well as four and five aza ring systems. Of the medium sized rings, nine membered rings have the largest strain energy ( $12.6 \text{ kcal mol}^{-1}$  in the case of the cyclononane) and for this reason the nine membered diazonane rings emerged as initial synthetic targets. It was

anticipated that the conformation of both fluorinated and non-fluorinated adducts will be assessed by both X-ray crystallography and DFT calculations for comparison.

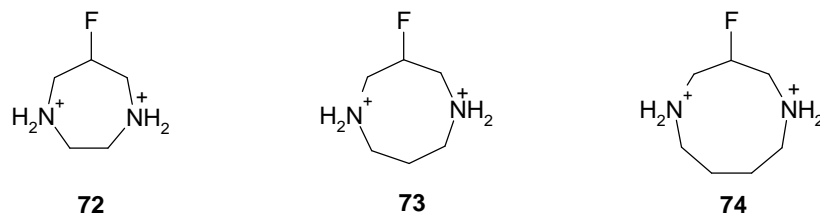
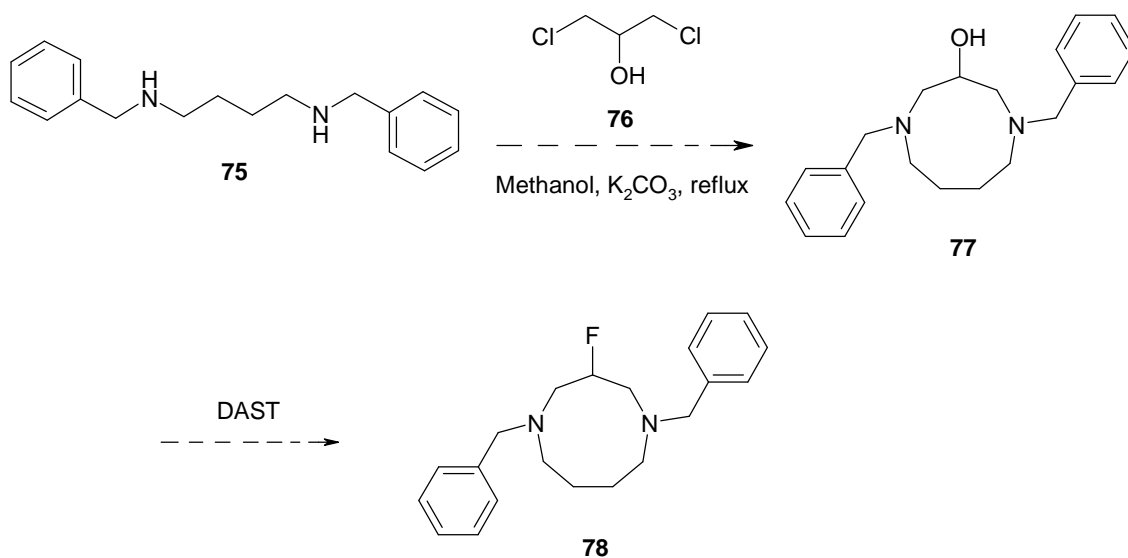


**Figure 2.9** Seven, eight and nine membered  $\beta$ -fluoro diaza rings as synthetic targets.

## 2.5 Synthesis of nine membered $\beta$ -fluoro aza rings :

### Strategy 1 – cyclisation *via* putricine

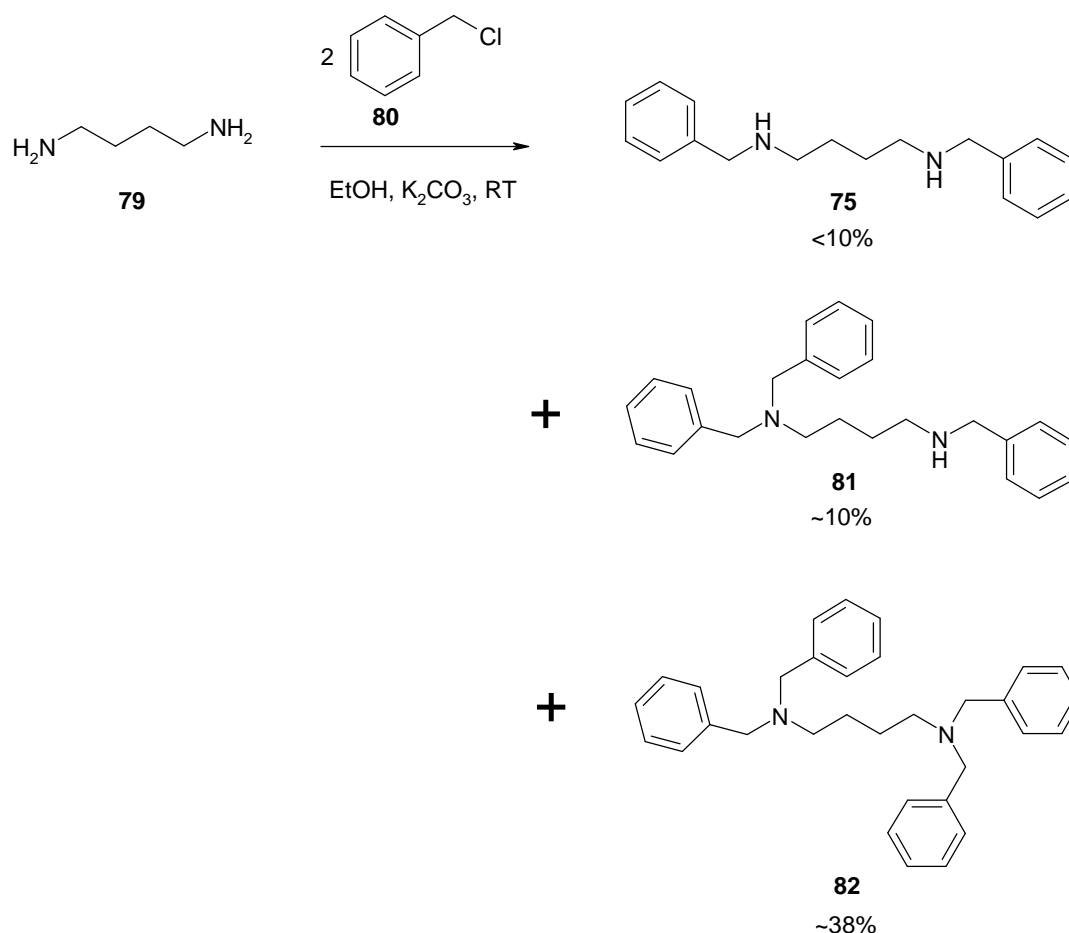
It was anticipated that a nine membered ring with *N*-benzyl protecting groups could be prepared by combination of a putricine derivative and a three carbon ( $C_3$ ) unit such as chloromethyl-oxirane or 1,3-dichloro-propan-2-ol as shown in **Scheme 2.2**. Incorporation of fluorine could then follow by direct fluorination of the resultant secondary alcohol using a reagent such as DAST or Deoxofluor.



**Scheme 2.2** Proposed route to diazonane **78**.

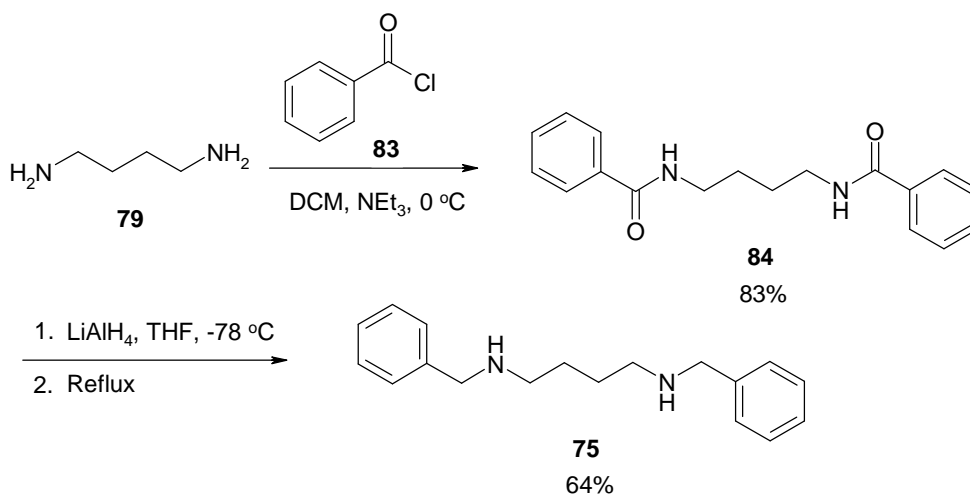
With this strategy in mind, the synthesis of diazonane **78** was explored. Initially diamine **75** was generated by the reaction of butane-1,4-diamine (putricine) **79** with two equivalents of benzylchloride (**Scheme 2.3**). The reaction gave a relatively complex mixture with **75** as a minor component. The over-alkylated products, **81** and **82** predominated even when an

excess of putricine was added and separating these benzylated amines by chromatography proved impractical.



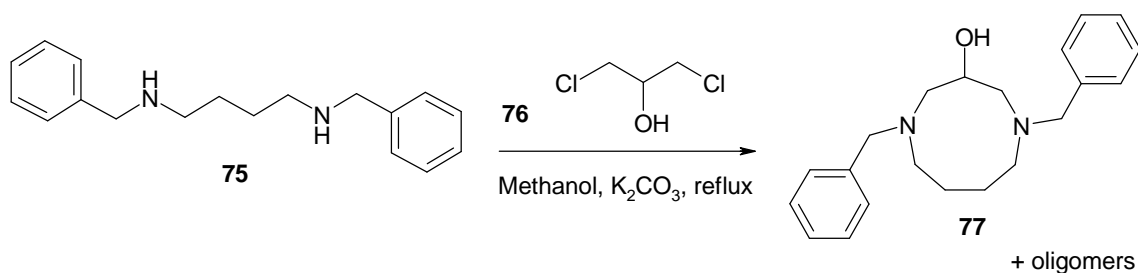
**Scheme 2.3** Reaction of putricine **79** with benzyl chloride gave a mixture of products.

In the main, this synthetic approach proved unsatisfactory and an alternative route to **75** was explored *via* **84**. The preparation of amide **84** was accomplished in good yield by the reaction of putricine **79** with benzoyl chloride. The resultant diamide **84** was then treated with LiAlH<sub>4</sub>. This proved to be a straightforward reaction and di-benzylamine **75** was isolated in a reasonable yield. The strategy was very effective and did not give rise to any other benzylated products, unlike direct benzylation (**Scheme 2.3**).



**Scheme 2.4** Preferred route to di-benzyl putricine **75**.

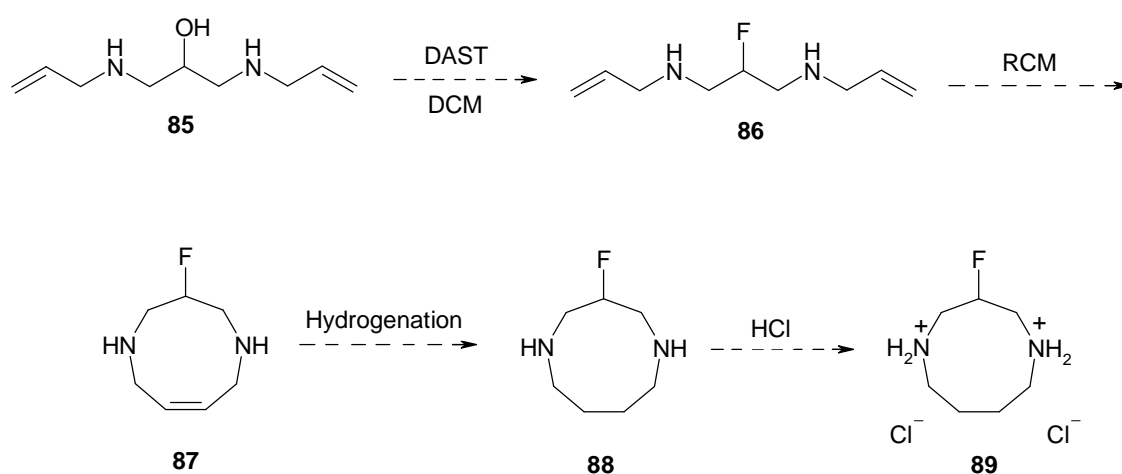
With dibenzylamine **75** in hand, cyclisation to form diazonane **77** was explored using 1,3-dichloropropan-2-ol **76**. However despite several attempts this method proved unsatisfactory. The  $^1\text{H}$  NMR was complex and inconclusive and chromatography did not result in the isolation of any pure products. Mass spectrometry (ES and GC-MS) indicated that the product had formed as a minor component among oligomers. Due to the inefficiency of this reaction another approach was investigated.



**Scheme 2.5** Inefficient route to **77**.

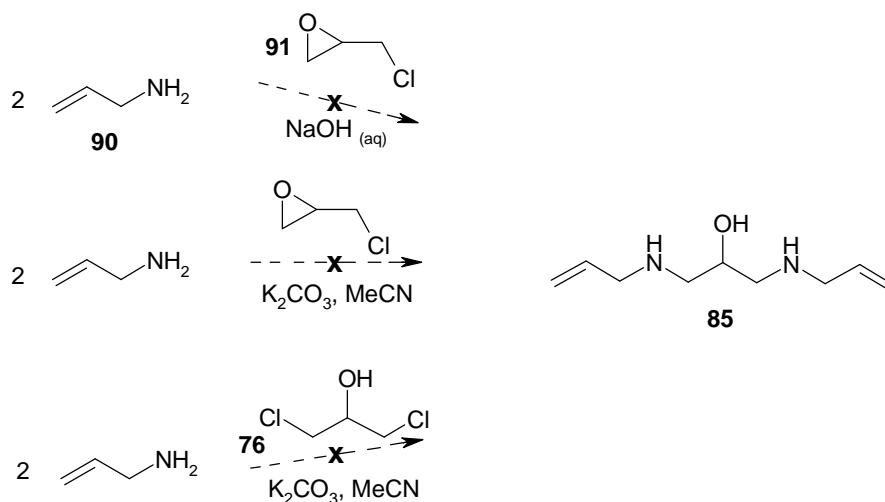
**Strategy 2 – Ring closing metathesis**

Ring closing metathesis (RCM) was explored as an alternative approach to the required diazonanes. Initially the synthesis of 3-fluoro-[1,5]diazonane **86** was investigated (**Scheme 2.6**), and it was envisaged that **86** could be cyclised using an intermolecular metathesis reaction.



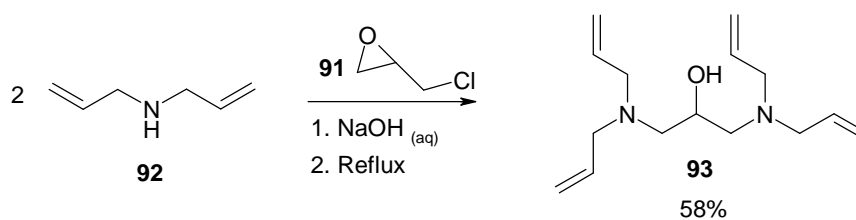
**Scheme 2.6** Proposed route to diazonane **89**.

Synthesis of alcohol **85** was explored by reaction of allylamine **90** with either epichlorohydrin **91** or 1,3-dichloropropanol **76**. Preliminary reaction products were monitored by GC-MS. Although several products were found to have been formed, none could be identified as product alcohol **85**.



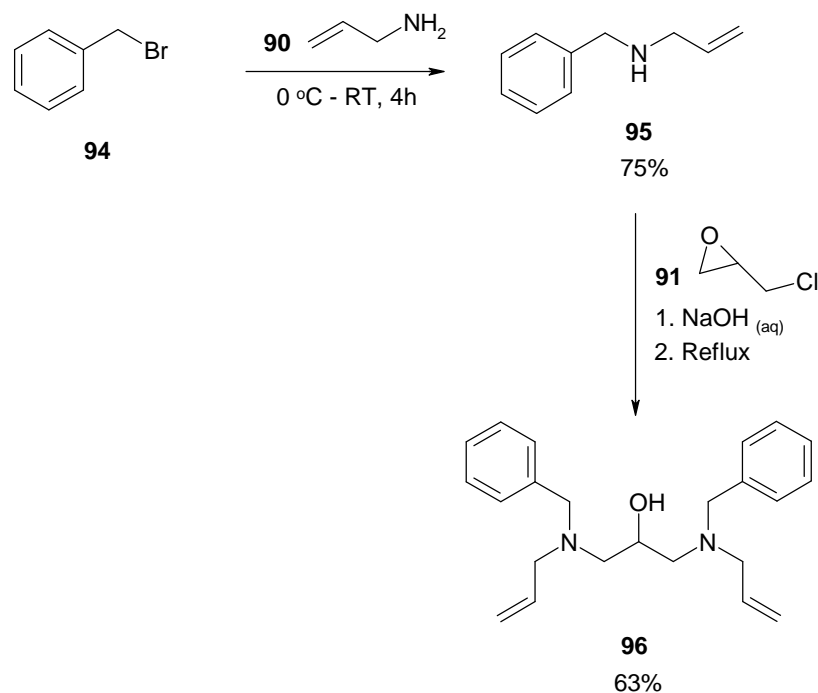
**Scheme 2.7** Attempted approaches to alcohol **85**.

Alternative routes were investigated. For example the tetra allyl amine alcohol analogue **93**<sup>12, 13</sup> and the *N,N'*-diallyl, *N,N'*-dibenzylamine **96** were successfully prepared as illustrated in **Schemes 2.8** and **2.9**. These alcohols were generated in moderate to good yields after treatment of *N,N'*-diallylamine **92** or *N*-benzyl-*N*-allylamine **95**, with epichlorohydrin **91** under basic conditions. Purification of both amines was accomplished by chromatography.



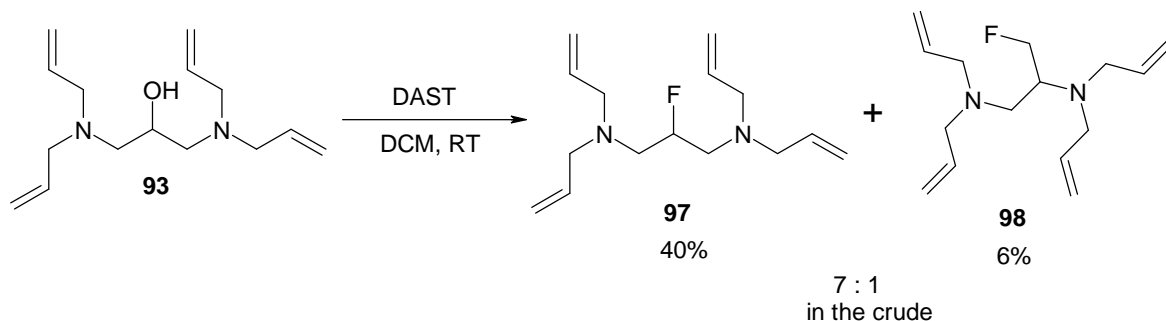
**Scheme 2.8** Synthesis of tetra allyl amine alcohol **93**.<sup>12</sup>





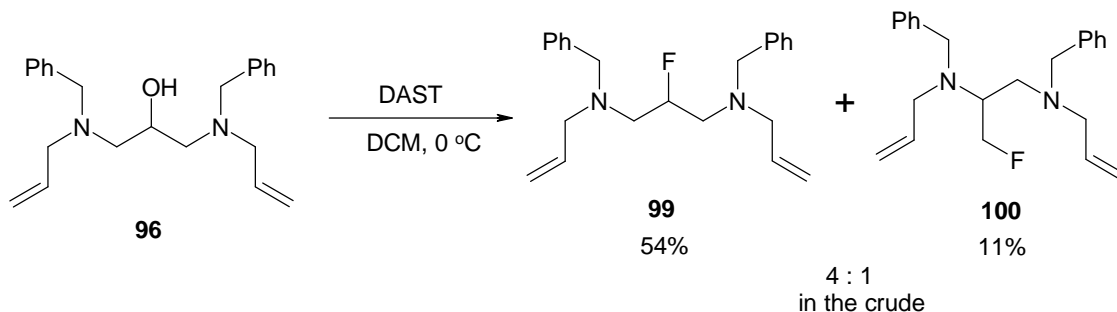
**Scheme 2.9** Synthesis of alcohol **96**.

Fluorination of alcohol **93** with DAST gave rise to two isomeric products. The major product was the desired fluoro diamine **97**, and the minor product contained a fluoromethyl group. NMR and mass spectrometry analyses showed this to be isomer **98**. These isomers could be separated by chromatography over silica gel.



**Scheme 2.10** Reaction of **93** with DAST gave two isomeric products.

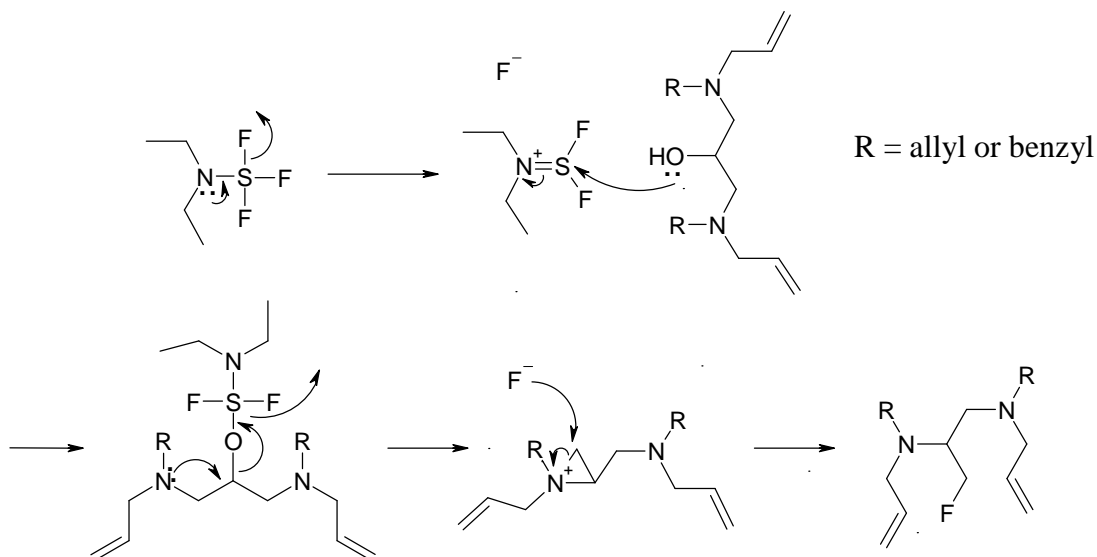
Similarly for diamine **96**, fluorination with DAST generated both the desired product **99** and its isomer **100**. Again both were cleanly separated by column chromatography.



**Scheme 2.11** Reaction of **96** with DAST gave two isomeric products.

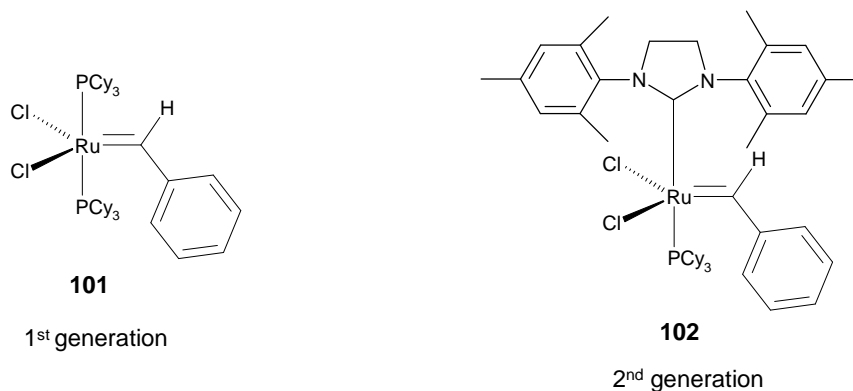
Both alcohols **93** and **96** gave rise to a significant level of isomerisation upon fluorination.

A putative mechanism is given in **Scheme 2.12** and has some literature precedent.<sup>14</sup>

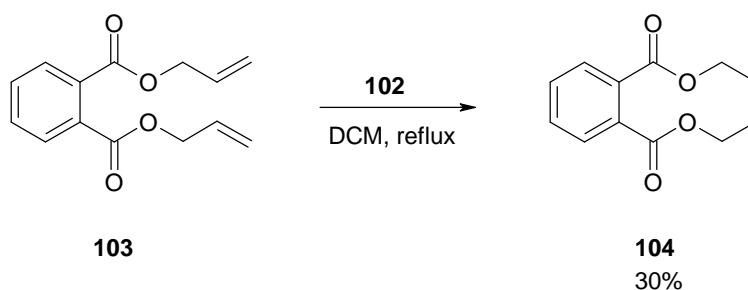


**Scheme 2.12** Putative mechanism for DAST mediated re-arrangement of **93** and **96**.

After purification the fluorinated amine **99** was then subjected to 1<sup>st</sup> and 2<sup>nd</sup> generation Grubbs catalysts, in order to explore the RCM cyclisation reactions.

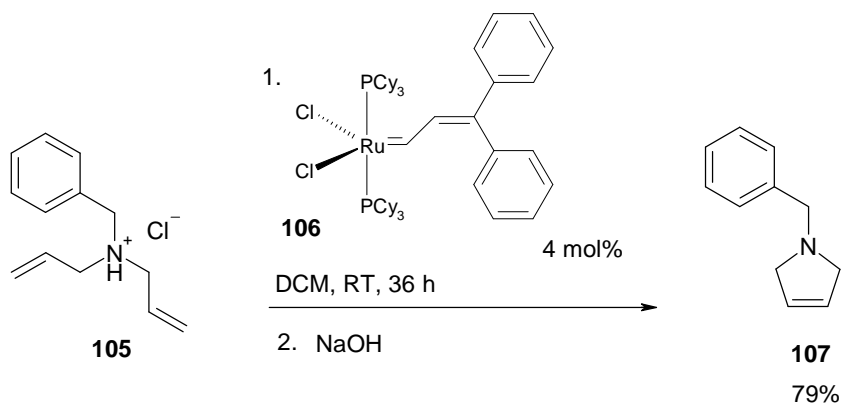


However the reaction was unsuccessful and only starting material was recovered. The 2<sup>nd</sup> generation catalyst was explored in a model reaction on diallyl phthalate and this verified that the catalyst was active and could mediate a ring closing metathesis.



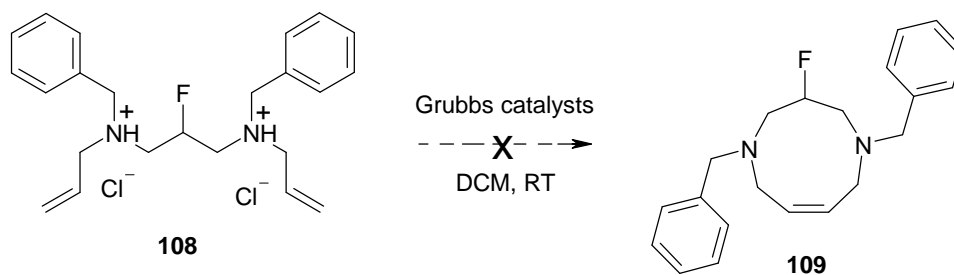
**Scheme 2.13** RCM of **103**.

The unsuccessful reaction with amine **99** as a free amine suggested that the co-ordinating ability of the basic nitrogen may be incompatible with the RCM catalysts. It has been reported<sup>15</sup> that protonated amines such as **105** have successfully undergone metathesis (**Scheme 2.14**) and clearly this strategy could be applied to **99** to promote ring closure.



**Scheme 2.14** RCM of hydrochloride salt **105**.<sup>15</sup>

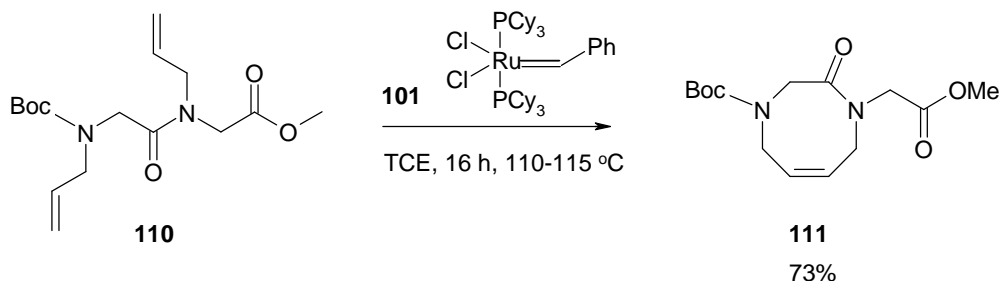
Diamine **99** was therefore acidified to generate the protonated amine **108** and this material was then subjected to RCM using both Grubbs 1<sup>st</sup> and 2<sup>nd</sup> generation catalysts. The reactions however yielded no new products (**Scheme 2.15**). It may be that the intermediate ring size results in too much torsional strain for this reaction to be successful.



**Scheme 2.15** Ring closing metathesis of hydrochloride salt **108** failed.

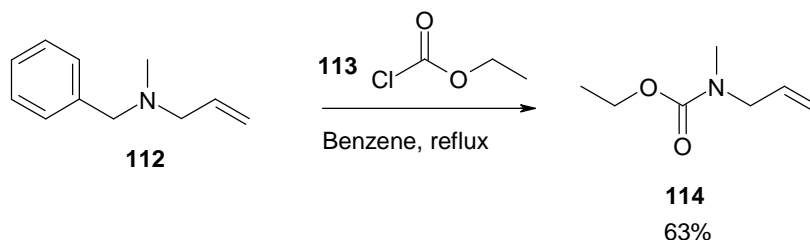
With metathesis of the amine **99** and its hydrochloride salt **108** proving unsuccessful, an alternative strategy to the diazocane ring system was explored. Amides, unlike amines, are well known to undergo metathesis reactions successfully. As previously discussed there are examples in the literature where medium ring size di-peptides have been synthesised by

ring closing metathesis. One example demonstrated by Grubbs involved cyclisation of the allyl substituents of amide **110** to generate an eight membered ring.<sup>16</sup>



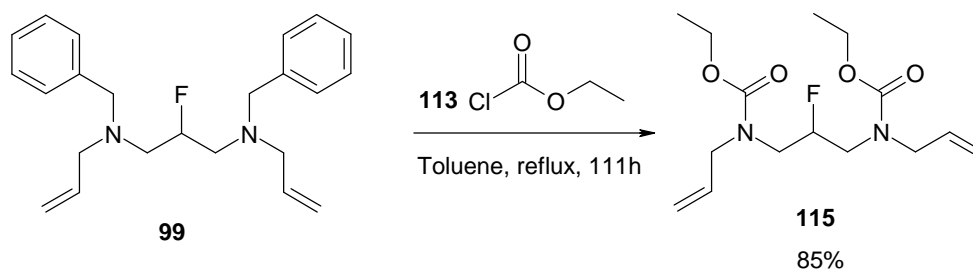
**Scheme 2.16** RCM with amide **110**.<sup>16</sup>

It has previously been shown that benzylamine **112** is converted to a carbamate **114** by benzyl cleavage but without the displacement of the allyl substituent.<sup>17</sup> This reaction presented an opportunity for an alternative approach.



**Scheme 2.17** Conversion of a benzyl group for a carbamate.<sup>17</sup>

Accordingly, treatment of **99**, with ethyl chloroformate in toluene, lead to the di-carbamate product **115** in an excellent yield (**Scheme 2.18**). This compound was purified by chromatography.



**Scheme 2.18** Preparation of dicarbamate **115**.

It is interesting to note that the  $^{19}\text{F}$  NMR spectrum of **115** was found to have at least six separate fluorine signals at room temperature, whereas the precursor **99** had only one. Variable temperature  $^1\text{H}$  and  $^{19}\text{F}$  NMR analysis at 470.3 MHz showed that these signals arose as a consequence of rotamers of **115** (**Figure 2.10**). At 20 °C (293K) three main signals were observed, along with three minor signals. Upon lowering the temperature to -4 °C (269K), the rotamer signals refine and 7 sharp signals are observed. However on heating coalescence of signals was observed (at 67 °C, 340K). At this temperature the molecule is sufficiently mobile for the rotamer signals to coalesce.

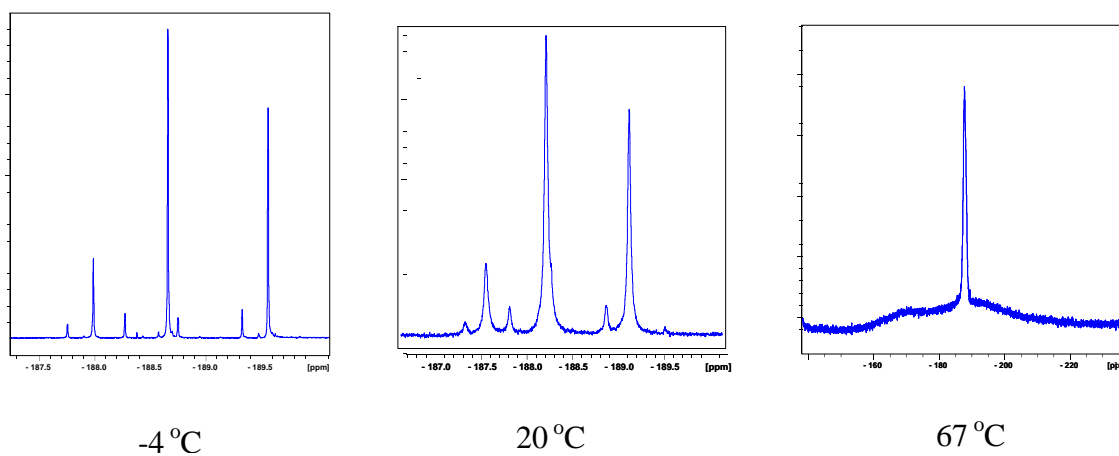


**Figure 2.10**  $^{19}\text{F}$  NMR analysis of **115** at -4 °C, 20 °C and 67 °C respectively. The rotamer signals coalesce at 67 °C.

Although we cannot assign specific  $^{19}\text{F}$  NMR signals to specific rotamers, it is clear that different rotamers can arise (**Figure 2.11**) by restricted rotation around the amide bonds and possibly the C-N bonds.

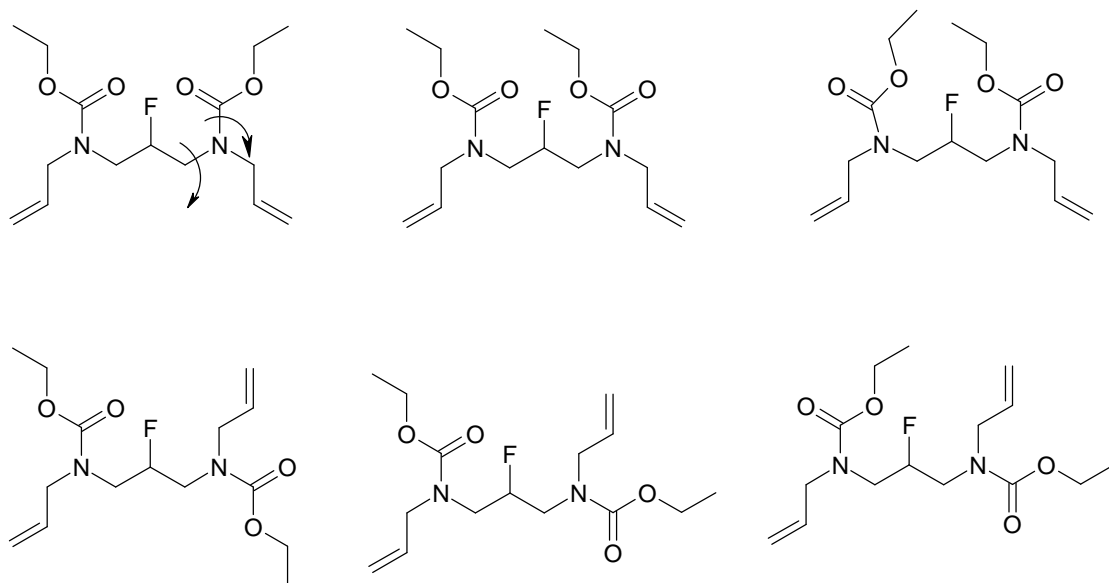
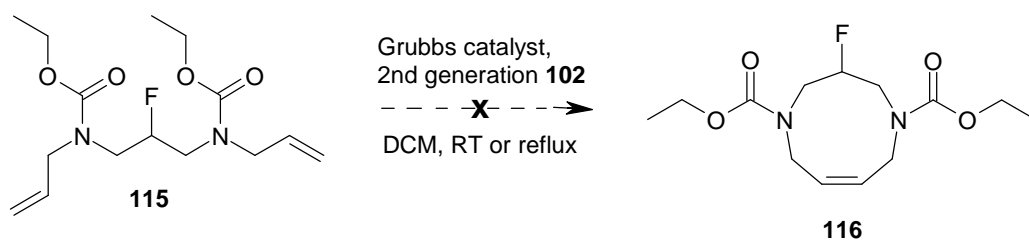


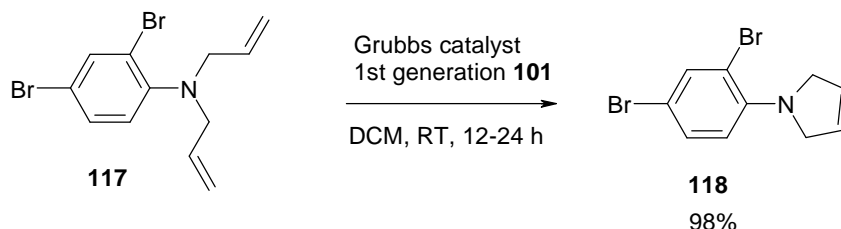
**Figure 2.11** Di-carbamate **115** has a number of rotamer conformations.

The di-carbamate **115** was then subjected to metathesis conditions, again however RCM proved unsuccessful.



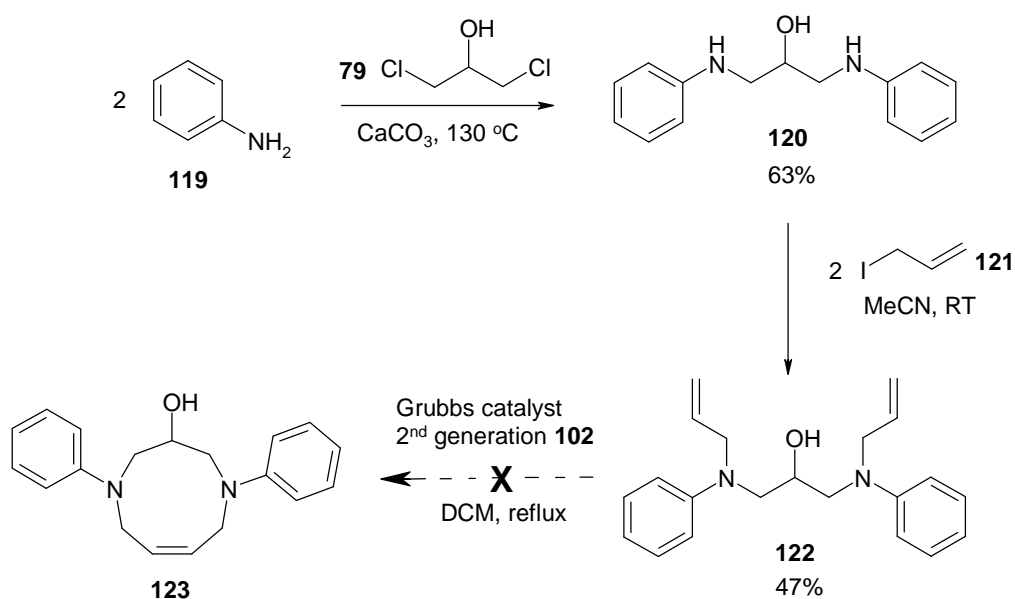
**Scheme 2.19** Di-carbamate **115** did not ring close.

Interestingly N,N'-di-allyl anilines have been shown to undergo RCM efficiently<sup>18, 19</sup>, for example to provide five and six membered rings, as shown in **Scheme 2.20**.



**Scheme 2.20** A RCM N,N-diallylamine **117**.<sup>18</sup>

This presented an alternative strategy of diazonane synthesis. Accordingly the di-allyl aniline **122** was prepared in two straightforward steps by treatment of aniline with 1,3-dichloropropanol **79** to generate alcohol **120**. Treatment of this alcohol with allyl iodide **121** then generated the N,N-diallylaniline **122**. This compound was subjected to RCM conditions, however this too was unsuccessful, and only gave rise to starting materials. Presumably these reactions are failing due to the unfavourable ring size.



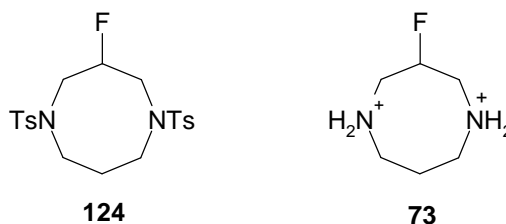
**Scheme 2.21** Synthesis of the di-allyl aniline **122** for RCM.



In conclusion the preparation of a fluorinated 1,5-diazonane was unsuccessful despite the exploration of a number of routes. It is thought that the ring size itself may contribute to the difficulty in mediating a ring closure, owing to entropic factors and transannular interactions.<sup>20</sup> In an effort to succeed on this aspect of the project eight rather than nine membered rings were therefore investigated.

## 2.6 Synthesis of eight membered rings:

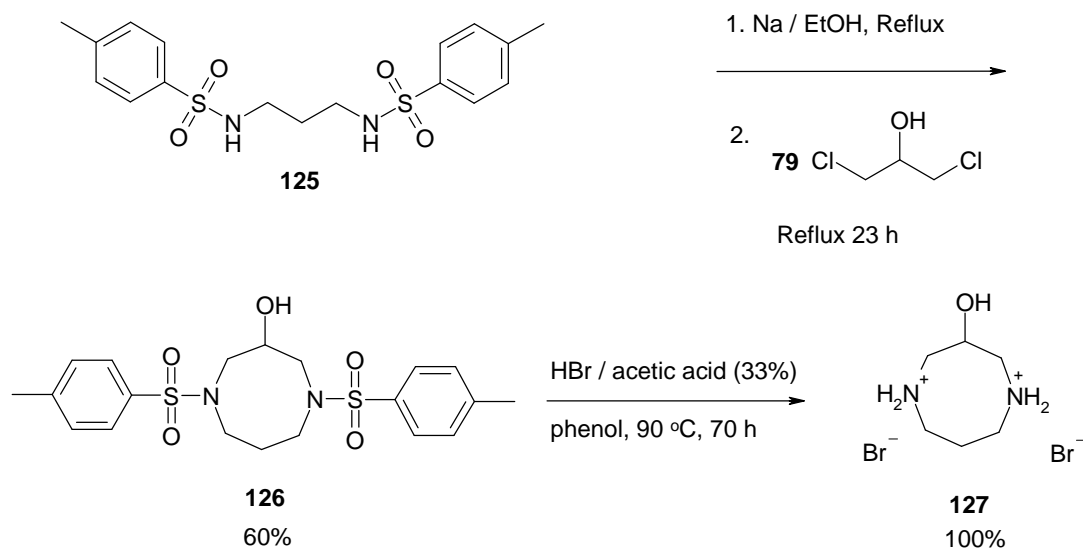
Three different synthetic approaches were taken to obtain the 3-fluoro-1,5-diaza cyclooctanes below.



### 2.6.1 Strategy 1 *via* fluorination of hydroxy-cyclooctane

A method for the synthesis of 3-hydroxyl-1,5-diazocane **126** has been described.<sup>21, 22</sup> It was anticipated that direct fluorination with either DAST or Deoxofluor would then give the fluorinated ring system.

Treatment of commercially available 1,3-bis-(toluene-4-sulfonylamino)-propane **125** with Na in either methanol or ethanol and then 1,3-dichloro-2-propanol **79** generated cyclic ditosylate **126**. The tosyl groups could then be removed after treatment with HBr (33%) in acetic acid.<sup>21, 23</sup> This resulted in the corresponding dihydrobromide salt which was then crystallised (**Scheme 2.22**) and a suitable crystal was used for X-ray structural analysis. An X-ray crystal structure was also determined for the alcohol **127** for future comparison with the corresponding fluorinated analogue.



**Scheme 2.22** Synthetic route to alcohol **127**.

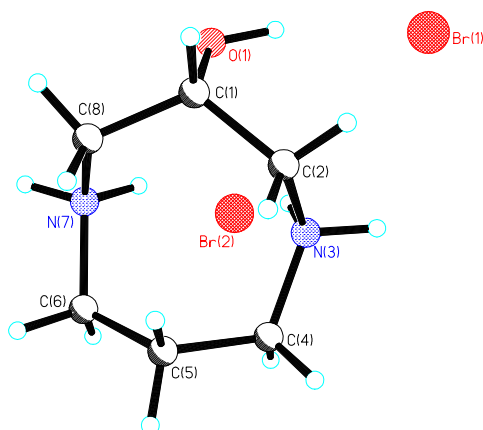
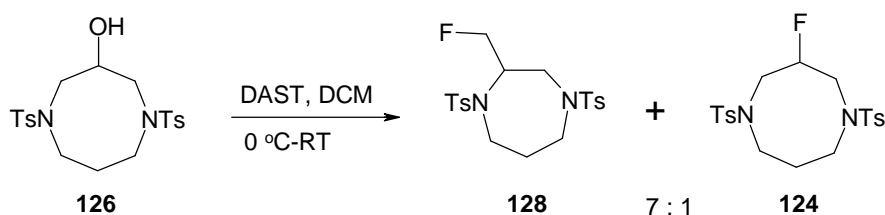


**Figure 2.12** X-ray crystal structure of **127**.

The N-C-C-O torsion angles were measured on either side of the ring and they were found to be 54° and 58°, consistent with relatively tight *gauche* conformations.

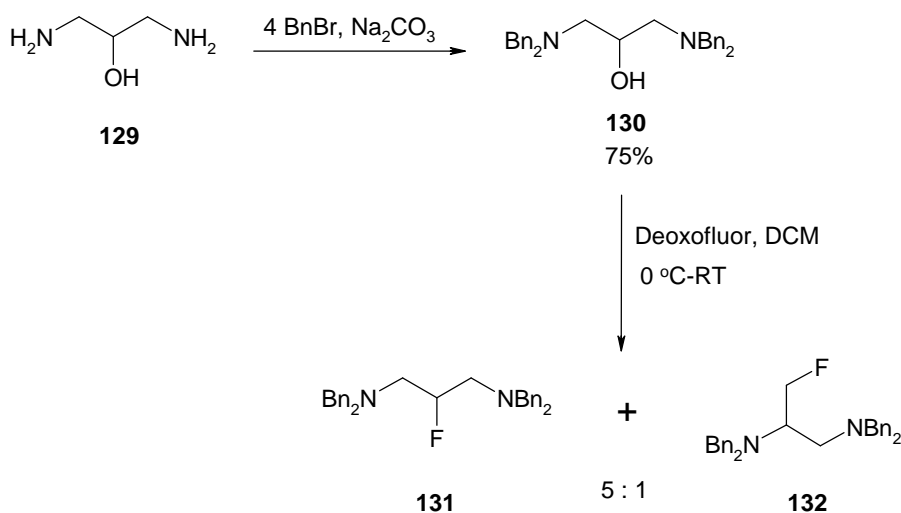
With alcohol **126** in hand, direct fluorination with DAST was then explored. This gave rise predominantly to the re-arranged ring-contracted product **128** and only a minor amount (7 : 1) of the desired 8-membered ring product was generated in the reaction. (**Scheme 2.23**).



**Scheme 2.23** Fluorination of **126** gives isomeric products **128** and **124**.

The predominance of the ring contracted product was unexpected. Clearly the seven membered ring is favoured over the eight in this case.

Another example of this type of re-arrangement emerged in this research. Tetrabenzyl diamine **130** was prepared after treatment of 1,3-diamino-2-propanol **129** with four equivalents of benzyl bromide in aqueous  $\text{Na}_2\text{CO}_3$ . Work-up and purification gave **130** in 75% yield, after silica gel chromatography. This material was then fluorinated with Deoxofluor. Both the directly fluorinated **131** and the re-arranged **132** product were clearly identifiable after  $^{19}\text{F}$  NMR analysis (**Scheme 2.24**). In this case the major isomer arose from direct fluorination and a small amount (17%) of the material isomerised.



**Scheme 2.24** Deoxofluor products of **130**.

Despite obtaining such a large proportion of the seven membered contracted product, purification was carried out on the isomers **128** and **124**. Column chromatography over silica gel was difficult, providing fractions of pure **128** but isomer **124** was always contaminated with **128**. Preparative TLC was however used to prepare an analytically pure sample of **124**. Crystallisation of these two isomers from hot ethanol gave suitable crystals for X-ray analysis and the resultant structures are shown in **Figure 2.13** and **2.14**. Note the structure for **128** shows two fluorines, each of 50% occupancy due to disorder.

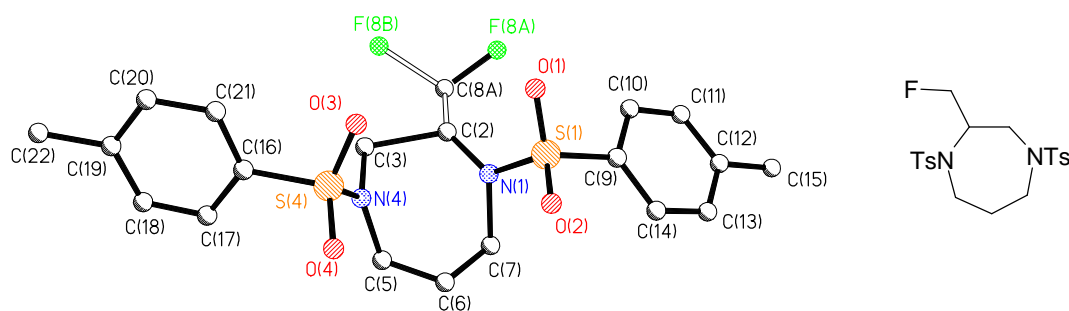


**Figure 2.13** X-ray crystal structure of **128**.

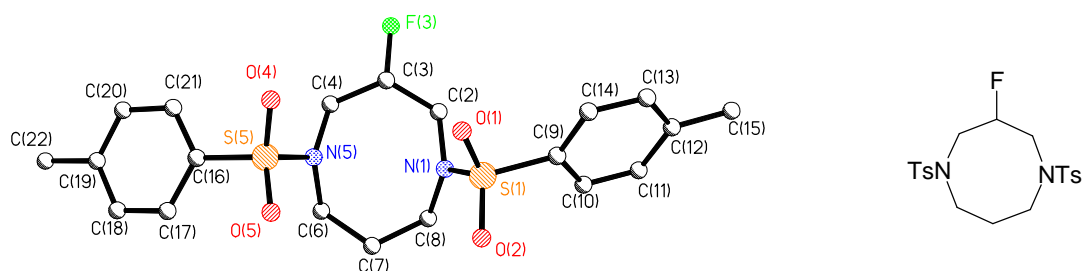
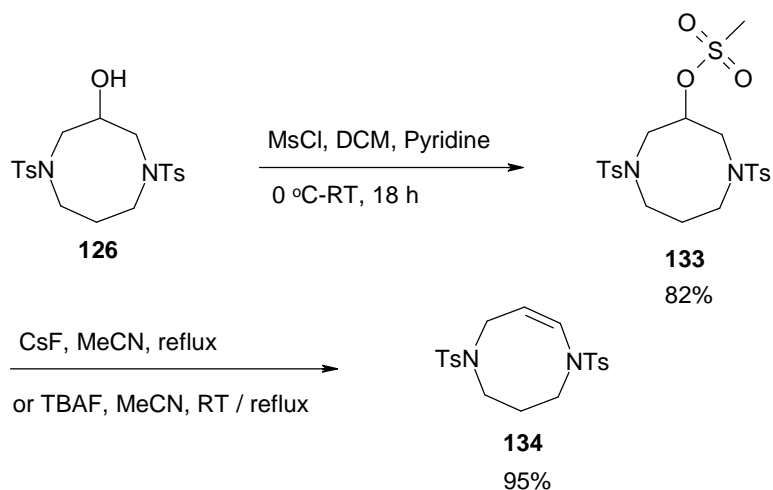


**Figure 2.14** The X-ray structure of **124**.

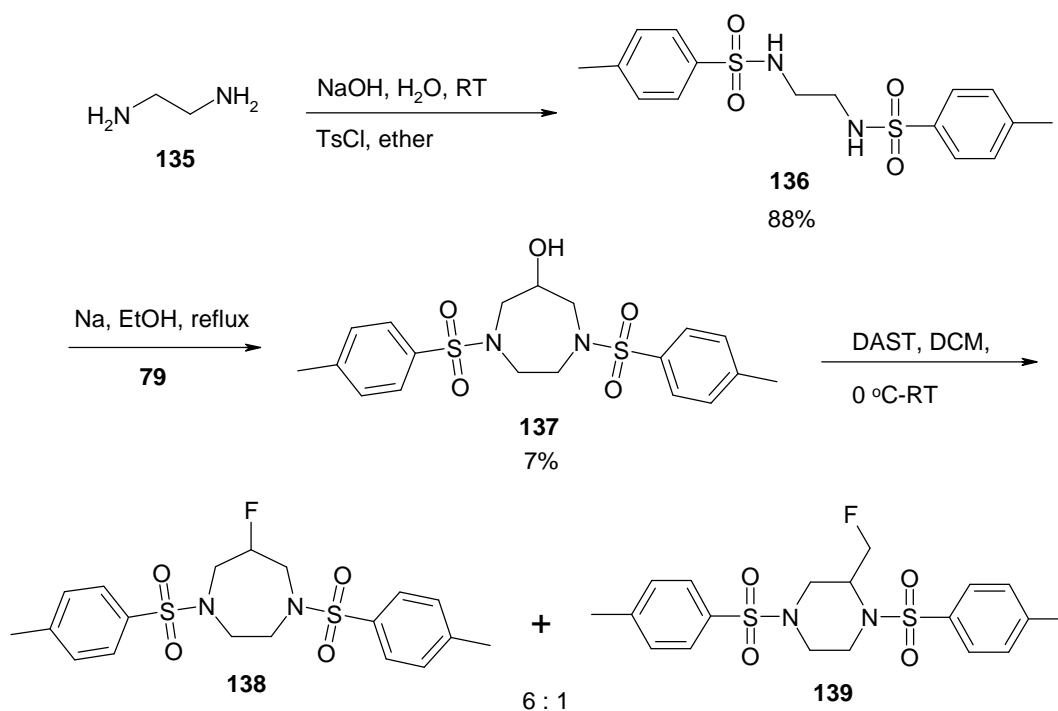
Although this route gave the target 3-fluoro-1,5-diaza octane **124**, this product was secured in a very low yield due to the difficulty in purifying each isomer. Insufficient material was prepared to attempt a removal of the tosyl groups and gain access to the parent ring system. An alternative method was therefore investigated for the preparation of **73**. Alcohol **126** was converted to mesylate **133** using mesyl chloride in pyridine. Nucleophilic fluorination with either CsF or TBAF was attempted to obtain **124**, however this also proved unsuccessful giving the elimination product **134** with an efficient conversion (95%).



**Scheme 2.25** Nucleophilic fluorination of **133** resulted in elimination.

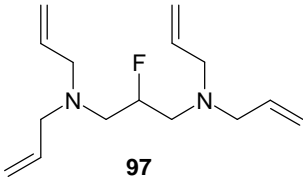
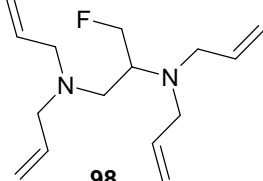
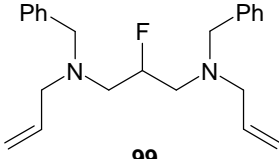
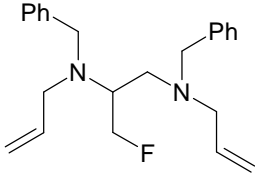
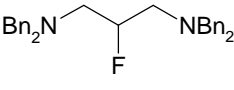
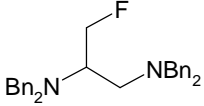
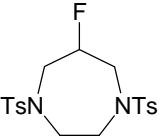
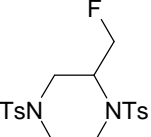
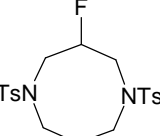
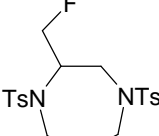
## 2.6.2 Synthesis of a fluoro diazepine

During the project fluorination of the seven membered ring 1,4-bis-(toluene-4-sulfonyl)-[1,4]diazepam-6-ol **137** was also explored. Alcohol **137** was prepared after tosylation of ethylene diamine **135** to generate **136**. Treatment of **136** with 1,4-dichloropropan-1-ol **79** under basic conditions then gave **137** although the conversion was poor. After careful purification over silica gel a pure sample of **137** was obtained but in low yield. A fluorination reaction with DAST was carried out by way of comparison with the eight membered analogue **126**. Interestingly here the direct fluorinated product **138** ( $^{19}\text{F}$  NMR = -180.5 ppm, CHF) dominated over the six membered ring product **139** ( $^{19}\text{F}$  NMR = -224.9 ppm,  $\text{CH}_2\text{F}$ ) in a 6 : 1 ratio (**Scheme 2.26**). Distinctive  $^1\text{H}$  and  $^{13}\text{C}$  NMR signals ( $\text{CDCl}_3$ , 400.13 MHz) for **138** were found respectively: 4.96 (1H, dm,  $J$  48.6, CHF) and 89.8 (d,  $J$  180.0,  $\text{CH}_2\text{F}$ ). Column chromatography (hexane : ethyl acetate, 3 : 1) again proved very difficult and the isomers could not be separated.



**Scheme 2.26** Fluoro diazepine **138** was formed by reaction of **137** with DAST.

**Table 2.1** summarises the fluorination reactions carried out in this research and illustrate the difference in direct fluorination : re-arrangement product ratios.

Fluorination reagent (in DCM)	Fluorinated product derived from the corresponding alcohol	Isomeric product	Isomer Ratio*
DAST	 <b>97</b>	 <b>98</b>	7 : 1
DAST	 <b>99</b>	 <b>100</b>	4 : 1
Deoxofluor	 <b>131</b>	 <b>132</b>	5 : 1
DAST	 <b>138</b>	 <b>139</b>	6 : 1
DAST	 <b>124</b>	 <b>128</b>	1 : 7

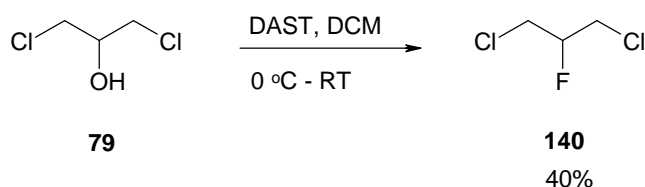
\* isomer ratios were determined by  $^{19}\text{F}$  NMR of crude products

**Table 2.1** Ratios of the CHF motif :  $\text{CH}_2\text{F}$  motif after various fluorination reactions of the precursor alcohols.



### 2.6.3 Strategy 2 - eight membered rings *via* cyclisation with a fluorinated C<sub>3</sub> unit

In order to obtain the parent 3-fluoro diazaoctane ring system a new approach was taken. This involved cyclisation with a fluorinated three carbon unit. 1,3-Dichloro-2-fluoropropane **140** was considered an appropriate starting material. This compound was not available commercially although it had been reported previously. The synthetic method to provide clean product in reasonable yield involved the use of chlorine monofluoride (ClF) and gaseous hydrogen fluoride (HF).<sup>24</sup> With neither of these reagents easily available, an alternative approach to **140** was considered. Commercially available 1,3-dichloropropan-2-ol **79** was directly fluorinated with DAST (Scheme 2.27) and the desired product was obtained cleanly after distillation. The <sup>19</sup>F NMR of **140** is shown in Figure 2.15. The coupling constants for this AA'BB'CX system have been derived from NMR simulation and found to be: <sup>2</sup>J<sub>HF</sub> = 45.8 Hz, <sup>3</sup>J<sub>HF</sub> = 19.0 Hz and <sup>3</sup>J<sub>HF</sub> = 16.4 Hz.



Scheme 2.27 Direct fluorination with DAST afforded **140**.

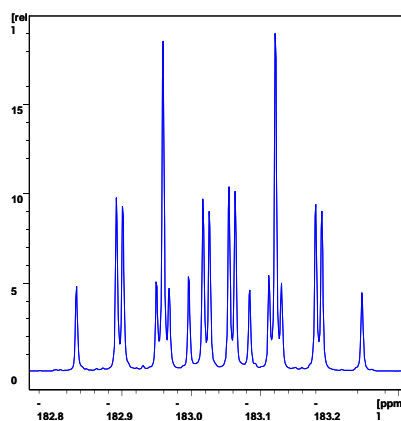
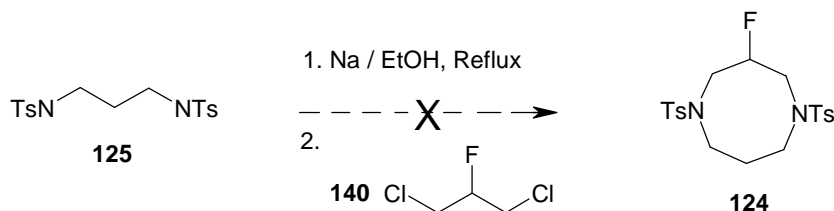


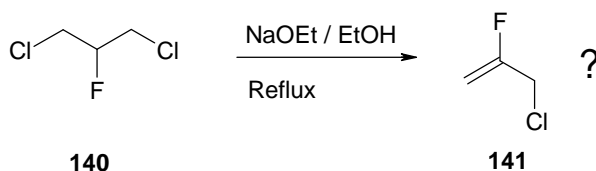
Figure 2.15 The <sup>19</sup>F NMR of 1,3-dichloro-2-fluoropropane **140**.

1,3-Dichloro-2-fluoro-propane **140** was then used in a ring closing reaction similar to that described in section 2.6.1. to try to generate the eight membered ring **124**. This involved treatment of the di-sulfonamide **125** with Na / EtOH, followed by addition of **140**. The reaction was however unsuccessful.



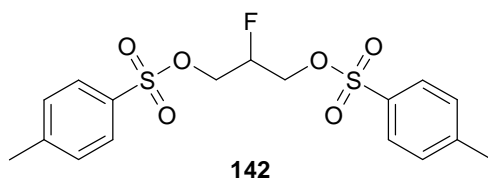
**Scheme 2.28** Cyclisation with the C<sub>3</sub> unit **140** was unsuccessful.

*In situ* <sup>19</sup>F NMR analysis showed a new fluorine signal at -102.8 ppm, consistent with a C=CF moiety. This suggested HCl elimination from **140** had occurred and appeared to generate 3-chloro-2-fluoro-1-propene **141** although this compound was not characterised.

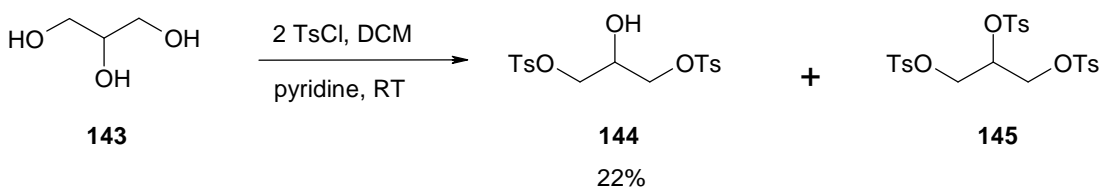


**Scheme 2.29** Proposed reaction of **140** generating vinyl fluoride **141**.

An alternative strategy to the 1,5-diaza cyclooctane ring system was investigated using 2-fluoro-1,3-bis-(toluene-4-sulfonyloxy)-propane **142**.

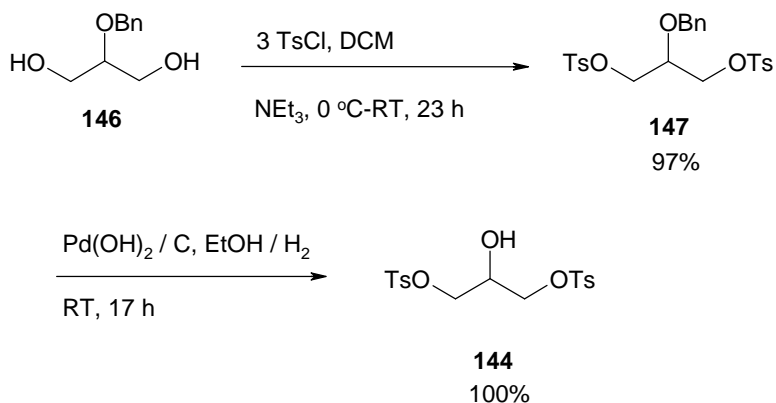


This compound has previously been prepared *via* di-tosylation of 2-fluoro-propane-1,3-diol or 1,3-dibromo-2-fluoropropane.<sup>25, 26</sup> The synthesis was approached *via* another method as it was considered that either 2-fluoropropane-1,3-diol or 1,3-dibromo-2-fluoropropane would be challenging to prepare. Initially alcohol **144** was generated in two different ways. The first involved tosylation of glycerol **143**, leaving the secondary alcohol unmodified. This however gave the desired product in a low yield due to the predominant formation of the trisubstituted product **145**.



**Scheme 2.30** The di-tosyl alcohol **144** was formed as a minor product.

The second approach involved a two step reaction where glycerol was benzyl protected at the 2 position. Treatment of **146** with an excess of tosyl chloride generated **147** and then hydrogenolysis of the benzyl ether gave alcohol **144** in excellent yield. This was found to provide a clean synthetic route to **144**, which could be scaled and provided an attractive intermediate.



**Scheme 2.31** Optimised route to 1,3-ditosylglycerol.

It was appealing at this stage to consider a direct fluorination of **144**, despite the two primary tosyl groups. In the event fluorination with either DAST or Deoxofluor generated **142** in good yield (67% e.g. with Deoxofluor), with no obvious by-products and only some residual starting material. Product **142** was readily purified by column chromatography and gave a solid material. This was amenable to crystallisation and a structure by X-ray analysis was determined as is shown in **Figure 2.16**.

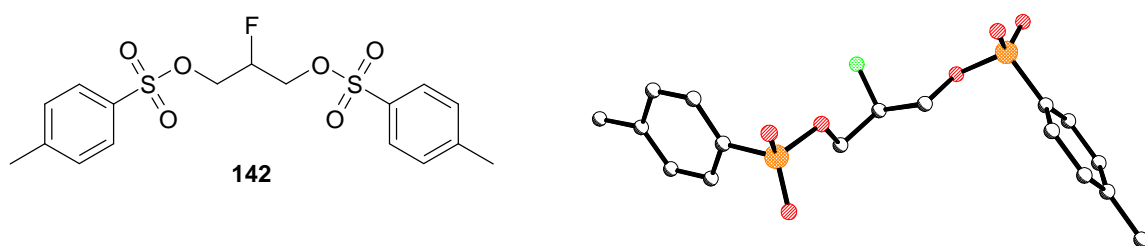
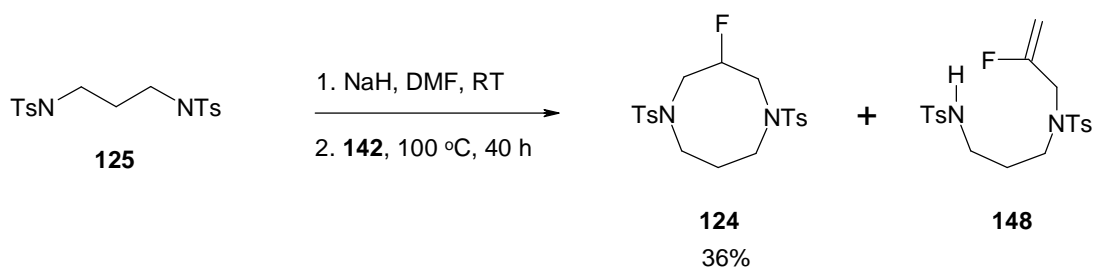


**Figure 2.16** X-ray crystal structure of **142**.

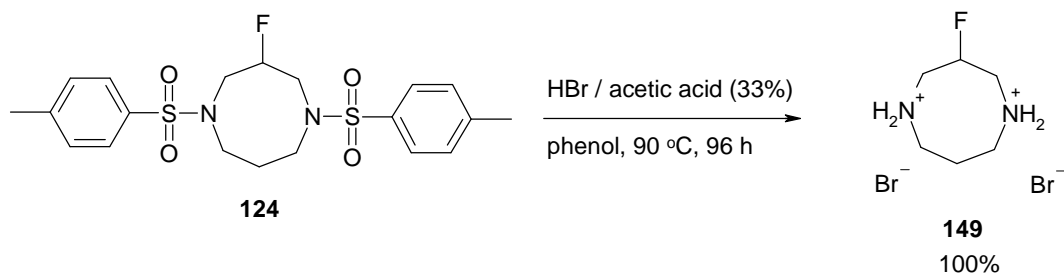
There are two O-C-C-F torsion angles and both show clear *gauche* angles ( $58^\circ$  and  $66^\circ$ ).

The fluoro ditosyl propane **142** was then utilised in a cyclisation reaction with disulfonamide **125** as shown in **Scheme 2.32**. This proved successful and finally the target 3-fluoro-1,3-diaza cyclooctane ring **124** was prepared by this method, despite a rather low yield (36%). The main by-product, was identified as the acyclic fluoro vinyl isomer **148**.  $^{19}\text{F}$  NMR analysis revealed a ddt for **148** with coupling constants: 47.4 Hz, 16.0 Hz and 15.7 Hz.



**Scheme 2.32** Successful synthesis of 3-fluoro-1,5-diazacyclooctane **124**.

Product **124** was purified by chromatography and was fully characterised. Despite the moderate yield it could be prepared in sufficient quantities to consider removal of the tosyl groups. Accordingly **124** was treated with HBr in acetic acid. This proved an efficient reaction and the HBr salt was recovered. Crystallisation from DMF / ether gave crystals suitable for X-ray structure analysis.



**Scheme 2.33** The preparation of 3-fluoro-1,5-diazacyclooctane hydrobromide **149**.

The X-ray derived structure is shown in **Figure 2.17**. It is very clear that the fluorine adopts an axial orientation, symmetrically located between the nitrogen atoms. The two  $N^+-C-C-F$  torsion angles are  $55^\circ$  and  $58^\circ$ , consistent with very tight *gauche* conformations.

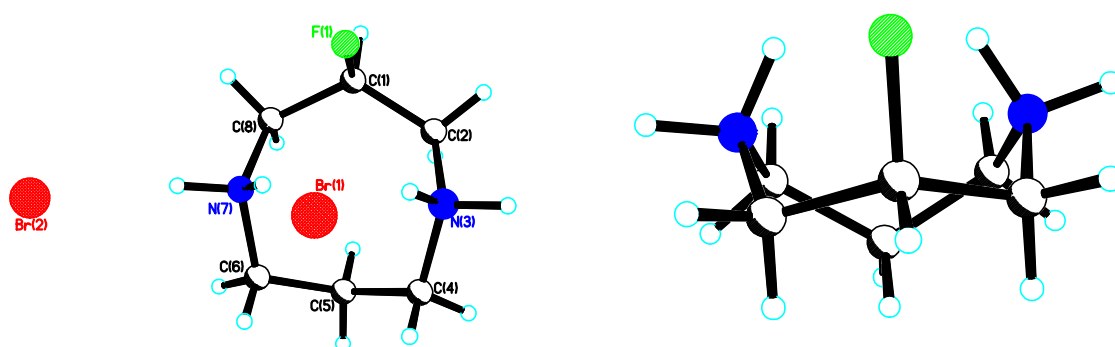


**Figure 2.17** Two views of the X-ray crystal structure of **149**.

To examine this structure more closely, the X-ray coordinates were sent to Dr David Tozer and co-workers at The University of Durham. With this data they carried out DFT calculations, measuring the absolute energy of this conformer, and this was compared to the conformer with the fluorine in an equatorial orientation. They found that there was a  $9.2 \text{ kcal mol}^{-1}$  preference in the ground state energies for the fluorine in the axial over the equatorial position.

If this energy difference is compared to the preference found in Lankin and Snyder's six membered piperidinium ring **51**<sup>1</sup>, then there is a substantial increase in the energy difference. 3-Fluoropiperidinium **51** was reported to have a  $3.3\text{--}4.3 \text{ kcal mol}^{-1}$  preference for the conformer with the axial conformation. It would appear from this study that such electrostatic interactions are at least additive, if not more.

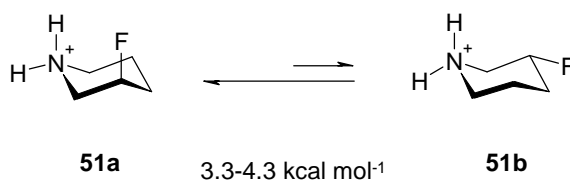


**Figure 2.18** Axial preference for **51**.

### 2.6.4 Synthesis of a di-fluoro-diazocane

Having successfully prepared the fluorinated di-aza eight membered heterocycle **149** attention focused on the synthesis of the di-fluorinated rings **150** and **151**. These compounds were investigated to explore the influence of a second fluorine in the ring (**Figure 2.19**). It should be noted that such compounds possess *cis* (**150a** and **151a**) and *trans* (**150b** and **151b**) isomers (**Figure 2.20**).

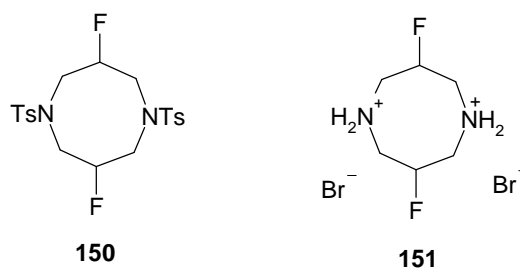


**Figure 2.19** The di-fluoro diazocane targets.

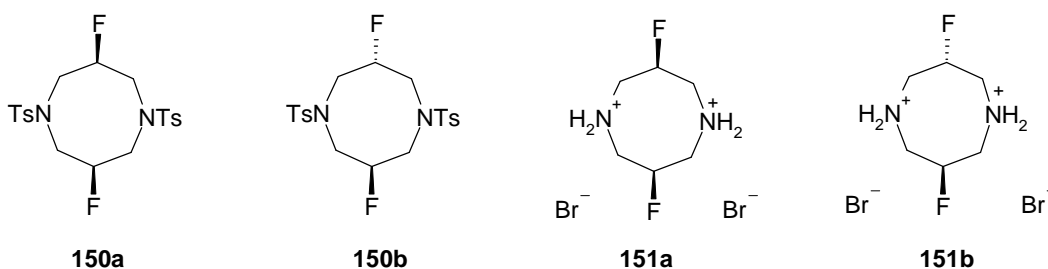
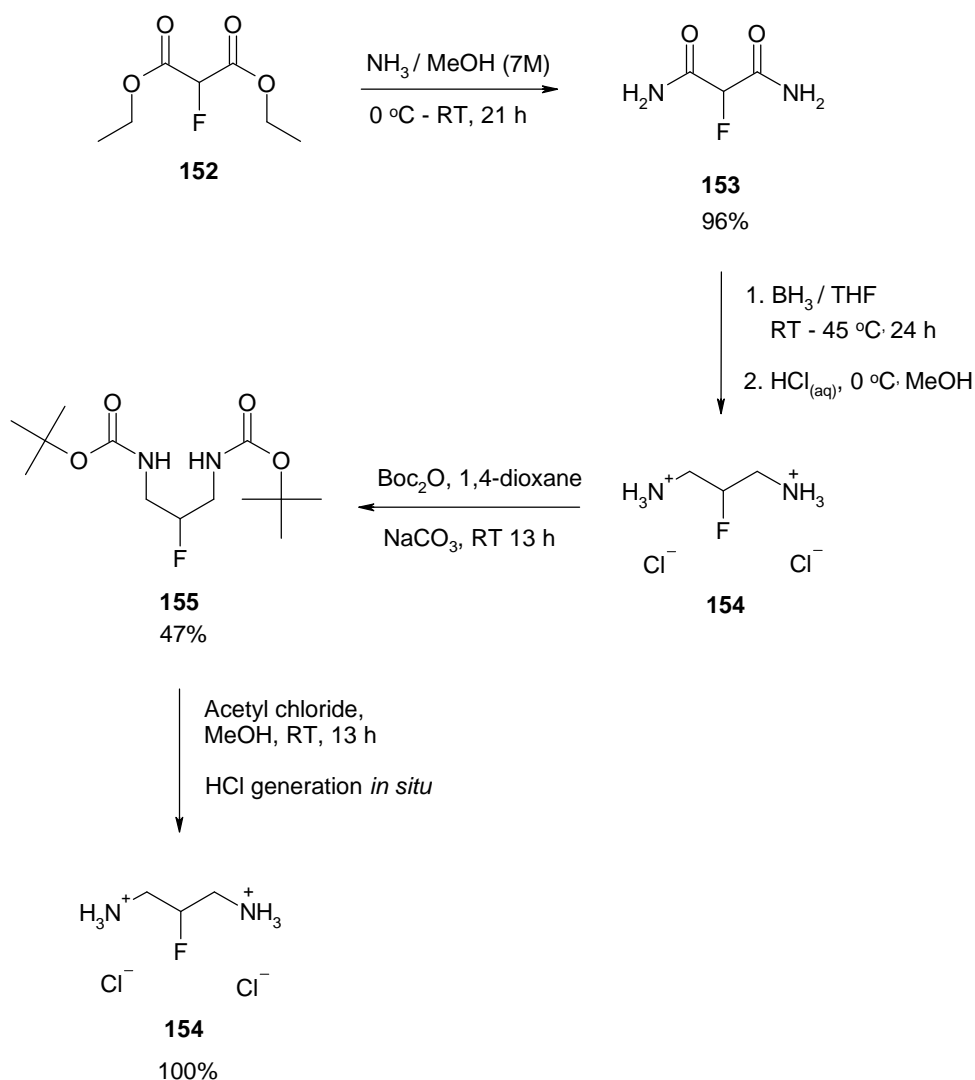


**Figure 2.20** The *cis* and *trans* isomers of the di-fluoro diazocane targets.

As a start point 1,3-diamino-2-fluoropropane **154** was prepared according to a literature procedure<sup>27</sup> via the reduction of 2-fluoromalonylamine **153**. 2-Fluoromalonylamine was prepared in good yield from commercially available diethyl fluoromalonate **152** upon reaction with ammonia in methanol. Treatment of **153** with diborane in THF then gave the

diamine **154** as a hydrochloride salt. Alternatively **154** could be obtained directly after the reduction of 2-fluoromalonamide **153** followed by passing the crude salts through a pre-packed SCX-2 column with water. The yield from this shortened procedure was quite low at 36%. However in order to get a pure product in good yield it proved necessary to prepare the di-Boc **155** derivative, purify it and then deprotect it. Accordingly **155** was treated with HCl, generated by the addition of acetyl chloride to a solution of **155** in methanol.



**Scheme 2.34** Optimised route for the preparation of **154**.



The hydrochloride salt **154** was crystallised and a X-ray structure obtained (**Figure 2.21**). Two F-C-C-N<sup>+</sup>H<sub>3</sub> torsion angles were measured at 66° and 62°, consistent with *gauche* conformations and an extended linear structure.

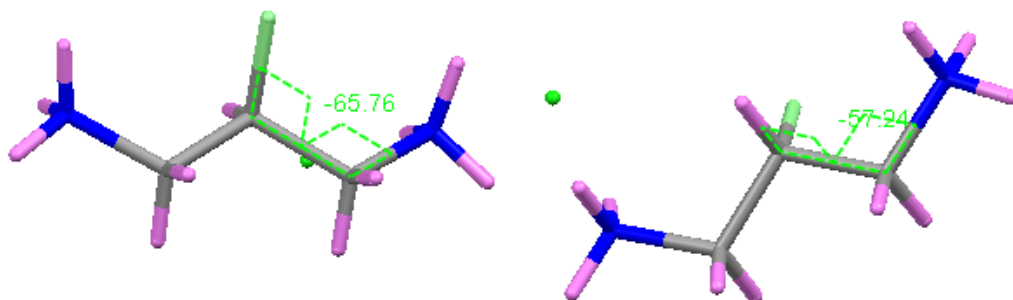
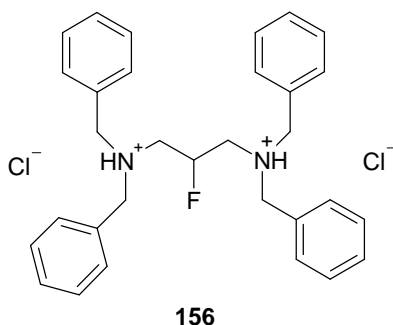


**Figure 2.21** X-ray structure of **154** showing an extended structure.

The F --- N<sup>+</sup> distances were measured and found to be 2.908Å and 2.899Å. This can be compared to those found in other N<sup>+</sup>CH<sub>2</sub>CHF motifs e.g. the fluoro eight membered ring **149** (2.85Å and 2.85Å), and the hydrochloride salt **156** of the previously prepared tetra benzyl amine **131** (3.10Å and 3.19Å). The distances vary very little between these systems.



The X-ray crystal structure of  $\alpha$ -fluoroamide **153**, an intermediate in the synthesis of **154** was also obtained. The fluorine orientates nearly *anti* to the carbonyl oxygens and *cis* to an

NH<sub>2</sub> with F-C-C(O)-N(H<sub>2</sub>) torsion angles of 15.3° and 19.3°. The intramolecular F---H distance was measured at 2.23Å and 2.20Å consistent with short contacts and stabilising F---H bonds. This conformation is another example of the preferred orientation of the fluorine within a  $\alpha$ -fluoroamide system as discussed in **Chapter 1**.

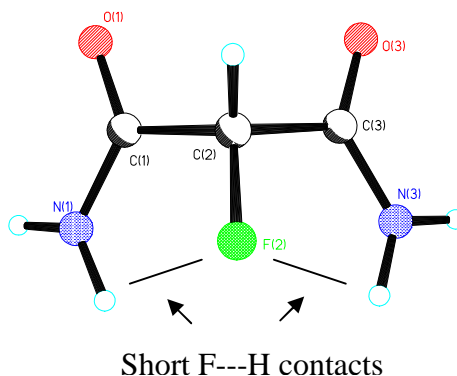
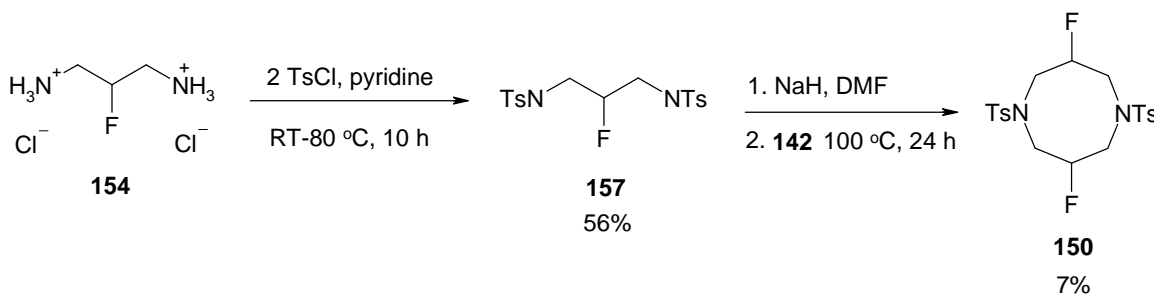


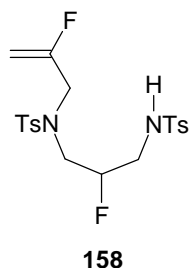
**Figure 2.22** X-ray structure of **153**.

It was anticipated that **157** could be prepared from **154** by reacting both amines with tosyl chloride. This reaction was carried out successfully and **157** could be prepared in 56% yield. Treatment of **157** with the previously prepared tosyl ester **142** with NaH in DMF gave rise to the intramolecular cyclised product **150** as a mixture of *cis* and *trans* isomers.

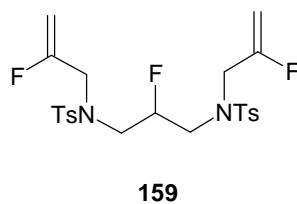


**Scheme 2.35** The di-tosylated ring **150** was successfully synthesised from **157**.

Purification of **150** proved difficult however, owing to the presence of a contaminating acyclic vinyl fluorine, presumably **158**. The  $^{19}\text{F}$  NMR signal at  $-103.1$  ppm ( $\text{CDCl}_3$ ,  $282.3$  MHz) is indicative of such a vinyl fluorine. Several attempts at both column chromatography as well as preparative plate chromatography gave an inefficient recovery of **150** (7%).

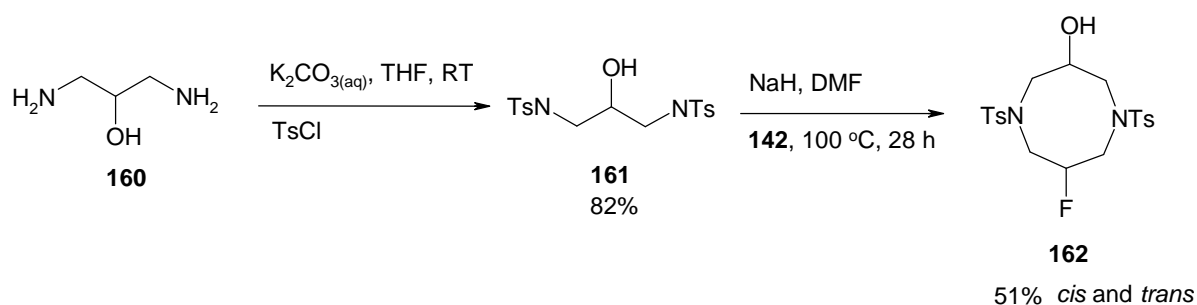


In a previous experiment, where an excess of NaH was used, the major product obtained was that containing fluorine with a  $^{19}\text{F}$  NMR chemical shift of  $-102.5$  ppm ( $\text{CDCl}_3$ ,  $282.3$  MHz). This material was identified by further NMR analyses and mass spectrometry (ES) to be **159**.



A pure sample of **150** obtained from extensive chromatography was then subjected to desilylation conditions (HBr, AcOH, phenol, reflux), however analyses ( $^1\text{H}$ ,  $^{19}\text{F}$  NMR and ES) of the crude product was inconclusive. Crystallisation of the product from aqueous acid to obtain **151** as a salt was also unsuccessful.

An alternative route to **150** was also explored, which envisaged direct fluorination of heterocyclic alcohol **162**. It was envisaged that **162** could be synthesised by ring closure of sulphonamide **161** with building block **142**, and then subsequent fluorination of the free hydroxyl group with Deoxofluor. In the event, treatment of **161** and **142** with NaH / DMF gave a relatively efficient preparation of **162**, as a mixture of *cis* and *trans* isomers. The ratio of the two isomers could not be determined by the  $^{19}\text{F}$  NMR owing to signal overlap, and the  $^1\text{H}$  NMR spectrum could not be assessed because of multiple signals. It is assumed that the isomer ratio will be very close to 1 : 1.



**Scheme 2.36** Route to the 3-fluoro-7-hydroxyl diaza ring **162**.

Crystallisation was carried out on an isomeric mixture of **162** and examination of a crystal by X-ray gave the structure of the *trans* isomer (**Figure 2.23**).

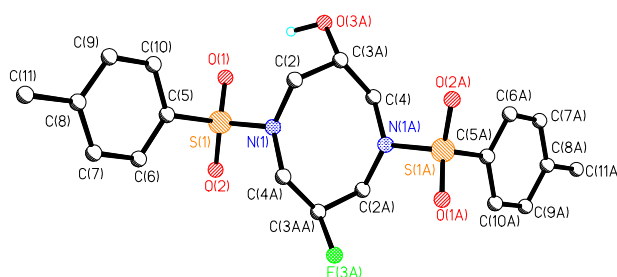


**Figure 2.23** X-ray structure of **162**.

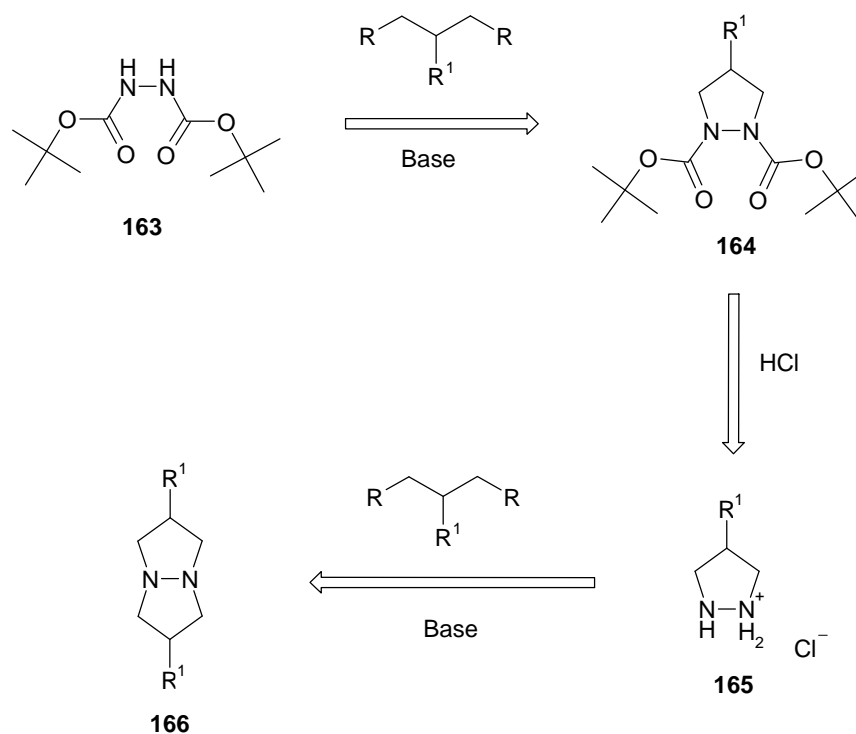
In this case, unlike that of **150**, the isomers were readily separated by column chromatography.

Fluorination of a *cis/trans* mixture of **162** with DAST again gave a predominant re-arrangement product (CH<sub>2</sub>F) as in the previous reaction with **126**. Purification by column chromatography was unsuccessful in separating the isomers.

In conclusion the 8 membered di-aza ring with a single fluorine  $\beta$  to both charged nitrogens was prepared as the hydrobromide salt **149**. The X-ray structure of **149** was determined and DFT calculations were performed on axial and equatorial fluorine conformations of the structure. Both the X-ray study and DFT analyse indicated that the fluorine has a strong axial preference and *gauche* to the charged nitrogens indicative of a strong  $\delta^- \text{F} \cdots \text{N}^+$  charge dipole interaction, consistent with the earlier conclusions of Lankin and Snyder. There is no doubt that the fluorine is constraining the conformational mobility of the ring.

**2.6.5 Strategy 3 - eight membered rings *via* cyclisation of a pyrazolidine ring**

As an alternative strategy towards the eight membered ring system, it was envisaged that a pyrazolidine ring could offer a synthetic intermediate. Further cyclisation with a C<sub>3</sub> unit such as 1,3-dibromo-propane would then generate the diazobicyclooctane **166** (Scheme 2.37). It was anticipated that the N-N bond could then be cleaved to mediate a ring expansion by hydrogenolysis.<sup>28</sup>

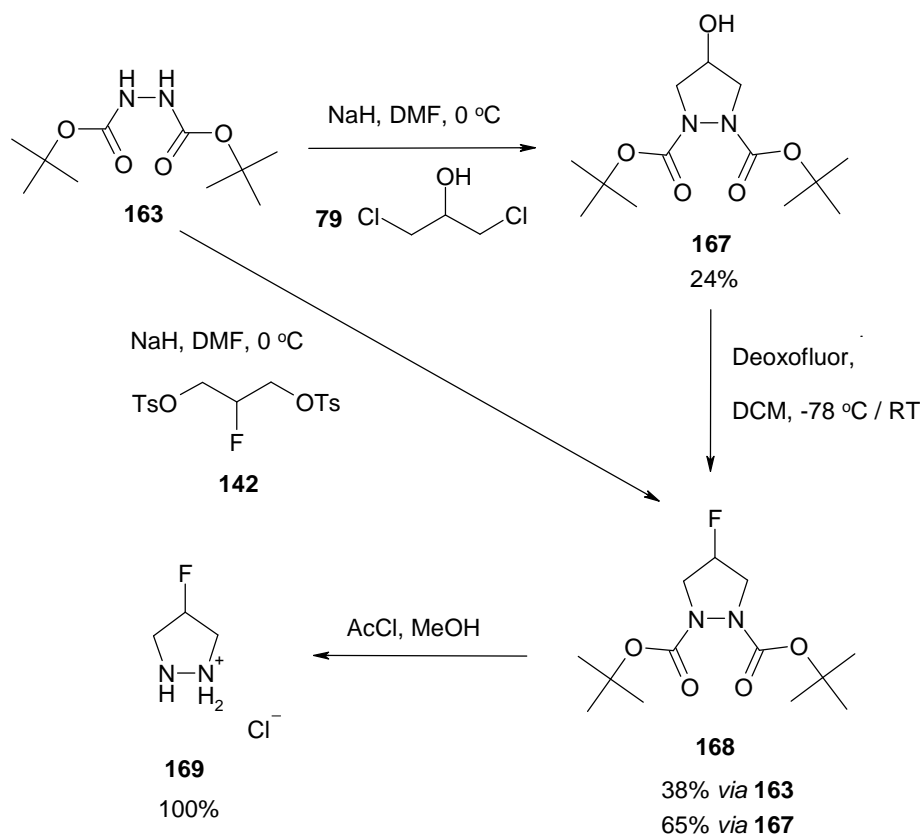


R = Br, Cl or TsO

R<sup>1</sup> = H, F, OH, OBn

**Scheme 2.37** Proposed route to a diazabicyclo octane.

A key intermediate in this study was 4-fluoro-pyrazolidine hydrochloride **169**. This was prepared *via* two different routes as shown in **Scheme 2.38**. Commercially available di-tert-butyl-hydrazodiformate **163** was treated with 1,3-dichloropropanol **79** and this afforded **167** in a modest yield. This alcohol was subsequently converted to the corresponding fluorinated product **168** after treatment with Deoxofluor. This reaction proved to be quite efficient and **168** was recovered in 65% yield. Alternatively **163** could be directly converted to **168**, by treatment with **142**, our novel fluorinated ditosylated building block. Although a modest yield of 38%, this was a little more efficient than the two step route. Pyrazolidine **168** was purified by column chromatography and with **168** in hand, removal of the Boc groups (AcCl / MeOH) proved efficient to generate hydrochloride salt **169**. This was found to be a crystalline compound, and a suitable crystal was subjected to X-ray structure analysis.



**Scheme 2.38** Routes for the preparation of **169**.

$^1\text{H}$  NMR (DMSO) variable temperature (VT) studies were carried out on the diboc precursor **168**. At RT there are four clear  $\text{NCH}_2\text{CHF}$  signals representing two rotamers due to restricted rotation around the carbamate  $(\text{O})\text{C}-\text{N}$  bonds. At  $105^\circ\text{C}$  these  $^1\text{H}$  signals broaden, presumably due to more rapid rotation on the NMR timescale.

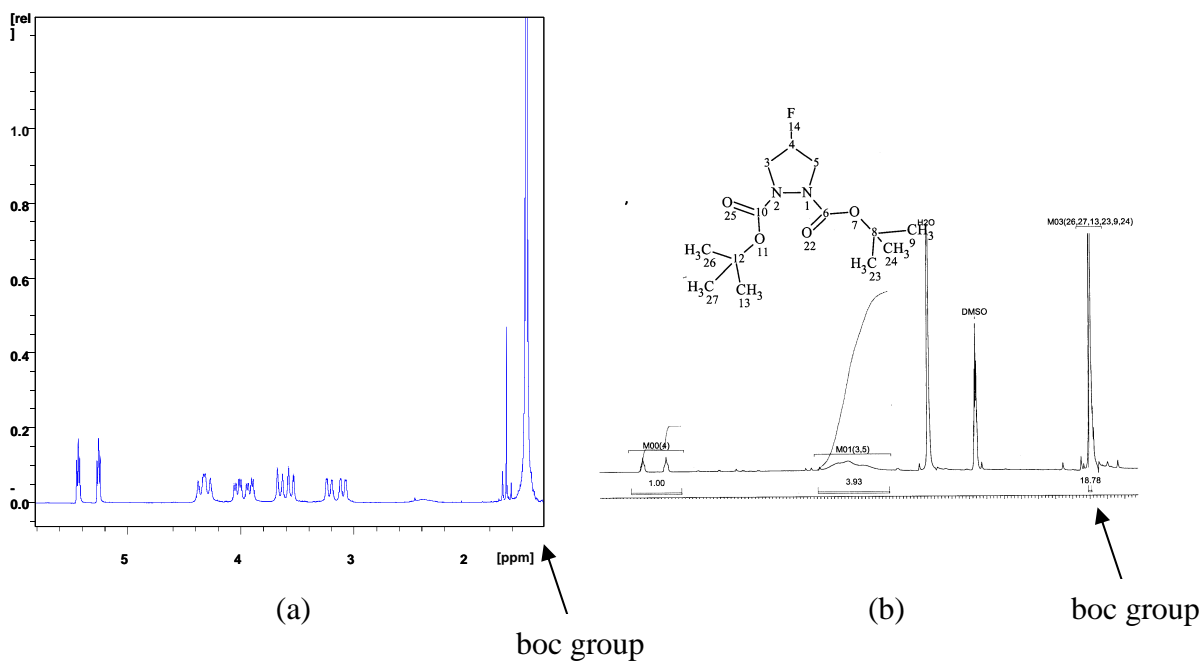


**Figure 2.24** (a)  $^1\text{H}$  NMR at RT of **168**, (b)  $^1\text{H}$  NMR at  $105^\circ\text{C}$  of **168** (DMSO).

After Boc removal the resulting pyrazolidine hydrochloride **169** was obtained and its X-ray crystal structure is shown in **Figure 2.25**.

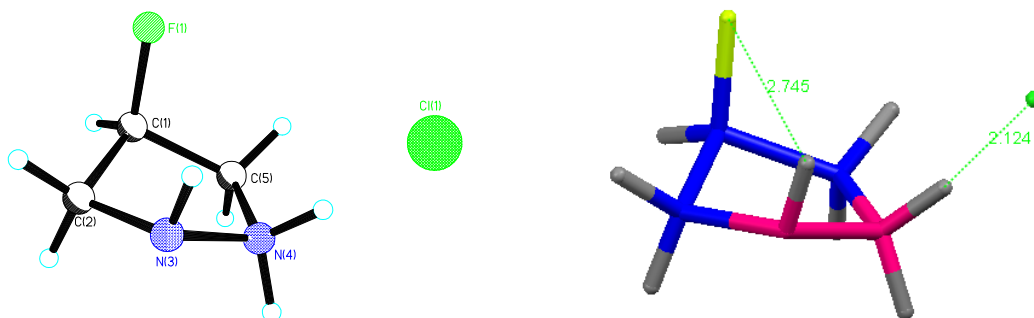


**Figure 2.25** The X-ray structure of 4-fluoro-pyrazolidine hydrochloride **169**.



It is interesting to observe the fluorine in a clear axial rather than equatorial orientation. The lone pair on the three valent N is orientated away from the fluorine atom, showing an anti-relationship between the two. Interestingly a comparison of the two F-C-C-N torsion angles shows that it is the non-protonated nitrogen which had a tighter torsion angle to the fluorine: F-C-C-NH = 77°, F-C-C-N<sup>+</sup>H = 89°, presumably a consequence of competing interactions e.g. CF----N<sup>+</sup> attraction and bond angles in the ring system.

We can compare structure **169** to that of the non-fluorinated pyrazolidinium **170** (as the azide salt) previously reported in the literature.<sup>29</sup> Analysis of this structure reveals that it is the non-protonated nitrogen which again contributes to a tighter torsion angle at 85°, compared to H<sup>1</sup>-C-C-N<sup>+</sup>H at 105° for the protonated N. But it is also notable that the corresponding torsional angle to the axial H (105°) is much wider than that in the fluorinated analogue (89°). This indicates a correspondingly tighter angle due to charge dipole attraction in the fluorinated system.

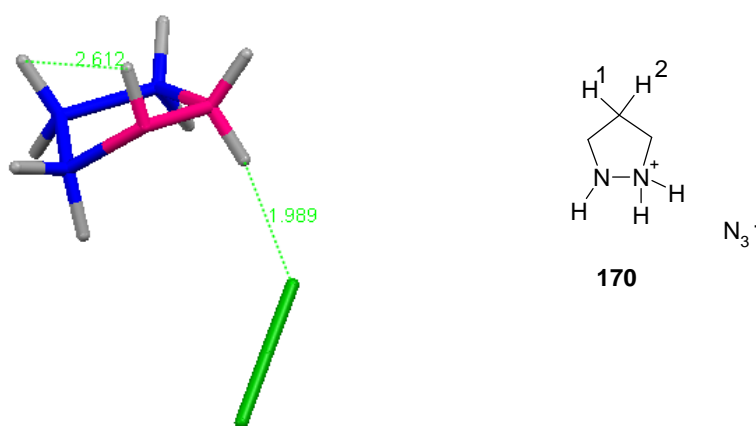


**Figure 2.26** Structure of **170**.

It may be that the different counter ions ( $\text{Cl}^-$  and  $\text{N}_3^-$ ) perturb the structures to some extent, but this is not expected to be very significant. It would appear the fluorine is influencing the conformation of the ring.

### Conversion of 4-fluoro-pyrazolidine hydrochloride **169** to the free base

The free base of **169** was easily obtained by use of a pre-packed Biotage Isolute® SCX-2 (Si-propylsulfonic acid) column: the salt was taken up into deionised water and passed through the column (**Figure 2.27**) under a low vacuum. This was then washed with deionised water followed by ammonia/ methanol (7N) solution and the fractions collected. To detect the presence of the amine, the fractions were spotted onto a TLC and those fractions which tested positive (a red spot) with ninhydrin spray were pooled and concentrated. The free base was recovered as an off white solid.

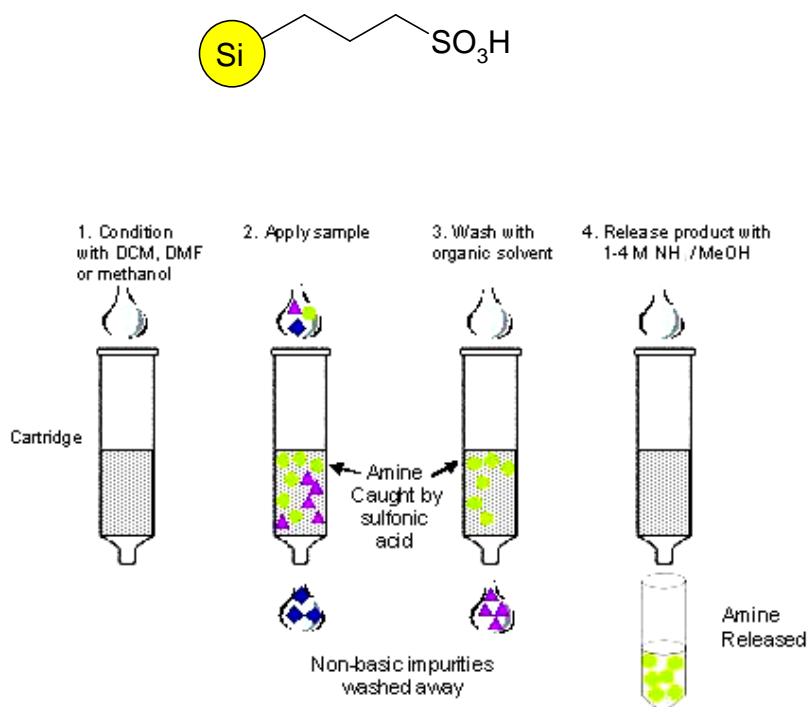
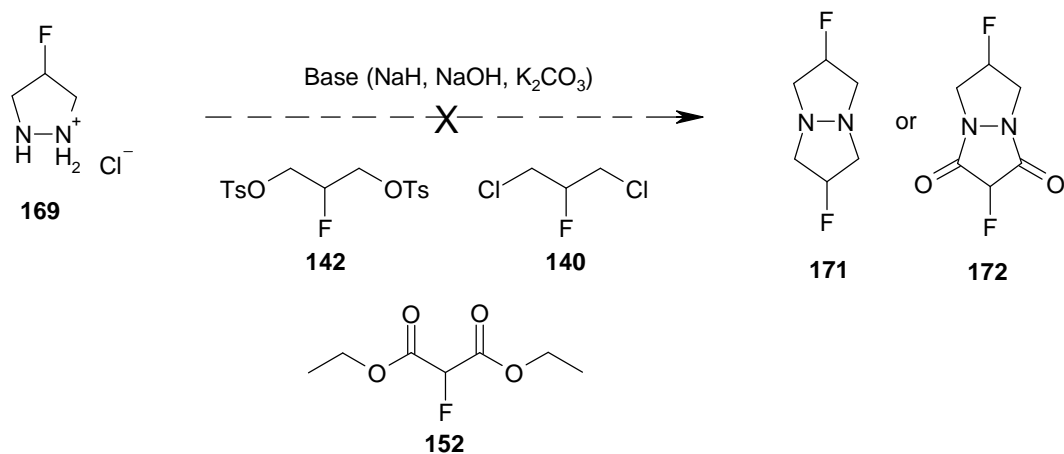


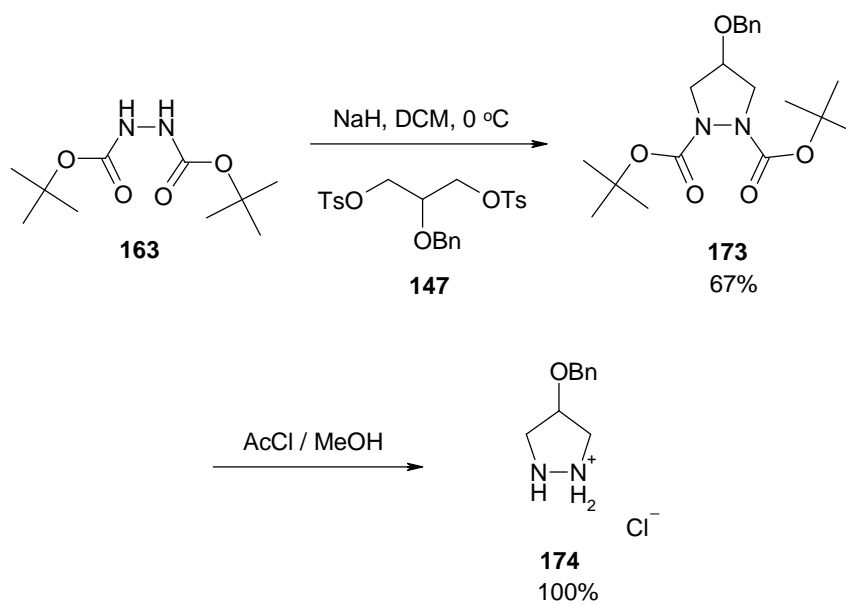
**Figure 2.27** The mechanism of the 'Catch and Release' process using SCX-2 / SCX-3.

With the fluoro pyrazolidinium **169** in hand, assembly of a second ring was attempted. After exploring a variety of methods, cyclisation proved unsuccessful (**Scheme 2.39**).



**Scheme 2.39** Cyclisation of **169** was unsuccessful.

An alternative method was investigated. It was thought that using a substrate with a bulky benzyl group would be easier to monitor and handle. The benzyl ether protected pyrazolidinium chloride **174** was therefore synthesised (**Scheme 2.40**). The intermediate **173** was prepared by ring formation between the commercially available hydrazine **163** and the previously prepared ditosylate **147**. The reaction was efficient and **173** was recovered in 67% yield. The Boc groups were then removed by straightforward acidification, which provided the pyrazolidinium as the hydrochloride salt **174**. Generation of a second ring however was once again unsuccessful, as previously experienced with the fluoro analogue **169**.



**Scheme 2.40** Synthesis of the benzyl ether analogue **174**.

## 2.7 Four membered $\beta$ -fluoro azetidinium rings

Small ring cycloalkanes possess eclipsing strain. For example cyclobutane prefers to adopt a puckered conformation to accommodate the close proximity of the vicinal hydrogens, thus reducing torsional strain which would be present in a planar conformation. (**Figure 2.28**). The angle of pucker is  $28^\circ$ .<sup>30</sup>



**Figure 2.28** The puckered conformation of cyclobutane.

Azetidine **176**, which is a liquid at room temperature, was recently crystallised<sup>31</sup> in a capillary at 170 K. The crystal was analysed by X-ray diffraction and shown to have a more planar conformation than cyclobutane. The structure also showed intermolecular N-H $\cdots$ N hydrogen bonding. The C-N-C bond is wider than the C-C-C leading to a more planar structure and the nitrogen puckers downwards slightly, allowing the NH hydrogen more steric space.

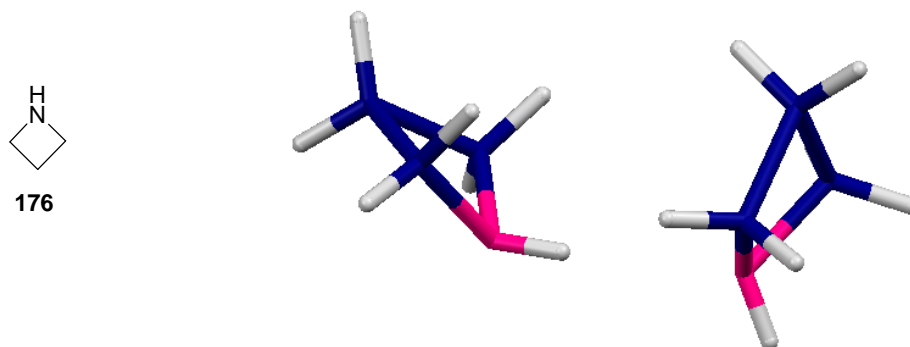


**Figure 2.29** The X-ray structure of azetidine **176**.

The alcohol, 3-azetidinol **177** has a higher melting point (114 °C) than **176**, due to intermolecular hydrogen bonding from the OH. The crystal structure <sup>32</sup> of **177** also revealed a puckered conformation for the azetidine ring and again the ring puckers presumably to accommodate the steric requirements of the NH hydrogen.

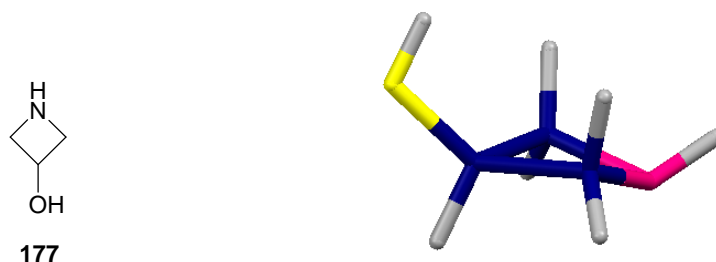


**Figure 2.30** The X-ray structure of 3-azetidinol **177**.

It is now interesting to compare the free base **176** with the salt **178**. Azetidinium perchlorate **178** has been crystallised and the resultant X-ray structure was found to adopt a perfectly planar conformation.<sup>33</sup> Here the preferred conformation is planar because of the symmetry of the molecule.

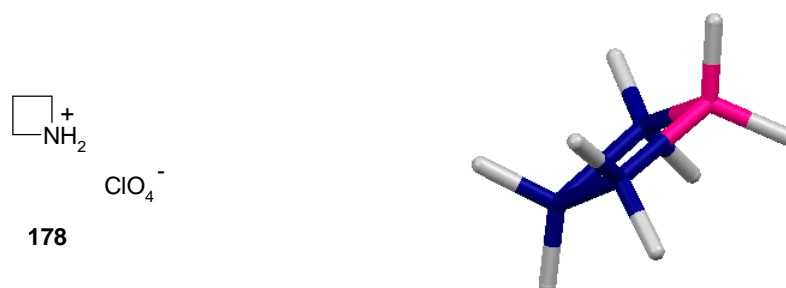


**Figure 2.31** The X-ray crystal structure of azetidinium perchlorate **178**.<sup>33</sup>

### 2.7.1 Evaluation of azetidinium hydrobromide by X-ray analysis

In order to explore an alternative counter ion to perchlorate, crystallisation of azetidinium hydrobromide was carried out in our study. The chloride salt is a yellow powdery solid and was not soluble in water and it proved difficult to dissolve in methanol or ethanol. However crystallisation was successful with the hydrobromide salt **179**, which was obtained after treatment of **176** with HBr in water (48%). A successful crystallisation was achieved from ethanol and ether. Subsequent analysis of this salt by X-ray crystallography again revealed a perfectly planar ring structure with 0° torsion angles, thus the counter ion ( $\text{ClO}_4^-$ ,  $\text{Br}^-$ ) has no effect on the ring conformation:

C(4)-N(1)-C(2)-C(3)	0.0°	N(1)-C(2)-C(3)-C(4)	0.0°
C(2)-N(1)-C(4)-C(3)	0.0°	C(2)-C(3)-C(4)-N(1)	0.0°

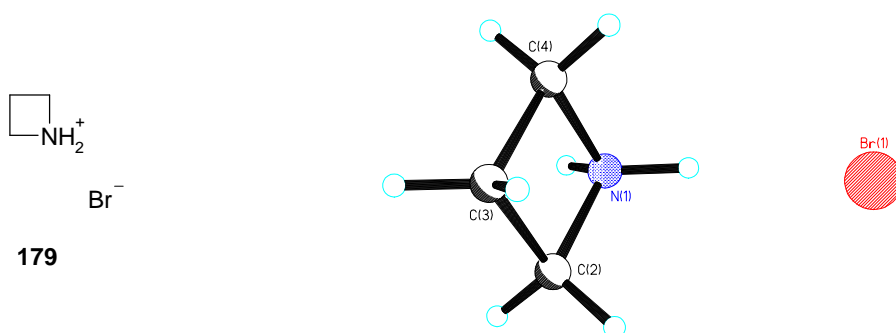
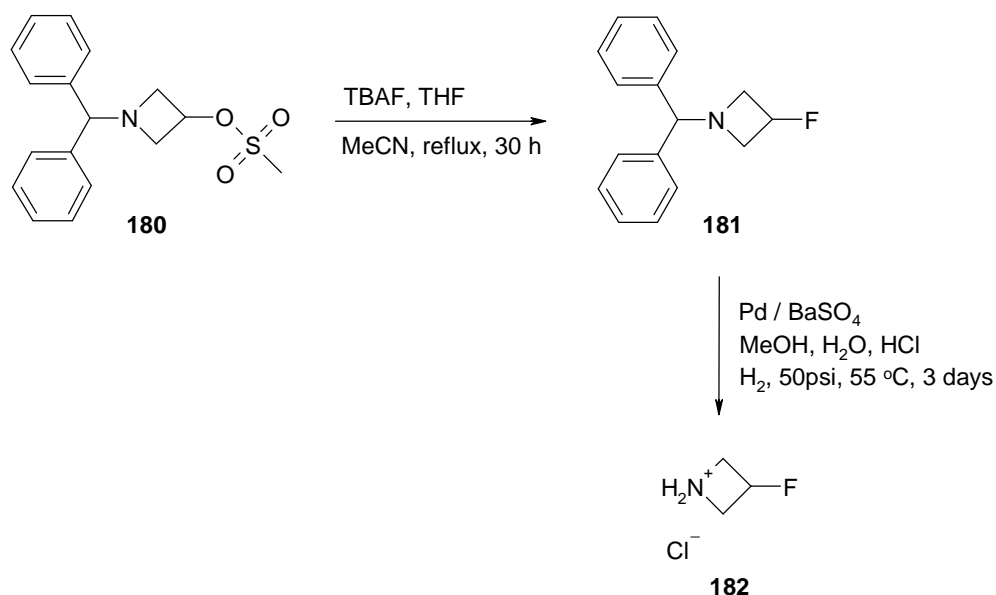


**Figure 2.32** The planar X-ray crystal structure of hydrobromide salt **179**.

### 2.7.2 X-ray analysis of 3-fluoroazetidinium hydrochloride and hydrobromide

In the context of this thesis it was of interest to investigate the effect of a fluorine atom on the ring conformation of an azetidinium salt. A sample of 3-fluoroazetidinium hydrochloride **182** was kindly provided by Steve Sollis at GlaxoSmithKline. This had previously been synthesised by Nathalie Valette within the company by the following route:<sup>34</sup>



**Scheme 2.39** GSK route to **182** .

3-Fluoroazetidinium hydrochloride **182** was subjected to X-ray diffraction analysis. The structure is shown in **Figure 2.33**. It is immediately apparent that the ring is puckered, and no longer planar, with a 6° deviation from planarity. The C-F $\cdots$ C-N<sup>+</sup> torsion angle is 107°, whereas the corresponding C-H $\cdots$ C-N<sup>+</sup> angle in **182** is wider at 116°.



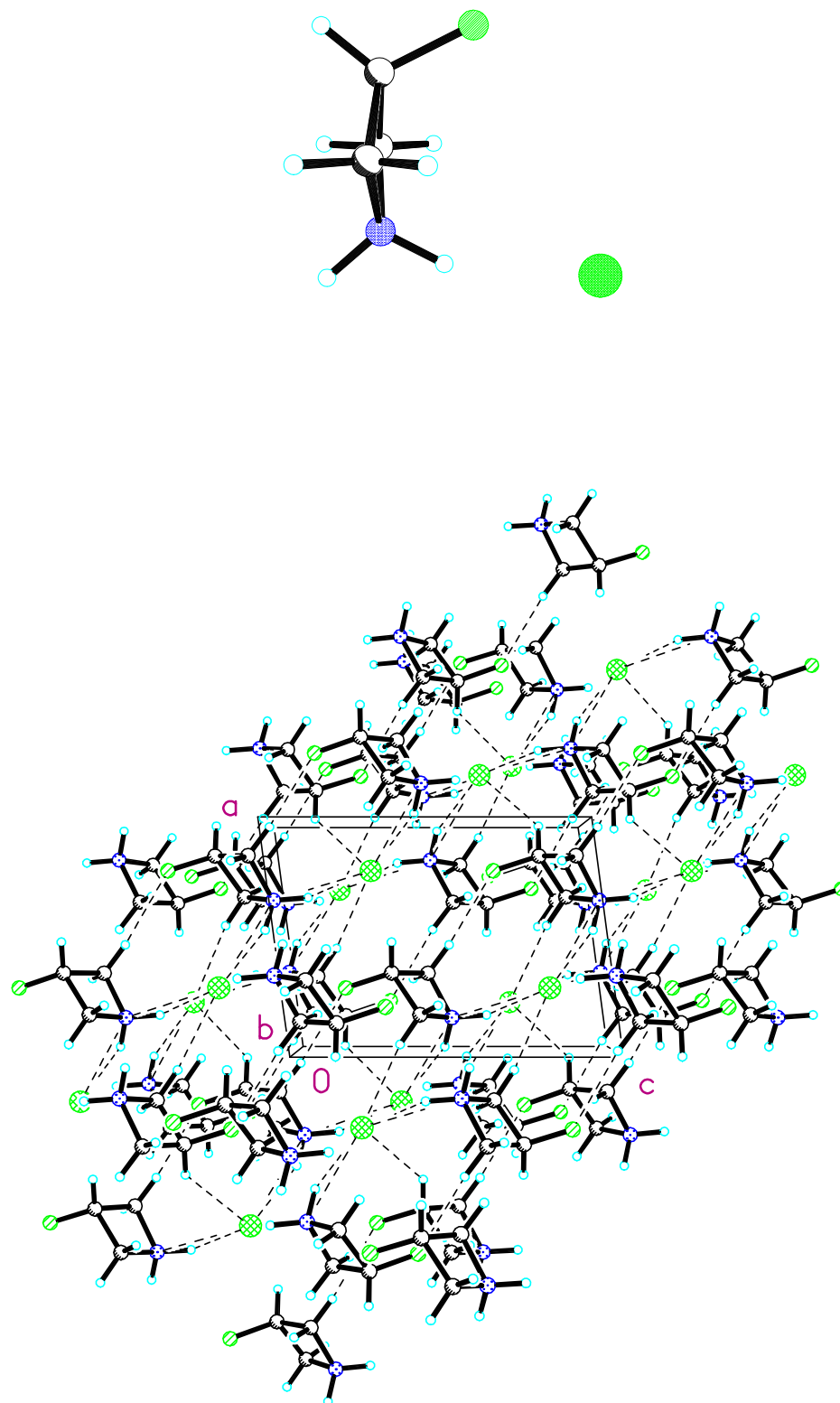


**Figure 2.33** X-ray structure and crystal packing of 3-fluoroazetidinium hydrochloride **182**.

$^{19}\text{F}$  NMR analysis generated a spectrum showing an AA'BB'CX system. The coupling constants:  $^2J_{\text{HF}} = 56.3$  Hz,  $^3J_{\text{HF}} = 22.0$  Hz and  $^3J_{\text{HF}} = 20.9$  Hz were extracted by simulation.

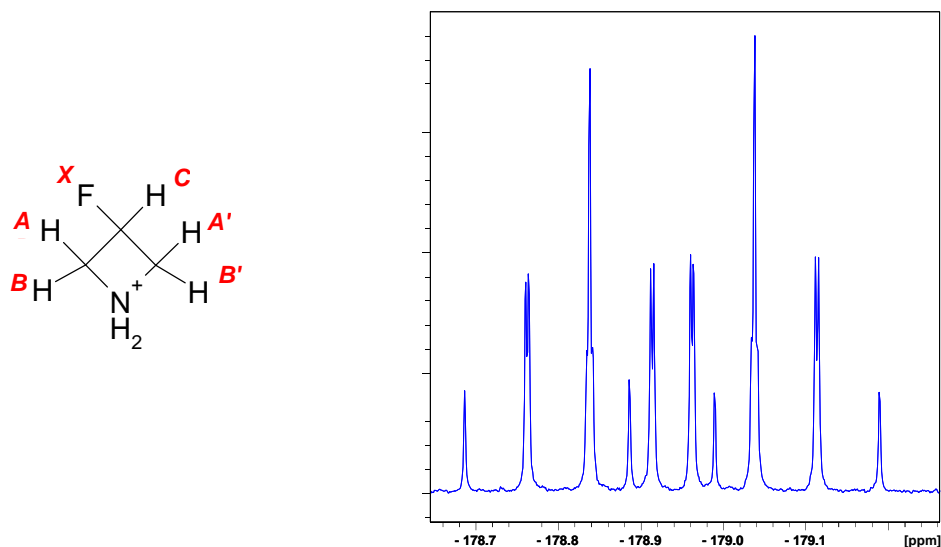


**Figure 2.34**  $^{19}\text{F}$  NMR spectrum of **182**.

For a direct comparison of structure **182** with the azetidinium salt **179** which has a bromide counter ion, the fluoro-azetidinium chloride was converted to its hydrobromide salt **183** by dissolving in aqueous HBr (48%). The aqueous was removed under reduced pressure and the salt was crystallised from ethanol and ether. Subsequent X-ray crystallography gave a structure for the hydrobromide salt **183**. The ring was also puckered, although only less so with a deviation from planarity of  $1.4^\circ$ . It appears the bromide may shield the electrostatic attraction between F and  $-\text{N}^+\text{H}_2$  a little, or there may be a different requirement for packing due to its larger size. This structure has a F-C-C-N torsion angle of  $113^\circ$ . The striking feature of these salts relative to azetidinium hydrobromide **179** is that they are non-planar and that the 4 membered ring is puckered towards fluorine, even though the fluorine is sterically more demanding than hydrogen.

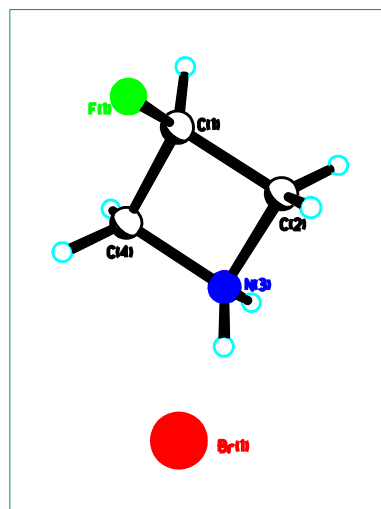
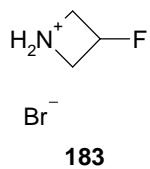
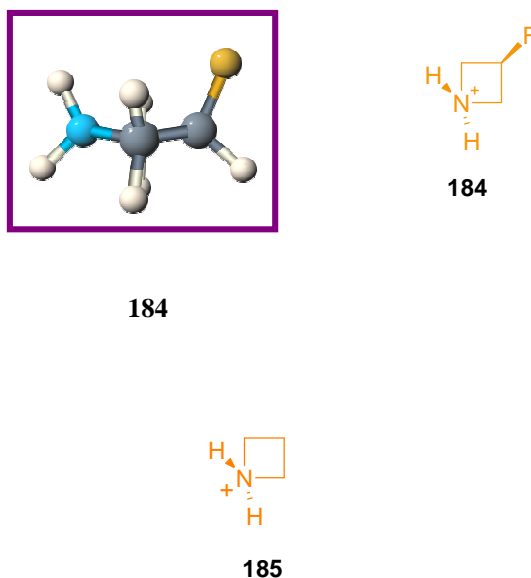


**Figure 2.35** X-ray crystal structure of 3-fluoroazetidinium hydrobromide **183**.

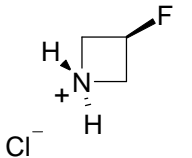
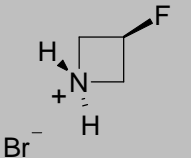
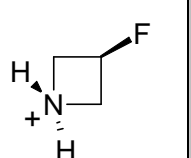
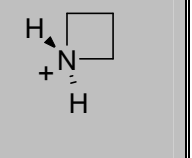
### 2.7.3 Theoretical evaluation of the 3-fluoroazetidinium conformation

Various forms of the 3-fluoroazetidinium ring were analysed by our collaborators, Dr David Tozer and Andrew Teale at The University of Durham.<sup>35</sup>

X-ray co-ordinates from the 3-fluoroazetidinium hydrochloride **182** structure were provided as a starting point for the calculations. DFT calculations on the 3-fluoroazetidinium cation **184** again revealed a puckered structure (**Figure 2.36**) although clearly counter ions are not considered in the theoretical structure. In this case the F-C-C-N<sup>+</sup> torsion angle is 100°, and much tighter than the hydrochloride and hydrobromide. It may be that the counter ions are partially shielding the electrostatic attraction, which results in a little angle widening in the experimental systems. The X-ray and DFT derived torsion angles are compared in **Table 2.2**.



**Figure 2.36** DFT analysis shows the 3-fluoroazetidinium cation **184** puckers to a greater extent than the azetidinium cation **185**.

	 $\text{Cl}^-$ <b>182 (X-ray)</b>	 $\text{Br}^-$ <b>183 (X-ray)</b>	 <b>184 (DFT)</b>	 <b>185 (DFT)</b>
F1-C1-C2-N3	107°	113°	<b>100.0°</b>	
H1-C1-C2-N3	122°	116°		<b>102.3°</b>

**Table 2.2** F-C-C-N and H-C-C-N torsion angles for **182** and **183**, **184** and **185**.

To further assess the effect of the positive charge on the conformation of the 3-fluoroazetidinium ring, in a theoretical experiment an extra electron was ‘added’ to **184** to generate a neutral, but protonated 3-fluoroazetidinium ring **186**. The nitrogen is now neutral. This is a hypothetical structure which can only be explored by theory, however it provides a very useful insight into the importance of the charge. The structure shows that the ring inverts, puckering now in the opposite direction with the fluorine on the more open face of the ring. This shows that there is no electrostatic attraction between F and H, and now the slightly larger size and steric influence of the fluorine is dominating the conformation.

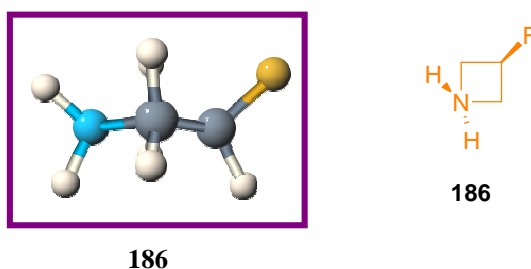
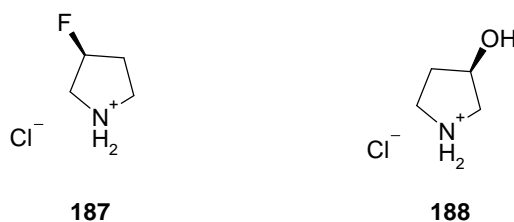


**Figure 2.37** The theoretical non-charged system **186**.

## 2.8 Conformation of $\beta$ -fluoro pyrrolidinium rings

It was of interest to extend the four membered ring study to the 3-fluoropyrrolidinium hydrochloride salt **187**. By way of a comparative study the pyrrolidinium ring systems with F, OH and H at the 3-position were evaluated. In this way the fluorine can be compared directly with OH and H, and as discussed in Chapter 1, fluorine has properties associated with each of these substituents. Both (*S*)-(+)-3-fluoropyrrolidine hydrochloride **187** and (*R*)-(-)-3-pyrrolidinol hydrochloride **188** were obtained commercially (Aldrich) and they were submitted for X-ray crystallography analysis. Interestingly the X-ray structure of **187** had never been previously reported.



The resultant crystal structures are shown in **Figure 2.38** below. Both structures have F and OH substituents in a clear axial orientation. The fluoropyrrolidine structure **187** had a N-C-C-F torsion angle of 81.0° and the pyrrolidinol structure **188** (N-C-C-O) has a similar torsion angle at 82.4°, suggesting similar electrostatic interactions for F and O. 3-fluoropyrrolidine **187** has a mean ring plane of 25.5°, 3-pyrrolidinol **188** is similar with a mean plane of 27.0°.

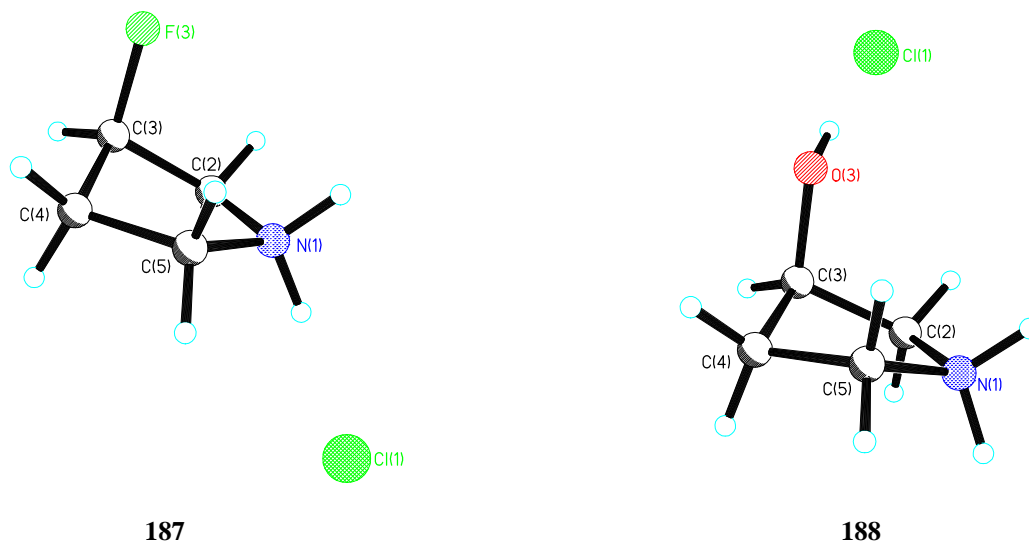


**Figure 2.38** X-ray structures for **187** and **188**.

If we compare these structures with those of the non-fluorinated, parent pyrrolidine salt **189** it is clear that the presence of a  $\beta$ -fluorine or  $\beta$ -hydroxyl strongly alters the ring conformation, bringing the C-F and C-O bonds closer to the charged nitrogen. Thus electronic/electrostatic interactions dominate these structures rather than sterics. It is interesting too that the hydroxyl group behaves like fluorine, rather than the structure being dominated by the consequences of intramolecular hydrogen-bonding. A search of the Cambridge Structural Database reveals several structures of the pyrrolidinium ring system. Both planar and slightly twisted forms of protonated pyrrolidine are deposited with various counter ions.<sup>36, 37</sup> For example two conformations for the pyrrolidinium rings **189** with a dinitronate counter ion are present in one structural study.<sup>36</sup> One of the rings is essentially planar and the other has a puckered conformation deviating  $12^\circ$  from the plane. The F and OH result in a substantial ring pucker.

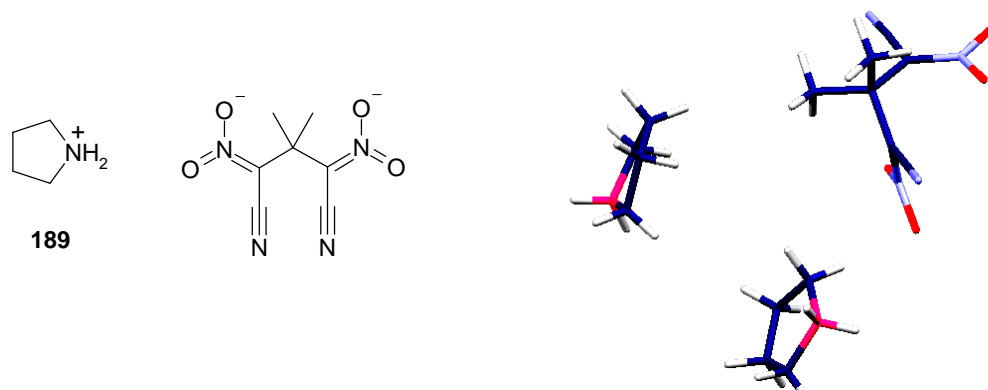


**Figure 2.39** The pyrrolidinium salt **189** is known to have an almost planar structure.

Another system, pyrrolidinium hexachloro-antimonate **190**<sup>37</sup> has been subjected to X-ray crystallography (twice). One pyrrolidinium ring was found to be planar ( $0.0^\circ$ ) (shown in Figure 2.40 in red), while the other deviated from the plane by  $17^\circ$ . Again it appears that the 5 membered ring varies a little in conformation, even with an identical counter ion.

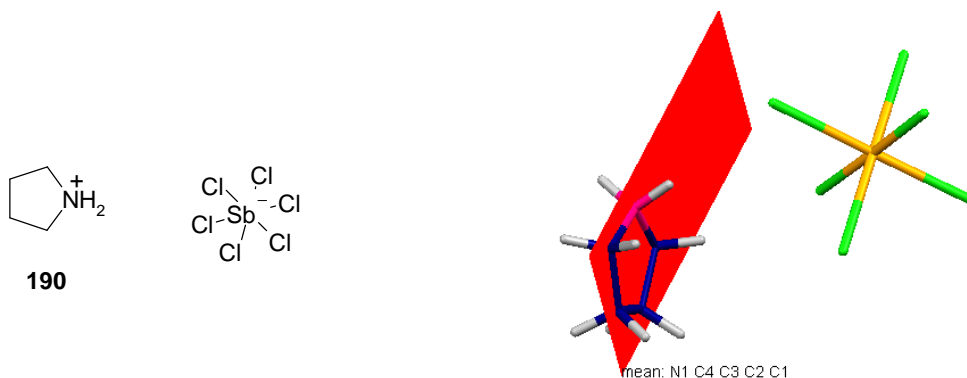


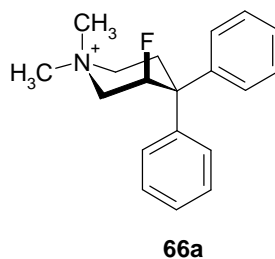
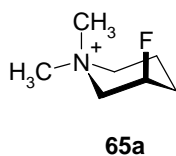
**Figure 2.40** The mean plane ( $0.0^\circ$ ) of **190** is shown in red.

Thus it is clear that in this case fluorine is behaving very similarly to the hydroxyl substituent, and differently from hydrogen. The cases of fluorine and hydroxyl can be interpreted in terms of intramolecular charge dipole interactions. This relationship between fluorine and the hydroxyl group is developed in the next section.

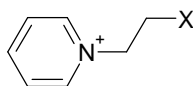


## 2.9 An electrostatic *gauche* effect in $\beta$ -fluoro- and $\beta$ -hydroxy- N-ethylpyridinium cations

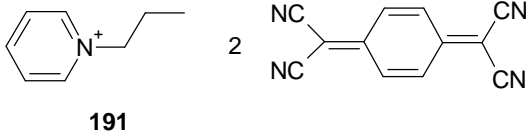
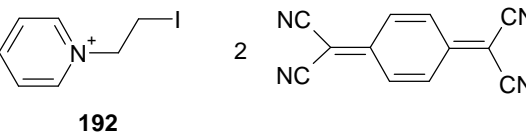
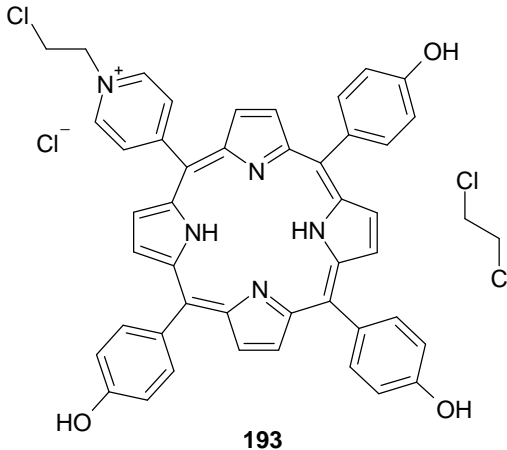
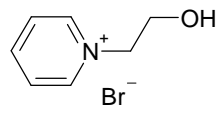
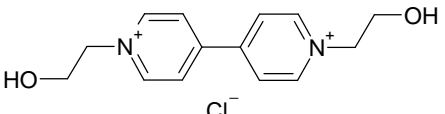
Prior to this study no data had emerged which focused on the electrostatic *gauche* effect with quaternary but non-protonated amines other than the work of Lankin and Snyder<sup>3</sup> (**Chapter 2, section 2.1**). Their systems do not differentiate between charge dipole interactions and the possibility of C-F----H-N<sup>+</sup> hydrogen bonding interactions.



In this study it was decided to explore N-alkylated pyridinium salts as a form of non-protonated quaternary nitrogens.

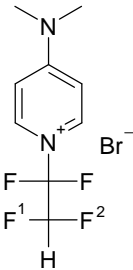
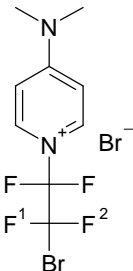


A search of the Cambridge Structural Database (CSD) provides some relevant information for N-alkylated pyridinium compounds but without a fluorine atom. The torsion angles between the N<sup>+</sup> and the X substituent  $\beta$  to the nitrogen was measured and is provided in **Table 2.3**. The Me and I substituents are *anti* whereas the Cl and OH substituents are *gauche*.

	Substituent	N <sup>+</sup> -C-C-X Torsion angle
 <p><b>191</b></p>	CH <sub>3</sub>	X = H 176.1° <sup>38</sup>
 <p><b>192</b></p>	I	X = I 173.7° <sup>39</sup>
 <p><b>193</b></p>	Cl	X = Cl 60.8° <sup>40</sup>
 <p><b>194</b></p>	OH	X = OH 63.5° <sup>41</sup>
 <p><b>195</b></p>	OH	X = OH 64.8° <sup>42</sup>

**Table 2.3** Torsion angles for pyridinium N<sup>+</sup>-C-C-X species from the CSD data base.

The structures of the multiply fluorinated pyridinium salts **196** and **197** (Table 2.4) have also been solved. Both molecules contained two fluorine atoms at  $\beta$  positions to the charged nitrogen.<sup>43</sup> Analysis of their X-ray structures show that in the case of **196** it is hydrogen and not one of the two fluorine atoms which is *anti* to  $N^+$ . This is not expected on steric grounds but is consistent with the electronic argument. In the case of **197**, the large bromine is found *anti* to the  $N^+$ , as expected on steric grounds, and the fluorines occupy *gauche* positions, consistent with developing electronic arguments.

	Torsion angle $N^+-C-C-X$
 <p style="text-align: center;"><b>196</b></p>	<p style="text-align: center;">57.4° (F<sup>1</sup>)</p> <p style="text-align: center;">58.7° (F<sup>2</sup>)</p> <p style="text-align: center;">179.5° (H)</p>
 <p style="text-align: center;"><b>197</b></p>	<p style="text-align: center;">57.8° (F<sup>1</sup>)</p> <p style="text-align: center;">57.9° (F<sup>2</sup>)</p> <p style="text-align: center;">180.0° (Br)</p>

**Table 2.4** The torsion angles of the N-ethyl substituents in **196** and **197**.

### 2.9.1 N-Ethylpyridinium targets

The N-ethylpyridinium compounds shown in **Figure 2.41** were identified as synthetic targets for X-ray structural studies. It was anticipated that the influence of the fluorine will be examined by determining the torsion angle between the  $\beta$  fluorine atom and the charged nitrogen.

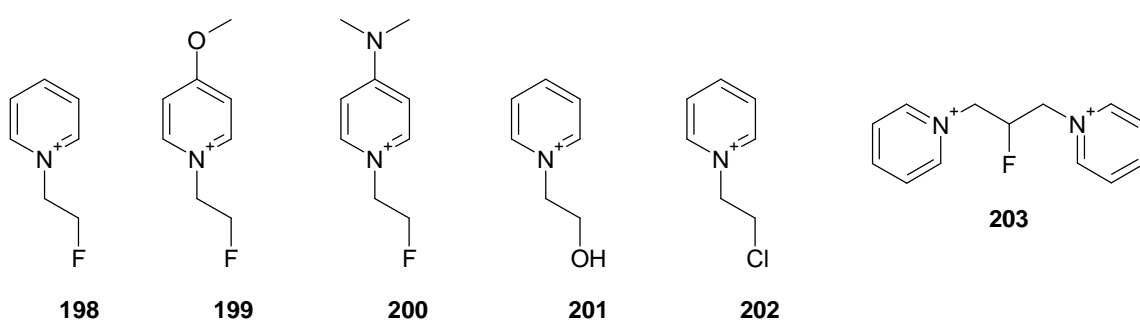
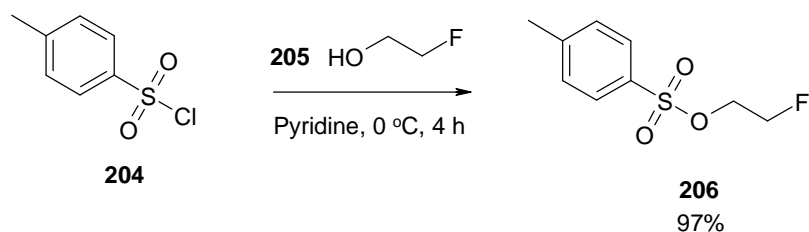


**Figure 2.41** N-alkylpyridinium rings as synthetic targets.

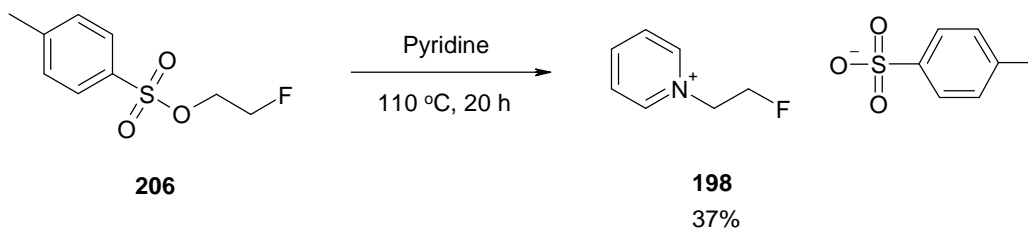
### 2.9.2 Synthesis of fluoro N-ethylpyridinium salts

It was necessary to obtain a suitable reagent for attachment of the fluoroethyl substituent to pyridine and it was envisaged that this could be achieved by activation of fluoroethanol. 2-Fluoroethylpyridinium bromide had previously been prepared in a reaction between pyridine and 1-bromo-2-fluoroethane.<sup>44</sup> Unfortunately this useful fluorinated reagent is no longer commercially available as it is classed as an ozone depleter. Accordingly 2-fluoroethyltosylate **206** was prepared following a literature procedure<sup>45</sup> and this was used as an alkylating reagent to access **198**, **199** and **200**.



**Scheme 2.40** Preparation of 2-fluoroethyltosylate **206**.

2-Fluoroethyltosylate was then heated in dry pyridine to generate **198**. Crystals suitable for X-ray crystallography were obtained by ensuring all traces of moisture had been removed and then crystallisation was achieved from ethanol and with slow migration of ether.



**Scheme 2.41** Preparation of the 1-(2-fluoro-ethyl)-pyridinium salt **198**.

The resultant X-ray crystal structure of **198** is shown in **Figure 2.42**. Interestingly the counter ion is Na 2(4-methylbenzenesulfonate). Sodium appears to have been introduced from the  $\text{Na}_2\text{CO}_3$  and  $\text{NaCl}$  solutions during work-up. The most obvious aspect of the structure relevant to this study is that the C-F bond aligns *gauche* to the C-N<sup>+</sup> bond, with a F-C-C-N<sup>+</sup> torsion angle of 68.1°. No intramolecular fluorine-hydrogen bonding is obvious.

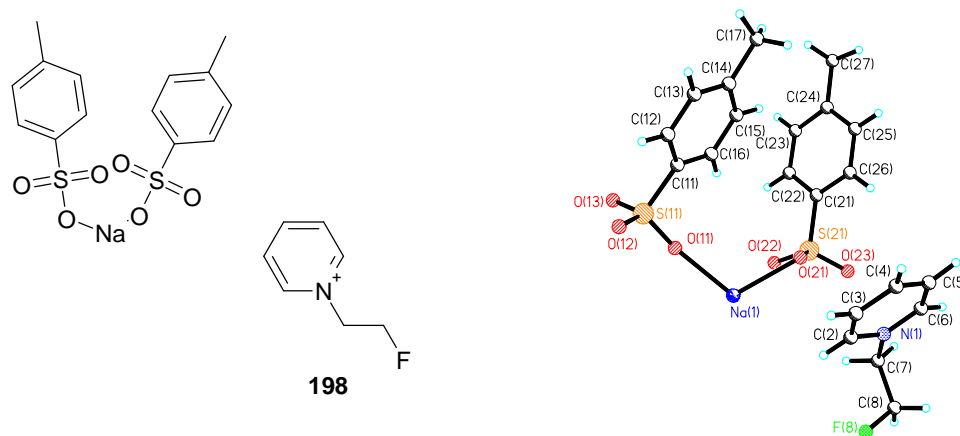


**Figure 2.42** X-ray crystal structure of **198**.

DFT calculations on **198** were carried out by Dr D. Tozer and Michael Peach at the University of Durham. They compared the energy differences between the *gauche* and *anti* conformers of **198** using the X-ray co-ordinates as a start point for their calculations. They found the relative ground state energy difference between the *anti* and *gauche* conformations of **198** be  $3.7 \text{ kcal mol}^{-1}$ , with a lower energy preference for the *gauche* conformer. This is the conformer observed in the X-ray diffraction study, and is entirely consistent with our charge dipole interaction hypothesis.

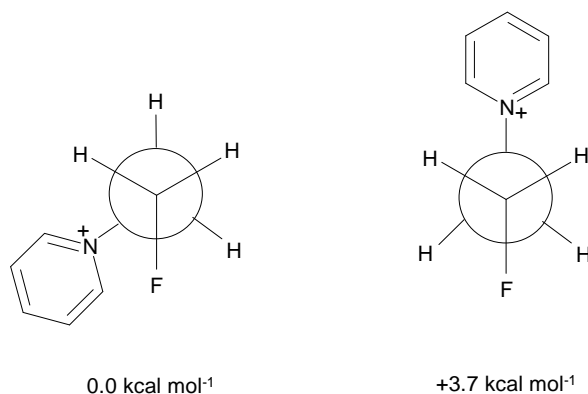
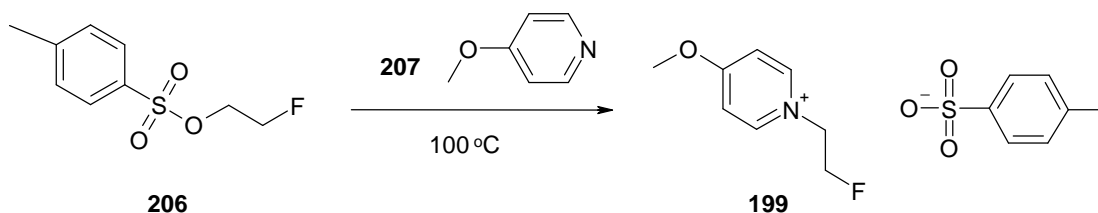


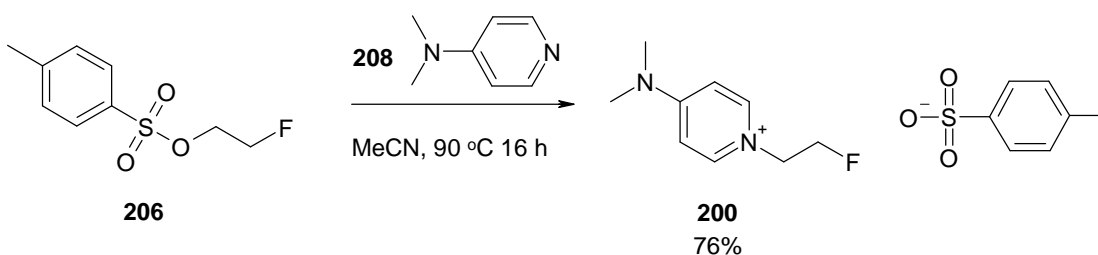
**Figure 2.43** Newman projections of the rotomers of *gauche* and *anti* **198**. The energy values emerge from DFT calculations (D. Tozer and M. Peach).

In order to examine the effect of an electron donating group the methoxy-pyridine analogue **199** was synthesised. It was thought that this could substantially neutralise the charge on the pyridinium nitrogen. However in this case the product was a liquid and no crystals could be obtained for X-ray diffraction studies.



**Scheme 2.42** Synthetic route to afford **199**.

An alternative electron donating group was explored and the pyridinium salt **200**, having a *p*-dimethylamino group presented an attractive system to study. Accordingly the 4-dimethylaminopyridine (DMAP) analogue was synthesised *via* a similar process to that of **198**. To enable DMAP **208** to become dissolved in the reaction, acetonitrile was employed as the solvent.



**Scheme 2.43** Preparation of **200**.

On work-up crystals of **200** were obtained from ethanol and ether. A suitable crystal was identified and X-ray crystallography generated the structure shown in **Figure 2.44**. In this case the F-C-C-N<sup>+</sup> torsion angle is 59.0°, consistent with a perfect *gauche* conformation. Thus the presence of the dimethylamino group does not override the electrostatic attraction between fluorine and N<sup>+</sup> in the solid state. Interestingly DFT calculations (University of Durham) estimate that the energy difference between the *gauche* and *anti* conformation for **200** is 3.1 kcal mol<sup>-1</sup>. So there is a reduction in the relative energy compared to **198**, but it is not sufficient to induce a repulsive effect.

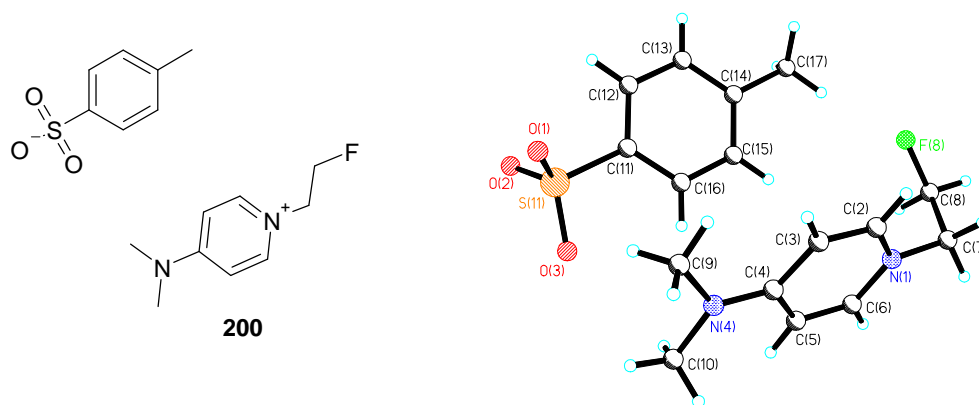
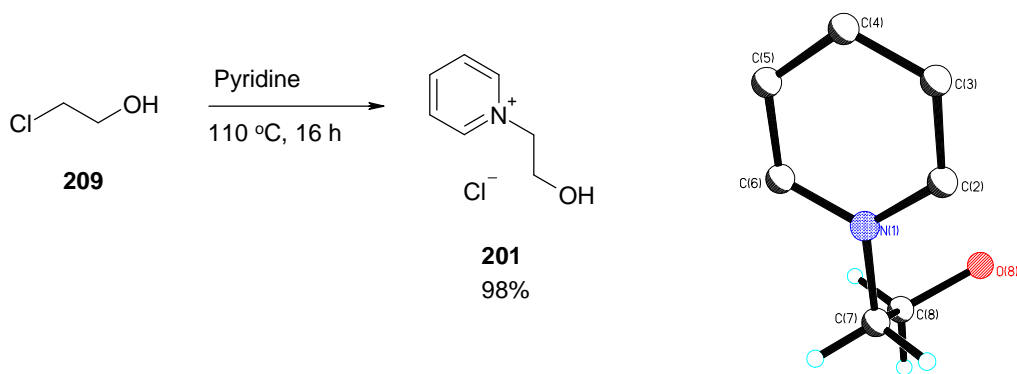


**Figure 2.44** X-ray crystal structure of **200**.

### 2.9.3 Synthesis and evaluation of the hydroxyl pyridinium salt

To extend the comparison of fluorine with a hydroxyl group the hydroxyl ethylpyridinium salt **201**, was prepared. This was achieved in a one step reaction by treatment of chloroethanol with pyridine. This salt has been synthesised previously and is reported in the literature, although the X-ray crystal structure of this chloride salt was not previously determined.<sup>46, 47</sup>





**Scheme 2.44** Preparation of **201** and its X-ray structure.

This gave rise to a crystalline chloride salt, a suitable crystal was selected for X-ray structure analysis and the resultant structure is shown above. Again a *gauche* conformation is observed with a HO-C-C-N<sup>+</sup> torsion angle of 61.2°. Both the fluorine and hydroxyl substituents have very similar conformations in these systems.

The bromide salt **194** has been previously prepared by combination of 2-bromoethanol and pyridine.<sup>48</sup> The crystal structure of the bromide<sup>41</sup> reports a very similar HO-C-C-N<sup>+</sup> torsion angle to that of the chloride salt with a value of 63.5°.

DFT calculations were carried out on **201** to measure the ground state energy difference between the *gauche* and *anti* conformations. Again the crystallographic co-ordinates were used as the starting point. Interestingly an identical value to **198** of 3.7 kcal mol<sup>-1</sup> in favour of the *gauche* conformer emerged.

A further calculation was carried out to explore the effect the positive charge on the conformation. Again in a hypothetical experiment an ‘electron’ was added to the system, to provide a neutral molecule. The energy difference now, between the *gauche* and *anti* conformers dramatically reduced to 0.05 kcal mol<sup>-1</sup> (**Figure 2.45**), indicating clearly that it is the positive charge on nitrogen that induces the large *gauche* preference in these salts.

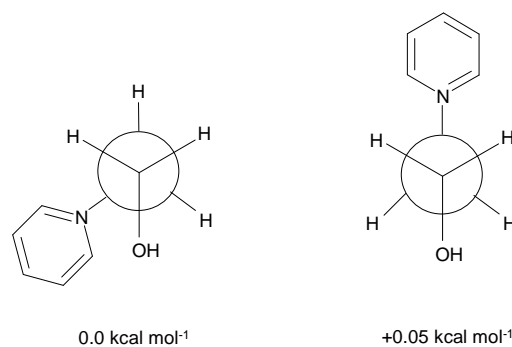
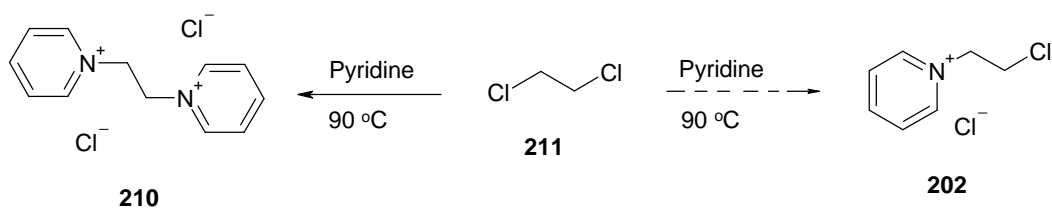


**Figure 2.45** Newman projections of the *gauche* and *anti* conformers of neutral **201** with an ‘extra electron’.

### 2.9.4 Synthesis of the chloro pyridinium salt

With the structures of the 2-fluoro **198** and 2-hydroxyl **201** ethylpyridinium salts evaluated, it appeared appropriate to prepare the chlorinated analogue **202**. This was attempted by combination 1,2-dichloroethane and pyridine at 90 °C.



**Scheme 2.45** The synthesis of **202** failed giving **210** as the major product.

Upon crystallising the product, small white needles were obtained. X-ray crystallography revealed an unexpected structure which was 1,1'-(ethane-1,2-diyl)dipyridinium dichloride **210**. The compound adopts a very clear *trans* conformation of the two pyridinium rings.

This is perhaps as one would expect where the positively charged nitrogens will repel each other electronically and the rings will avoid each other on steric grounds.

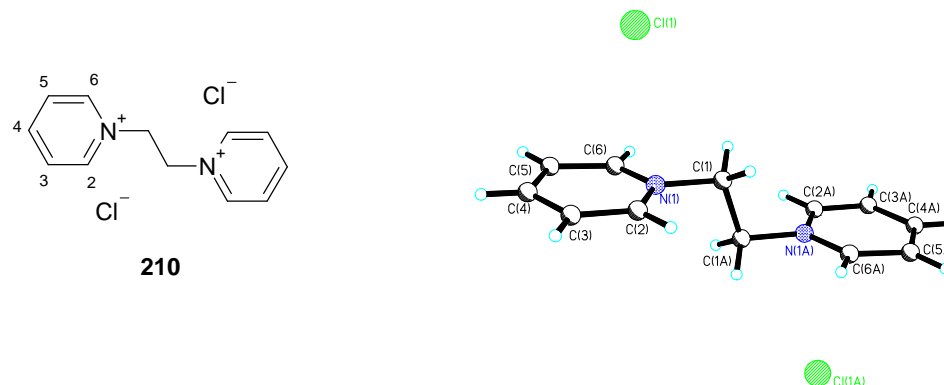


**Figure 2.46** X-ray crystal structure of **210**.

The 2-chloroethyl pyridinium salt **202** was then successfully purified from the residue by decanting off **210**, unfortunately suitable crystals of this product could not be obtained for X-ray studies. Because of the difficulty in preparing 1-(2-chloroethyl)pyridinium chloride **202**, a search on the CSD was carried out to explore related structures. Only one compound relevant to the study was found, and its structure is shown in **Figure 2.47** below and **Table 2.3**.<sup>40</sup> The crystalline salt was most probably prepared by treatment of the precursor pyridine with 1,2-dichloroethane because the reagent is present in the product in a 1:1 stoichiometry. The chlorines are *trans* in the crystal structure of 1,2-dichloroethane, and the Cl-C-C-N<sup>+</sup> torsion angle in the pyridine is measured at 60.8°. So the chlorine is sufficiently attracted to the positive nitrogen *via* an electrostatic interaction rather than the conformation being dominated by steric repulsion. Steric repulsion of the chlorines however dominates the conformation of 1,2-dichloroethane in this case.

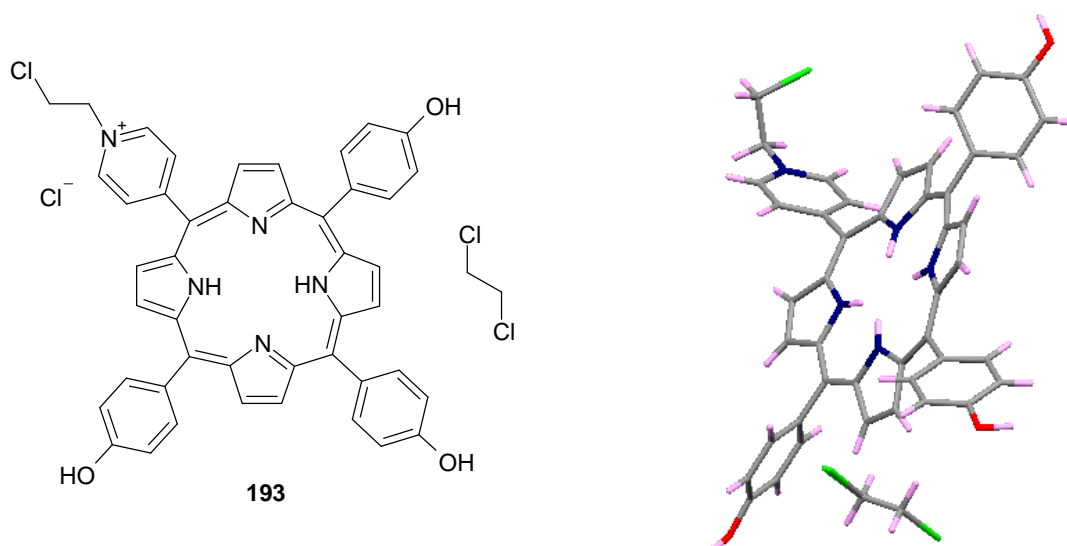
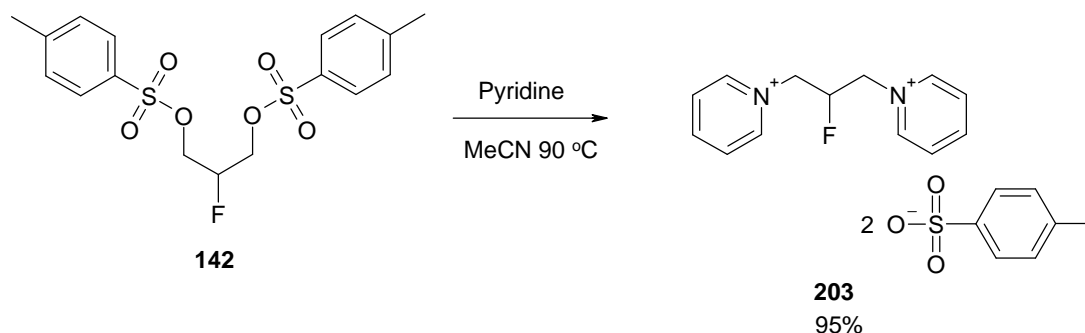


**Figure 2.47** X-ray diffraction studies found **193** to have a Cl-C-C-N<sup>+</sup> torsion angle of 60.8° and a Cl-C-C-Cl angle of 180°.

### 2.9.5 Synthesis of the fluoro bis-pyridinium salt

With previously prepared **142** in hand (section 2.6.3), this alkylating agent was treated with pyridine to generate a bis- salt, with a single fluorine  $\beta$  to two N<sup>+</sup> pyridinium atoms. It is interesting to consider the conformational preference when the bulky pyridinium species compete for the single electronegative fluorine. Accordingly crystallisation was accomplished after treating the tosylate salt **203** with aqueous HBr and removal of water by freeze drying. The resultant solid was crystallised from ethanol and ether and X-ray crystallography was carried out. The resultant structure was found to consist of a metal tetra bromide counter ion (MBr<sub>4</sub>) which we tentatively guess is nickel as it is believed the needle which was used to remove excess HBr was made of this metal. The X-ray structure is shown in **Figure 2.48**. The two N<sup>+</sup>-C-C-F torsion angles have been measured at 59.6 ° and 71.5 °, both consistent with a *gauche* conformation. This is the first example of a di

( $N^+-C-C$ )<sub>2</sub>-F system, possessing no hydrogen bonding which clearly shows two *gauche* conformations within the one molecule.



**Scheme 2.46** Preparation of **203** from the 2-fluoro-1,3-propane unit **142**.

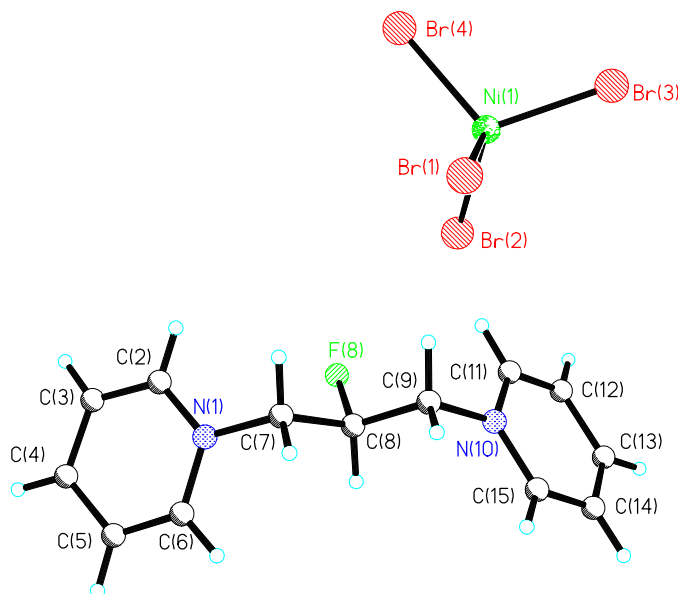


**Figure 2.48** X-ray crystal structure of **203** with a  $NiBr_4$  counter ion. The ( $N^+-C-C$ )<sub>2</sub>-F *gauche* angles are 59.6° and 71.5°.

**$^{19}\text{F}$  NMR analysis of **203****

The  $^{19}\text{F}$  NMR of **203** displays a doublet of triplets of triplets (dt) (**Figure 2.49**), showing 10 peaks from a theoretical 18, owing to overlap. The methylene hydrogens are non equivalent due to the CHF group.

The coupling constants have been estimated using DAISY from the Bruker Topspin NMR data program to be approximately  $^2J = 50$  Hz,  $^3J = 32$  Hz and  $^3J = 16$  Hz. On inspection of the spectrum it can be seen that the  $J$  values are:  $^2J = 48.9$  Hz,  $^3J = 33.0$  Hz and  $^3J = 16.8$  Hz.

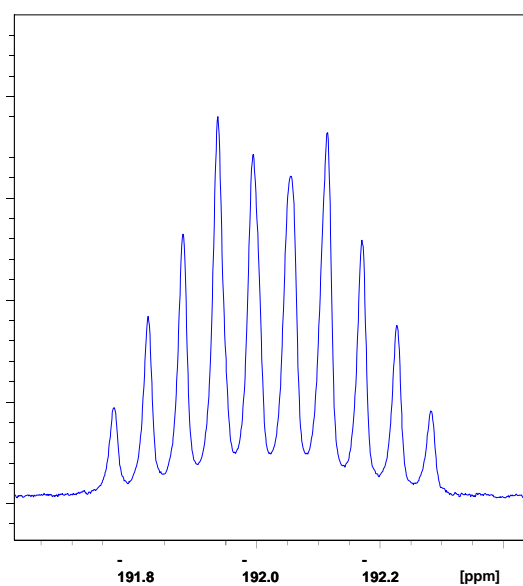


**Figure 2.49**  $^{19}\text{F}$  NMR spectrum of **203**.

In conclusion, the preparation of a number of protonated  $\text{HN}^+\text{-----F-C}$  and non protonated  $\text{N}^+\text{-----F-C}$  systems with a  $\beta$  fluorine was explored. X-ray crystallography was carried out on these salts and the fluorine-nitrogen<sup>+</sup> torsion angle was measured. It was found that in the protonated systems that there was a clear *gauche* torsion angle, consistent with a charge dipole interaction. When pyridiniums with a  $\beta$  fluorine were examined they too were found to exhibit a *gauche* torsion angle. This showed that the charge dipole interaction was indeed independent of any hydrogen bonding. DFT calculations were also carried out to examine the conformational preference and it was found in the case of the fluoro diaza cyclooctane **149**, that there was a large preference for an axial fluorine over equatorial (9.2 kcal mol<sup>-1</sup>). DFT calculations were also performed on the pyridinium systems, **198** and **200**. Again X-ray structure results agreed with the DFT findings of a lower energy preference for the *gauche* conformer, (3.7 and 3.1 kcal mol<sup>-1</sup> respectively).

## 2.10 References for chapter two

1. D. C. Lankin, N. S. Chandrakumar, S. N. Rao, D. P. Spangler and J. P. Snyder, *J. Am. Chem. Soc.*, 1993, **115**, 3356-3357.
2. J. P. Snyder, N. S. Chandrakumar, H. Sato and D. C. Lankin, *J. Am. Chem. Soc.*, 2000, **122**, 544-545.
3. A. Sun, D. C. Lankin, K. Hardcastle and J. P. Snyder, *Chem. Eur. J.*, 2005, **11**, 1579-1591.
4. C. R. S. Briggs, M. J. Allen, D. O'Hagan, D. J. Tozer, A. M. Z. Slawin, A. E. Goeta and J. A. K. Howard, *Org. Biomol. Chem.*, 2004, **2**, 732-740.
5. F. A. L. Anet, *Fortschr. Chem. Forsch.*, 1974, **45**, 169-220.
6. U. Nubbemeyer, *Top. Curr. Chem.*, 2001, **216**, 125-196.
7. L. Yet, *Chem. Rev.*, 2000, **100**, 2963-3007.
8. G. Vo-Thanh, V. Boucard, H. Sauriat-Dorizon and F. Guibe, *Synlett*, 2001, 37-40.
9. I. L. C. Hernandez, M. L. Macedo, R. G. S. Berlinck, A. G. Ferreira and M. J. L. Godinho, *J. Braz. Chem. Soc.*, 2004, **15**, 441-444.
10. M. Mitova, G. Tommonaro, U. Hentschel, W. E. G. Mueller and S. De Rosa, *Mar. Biotechnol.*, 2004, **6**, 95-103.
11. J. W. Blunt, B. R. Copp, M. H. G. Munro, P. T. Northcote and M. R. Prinsep, *Nat. Prod. Rep.*, 2005, **22**, 15-61.
12. M. A. Korshunov, F. N. Bodnaryuk and V. S. Mikhlin, *Zh. Org. Khim.*, 1969, **5**, 1947-1952.
13. M. A. Korshunov, B. F. N. and M. V. S., *Zh. Org. Khim.*, 1969, **5**, 1893-1898.
14. J.-W. Chern, J.-Y. Chang, C. O. Usifoh and A. Gutsait, *Tetrahedron Lett.*, 1998, **39**, 8483-8486.



15. G. C. Fu, S. T. Nguyen and R. H. Grubbs, *J. Am. Chem. Soc.*, 1993, **115**, 9856-9857.
16. J. F. Reichwein and R. M. J. Liskamp, *Eur. J. Org. Chem.*, 2000, 2335-2344.
17. H. Kapnang and G. Charles, *Tetrahedron Lett.*, 1983, **24**, 3233-3236.
18. P. Evans, R. Grigg and M. Monteith, *Tetrahedron Lett.*, 1999, **40**, 5247-5250.
19. R. C. Buijsman, E. van Vuuren and J. G. Sterrenburg, *Org. Lett.*, 2001, **3**, 3785-3787.
20. G. Illuminati and L. Mandolini, *Acc. Chem. Res.*, 1981, **14**, 95-102.
21. G. P. Xue, H. Liu, e. Q. Fu, H. S. Xu and C. T. Wu, *Chin. Chem. Lett.*, 1994, **5**, 457-458.
22. M. Wu, G. Cheng, Y. He and C. Wu, *Synth. Commun.*, 1995, **25**, 1427-1431.
23. J. A. Halfen, H. L. Moore and D. C. Fox, *Inorg. Chem.*, 2002, **41**, 3935-3943.
24. N. N. Chuvatkin, I. Y. Panteleeva and L. S. Boguslavskaya, *Zh. Org. Khim.*, 1982, **18**, 946-953.
25. F. L. M. Pattison, D. A. V. Peters and F. H. Dean, *Can. J. Chem.*, 1965, **43**, 1689-1699.
26. R. Harrison, R. Eisenthal, W. J. Lloyd and N. F. Taylor, *Chem. Commun.*, 1970, 1507-1508.
27. P. Najappan, N. Raju, K. Ramalingam and D. P. Nowotnik, *Tetrahedron*, 1994, **50**, 8617-8632.
28. H. Stetter and H. Spangenberger, *Chem. Ber.*, 1958, **91**, 1982-1988.
29. A. Hammerl, G. Holl, M. Kaiser, T. M. Klapotke, R. Kranzle and M. Vogt, *Z. Anorg. Allg. Chem.*, 2002, **628**, 322-325.
30. T. Egawa, T. Fukuyama, S. Yamamoto, F. Takabayashi, H. Kambara, T. Ueda and K. Kuchitsu, *J. Chem. Phys.*, 1987, **86**, 6018-6026.

31. G. M. Day, W. D. S. Motherwell, H. L. Ammon, S. X. M. Boerrigter, R. G. Della Valle, E. Venuti, A. Dzyabchenko, J. D. Dunitz, B. Schweizer, B. P. van Eijck, P. Erk, J. C. Facelli, V. E. Bazterra, M. B. Ferraro, D. W. M. Hofmann, F. J. J. Leusen, C. Liang, C. C. Pantelides, P. G. Karamertzanis, S. L. Price, T. C. Lewis, H. Nowell, A. Torrisi, H. A. Scheraga, Y. A. Arnautova, M. U. Schmidt and P. Verwer, *Acta Crystallogr., Sect. B: Struct. Sci.*, 2005, **B61**, 511-527.
32. M. Gajhede, U. Anthoni, C. Christophersen and P. Halfdan Nielsen, *Acta Crystallogr., Sect. B: Struct. Sci.*, 1989, **B45**, 562-566.
33. P. Huszthy, J. S. Bradshaw, K. E. Krakowiak, T. Wang and N. K. Dalley, *J. Heterocycl. Chem.*, 1993, **30**, 1197-1207.
34. *Application: WO Pat.*, 2003-EP3299, 2003087064, 2003.
35. N. E. J. Gooseman, D. O'Hagan, A. M. Z. Slawin, A. M. Teale, D. J. Tozer and R. J. Young, *Chem. Commun.*, 2006, 3190-3192.
36. N. Nishiwaki, T. Nogami, C. Tanaka, F. Nakashima, Y. Inoue, N. Asaka, Y. Tohda and M. Ariga, *J. Org. Chem.*, 1999, **64**, 2160-2162.
37. R. Jakubas, B. Bednarska-Bolek, J. Zaleski, W. Medycki, K. Holderna-Natkaniec, P. Zielinski and M. Galazka, *Solid State Sci.*, 2005, **7**, 381-390.
38. M. Konno and Y. Saito, *Acta Crystallogr. B*, 1981, **B37**, 2034-2043.
39. O. A. D'Yachenko, V. V. Gritsenko, G. G. Abashev, E. V. Shklyueva and V. S. Russkikh, *Russ. Chem. Bull.*, 1997, **46**, 1555-1559.
40. M. Vinodu and I. Goldberg, *CrystEngComm*, 2003, **5**, 204-207.
41. O. N. Kataeva, I. A. Litvinov, I. Y. Strobrykina and V. E. Kataev, *Izv. Akad. Nauk, Ser. Khim.*, 1990, 2617-2619.
42. I. Y. Polishchuk, L. G. Grineva, A. P. Polishchuk and A. N. Chernega, *Russ. J. Gen. Chem.*, 1997, **67**, 1782-1790.

43. R. M. Schoth, E. Lork, A. A. Kolomeitsev and G. V. Roeschenthaler, *J. Fluorine Chem.*, 1997, **84**, 41-44.
44. B. C. Saunders and I. G. E. Wilding, *J. Chem. Soc.*, 1949, 1279-1282.
45. A. D. C. Parenty, L. V. Smith and L. Cronin, *Tetrahedron*, 2005, **61**, 8410-8418.
46. J.-C. Legeay, J. J. Vanden Eynde and J. P. Bazureau, *Tetrahedron*, 2005, **61**, 12386-12397.
47. D. Kuhnen-Clausen, I. Hagedorn and R. Bill, *J. Med. Chem.*, 1979, **22**, 177-178.
48. K. L. Meyer, C. J. Marasco, Jr., S. L. Morris-Natschke, K. S. Ishaq, C. Piantadosi and L. S. Kucera, *J. Med. Chem.*, 1991, **34**, 1377-1383.
49. R. G. Gafurov, V. Y. Grigor'ev, A. N. Proshin, V. G. Chistyakov, I. V. Martynov and N. S. Zefirov, *Russ. J. Bioorg. Chem.*, 2004, **30**, 592-598.
50. Y. Gao and J. n. M. Shreeve, *Synthesis*, 2004, 1072-1082.
51. *Application: US Pat.*, 97-825786, 5756725, 1998.
52. G. R. Pettit, D. C. Fessler and J. A. Settepani, *J. Org. Chem.*, 1969, **34**, 2978-2981.

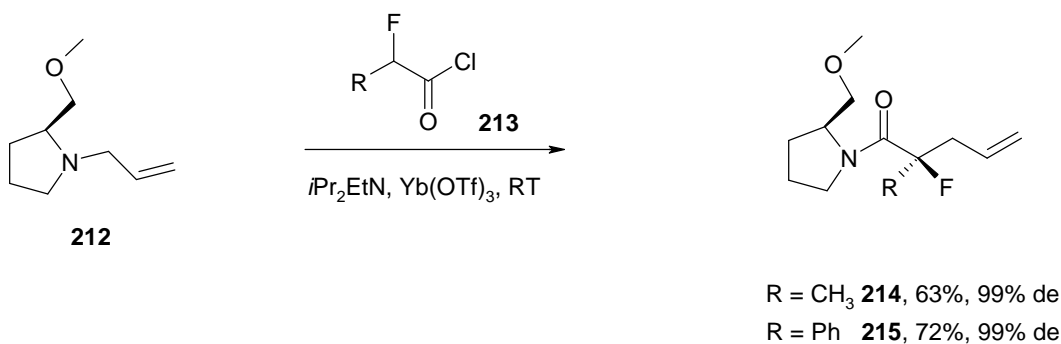
## Chapter 3

# CHARGED C-O<sup>+</sup> ----- F-C DIPOLE INTERACTIONS

### 3.1 Introduction

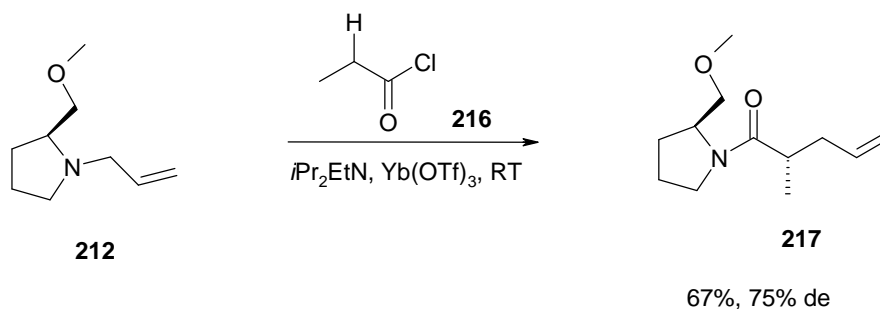
The charge dipole interaction of a charged nitrogen with a fluorine atom in a C-F bond was described in **Chapter 2**.

Recently a C-N<sup>+</sup> ---- F-C dipole interaction was proposed as significant in promoting the stereoselectivity in an aza-Claisen reaction.<sup>1</sup> When allyl amine **212** was treated with 2-fluoropropionyl chloride **213**, Hünig's base and Yb(OTf)<sub>3</sub>. A highly diastereoselective aza-Claisen rearrangement product emerged (**Scheme 3.1**).



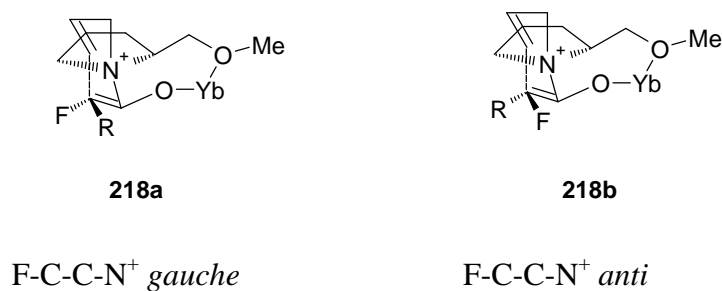
**Scheme 3.1** Diastereoselective aza-Claisen rearrangement.<sup>1</sup>

Interestingly, when the reaction was carried out with propionyl chloride **216** rather than an  $\alpha$  fluorinated substrate such as **213**, then a lower diastereoselectivity for **217** emerged (75% de).



**Scheme 3.2** Aza-Claisen rearrangement with **212** and propionyl chloride.<sup>1</sup>

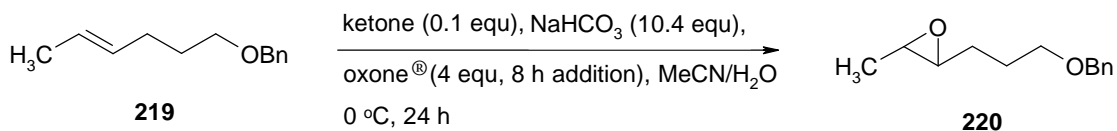
The influence of the fluorine atom in the production of **214** and **215**, can be assessed by evaluation of the two putative transition states **218a** and **218b**. In **218a** the fluorine has a *gauche* relationship to the  $\text{N}^+$  ( $\text{F-C-C-N}^+$ ), whereas in **218b** this relationship is *anti*.



Because of the charge-dipole interaction stabilising **218a**, this transition state is anticipated to be lower in energy than **218b** and therefore would in turn dominate the reaction path. This transition state provides products with the stereochemistry observed in **214** or **215**, accounting for the high diastereoselectivity of the reaction as depicted in **Scheme 3.1**.

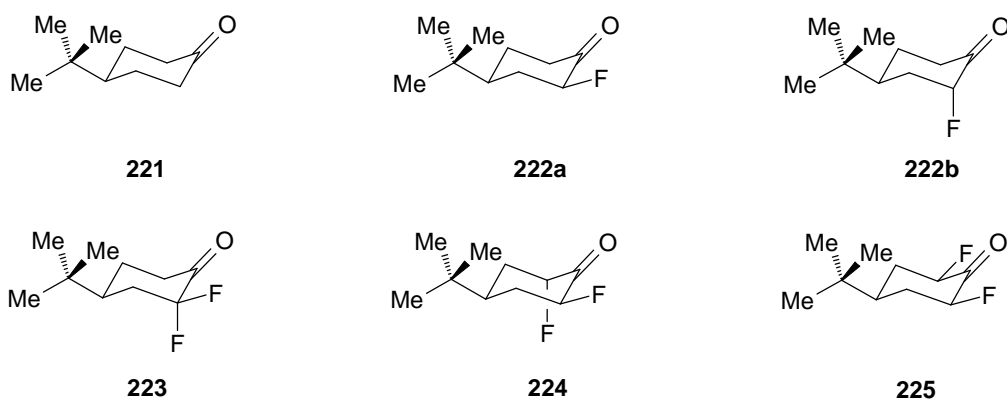
It is also of interest to consider the influence of a fluorine atom with respect to a charged  $\text{C-O}^+$  system.

Denmark has demonstrated that fluorine has the ability to influence the epoxidation of alkenes by oxone<sup>®</sup> using fluoro ketones as catalysts.<sup>2</sup> The general scheme is given below.



**Scheme 3.3** General epoxidation reaction of an alkene.<sup>2</sup>

Five different fluorinated 4-*tert*-butylcyclohexanones were assessed as catalysts for the epoxidation reaction (**Figure 3.1**). It was found that all of the fluorinated ketones **222–225** were better catalysts than the non fluorinated counterpart 4-*tert*-butylcyclohexanone **221**. Interestingly the mono **222a** and di-fluorinated **225** ketones, where the fluorines are equatorial, gave better conversions relative to those with axial fluorines (**222b**, **223** and **224**).



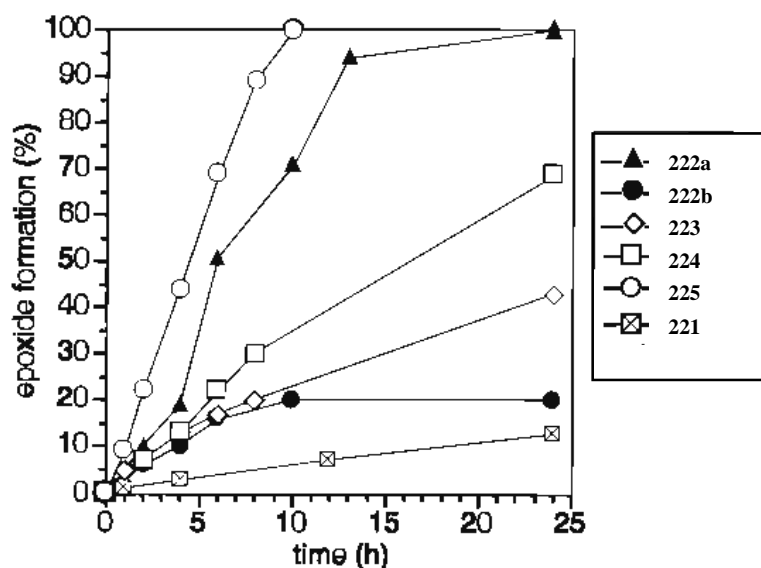
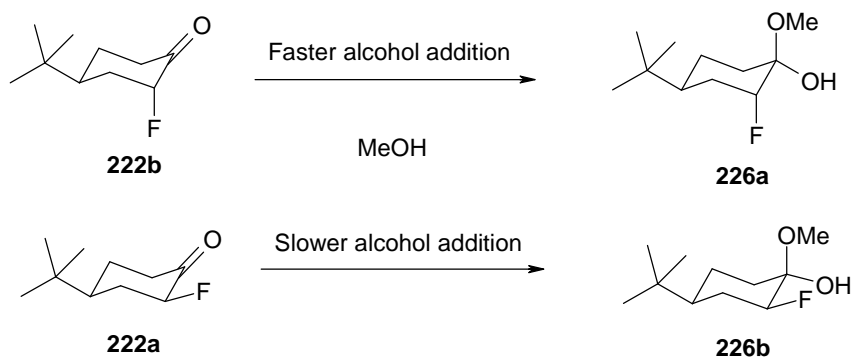


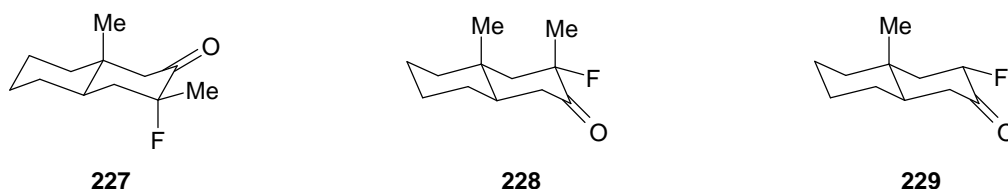
**Figure 3.1** *t*-Butylcyclohexanone epoxidation catalysts and the epoxidation reaction profiles.<sup>2</sup>

Denmark attributed these differences to stereoelectronic effects. He concluded that slow reactions could be explained by nucleophilic attack to the carbonyl, *anti* to the fluorine, forming a stable hemi-ketal. In a comparative experiment both equatorial and axial fluoro ketones were treated with methanol to form hemi-ketals. The axial fluoro ketones were found to form the more stable hemi-ketals. This suggests that the Criegee intermediates formed after oxone<sup>®</sup> addition would turn over more slowly or would be inhibited by any water or alcohol thus slowing the rate of the reaction.

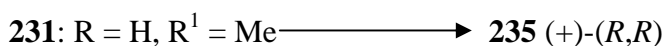
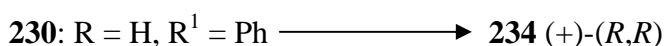
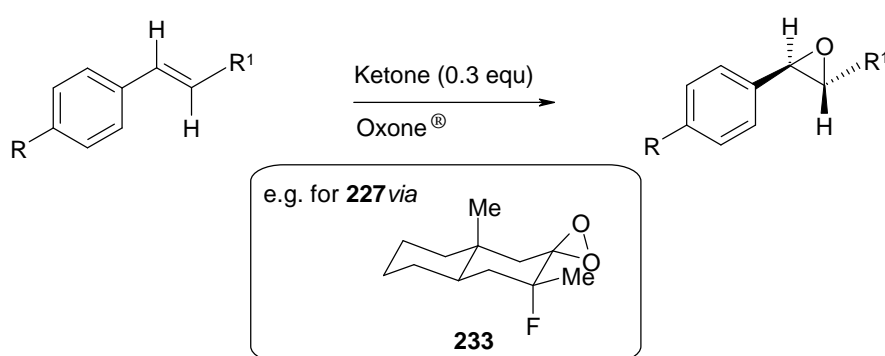


**Scheme 3.4** The rates of methanol addition are inverse to the rate of epoxidation.

More recently in 2004, Solladié-Cavallo *et al.*, discussed the effect of fluorine in  $\alpha$ -fluoro decalones, also used as catalysts in the epoxidation of alkanes with oxone<sup>®</sup>.<sup>3</sup> Axial and equatorial fluoro decalone catalysts **227**, **228** and **229** were evaluated as these rigid systems cannot undergo ring inversion.



These catalysts were utilised in the epoxidation of **230**, **231** and **232** via a dioxirane intermediate **233** (Scheme 3.5). The conversions and enantiomeric excesses of **234**, **235** and **236** were measured and in conclusion it was found that **227** was the most effective catalyst giving higher ee's than **228** and **229**. This contradicts Denmark's 'axial' conclusions, however steric effects from the axial methyl groups clearly complicate this case and a direct comparison is not straightforward.



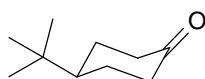
**Scheme 3.5** Epoxidation reactions using fluoro ketones as catalysts.<sup>3</sup>



### 3.2 A stereoselective study on fluorine, C-F-----<sup>+</sup>O-R

This study aimed to explore the effect of a fluorine substituent on a reaction that involves a protonated oxygen as an intermediate ( $O^+$ ). If a  $\beta$  fluorine orientates *gauche* to an  $O^+$ , then it is anticipated that a  $C-O^+ \cdots F-C$  charge dipole interaction will act to stabilise a *gauche* conformer relative to a structure where the fluorine is *anti* to  $O^+$ . Such stabilisation should lower the energy of one diastereoisomer relative to the other and accelerate the rate of reaction. A model reaction was selected to explore this. It was anticipated that the rates of ketal hydrolysis of diastereoisomers **237a** ( $H^+$ ) and **237b** ( $H^+$ ) would differ as a result of this effect.

In *t*-butylcyclohexanone **221** the *t*-butyl group will force a chair conformation with the *t*-butyl group lying equatorial. Although this is not a rigid conformation, the axial value (A value) of the *t*-butyl group is large ( $4.7 \text{ Kcal mol}^{-1}$ ) and therefore the equatorial conformer is expected to predominate in solution.



**221**

**Figure 3.2** shows the conformations anticipated in solution for the protonated ketals **237a** ( $H^+$ ) and **237b** ( $H^+$ ). This illustrates a reaction intermediate in the acid catalysed formation / breakdown of the ketal. *Gauche/gauche* or *anti/gauche* refers to the relationship between fluorine and each of the ketal oxygens. Protonation may of course occur to either oxygen. However it is envisaged that the axial C–O bond of the ketals, on protonation will be weaker than the equatorial C–O bond. The axial oxygen is the sterically more congested and thus this bond will be predisposed to cleave more readily relative to the equatorial C–

O bond. It is also assumed that the introduction of fluorine will slow C–O bond cleavage quite dramatically in both cases. A *gauche* O<sup>+</sup> / F relationship is anticipated to stabilise intermediate **237a** (H<sup>+</sup>), due to the C–O<sup>+</sup>·····F–C charge dipole interaction, whereas an axial fluorine will not achieve such stabilisation. Accordingly at the outset the axial conformer of intermediate **237b** (H<sup>+</sup>) is anticipated to be more difficult to attain and therefore it will react at a slower rate than the equatorial diastereoisomer **237a** (H<sup>+</sup>).

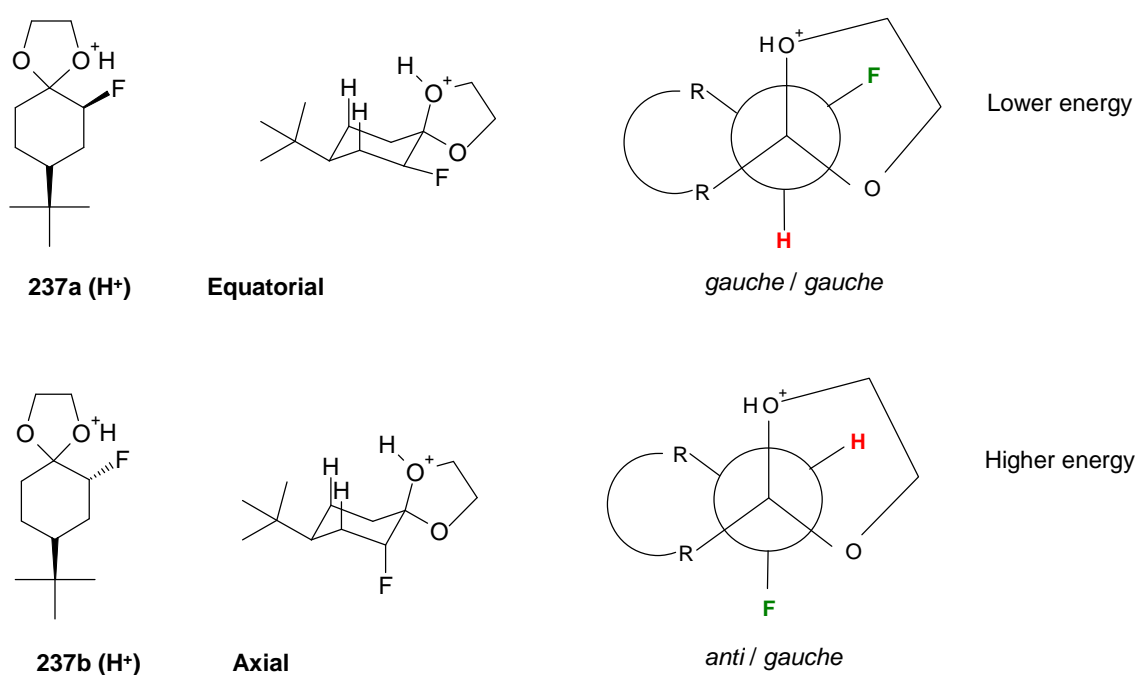
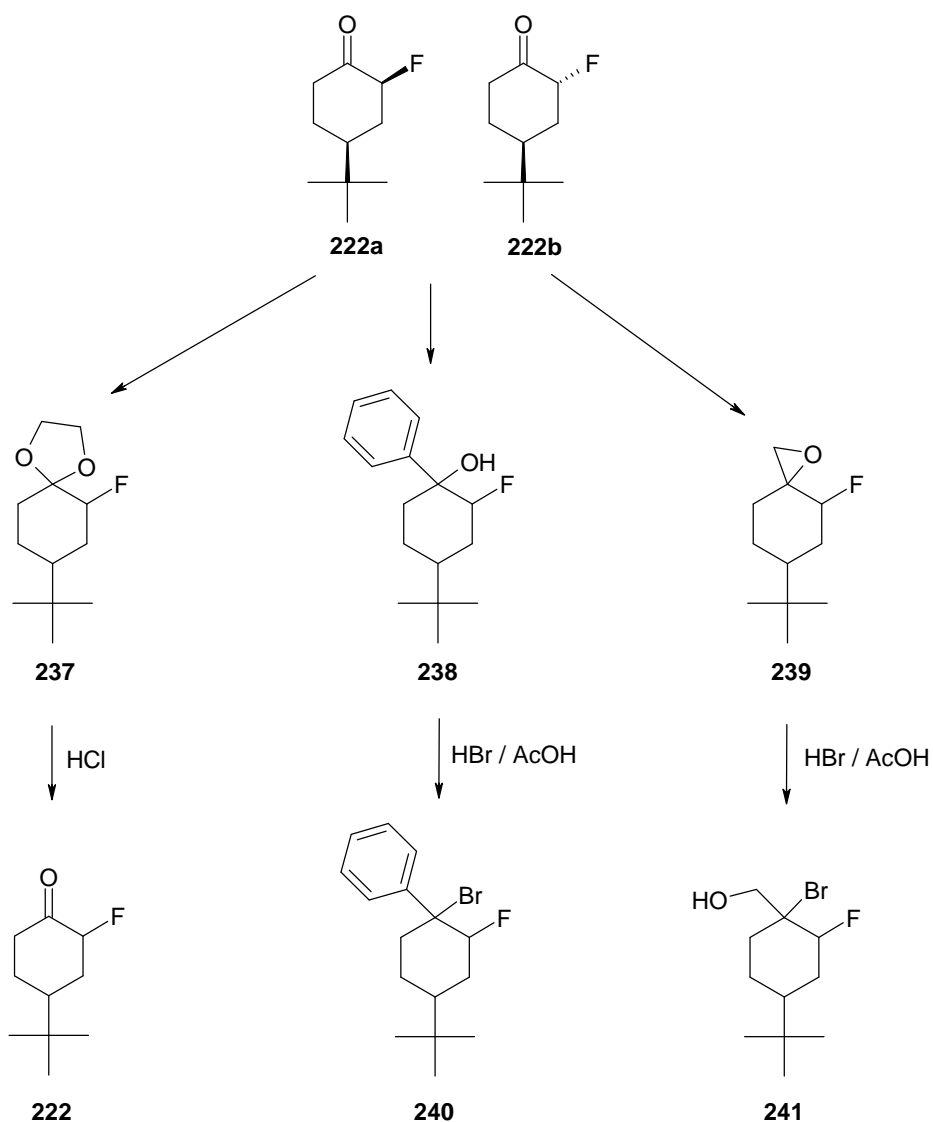


**Figure 3.2** Protonated intermediates in acetal hydrolysis of **237a** (H<sup>+</sup>) and **237b** (H<sup>+</sup>).

The three fluoro cyclohexanes **237**, **238** and **239** were identified as candidate substrates in which to explore reactions where the influence of axial and equatorial fluorines could be compared (**Scheme 3.6**). It was planned to monitor reactions of these substrates by <sup>19</sup>F NMR and analyse the relative rates of reaction of the diastereoisomers.



**Scheme 3.6** Fluorocyclohexane substrates **237** – **239** and proposed reactions.

Thus the aim of this study was to explore the relative rate of hydrolysis of both the C-F equatorial and C-F axial fluoroketals under acidic conditions, back to their respective ketones **222a** and **222b**. For the tertiary alcohols **238**, it was anticipated that both the C-F axial and C-F equatorial diastereoisomers will react in  $S_N1$  reactions at different rates e.g. in a bromination reaction with HBr to afford **240**. And for **239** epoxide ring opening will be explored.

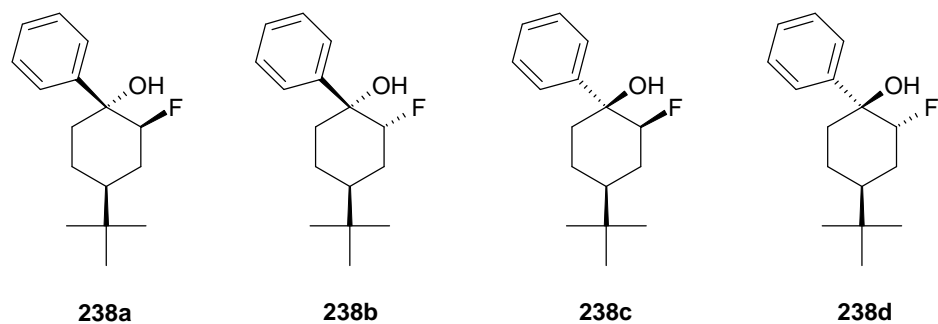
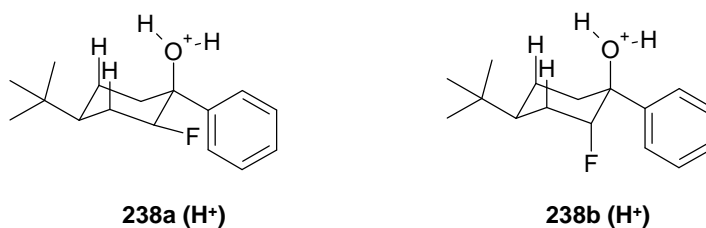


**Figure 3.3** Tertiary alcohol **238** diastereoisomers.

An  $S_N1$  reaction of tertiary alcohols **238a** / **238b** involves an  $RO^+H_2$  species, the stability of which is expected to vary depending on the orientation of fluorine. The intermediate species are given below.



The fluoro epoxides **239** also have four diastereoisomers and thus the appropriate pairs of diastereoisomers have to be compared (**Figure 3.4**).

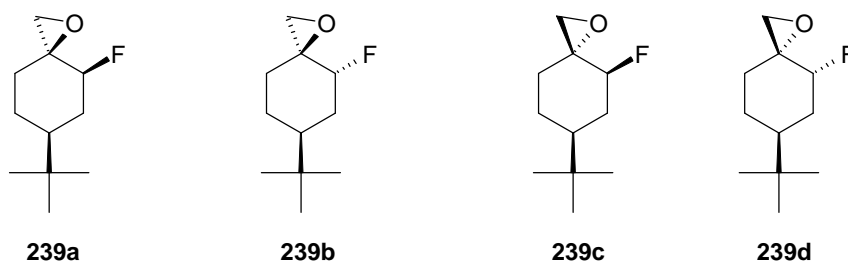
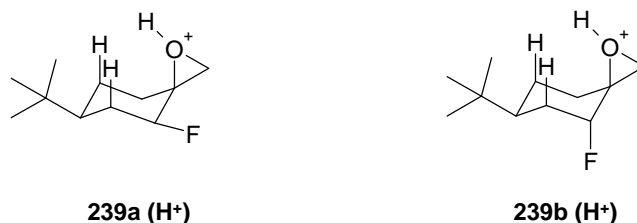


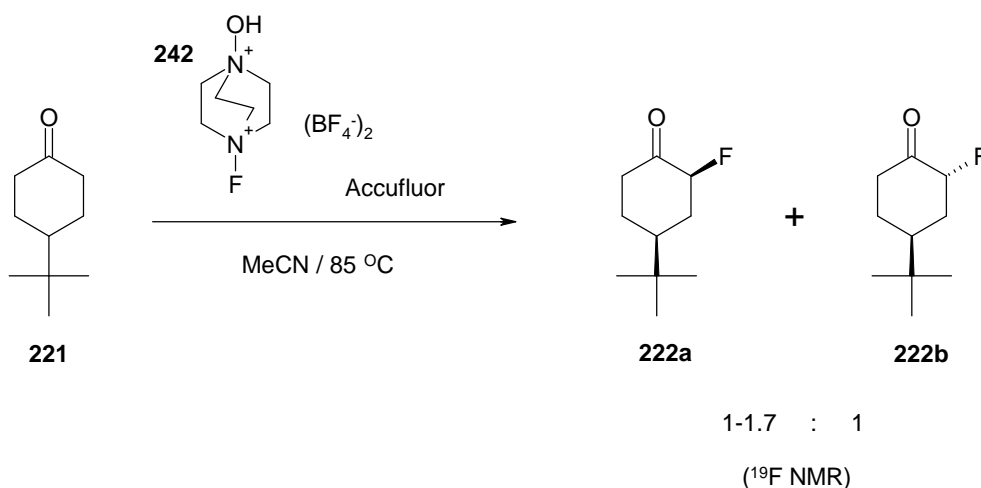
**Figure 3.4** Fluoro epoxide **239** diastereoisomers.

For example protonation of diastereoisomers **239a** and **239b** will give the intermediates shown below. The equatorial fluoro epoxide is expected to be more readily attained and thus react faster than the axial **239b**.



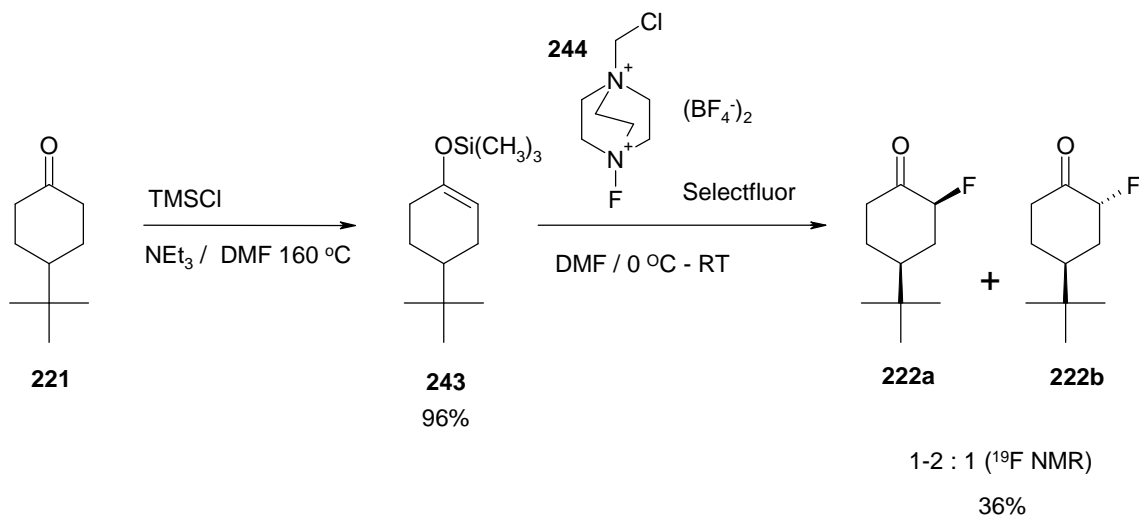
### 3.3 Synthesis of 2-fluoro-4-(1,1-dimethylethyl)cyclohexanone

The ketone diastereoisomers **222a** and **222b** in **Scheme 3.7** are required to make the appropriate substrates to explore these reactions. Two synthetic routes to this ketone have been described in the literature. Zupan<sup>4</sup> has shown that direct fluorination of 4-*t*-butylcyclohexanone **221** with Accufluor™ **242** on alumina provides a mixture of both **222a** and **222b**. This reaction was carried out, and in our hands a mixture of *eq* and *ax* diastereoisomers was generated in a ratio of 1–1.7 : 1 respectively. Column chromatography over silica proved difficult in separating these isomers.



**Scheme 3.7** Synthesis of **222a** and **222b** with Accufluor™.

An alternative procedure (**Scheme 3.8**) involving electrophilic fluorination of the silyl enol ether **243** with Selectfluor™ **244** afforded **222a** and **222b**.<sup>2</sup> Since this method generates a larger proportion of the axial fluoro isomer **222b**, it became the favoured method. Careful column chromatography over silica enabled separation of the individual diastereoisomers.



**Scheme 3.8** Two step synthesis of **222a** and **222b**.

Overall the second method, despite involving two steps provided a more equal ratio of the two isomers. In general the F-axial isomer **222b** proved to be the more difficult to isolate by chromatography. The F-axial isomer is the more reactive and appeared to be more sensitive to acidic / basic conditions than the equatorial isomer consistent with Denmark's observations. Basic (NaOH) or acidic (HCl) mediated equilibrium caused the ratio of the isomers to alter in favour of the F-equatorial isomer **222a** which then became the dominant isomer.

A suitable crystal of the equatorial isomer **222a** was subjected to X-ray crystallography analysis (**Figure 3.5**).

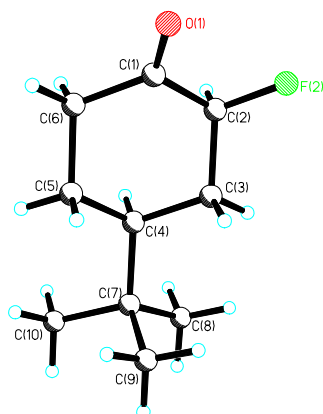


**Figure 3.5** X-ray crystal structure of **222a**.

It is interesting to note the very different  $^{19}\text{F}$  NMR ( $\text{CDCl}_3$ ), coupling patterns of the F-equatorial and F-axial diastereoisomers as shown in **Figure 3.6**. The coupling constants are most readily abstracted for the F-axial diastereoisomer and are consistent with the expected  $J_{\text{HF}}$  Karplus relationships. This is a dddd with the following coupling constants:  $^4J_{\text{HF}}$  5.3Hz,  $^3J_{\text{HF}}$  12.7Hz,  $^3J_{\text{HF}}$  43.5Hz and  $^2J_{\text{HF}}$  coupling of 49.8 Hz.

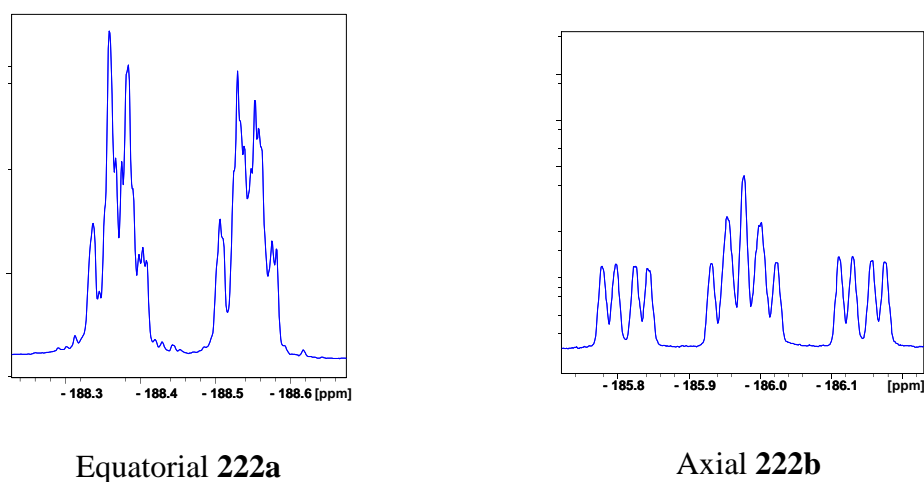
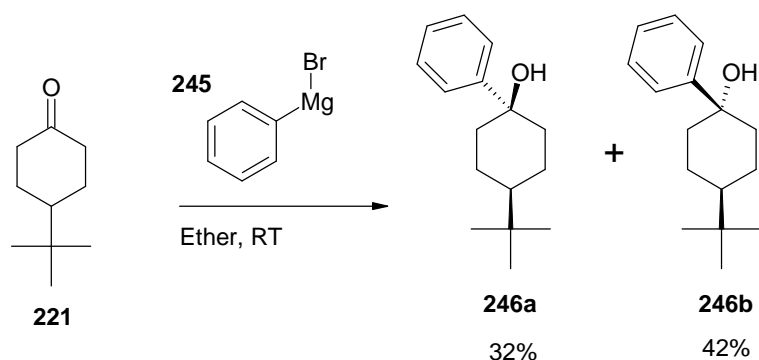


**Figure 3.6**  $^{19}\text{F}$  NMR of F-equatorial **222a** and F-axial **222b**.

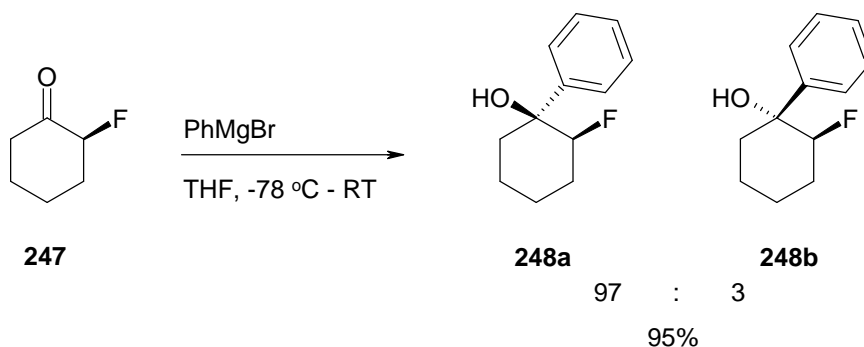
### 3.4 Grignard reactions

It was envisaged that the 2-fluorophenylcyclohexanol **238** could be prepared by a Grignard reaction on the corresponding cyclohexanone **222**. As a model reaction 1-phenyl-4-*t*-butylcyclohexanol **246** was prepared from **221** using phenylmagnesium bromide.<sup>5</sup> This reaction gave a 1 : 1 ratio of isomers **246a** and **246b** (GC-MS) and upon purification over silica gel the two isomers were separated in good overall yield (**Scheme 3.9**).



**Scheme 3.9** *t*-Butylcyclohexanol **246a** and **246b** was prepared *via* a Grignard reaction.

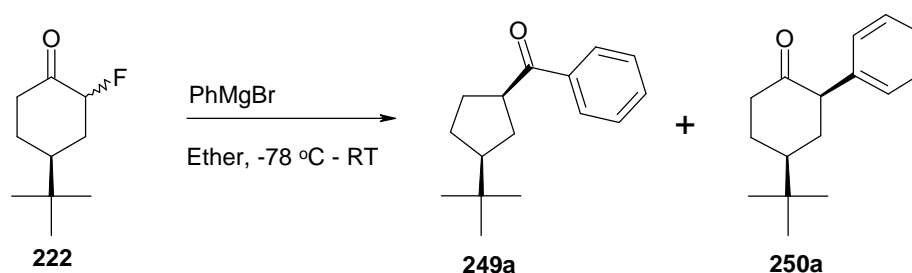
It is of significance to highlight the recently reported (2006)<sup>6</sup> synthesis of 2-fluoro-1-phenylcyclohexanol **248** by reaction of 2-fluorocyclohexanone **247** with PhMgBr in THF. This gave the expected product **248** in a 95% yield with a high diastereoselectivity (97:3).



**Scheme 3.10** Grignard reaction of 2-fluorocyclohexanone **247**.<sup>6</sup>



Attention was therefore directed towards the Grignard reaction of ketone **222**. In the first instance this reaction was carried out as a mixture of isomers and in the event no fluorinated products were generated. However two unexpected products were isolated. Characterisation using GC-MS, NMR and X-ray crystallography identified the major product to be the cyclopentane ketone **249a** and the minor product to be the *cis* cyclohexanone **250a**.



**Scheme 3.11** Products of the Grignard reaction of **222**.

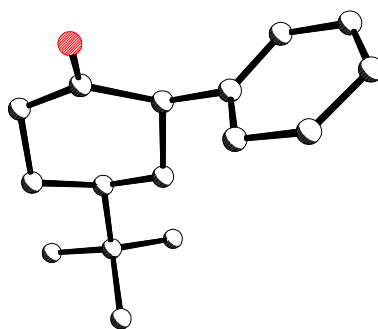


**Figure 3.7** X-ray structure of **250a**.

The major isomer **249a** was obtained as a viscous liquid. In order to clarify unambiguously the identity of this product by crystallography, the corresponding dinitrophenylhydrazone was prepared by reaction with dinitrophenylhydrazine in  $\text{H}_2\text{SO}_4$  / ethanol. X-ray diffraction analysis revealed **251** with the *t*-butyl and  $\text{CHC}(\text{Ph})$  groups *cis* to each another suggesting the major isomer from the Grignard reaction was **249a**.

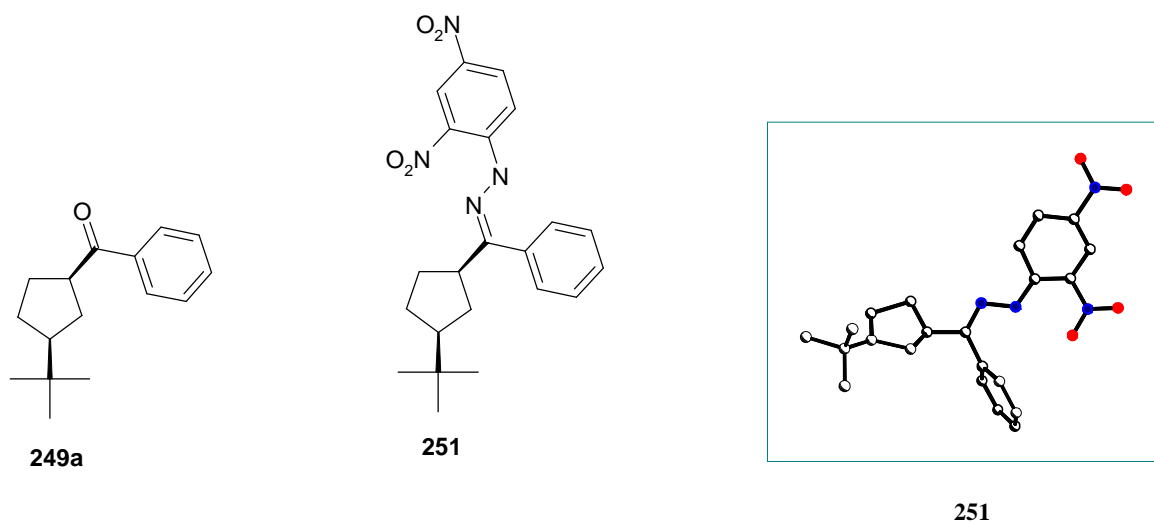
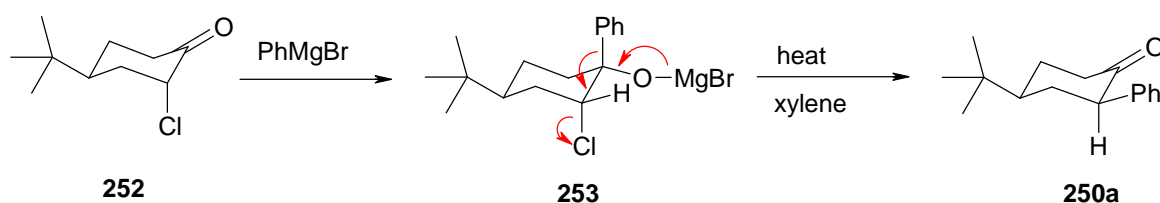


**Figure 3.8** The major product **249a** and its dinitrophenylhydrazone derivative **251**.

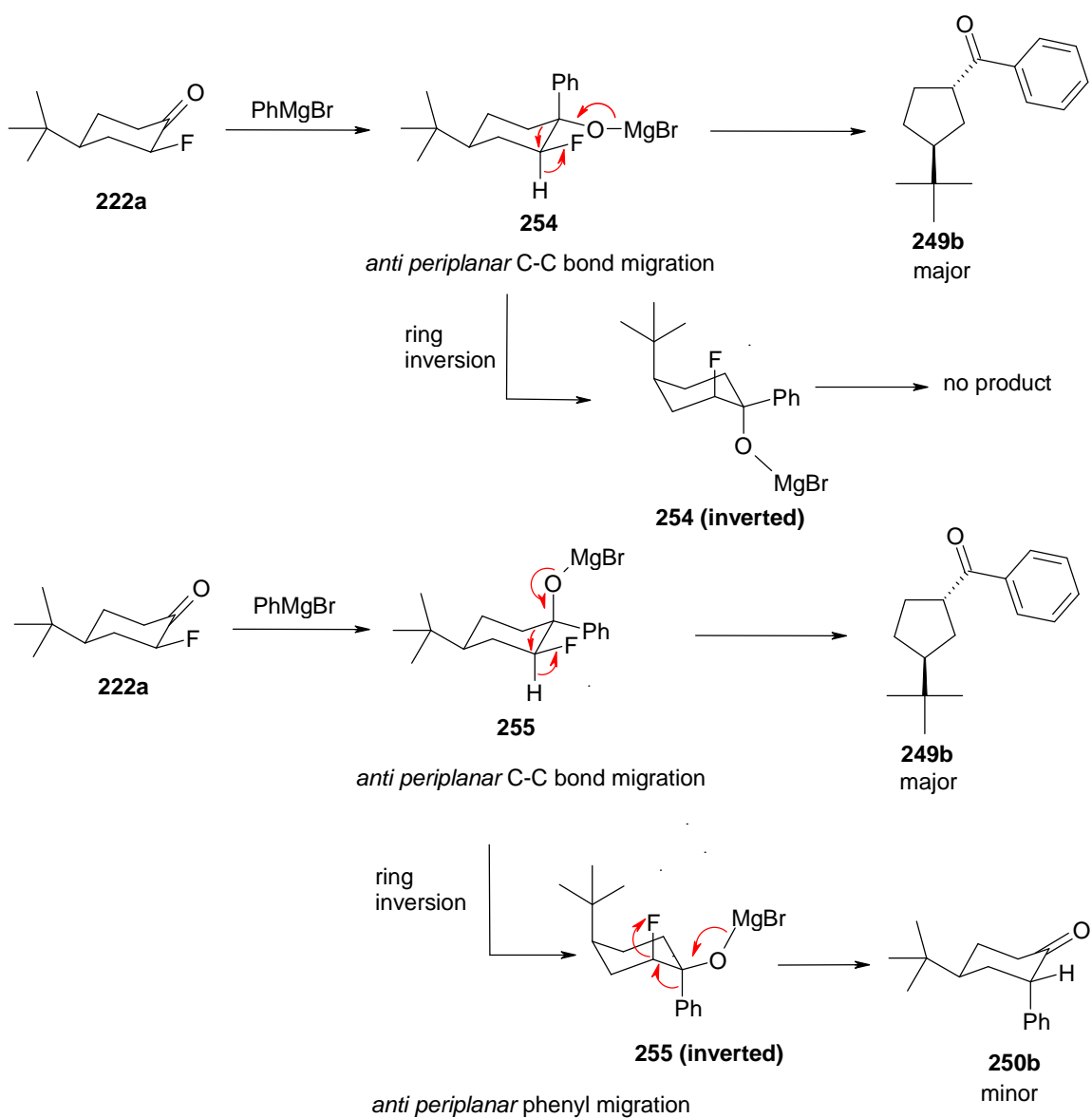
The rearrangements during the Grignard reaction were unexpected however a search of the literature found that such rearrangements have been observed in the organo chloro and organo bromo analogues.<sup>7-10</sup> Yee and Bordwell have reported the preparation of *cis* phenylcyclohexanone **250a** (Scheme 3.12) from the  $\alpha$ -chloro ketone **252**,<sup>7</sup> a reaction previously described by Tiffeneau<sup>11</sup> in 1934. The reaction was interpreted as one where the addition of the Grignard reagent provided a magnesium salt of a chlorohydrin which underwent rearrangement driven by chlorine elimination. Stereoelectronic considerations suggest that the migrating phenyl group will be *anti-periplanar* to the C-Cl bond, for such a rearrangement.



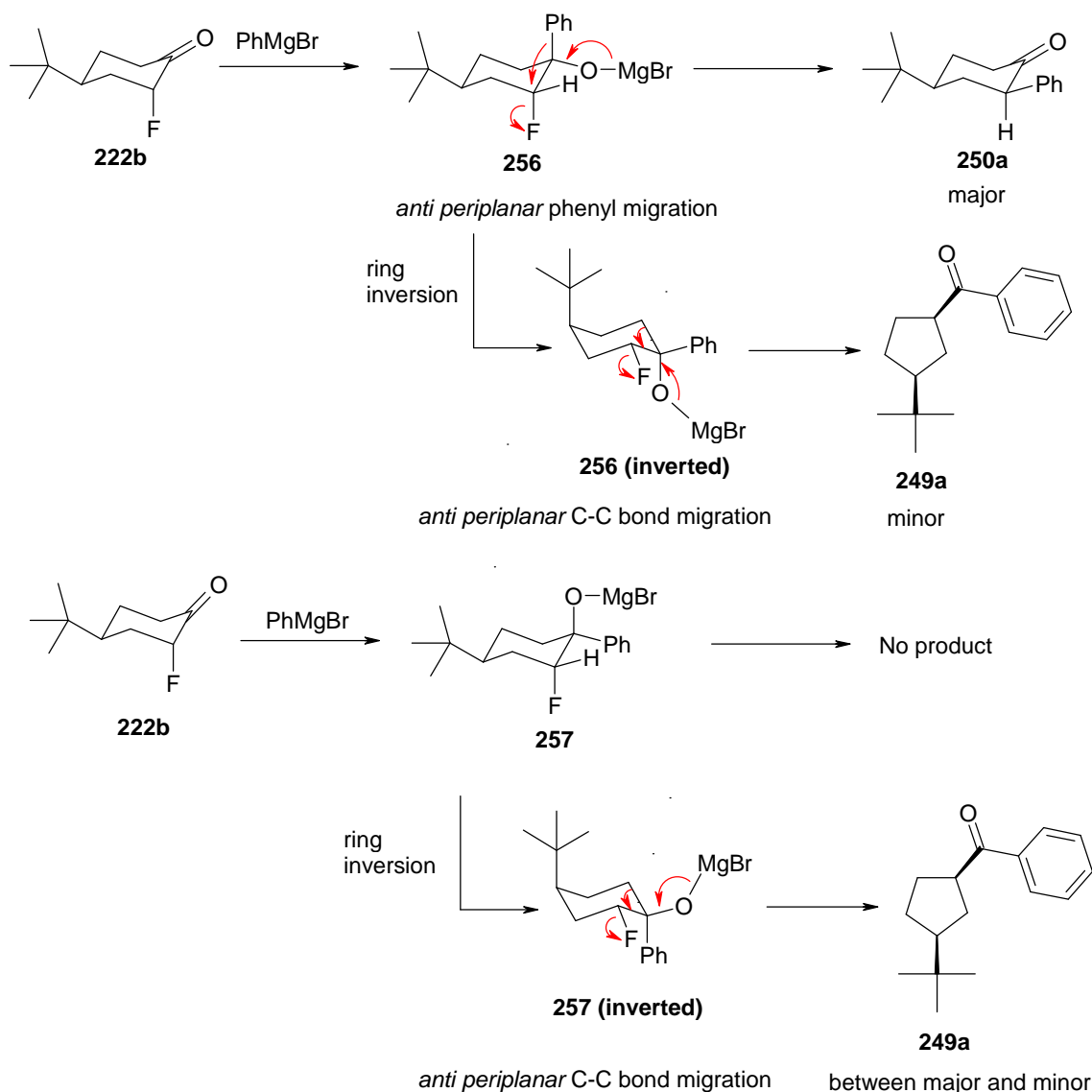
**Scheme 3.12** Proposed elimination mechanism of intermediate **253**.<sup>7</sup>

In the case of **222**, the rearrangement seems quite efficient despite fluorine being the poorest of the halogen leaving groups.

Conformations of the magnesium salts, which fulfil the stereoelectronic requirements to afford both the 5- and 6- membered phenyl ketones are proposed in **Scheme 3.13** and **Scheme 3.14**. In **Scheme 3.13** the possible outcomes for an equatorial fluorine in **222a** are shown, and **Scheme 3.14** predicts the outcome for an axial fluorine in **222b**.



**Scheme 3.13** Possible product outcomes for **222a** (equatorial fluorine).



**Scheme 3.14** Possible product outcomes for **222b** (axial fluorine).

The predominant conformers will have the *t*-butyl group equatorial. The  $\alpha$ -phenyl cyclohexanones should arise from an *anti-periplanar* migration of the phenyl group, and the cyclopentanone ketone, from an *anti-periplanar* migration of the C-C bond.

To gain a better understanding of the product outcomes of these reactions, the fluorinated ketones **222a** and **222b** were prepared as individual isomers. After chromatography the samples were substantially clean of the other isomer.  $^{19}\text{F}$  NMR spectra of the individual ketones are shown in **Figure 3.9**. Cross contamination is estimated to be ~5% for the equatorial ketone and ~1% for the axial ketone.

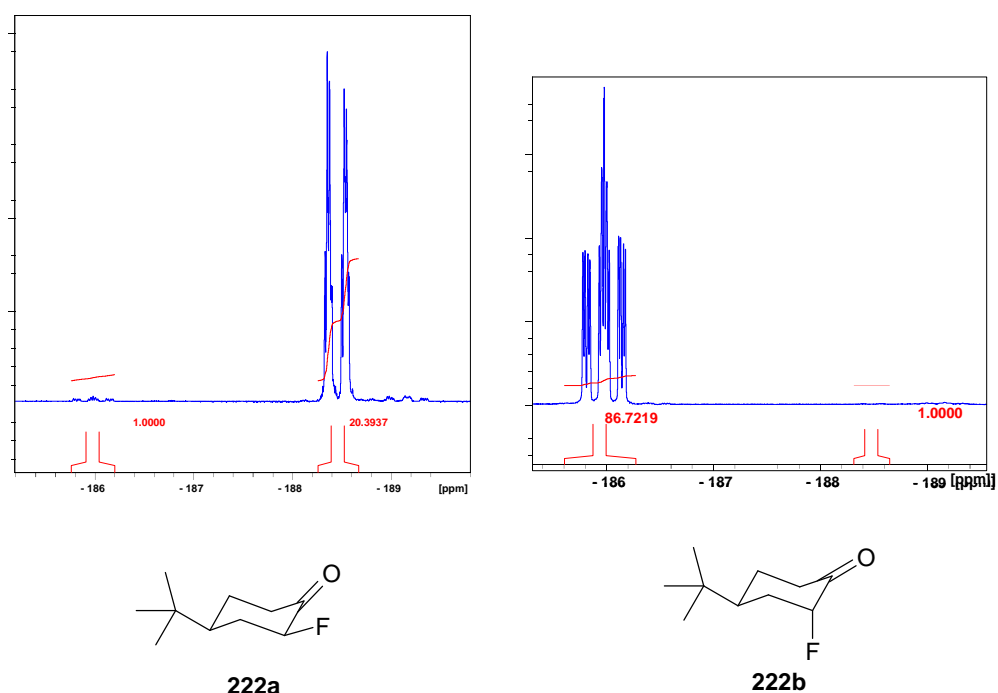
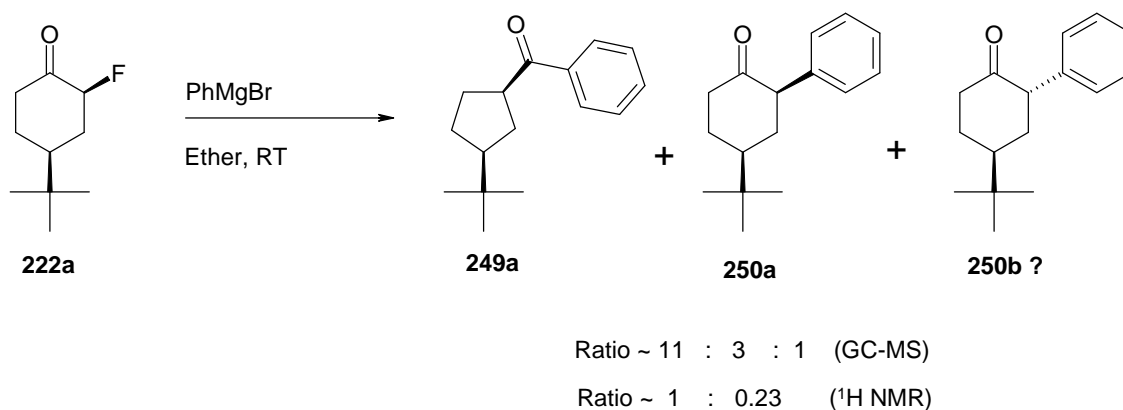


**Figure 3.9**  $^{19}\text{F}$  NMR of fluoro ketones **222a** and **222b** as used in Grignard reactions.

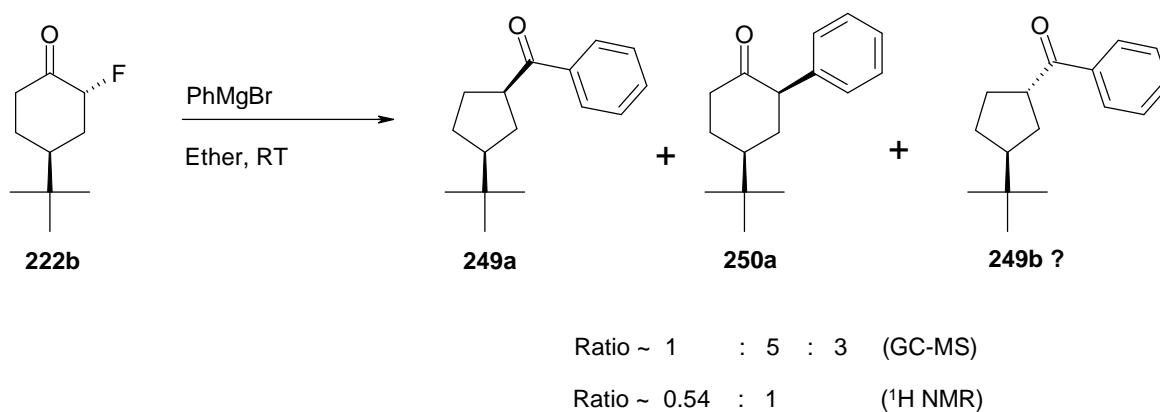
The individual isomers were then subjected to Grignard reactions with  $\text{PhMgBr}$  in ether.  $^1\text{H}$  NMR and GC-MS analysis was carried out on the product mixture. Ketone **222a** gave predominantly the five membered ring product **249a**, with a ratio of 5 to 6 membered ring product **250a** at 11 : 3. A third isomer was observed by GC-MS which had an identical mass and is tentatively suggested to be **250b** (**Scheme 3.15**).



**Scheme 3.15** Product ratio from Grignard reaction of **222a**.

This outcome is different to the predicted outcome (**Scheme 3.13**) as the cyclopentane ketone **249a** is the major product rather than the predicted **249b**. This and the minor isomer **250a** can perhaps be explained by epimerisation of **249b** and the cyclohexane product **250b** under the basic conditions.

For ketone **222b** (axial fluorine), the product outcome broadly agrees with the stereoelectronic analysis. This time the  $\alpha$ -phenyl cyclohexane **250a** predominates (**Scheme 3.16**). So clearly the stereochemistry of the fluorine can influence the product outcome in a predictable way. A third isomer was present which is tentatively attributed to **249b**.

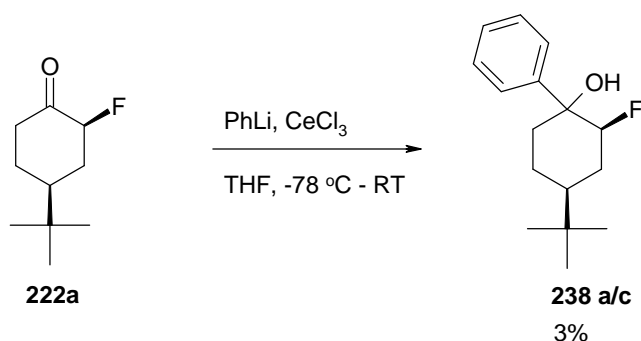


**Scheme 3.16** Product ratio from Grignard reaction of **222b**.

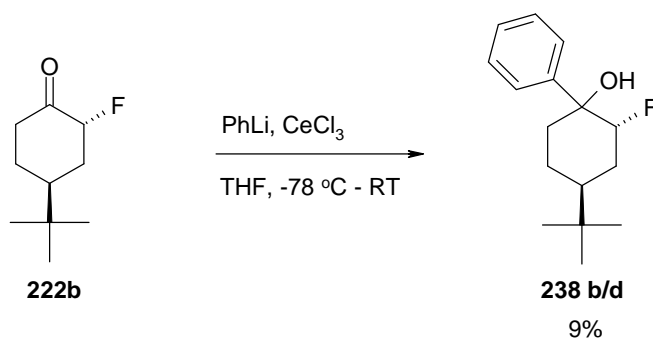
It was surprising to compare this reaction with the Grignard on 2-fluorocyclohexanone **247** described earlier (**Scheme 3.10**). In that case a straight forward addition of phenyl to the ketone carbonyl occurs, without subsequent rearrangement. In substrate **222** the *t*-butyl group must constrain the conformation in a manner which promotes stereoelectronic migration and fluoride ion elimination.

### 3.5 Synthesis of the 3-fluorophenylcyclohexanols with phenyl lithium

An alternative method to the required tertiary alcohols **238** was investigated using phenyllithium in the presence of cerium trichloride.<sup>12</sup> However, these were poor reactions giving the desired product in very low yields (3% and 9%). The rearranged products **249a** and **250a** were also evident in the product mixtures.



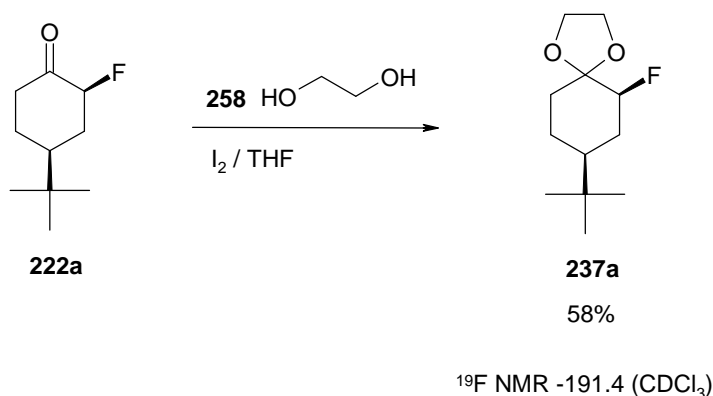
**Scheme 3.17** Phenyllithium afforded the tertiary alcohol **238 a/c** from fluoro ketone **222a**.



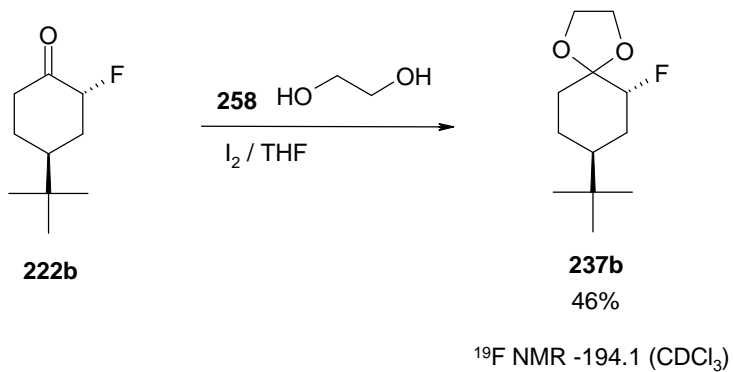
**Scheme 3.18** Phenyllithium afforded the tertiary alcohol **238 b/d** from **222b**.

### 3.6 Fluoro ketal study

Due to the inability of obtaining sufficient and analytically pure samples of tertiary alcohols **238**, attention turned to exploring ketal formation / reaction of ketones **222a** and **222b**. The fluoro ketals **237a** and **237b** were separately prepared from both fluoro ketone isomers **222a** and **222b**, using ethylene glycol and either  $I_2$ <sup>13</sup> or p-TSA as catalysts.<sup>14</sup> These reactions were relatively straightforward and the resultant ketals could be recovered and characterised.



**Scheme 3.19** Ketal **237a** synthesis from equatorial fluoro **222a**.

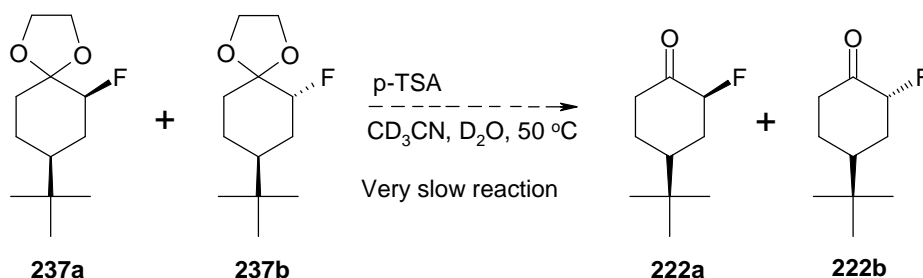


**Scheme 3.20** Ketal **237b** synthesis from axial fluoro **222b**.



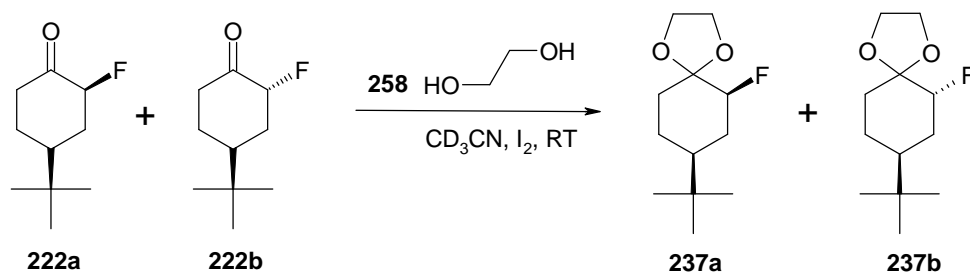
Attention then turned to exploring the difference in the rates of hydrolysis of the two ketal isomers **237a** and **237b**.

The hydrolysis reaction on a mixture of **237a** and **237b** (Scheme 3.21) was investigated employing p-TSA in CD<sub>3</sub>CN / D<sub>2</sub>O, however, in the event this reaction proved too slow to be monitored by <sup>19</sup>F NMR. Even addition of HCl (aq) and TFA with heating did not move the reaction forward fast enough to provide reasonable <sup>19</sup>F NMR time course analyses. The presence of the α-fluorine is clearly stabilising the ketals.



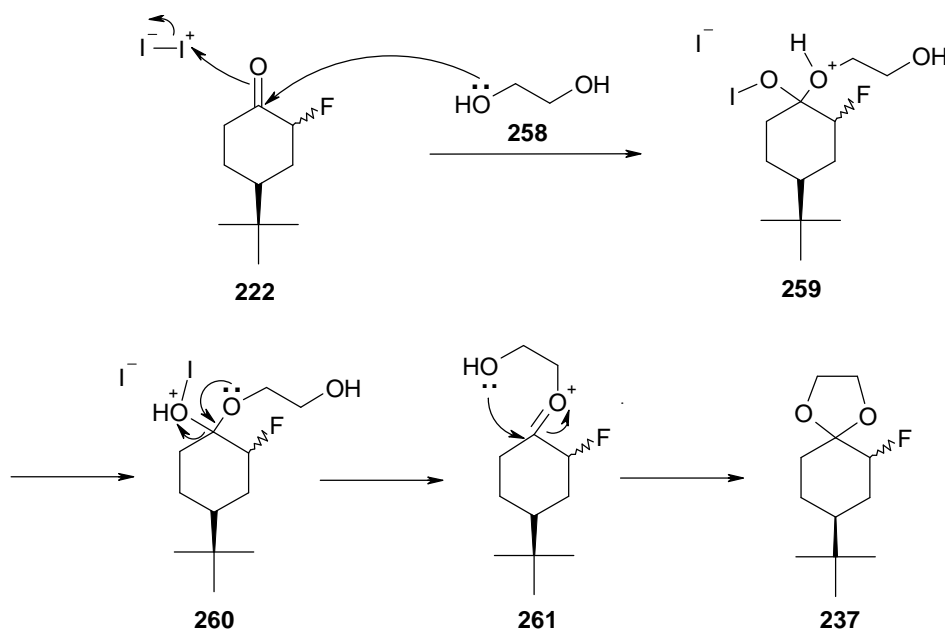
**Scheme 3.21** The hydrolysis of ketals **237a** and **237b** was too slow for <sup>19</sup>F NMR analyses.

Due to the very slow rate of the ketal hydrolysis, the relative rate of ketal formation was explored. Both fluoro cyclohexanone isomers **222a** and **222b** were combined in an NMR tube in a 1 : 1 ratio with less than 1 equivalent of ethylene glycol in CD<sub>3</sub>CN.



**Scheme 3.22** Ketal formation from **222a** and **222b**.

Iodine ( $I_2$ ) as a catalyst in the formation of a ketal has been reported by B. K. Banik<sup>13</sup>, where it was concluded that there is a “*complexation role for molecular iodine apart from its acidity*”.<sup>15</sup> Thus the process does not appear to involve HI as the catalyst, and a mechanism such as that illustrated in **Scheme 3.23** is proposed.



**Scheme 3.23** Proposed mechanism when  $I_2$  is the catalyst and undergoes complexation.

The reaction was followed by  $^{19}F$ -NMR from reaction initiation, by addition of  $I_2$ . The corresponding pairs of  $^{19}F$ -NMR coupled signals **222a** /**237a** and **222b**/**237b** were then integrated and the progress of the reaction was determined in terms of the % converted to the ketals **237a** and **237b**. An example of an intermediate  $^{19}F$  NMR for the reaction is shown in **Figure 3.10**.

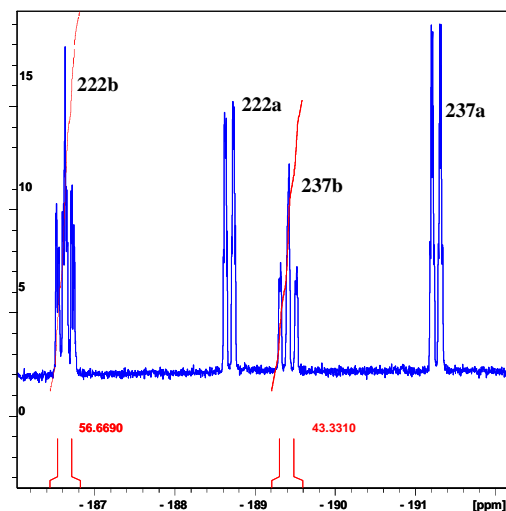


**Figure 3.10**  $^{19}\text{F}$ -NMR at approximately 40% conversion during ketal **237a/b** from ketones **222a/b** (see **Scheme 3.23**).

It can be seen that the initial rates of ketal **237a/b** formation from **222a/b** are very similar (**Figure 3.11**). The forward reactions to the ketals were not sufficiently different to differentiate the relative rates of reaction and the reverse reaction to form the ketones was too slow to be assessed by  $^{19}\text{F}$  NMR. Thus, in the end, these reactions were unsuitable for exploring the influence of the orientation of the fluorine on the reactivity.

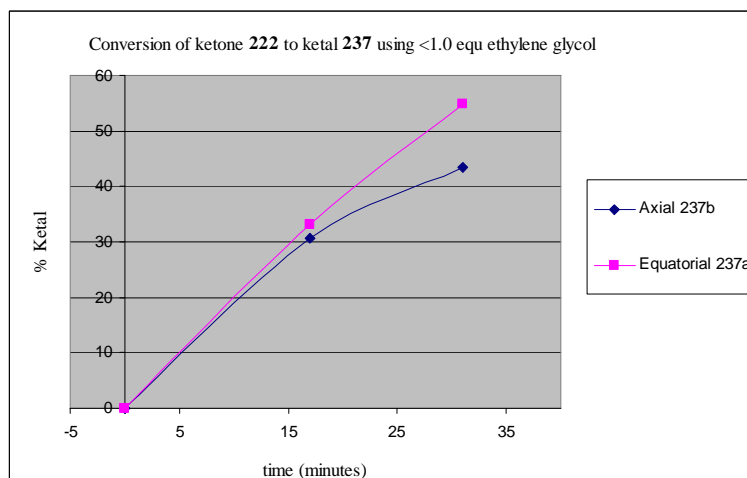
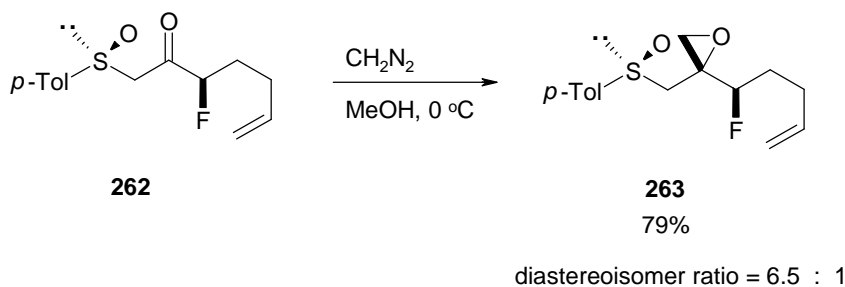


**Figure 3.11** The rate of reaction of ketal **237a/b** formation from **222a/b** was similar for axial and equatorial **237**.

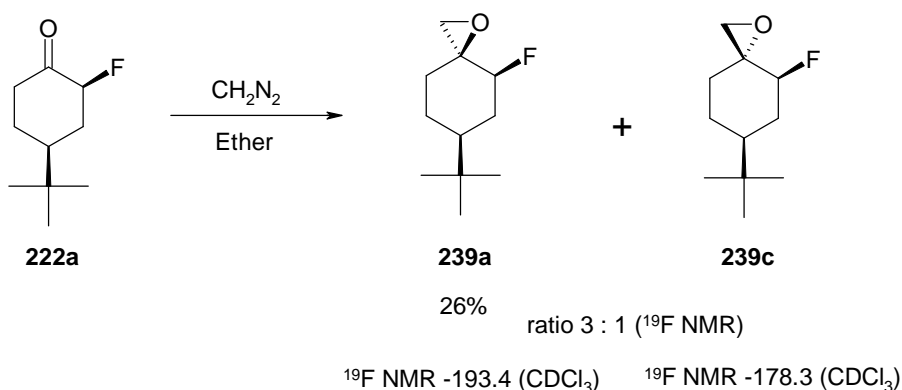
### 3.7 Synthesis of $\alpha$ -fluoro epoxides

Epoxide formation by methylene homologation of an  $\alpha$ -fluoro cyclohexanone has not been reported in the literature, however it is known that ketones including  $\alpha$ -fluoroketones, can be treated with diazomethane to afford the corresponding epoxides in good yield.



**Scheme 3.24** An example of a diazomethane mediated epoxidation of an  $\alpha$ -fluoroketone.<sup>16</sup>

Such a reaction was explored with **222a** and **222b**, diazomethane was prepared freshly from Diazald, 2-(2-ethoxyethoxy)ethanol and KOH,<sup>17</sup> and the diazomethane was then used in a reaction with the equatorial fluoro ketone **222a**. This resulted in two diastereoisomers in a ratio of 3 : 1 (**Scheme 3.25**).



**Scheme 3.25** Preparation of epoxides **239a** and **239c** from **222a** with diazomethane.

The major epoxide **239a** was subjected to NOESY-NMR analysis in an attempt to establish its relative stereochemistry. Both the CH<sub>2</sub>O protons were irradiated individually (**Figure 3.12**) and the nOe response was observed. The H<sub>a</sub> proton was observed to have an nOe with CHF as well as H<sub>b</sub>, suggesting that the major epoxide is **239a**.

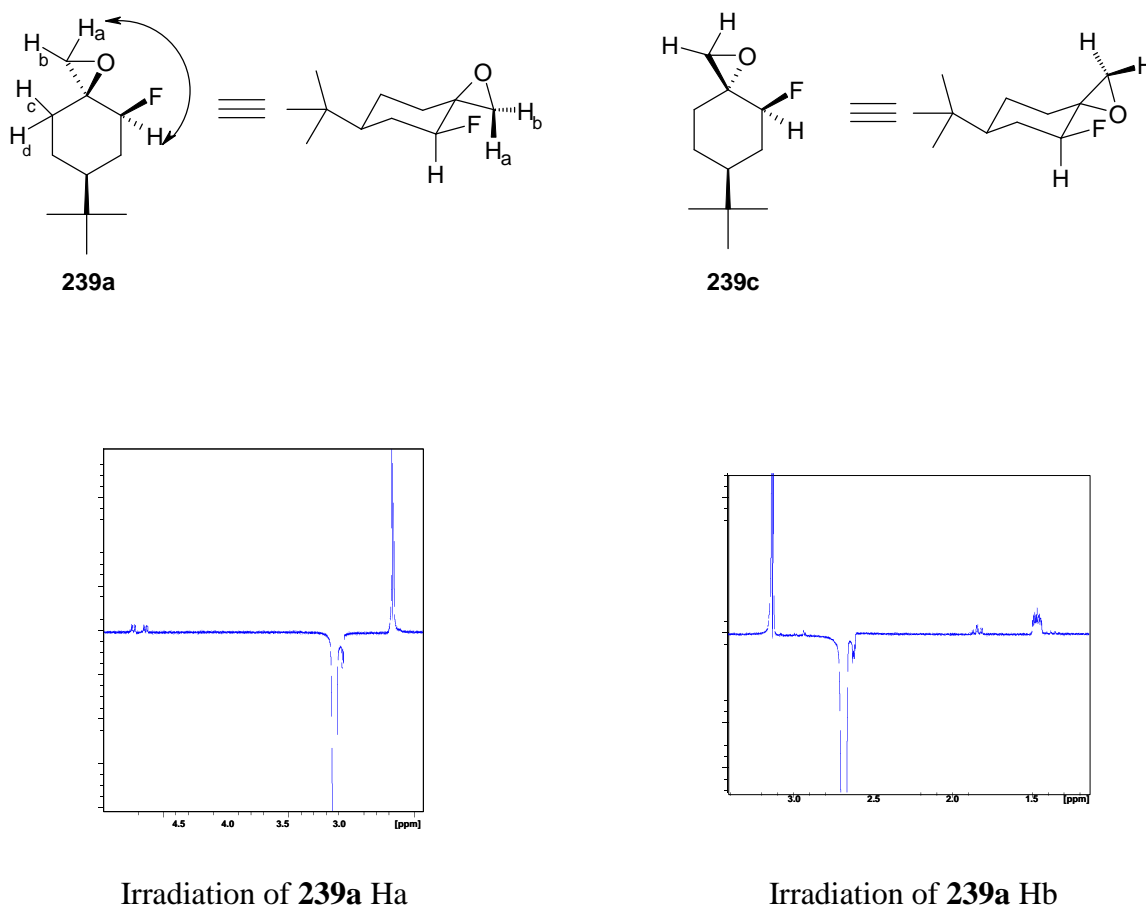
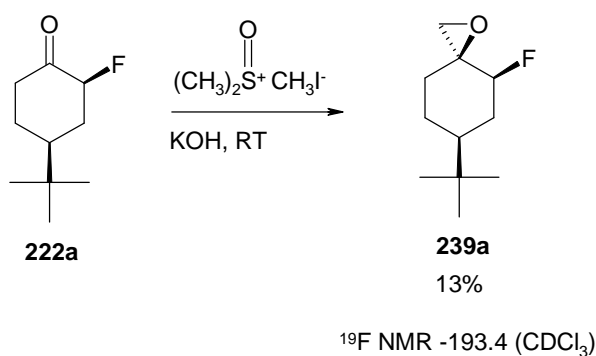


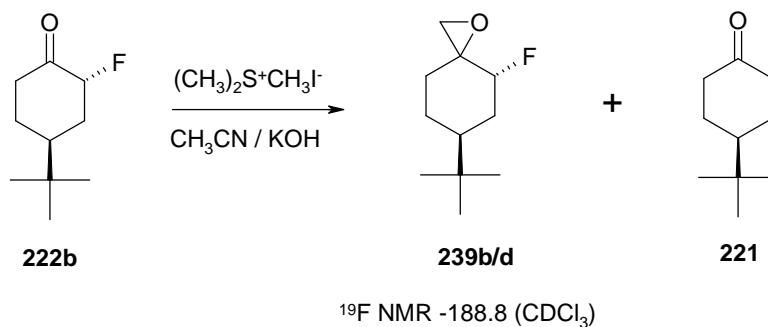
**Figure 3.12** The stereochemistry of the major epoxide was determined by nOe studies.

An alternative method for epoxidation was investigated in anticipation that a better yield of the isomer **239c** could be obtained. The reaction of 4-*tert*-butylcyclohexanone **221** with a ylide in both acetonitrile and in the solid state have been reported.<sup>18, 19</sup>

Accordingly a solid state reaction on **222a** was carried out by combining the ketone with trimethyloxosulfonium iodide and ground KOH and rotating this mixture at RT. Epoxide **239a** was isolated. However, the yield was again poor (**Scheme 3.26**). A similar ylide reaction (**Scheme 3.27**) was attempted on the diastereoisomer **222b**, however this reaction was also poor (<10%).

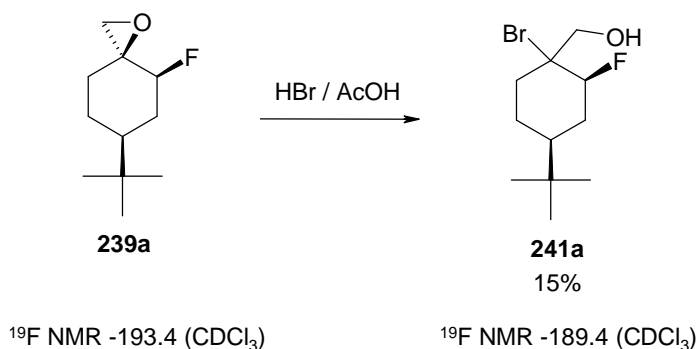


**Scheme 3.26** Synthesis of epoxide **239a** via an ylide reaction.



**Scheme 3.27** Synthesis of epoxide **239b/d** from **222b** via an ylide reaction.

Although conversion of **239a** to the bromo alcohol **241a** was achieved, the study of these epoxides was not progressed owing to synthetic difficulties in obtaining both of the epoxide diastereoisomers in an adequate yield.



**Scheme 3.28** The bromo alcohol **241a** was provided by reaction with HBr.

In conclusion the C-O<sup>+</sup>-----F-C charge dipole interaction was explored *via* a number of synthetic routes. During this research however, unexpected products from a Grignard reaction on the fluorocyclohexanone **222** were observed. It appears that re-arrangement of **222b** followed by fluorine elimination accounts for the synthesis of **249a** and that the *anti periplanar* phenyl migration, followed by fluorine elimination explains the observation of **250a**. In the case of fluorocyclohexanone **222a**, Grignard reaction again provided **249a** which differs from the predicted diastereoisomer (**249b**), this indicated that **249a** was possibly a product of epimerisation of the product **249b**.

### 3.8 References for chapter three

1. K. Tenza, J. S. Northen, D. O'Hagan and A. M. Z. Slawin, *Beilstein J. Org. Chem.*, 2005, **1**, 13.
2. S. E. Denmark, Z. Wu, C. M. Crudden and H. Matsuhashi, *J. Org. Chem.*, 1997, **62**, 8288-8289.
3. A. Solladie-Cavallo, L. Jierry, A. Klein, M. Schmitt and R. Welter, *Tetrahedron: Asymmetry*, 2004, **15**, 3891-3898.
4. S. Stavber and M. Zupan, *Tetrahedron Lett.*, 1996, **37**, 3591-3594.
5. C. M. Garner, P. Terech, J.-J. Allegraud, B. Mistrot, P. Nguyen, A. de Geyer and D. Rivera, *J. Chem. Soc. Faraday Trans.*, 1998, **94**, 2173-2179.
6. S. B. Billings and K. A. Woerpel, *J. Org. Chem.*, 2006, **71**, 5171-5178.
7. F. G. Bordwell and K.-C. Yee, *J. Am. Chem. Soc.*, 1970, **92**, 5933-5938.
8. M. Hori, T. Kataoka, H. Shimizu, E. Imai, T. Iwamura and K. Maeda, *Chem. Pharm. Bull.*, 1986, **34**, 3599-3605.
9. J.-H. Xie, S. Liu, X.-H. Huo, X. Cheng, H.-F. Duan, B.-M. Fan, L.-X. Wang and Q.-L. Zhou, *J. Org. Chem.*, 2005, **70**, 2967-2973.
10. R. J. Spear and S. Sternhell, *Aust. J. Chem.*, 1985, **38**, 889-897.
11. M. Tiffeneau and B. Tchoubar, *Compt. Rend.*, 1934, **199**, 360-362.
12. L. A. Paquette and C. S. Ra, *J. Org. Chem.*, 1988, **53**, 4978-4985.
13. B. K. Banik, M. Chapa, J. Marquez and M. Cardona, *Tetrahedron Lett.*, 2005, **46**, 2341-2343.
14. J. J. Wolff, G. Frenking and K. Harms, *Chem. Ber.*, 1991, **124**, 551-561.
15. B. K. Banik, M. Fernandez and C. Alvarez, *Tetrahedron Lett.*, 2005, **46**, 2479-2482.



16. P. Ambrosi, A. Arnone, P. Bravo, L. Bruche, A. De Cristofaro, V. Francardi, M. Frigerio, E. Gatti, G. S. Germinara, W. Panzeri, F. Pennacchio, C. Pesenti, G. Rotundo, P. F. Roversi, C. Salvadori, F. Viani and M. Zanda, *J. Org. Chem.*, 2001, **66**, 8336-8343.
17. A. I. Vogel, *Vogels Textbook of Practical Organic Chemistry*, 1989.
18. E. Borredon, M. Delmas and A. Gaset, *Tetrahedron Lett.*, 1987, **28**, 1877-1880.
19. F. Toda and N. Imai, *J. Chem. Soc., Perkin Trans. 1*, 1994, 2673-2674.

## **Chapter 4                      Experimental**

### **4.1 General experimental procedures**

#### **4.1.1 Reagents and solvents**

Commercially available reagents and solvents were used where available and purchased from Aldrich, Fluka, Lancaster and Acros. The solvents used in reactions were dried, distilled and stored under nitrogen prior to use. Some solvents were commercially available as dry and were used as such.

#### **4.1.2 Reaction conditions**

Where dry conditions were required, glassware was oven dried and reactions were carried out under a nitrogen atmosphere. Reaction temperatures of  $-78\text{ }^{\circ}\text{C}$  were obtained using solid  $\text{CO}_2$  and isopropyl alcohol or acetone. For those at  $0\text{ }^{\circ}\text{C}$ , an ice bath was employed and where heat was required an oil bath with contact thermometer was used. Reactions were monitored by TLC, GC-MS or LC-MS where available. TLC was carried out using Machery-Nagel Polygram® SIL G UV<sub>254</sub> pre-coated plastic sheets with 0.20 mm silica gel and fluorescent indicator. Indicators used included potassium permanganate stain, molybdenum based stain and ninhydrin spray.

### **4.1.3 Purification techniques:**

#### **Column chromatography**

Silica gel, 40–63 micron grade from Apollo was used in the purification of crude products by column chromatography. The samples were either applied directly to the top of the silica / solvent column or applied as a dry silica gel slurry.

#### **Teledyne Isco Combiflash Companion™ purification system**

**(on placement at GSK)**

Crude samples were dissolved in a small amount of DCM and applied to RediSep® pre-packed columns. The column was placed within the Teledyne Isco Combiflash Companion® purification system and automated purification was carried out using a solvent gradient program. The system was used either with the automated fraction collection facility where compounds were detected by UV or by collecting all fractions.

#### **Preparative TLC**

Analtech Uniplat™ glass sheets (20 x 20 cm) coated with silica gel (1000 microns) and UV<sub>254</sub> indicator were used on a small amount of sample requiring a delicate purification method.

#### 4.1.4 Nuclear Magnetic Resonance Spectroscopy (NMR)

NMR was recorded on Bruker Avance instruments operating at 300 and 400 MHz ( $^1\text{H}$ ), 75 and 100 MHz ( $^{13}\text{C}$ ), 282 and 376 MHz ( $^{19}\text{F}$ ). Calibration was carried out using the residual solvent shift from the deuterated solvent.<sup>1</sup> Where  $\text{CDCl}_3$  was employed as the solvent, calibration was carried out on this solvent signal at 7.26 ( $^1\text{H}$ ) and 77.16 ( $^{13}\text{C}$ ). Where aromatics were present in the sample to be analysed,  $\text{Me}_4\text{Si}$  was added to  $\text{CDCl}_3$  and the spectra were calibrated at 0.0 ( $^1\text{H}$ ). Where  $\text{D}_2\text{O}$  was used the water signal was designated the internal reference at 4.79ppm ( $^1\text{H}$ ), for  $\text{CD}_3\text{OD}$ , the internal reference was designated at 3.31ppm ( $^1\text{H}$ ) and 49.0ppm ( $^{13}\text{C}$  NMR), for  $(\text{CD}_3)_2\text{SO}$  the internal reference was designated at 2.50ppm ( $^1\text{H}$ ) and 39.5ppm ( $^{13}\text{C}$ ). For  $^{19}\text{F}$ ,  $\text{CFCl}_3$  as an external reference was used.

Chemical shifts are reported in parts per million (ppm) and coupling constants are given in Hertz (Hz). The abbreviations for the multiplicity of the proton and carbon signals are as follows: s singlet, d doublet, dd doublet of doublet, dt doublet of triplets, ddt doublet of doublet of triplets, t triplet, tt triplet of triplets, q, quintet, m multiplet.

#### 4.1.5 Mass spectroscopy

High resolution mass analysis was carried out by Caroline Horsburgh, spectra were recorded on a Micromass LCT TOF mass spectrometer using ES ionization in +ve ion mode. Where this method was not adequate CI was employed using a Micromass GCT instrument.

#### **4.1.6 Elemental analyses**

Elemental analyses were carried out by Silvia Williamson using a CE instrument EA 1110 CHNS analyser.

#### **4.1.7 Melting point analyses**

Melting points were measured on a Gallenkamp Griffin MPA350.BM2.5 instrument.

#### **4.1.8 GC-MS**

Low resolution GC-MS analysis was carried out using an Agilent 6890 plus gas chromatograph coupled to a 5973N mass selective detector in EI mode, with helium carrier gas. Automatic injections using a 7683 series injector were made into both non-chiral and chiral columns. Separations were achieved with an Agilent HP 19091S-433, 5% phenyl methyl siloxane, 30m x 250 $\mu$ m, film thickness 0.25  $\mu$ m, non-chiral column and a  $\beta$ -DEX 120 Supercosil chiral column. The HP 6890 chemstation software was used for data processing.

#### **4.1.9 LC-MS**

Low resolution LC-MS analysis was carried out on a Supelcosil ABZ+PLUS column (3  $\mu$ m, 3.3 cm x 4.6 mm ID) eluting with 0.1% HCO<sub>2</sub>H and 0.01 M ammonium acetate in water (solvent A), and 95% CH<sub>3</sub>CN and 5% water (containing 0.5% HCO<sub>2</sub>H) (solvent B). The elution gradient was as follows: 0–0.7 min 0% B, 0.7–4.2 min 0–100% B, 4.2–4.6 min 100% B with a flow rate of 3 cm<sup>3</sup> / min. Three modes of detection were used: electrospray

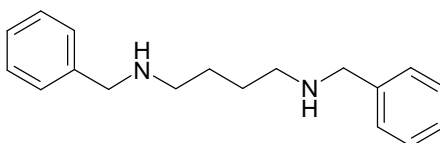
in positive mode, electrospray in negative mode which were recorded on a Waters ZQ mass spectrometer and diode array UV detection which was carried out in the range 215–330 nm.

#### **4.1.10 IR**

IR spectra were recorded on a Perkin Elmer, Spectrum GX, FT-IR system as a fine film on poly-tetrafluoroethylene IR cards.

## 4.2 Experimental protocols

### 4.2.1 *N,N'*-Dibenzylbutane-1,4-diamine **75** <sup>2</sup>, *N, N, N'*-tribenzylbutane-1,4-diamine **81** and tetra-*N*-benzylbutanediyldiamine **82** <sup>3</sup>



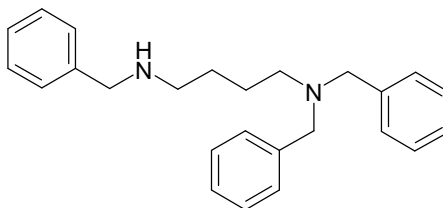
$\text{K}_2\text{CO}_3$  (0.81 g, 5.86 mmol) and chloromethyl benzene (4.3 cm<sup>3</sup>, 37.3 mmol) was added to a solution of butane-1,4-diamine (1.61 g, 18.31 mmol) in EtOH (20 cm<sup>3</sup>) at RT. The reaction was stirred for 48 h then heated to 100 °C for 26 h, after which the reaction was cooled and EtOH removed under reduced pressure. The crude product was taken up into water and the pH adjusted from 10 to 14 with NaOH (20%). Organic material was extracted into DCM, and the solvent was removed under reduced pressure. Purification over silica gel (DCM: MeOH 9:1) was carried out to give the title product and by-product; *N, N, N'*-tribenzylbutane-1,4-diamine **81**.

**75**

m/z (EI): 267 [M-H]<sup>+</sup> (35%), 160 (52), 106 [C<sub>6</sub>H<sub>5</sub>CH<sub>2</sub>NH]<sup>+</sup> (10), 91 [C<sub>6</sub>H<sub>5</sub>CH<sub>2</sub>]<sup>+</sup> (100).

LRMS (EI): found 269.15 Calcd. for C<sub>18</sub>H<sub>24</sub>N<sub>2</sub>+H, 269.20.

81

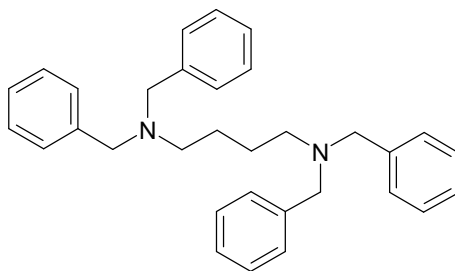


**81** was obtained as a yellow oil (0.49 g, 10%).

$\delta_{\text{H}}$  ( $\text{CDCl}_3$ , 300.13 MHz): 1.37–1.47 (2 H, m,  $\text{NCH}_2\text{CH}_2$ ), 1.56–1.67 (2 H, m,  $\text{NCH}_2\text{CH}_2$ ), 2.27–2.33 (2 H, m,  $\text{NCH}_2\text{CH}_2$ ), 2.44–2.51 (2 H, m,  $\text{NCH}_2\text{CH}_2$ ), 3.43 (4 H, s,  $\text{CH}_2\text{Ph}$ ), 3.75 (2 H, s,  $\text{NHCH}_2\text{Ph}$ ), 7.12–7.36 (15 H, m, Ph-H).  $\delta_{\text{C}}$  ( $\text{CDCl}_3$ , 75.48 MHz): 24.5 ( $\text{NCH}_2\text{CH}_2$ ), 24.8 ( $\text{NCH}_2\text{CH}_2$ ), 46.9 ( $\text{NCH}_2\text{CH}_2$ ), 54.6 ( $\text{NHCH}_2\text{Ph}$ ), 52.6 ( $\text{NCH}_2\text{CH}_2$ ), 58.4 ( $\text{CH}_2\text{Ph}$ ), 127.0 (CH), 128.4 (CH), 128.7 (CH), 129.0 (CH), 129.0 (CH), 129.8 (CH), 133.5 (C), 139.6 (C).  $m/z$  (EI): 357  $[\text{M}-\text{H}]^+$  (60%), 210 (18), 160 (62), 91  $[\text{C}_6\text{H}_5\text{CH}_2]^+$  (100). HRMS (CI): found 359.2493. Calcd. for  $\text{C}_{25}\text{H}_{30}\text{N}_2+\text{H}$ , 359.2487.

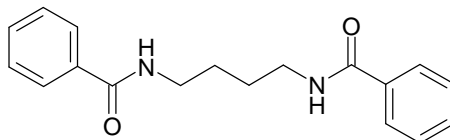


82



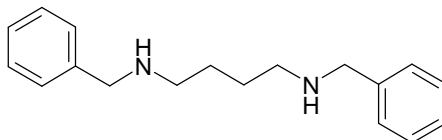
**82** was obtained as a white solid (1.89 g, 38%).

Mp 130–132 °C (from hexane), (Lit.,<sup>3</sup> 90 °C).  $\delta_{\text{H}}$  (CDCl<sub>3</sub>, 300.13 MHz): 1.36–1.44 (4 H, m, NCH<sub>2</sub>CH<sub>2</sub>), 2.23–2.30 (4 H, m, NCH<sub>2</sub>CH<sub>2</sub>), 3.43 (8 H, s, CH<sub>2</sub>Ph), 7.10–7.30 (20 H, m, Ph-H).  $\delta_{\text{C}}$  (CDCl<sub>3</sub>, 75.48 MHz): 24.8 (NCH<sub>2</sub>CH<sub>2</sub>), 53.4 (NCH<sub>2</sub>CH<sub>2</sub>), 58.4 (CH<sub>2</sub>Ph), 126.8 (CH), 128.2 (CH), 128.9 (CH) 140.1 (C). Elemental analysis: found C, 85.5; H, 8.3; N, 6.2. Calc. for C<sub>32</sub>H<sub>36</sub>N<sub>2</sub>: C, 85.7; H, 8.1; N, 6.2%. LRMS (EI): found 449.17. Calcd. for C<sub>32</sub>H<sub>36</sub>N<sub>2</sub>+H, 449.30.

4.2.2 *N,N'*-Butanediylbisbenzamide **84**<sup>4</sup>

Triethylamine (4 cm<sup>3</sup>) was added to a solution of butane-1,4-diamine (1.62 g, 18.2 mmol) in DCM (20 cm<sup>3</sup>) at 0 °C. Benzoyl chloride (5.13 g, 36.5 mmol) in DCM (10 cm<sup>3</sup>) was then added slowly and the reaction was stirred for 21 h at RT. The DCM was removed under reduced pressure and the resulting solid was washed with water (200 cm<sup>3</sup>) and HCl (2 cm<sup>3</sup>), followed by three washes of sodium carbonate (aq) solution (3 x 15 cm<sup>3</sup>). The resultant white solid **84** was filtered and dried at 80 °C overnight. (4.46 g, 83%).

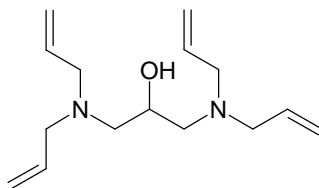
Mp 175–176 °C (from ethyl acetate), (Lit.,<sup>4</sup> 176–177 °C).  $\delta_{\text{H}}$  (CDCl<sub>3</sub>, 300.06 MHz): 1.72–1.77 (4 H, m, NCH<sub>2</sub>CH<sub>2</sub>), 3.52–3.58 (4 H, m, NCH<sub>2</sub>CH<sub>2</sub>), 6.53 (2 H, br s, NH), 7.40–7.53 (6 H, m, Ph-H), 7.79–7.83 (4 H, m, Ph-H).  $\delta_{\text{C}}$  ((CD<sub>3</sub>)<sub>2</sub>SO, 100.62 MHz): 26.8 (NCH<sub>2</sub>CH<sub>2</sub>), 39.0 (NCH<sub>2</sub>CH<sub>2</sub>), 127.2 (CH), 128.3 (CH), 131.1 (CH), 134.7 (C), 166.2 (C=O). *m/z* (EI): 281 [M-O]<sup>+</sup> (13%), 207 (55), 191 [M-C<sub>6</sub>H<sub>5</sub>CO]<sup>+</sup> (15), 174 (30), 162 [C<sub>6</sub>H<sub>5</sub>CONHCH<sub>2</sub>CH<sub>2</sub>CH<sub>2</sub>]<sup>+</sup> (13), 148 [C<sub>6</sub>H<sub>5</sub>CONHCH<sub>2</sub>CH<sub>2</sub>]<sup>+</sup> (15), 134 [C<sub>6</sub>H<sub>5</sub>CONHCH<sub>2</sub>]<sup>+</sup> (15), 105 [C<sub>6</sub>H<sub>5</sub>CO]<sup>+</sup> (100), 77 [C<sub>6</sub>H<sub>5</sub>]<sup>+</sup> (73). LRMS (EI): found 297.04. Calcd. for C<sub>18</sub>H<sub>20</sub>O<sub>2</sub>N<sub>2</sub>+H, 297.16. Elemental analysis found: C, 72.4; H, 7.0; N, 9.2. Calc. for C<sub>18</sub>H<sub>20</sub>N<sub>2</sub>O<sub>2</sub>: C, 72.9; H, 6.8; N, 9.5%.

4.2.3 *N, N'*-Dibenzylbutane-1,4-diamine **75**<sup>2</sup>

LiAlH<sub>4</sub> (1.80 g, 47.5 mmol) was added to a solution of *N, N'*-butanediylbisbenzamide (1.45 g, 4.9 mmol) in THF (30 cm<sup>3</sup>) at 0 °C. The reaction was stirred for 22 h at RT and was then quenched at 0 °C with water (10 cm<sup>3</sup>) followed by NaOH 30% (3 cm<sup>3</sup>). Ether (10 cm<sup>3</sup>) was added to aid stirring. The mass was filtered and the solvents removed under reduced pressure. The resulting crude liquid was partitioned between DCM and water and the DCM phase was dried with MgSO<sub>4</sub> and the solvent removed under reduced pressure. The product was obtained as a yellow liquid (0.84 g, 64%) without further purification.

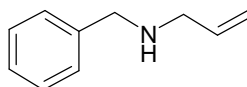
$\delta_{\text{H}}$  (CDCl<sub>3</sub>, 300.06 MHz): 1.41–1.51 (4 H, m, NCH<sub>2</sub>CH<sub>2</sub>), 2.60–2.66 (4 H, m, NCH<sub>2</sub>CH<sub>2</sub>), 3.77 (4 H, s, CH<sub>2</sub>Ph), 7.21–7.32 (10 H, m, Ph-H).  $\delta_{\text{C}}$  (CDCl<sub>3</sub>, 75.48 MHz): 28.0 (NCH<sub>2</sub>CH<sub>2</sub>), 49.4 (NCH<sub>2</sub>CH<sub>2</sub>), 54.1 (CH<sub>2</sub>Ph), 127.0 (CH), 128.2 (CH), 128.5 (CH) 140.5 (C).

**75** was also characterised by GC-MS and LRMS. The analysis was found to be identical to that in **section 4.2.1**.

4.2.4 1,3-Bis(diallylamino)-2-propanol 93 <sup>5</sup>

NaOH 25% (8 cm<sup>3</sup>) was added to a solution of diallylamine (7.77 g, 80.0 mmol) in MeCN (10 cm<sup>3</sup>) at 0 °C, and then chloromethyloxirane (3.66 g, 39.6 mmol) was added, and the mixture was heated under reflux for 22 h. After cooling, the NaOH phase was separated and the acetonitrile evaporated under reduced pressure. The product was extracted into DCM, washed with water, dried (MgSO<sub>4</sub>) and re-concentrated. Purification by distillation gave the product as a clear liquid (5.79 g, 58%).

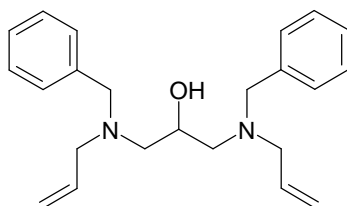
$\delta_{\text{H}}$  (CDCl<sub>3</sub>, 300.06 MHz): 2.41–2.44 (4 H, m, CH(OH)CH<sub>2</sub>), 3.08 (4 H, dddd, *J* 1.2, *J* 1.2, *J* 6.9, *J* 14.1, CH<sub>2</sub>CH=CH<sub>2</sub>), 3.18 (4 H, dddd, *J* 1.2, *J* 1.2, *J* 6.1, *J* 14.1, CH<sub>2</sub>CH=CH<sub>2</sub>), 3.55 (1 H, br s, OH), 3.78 (1 H, m, CH(OH)CH<sub>2</sub>), 5.10–5.19 (8 H, m, CH=CH<sub>2</sub>), 5.82 (4 H, m, CH<sub>2</sub>CH=CH<sub>2</sub>).  $\delta_{\text{C}}$  (CDCl<sub>3</sub>, 75.46 MHz): 57.4 (NCH<sub>2</sub>CH=CH<sub>2</sub>), 57.7 (NCH<sub>2</sub>CHOH), 65.5 (CHOH), 117.8 (CH=CH<sub>2</sub>), 135.6 (CH=CH<sub>2</sub>). *m/z* (EI): 140 [NCH<sub>2</sub>CHOH(CH<sub>2</sub>CH=CH<sub>2</sub>)<sub>2</sub>]<sup>+</sup> (57%), 110 [NCH<sub>2</sub>(CH<sub>2</sub>CH=CH<sub>2</sub>)<sub>2</sub>]<sup>+</sup> (100), 41 [CH<sub>2</sub>CH=CH<sub>2</sub>]<sup>+</sup> (28).

4.2.5 *N*-Allylbenzylamine **95**<sup>6</sup>

Benzyl bromide (7.8 cm<sup>3</sup>, 65.89 mmol) was added slowly to neat allylamine (29 cm<sup>3</sup>, 391.8 mmol) over 50 min at 0 °C. The reaction was then stirred for 4 h, warming to ambient temperature and once the benzyl bromide had fully reacted the reaction was quenched with aqueous sodium bicarbonate. The reaction was extracted into diethylether and dried with potassium carbonate, concentrated and purified over silica gel (hexane : ethyl acetate 1:2), to give the product as a clear yellow liquid (7.26 g, 75%).

$\delta_{\text{H}}$  (CDCl<sub>3</sub>, 300.13 MHz): 1.30 (1 H, br s, NH), 3.19 (2 H, ddd, *J* 1.4, *J* 1.4, *J* 5.9, NCH<sub>2</sub>CH), 3.70 (2 H, s, PhCH<sub>2</sub>), 5.03 (1 H, ddt, *J* 1.4, *J* 1.8, *J* 10.2, *cis* CH=CH<sub>2</sub>), 5.11 (1 H, ddt, *J* 1.7, *J* 1.7, *J* 17.3, *trans* CH=CH<sub>2</sub>), 5.85 (1 H, ddt, *J* 5.9, *J* 10.3, *J* 17.2, CH<sub>2</sub>CH=CH<sub>2</sub>), 7.13–7.25 (5 H, m, Ph-H).  $\delta_{\text{C}}$  (CDCl<sub>3</sub>, 75.48 MHz): 51.9 (NCH<sub>2</sub>CH), 53.4 (PhCH<sub>2</sub>), 116.1 (CH=CH<sub>2</sub>), 127.0 (CH), 128.3 (CH), 128.5 (CH), 136.9 (CH=CH<sub>2</sub>), 140.4 (C). *m/z* (EI): 146 [M-H]<sup>+</sup> (39%), 91 [Bn]<sup>+</sup> (100), 56 [NHCH<sub>2</sub>CHCH<sub>2</sub>]<sup>+</sup> (21).

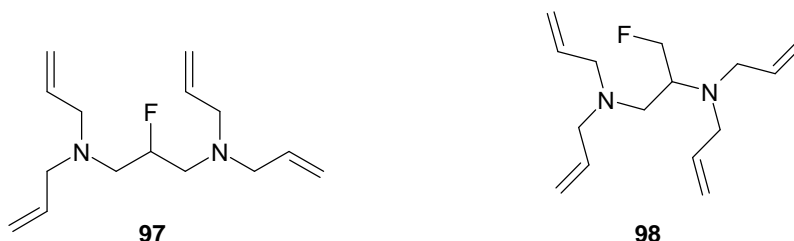
## 4.2.6 1,3-Bis[allyl(benzyl)amino]-2-propanol 96



A mixture of allylbenzylamine (13.79 g, 93.8 mmol), chloromethyl-oxirane (4.66 g, 49.0 mmol) and NaOH 20% (10 cm<sup>3</sup>) was heated to 113 °C. The reaction was stirred for 47 h and monitored by GC-MS. When the allylbenzylamine ceased to react, the reaction was quenched with water. The product was then extracted into DCM, dried (MgSO<sub>4</sub>), and concentrated under reduced pressure. Purification was carried out over silica gel using two sequential columns (hexane: ethyl acetate 1:3) then (17:1). The product was obtained as a clear yellow liquid (10.3 g, 63%).

$\delta_{\text{H}}$  (CDCl<sub>3</sub>, 300.06 MHz): 2.48–2.52 (4 H, m, NCH<sub>2</sub>CHOH), 3.08 (2 H, dddd, *J* 1.8, *J* 1.8, *J* 6.9, *J* 14.1, CH<sub>2</sub>CH=CH<sub>2</sub>), 3.18 (2 H, dddd, *J* 1.8, *J* 1.8, *J* 6.1, *J* 14.1, CH<sub>2</sub>CH=CH<sub>2</sub>), 3.64 (4 H, dd, *J* 13.7, *J* 37.9, PhCH<sub>2</sub>), 3.84 (1 H, m, CH(OH)), 5.15–5.22 (4 H, m, CH=CH<sub>2</sub>), 5.87 (2 H, m, CH=CH<sub>2</sub>), 7.23–7.33 (10 H, m, Ph-H).  $\delta_{\text{C}}$  (CDCl<sub>3</sub>, 75.46 MHz): 57.4 (NCH<sub>2</sub>CH=CH<sub>2</sub>), 57.8 (NCH<sub>2</sub>CHOH), 58.7 (PhCH<sub>2</sub>), 65.7 (CHOH), 117.8 (CH=CH<sub>2</sub>); 127.1 (CH), 128.3 (CH), 129.1 (CH), 135.5 (CH=CH<sub>2</sub>), 139.1 (C). *m/z* (EI): 190 [M]<sup>+</sup> (33%), 160 [BnN(CH<sub>2</sub>)CH<sub>2</sub>CH=CH<sub>2</sub>]<sup>+</sup> (48), 91 [Bn]<sup>+</sup> (100). HRMS (ES): Found 373.2258. Calcd. for C<sub>23</sub>H<sub>30</sub>N<sub>2</sub>ONa, 373.2256.

**4.2.7**      ***N, N, N', N'* -Tetraallyl-2-fluoro-1,3-propanediamine **97****  
**and *N, N, N', N'*-tetraallyl-3-fluoro-1,2-propanediamine **98****



DAST (1.2 cm<sup>3</sup>, 10.1 mmol) was added to a solution of 1,3-bis(diallylamino)-2-propanol (2.51 g, 10.0 mmol) in DCM (10 cm<sup>3</sup>) at -78 °C. The reaction was allowed to warm to ambient temperature and was stirred for 24 h before quenching with aqueous sodium bicarbonate. The product was then extracted into DCM, dried (MgSO<sub>4</sub>) and concentrated under reduced pressure. The product **97** : isomer **98** ratio was present in a ratio of 7 : 1 (by <sup>19</sup>F NMR). Purification over silica gel (hexane : ethyl acetate 5:1) allowed separation of the isomers **97** (1.02 g, 40%) and **98**(162 mg, 6%) as light yellow liquids.

**97**

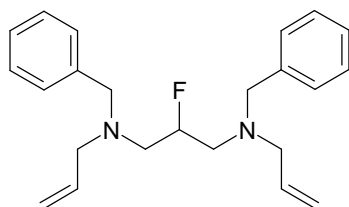
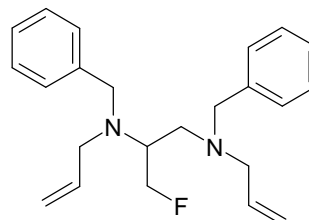
$\delta_{\text{H}}$  (CDCl<sub>3</sub>, 300.06 MHz): 2.57–2.67 (4 H, m, CHFCH<sub>2</sub>), 3.12 (8 H, d, *J* 6.4, NCH<sub>2</sub>CH=CH<sub>2</sub>), 4.72 (1 H, dm, *J* 49.9, CHFCH<sub>2</sub>), 5.07–5.18 (8 H, m, CH=CH<sub>2</sub>), 5.80 (4 H, m, CH<sub>2</sub>CH=CH<sub>2</sub>).  $\delta_{\text{C}}$  (CDCl<sub>3</sub>, 75.46 MHz): 55.4 (d, *J* 21.6, NCH<sub>2</sub>CHF), 57.7 (NCH<sub>2</sub>CH=CH<sub>2</sub>), 92.0 (d, *J* 171.4, CHF), 117.6 (CH=CH<sub>2</sub>), 135.6 (CH=CH<sub>2</sub>).  $\delta_{\text{F}}$  (CDCl<sub>3</sub>, 282.29 MHz): -184.0 (m, CHF).  $\nu_{\text{max}}$  /cm<sup>-1</sup> (film): 3077, 2809, 1746, 1644, 1447, 1418, 1355, 1212, 1153. *m/z* (EI): 136 [NCH<sub>2</sub>CCH<sub>2</sub>(CH<sub>2</sub>CH=CH<sub>2</sub>)<sub>2</sub>]<sup>+</sup> (100%), 110 [NCH<sub>2</sub>(CH<sub>2</sub>CH=CH<sub>2</sub>)<sub>2</sub>]<sup>+</sup> (84), 41 [CH<sub>2</sub>CH=CH<sub>2</sub>]<sup>+</sup> (45). HRMS (ES): Found 253.2073. Calcd. for C<sub>15</sub>H<sub>26</sub>N<sub>2</sub>F, 253.2080.

**98**

$\delta_{\text{H}}$  ( $\text{CDCl}_3$ , 300.06 MHz): 2.40 (1 H, ddd,  $J$  3.2,  $J$  5.3,  $J$  13.0,  $\text{CHCH}_2$ ), 2.48 (1 H, dd,  $J$  9.0,  $J$  13.0,  $\text{CHCH}_2$ ), 2.87–3.21 (8 H, m,  $\text{NCH}_2\text{CH}=\text{CH}_2$ ) (1 H, m, NCH), 4.50 (2 H, dd,  $J$  4.6,  $J$  47.9,  $\text{CH}_2\text{F}$ ), 4.99–5.18 (8 H, m,  $\text{CH}=\text{CH}_2$ ), 5.66–5.81 (4 H, m,  $\text{CH}_2\text{CH}=\text{CH}_2$ ).  $\delta_{\text{C}}$  ( $\text{CDCl}_3$ , 75.46 MHz): 51.1 (d,  $J$  7.2,  $\text{NCH}_2\text{CHN}$ ), 53.9 ( $\text{CHNCH}_2\text{CH}=\text{CH}_2$ ), 56.9 (d,  $J$  17.1, CH), 57.4 ( $\text{CH}_2\text{NCH}_2\text{CH}=\text{CH}_2$ ), 83.7 (d,  $J$  170.2,  $\text{CH}_2\text{F}$ ), 116.6 ( $\text{CH}=\text{CH}_2$ ), 117.4 ( $\text{CH}=\text{CH}_2$ ), 135.9 ( $\text{CH}=\text{CH}_2$ ), 137.5 ( $\text{CH}=\text{CH}_2$ ).  $\delta_{\text{F}}$  ( $\text{CDCl}_3$ , 282.29 MHz): -226.7 (m,  $\text{CH}_2\text{F}$ ).  $\nu_{\text{max}}/\text{cm}^{-1}$  (film): 3077, 2810, 1737, 1642, 1446, 1418, 1212, 1153.  $m/z$  (ED): 142 [ $\text{NCHCH}_2\text{F}(\text{CH}_2\text{CH}=\text{CH}_2)_2$ ]<sup>+</sup> (19%), 122 [ $\text{NCCH}_2(\text{CH}_2\text{CH}=\text{CH}_2)_2$ ]<sup>+</sup> (51), 110 [ $\text{NCH}_2(\text{CH}_2\text{CH}=\text{CH}_2)_2$ ]<sup>+</sup> (100), 81 [ $\text{N}(\text{CH}_2\text{C})\text{CH}_2\text{CH}=\text{CH}_2$ ]<sup>+</sup> (17), 41 [ $\text{CH}_2\text{CH}=\text{CH}_2$ ]<sup>+</sup> (40). HRMS (ES): Found 253.2079. Calcd. for  $\text{C}_{15}\text{H}_{26}\text{N}_2\text{F}$ , 253.2080.



**4.2.8** *N*<sup>1</sup>, *N*<sup>3</sup>-Diallyl-*N*<sup>1</sup>, *N*<sup>3</sup>-dibenzyl-2-fluoro-1,3-propanediamine **99**  
and *N*<sup>1</sup>, *N*<sup>2</sup>-diallyl-*N*<sup>1</sup>, *N*<sup>2</sup>-dibenzyl-3-fluoro-1,2-propanediamine **100**

**99****100**

DAST (1.10 cm<sup>3</sup>, 8.9 mmol) was added to a solution of 1,3-bis[allyl(benzyl)amino]-2-propanol (3.14 g, 8.97 mmol) in DCM (10 cm<sup>3</sup>) at 0 °C. The reaction was then stirred for 5 h at RT and was then quenched with aqueous sodium bicarbonate. The crude product was extracted into DCM and concentrated under reduced vacuum. The isomer ratio **99** : **100** was 4 : 1 (<sup>19</sup>F NMR). Purification over silica gel (hexane: ethyl acetate 15:1) gave **99** (1.72 g, 54 %) and isomer **100** (0.33 g, 11%) as clear yellow viscous liquids.

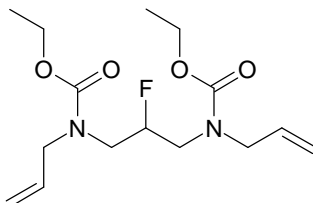
**99**

$\delta_{\text{H}}$  (CDCl<sub>3</sub>, 300.06 MHz): 2.50–2.61 (4 H, m, NCH<sub>2</sub>CHF), 2.94–3.09 (4 H, m, CH<sub>2</sub>CH=CH<sub>2</sub>), 3.51 (4 H, dd, *J* 13.7, *J* 27.9, PhCH<sub>2</sub>), 4.67 (1 H, dm, *J* 49.7, CHF), 5.0–5.10 (4 H, m, CH=CH<sub>2</sub>), 5.73 (2 H, m, CH=CH<sub>2</sub>), 7.09–7.20 (10 H, m, Ph-H).  $\delta_{\text{C}}$  (CDCl<sub>3</sub>, 75.46 MHz): 55.6 (d, *J* 21.6, NCH<sub>2</sub>CHF), 57.7 (NCH<sub>2</sub>CH=CH<sub>2</sub>), 58.9 (PhCH<sub>2</sub>), 92.3 (d, *J* 170.8, CHF), 117.6 (CH=CH<sub>2</sub>), 127.0 (CH), 128.3 (CH), 129.0 (CH), 135.8 (CH=CH<sub>2</sub>), 139.3 (C).  $\delta_{\text{F}}$  (CDCl<sub>3</sub>, 282.29 MHz): -183.03 (CHF).  $\nu_{\text{max}}$  /cm<sup>-1</sup> (film): 3064, 2927, 2802, 1643, 1494, 1453, 1211, 1153. *m/z* (EI): 186 [BnN(CH<sub>2</sub>CCH<sub>2</sub>)CH<sub>2</sub>CH=CH<sub>2</sub>]<sup>+</sup> (77%), 174 [BnN(CH<sub>2</sub>CH)CH<sub>2</sub>CH=CH<sub>2</sub>]<sup>+</sup> (12), 160 [BnN(CH<sub>2</sub>)CH<sub>2</sub>CH=CH<sub>2</sub>]<sup>+</sup> (23), 91 [Bn]<sup>+</sup> (100). HRMS (ES): Found 353.2400. Calcd. for C<sub>23</sub>H<sub>30</sub>N<sub>2</sub>F, 353.2393.

**100**

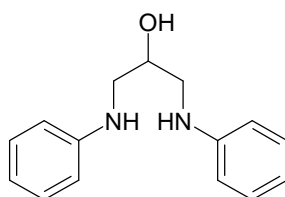
$\delta_{\text{H}}$  ( $\text{CDCl}_3$ , 300.06 MHz): 2.46–2.50 (2 H, m,  $\text{NCH}_2\text{CHCH}_2\text{F}$ ), 2.82–3.11 (4 H, m,  $\text{CH}_2\text{CH}=\text{CH}_2$ ) (1 H, m,  $\text{NCHCH}_2\text{F}$ ), 3.33–3.67 (4 H, m,  $\text{PhCH}_2$ ), 4.48 (2 H, dm,  $J$  48.0,  $\text{CH}_2\text{F}$ ), 4.93–5.11 (4 H, m,  $\text{CH}=\text{CH}_2$ ), 5.62–5.81 (2 H, m,  $\text{CH}=\text{CH}_2$ ), 7.08–7.27 (10 H, m, Ph-H).  $\delta_{\text{C}}$  ( $\text{CDCl}_3$ , 75.46 MHz): 51.7 (d,  $J$  7.2,  $\text{NCH}_2\text{CHCH}_2\text{F}$ ), 53.9 ( $\text{NCH}_2\text{CH}=\text{CH}_2$ ), 54.6 ( $\text{PhCH}_2$ ), 56.3 (d,  $J$  17.2,  $\text{CHCH}_2\text{F}$ ), 57.4 ( $\text{NCH}_2\text{CH}=\text{CH}_2$ ), 59.0 ( $\text{PhCH}_2$ ), 83.6 (dm,  $J$  170.8,  $\text{CH}_2\text{F}$ ), 116.7 ( $\text{CH}=\text{CH}_2$ ), 117.6 ( $\text{CH}=\text{CH}_2$ ), 126.8 (CH), 127.0 (CH), 128.2 (CH), 128.5 (CH), 129.0 (CH), 135.7 ( $\text{CH}=\text{CH}_2$ ), 137.5 ( $\text{CH}=\text{CH}_2$ ), 139.4 (C), 140.6 (C).  $\delta_{\text{F}}$  ( $\text{CDCl}_3$ , 282.29 MHz): -226.2 (dt,  $J$  24.1,  $J$  47.7,  $\text{CH}_2\text{F}$ ).  $\nu_{\text{max}}/\text{cm}^{-1}$  (film): 3064, 3028, 2924, 2806, 1642, 1453, 1211, 1154.  $m/z$  (EI): 186 [ $\text{BnN}(\text{CH}_2\text{CCH}_2)\text{CH}_2\text{CH}=\text{CH}_2$ ]<sup>+</sup> (15%), 172 [ $\text{BnN}(\text{CH}_2\text{C})\text{CH}_2\text{CH}=\text{CH}_2$ ] (33), 173 [ $\text{BnN}(\text{CH}_2\text{CH})\text{CH}_2\text{CH}=\text{CH}_2$ ] (33), 160 [ $\text{BnN}(\text{CH}_2)\text{CH}_2\text{CH}=\text{CH}_2$ ]<sup>+</sup> (45), 91 [ $\text{Bn}$ ]<sup>+</sup> (100). HRMS (ES): Found 353.2397. Calcd. for  $\text{C}_{23}\text{H}_{30}\text{N}_2\text{F}$ , 353.2393.

**4.2.9 Allyl-[3(allylethoxycarbonylamino)-2-fluoropropyl]carbamic acid diethyl ester **115****



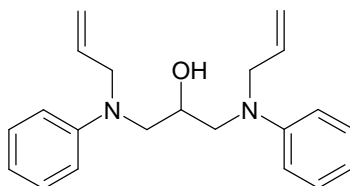
Ethyl chloroformate (335 mg, 3.08 mmol) was added to a solution of **xxx** (434 mg, 1.2 mmol) in toluene (15 cm<sup>3</sup>) at room temperature. The reaction was heated under reflux and monitored by GC-MS. On completion the reaction was then quenched with water, the phases were separated and the toluene evaporated under reduced pressure. Purification over silica gel (hexane:ethyl acetate 8:1) afforded **115** as a clear orange liquid (332 mg, 85%).

$\delta_{\text{H}}$  (CDCl<sub>3</sub>, 300.06 MHz): 1.26 (6 H, t, *J* 7.1, CH<sub>3</sub>), 3.23–3.67 (4 H, m, NCH<sub>2</sub>CHF), 3.77–4.08 (4 H, m, CH<sub>2</sub>CH=CH<sub>2</sub>), 4.10–4.19 (4 H, m, CH<sub>2</sub>CH<sub>3</sub>), 4.85 (1 H, dm, *J* 50.7, CHF), 5.07–5.20 (4 H, m, CH=CH<sub>2</sub>), 5.69–5.84 (2 H, m, CH=CH<sub>2</sub>).  $\delta_{\text{C}}$  (CDCl<sub>3</sub>, 75.46 MHz): 14.6 (CH<sub>3</sub>), 48.0 (d, *J* 22.1, NCH<sub>2</sub>CHF (rotamer)), 48.6 (d, *J* 21.3, NCH<sub>2</sub>CHF (rotamer)), 50.7 (NCH<sub>2</sub>CH=CH<sub>2</sub>), 61.6 (CH<sub>2</sub>CH<sub>3</sub>), 92.4 (d, *J* 175.0, CHF), 117.3 (CH=CH<sub>2</sub>), 133.4 (CH=CH<sub>2</sub>), 156.0 (C=O).  $\delta_{\text{F}}$  (CDCl<sub>3</sub>, 282.29 MHz): -189.04, -189.59, -190.50 (CHF rotamers).  $\nu_{\text{max}}$ /cm<sup>-1</sup> (film): 3518, 2983, 1699, 1471, 1416, 1245, 1154. *m/z* (EI): 267 [M-F-Et]<sup>+</sup> (32%), 255 [M-F-CH<sub>2</sub>CH=CH<sub>2</sub>]<sup>+</sup> (68), 223 [M-F-COOEt]<sup>+</sup> (35), 168 [NCH<sub>2</sub>CHCH<sub>2</sub>(CH<sub>2</sub>CH=CH<sub>2</sub>)(COOEt)]<sup>+</sup> (62), 142 [NCH<sub>2</sub>(CH<sub>2</sub>CH=CH<sub>2</sub>)(COOEt)]<sup>+</sup> (100), 70 [NCH<sub>2</sub>(CH<sub>2</sub>CH=CH<sub>2</sub>)]<sup>+</sup> (45), 41 [CH<sub>2</sub>CH=CH<sub>2</sub>]<sup>+</sup> (50). HRMS (ES): Found 339.1686. Calcd. for C<sub>15</sub>H<sub>25</sub>N<sub>2</sub>O<sub>4</sub>FNa, 339.1696.

**4.2.10 1,3-Dianilinopropan-2-ol** <sup>7</sup>

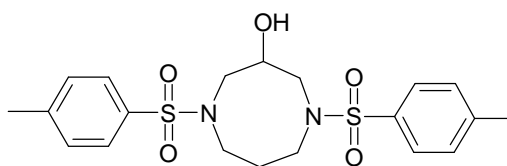
A mixture of aniline (5.20 g, 55.8 mmol) and 1,3-dichloropropan-2-ol (1.80 g, 13.9 mmol) were heated to 130 °C and stirred for 69 h. Water (50 cm<sup>3</sup>) was then added and the mixture was heated under reflux for 30 min, after which the reaction was cooled and the water was decanted off. The product was partitioned between DCM and water, and the DCM was separated and the solvent was removed under reduced pressure. Purification over silica gel (hexane : ethyl acetate 1:1) gave the compound as a brown solid (2.13 g, 63%).

Mp 56–58 °C (ether), (Lit.,<sup>7</sup> 56–57 °C).  $\delta_{\text{H}}$  (CDCl<sub>3</sub>, 300.06 MHz): 3.14 (2 H, dd, *J* 7.8, *J* 13.0, PhNCH<sub>2</sub>), 3.34 (2 H, dd, *J* 3.8, *J* 13.0, PhNCH<sub>2</sub>), 4.10 (1 H, m, CHOH), 6.65–6.78 (6 H, m, Ph-H), 7.16–7.22 (4 H, m, Ph-H).  $\delta_{\text{C}}$  (CD<sub>3</sub>OD, 75.46 MHz): 47.8 (PhNCH<sub>2</sub>), 68.3 (CHOH), 113.5 (CH), 117.0 (CH), 129.2 (CH), 149.2 (C). *m/z* (EI): 242 [M]<sup>+</sup> (33%), 132 (42), 106 [C<sub>6</sub>H<sub>5</sub>NHCH<sub>2</sub>]<sup>+</sup> (100), 93 (90), 77 [C<sub>6</sub>H<sub>5</sub>]<sup>+</sup> (28).

**4.2.11 1,3-Bis(allyl(phenyl)amino)propan-2-ol 122**

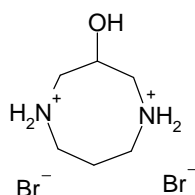
Allyl iodide (2.7 cm<sup>3</sup>, 29.8 mmol) was added to a solution of 1,3-dianilinopropan-2-ol (3.78 g, 15.6 mmol) in MeCN (40 cm<sup>3</sup>) at RT. The reaction was stirred for 89 h and then the MeCN was removed under reduced pressure. The product was partitioned between DCM and water, the DCM phase was separated and the solvent removed under reduced pressure. Purification over silica gel (hexane : ethyl acetate, 2:1) gave the title compound as a viscous brown liquid (2.36 g, 47 %).

$\delta_{\text{H}}$  (CDCl<sub>3</sub>, 300.13 MHz): 3.32 (2 H, dd, *J* 8.2, *J* 15.0, NCH<sub>2</sub>CHOH), 3.47 (2 H, dd, *J* 4.0, *J* 15.0, NCH<sub>2</sub>CHOH), 3.96–4.01 (4 H, m, NCH<sub>2</sub>CH=CH<sub>2</sub>), 4.23 (1 H, m, NCH<sub>2</sub>CHOH), 5.10–5.18 (4 H, m, NCH<sub>2</sub>CH=CH<sub>2</sub>), 5.85 (2 H, m, NCH<sub>2</sub>CH=CH<sub>2</sub>), 6.68–6.78 (6 H, m, Ph-H), 7.16–7.23 (4 H, m, Ph-H).  $\delta_{\text{C}}$  (CDCl<sub>3</sub>, 75.48 MHz): 54.5 (NCH<sub>2</sub>CH=CH<sub>2</sub>), 55.5 (NCH<sub>2</sub>CHOH), 68.3 (CHOH), 113.3 (CH), 116.7 (CH=CH<sub>2</sub>), 117.3 (CH), 129.3 (CH), 133.9 (CH=CH<sub>2</sub>), 148.8 (C). *m/z* (EI): 172 (53%), 146 [C<sub>6</sub>H<sub>5</sub>N(CH<sub>2</sub>)CH<sub>2</sub>CH=CH<sub>2</sub>]<sup>+</sup> (100), 133 (10), 104 (25), 77 [C<sub>6</sub>H<sub>5</sub>]<sup>+</sup> (12).

4.2.12 1,5-Bis-(toluene-4-sulfonyl)-1[1,5]diazocan-3-ol **126** <sup>8,9</sup>

Sodium (0.79 g, 34.4 mmol) in EtOH (20 cm<sup>3</sup>) was added to a solution of 1,3-bis-(toluene-4-sulfonylamino)-propane (4.88 g, 12.8 mmol) in EtOH (200 cm<sup>3</sup>) under reflux. The reaction was stirred for 3 h then 1,3-dichloro-2-propanol (2.47 g, 19.2 mmol) was added. After a further 11 h at reflux the reaction mixture was cooled to RT and was filtered. The resultant white solid was crystallised from hot ethanol to provide **126** as white needles (3.38 g, 60%).

Mp 206–208 °C (ethanol), (Lit.,<sup>8</sup> 206–208 °C) (Lit.,<sup>9</sup> 208–209 °C).  $\delta_{\text{H}}$  (CDCl<sub>3</sub>, 300.13 MHz): 2.05–2.14 (2 H, m, NCH<sub>2</sub>CH<sub>2</sub>CH<sub>2</sub>N), 2.45 (6 H, s, CH<sub>3</sub>), 3.16–3.78 (6 H, m, NCH<sub>2</sub>CHOH, NCH<sub>2</sub>CH<sub>2</sub>CH<sub>2</sub>N), 3.47 (2 H, dd, *J* 4.7, *J* 15.3, NCH<sub>2</sub>CHOH), 3.80 (1 H, d, *J* 9.0, OH, exchanges with D<sub>2</sub>O), 4.14–4.25 (1 H, m, CHOH), 7.30–7.36 (4 H, m, Ts-H), 7.66–7.71 (4 H, m, Ts-H).  $\delta_{\text{C}}$  (CD<sub>3</sub>)<sub>2</sub>SO, 100.62 MHz): 21.0 (CH<sub>3</sub>), 30.0 (NCH<sub>2</sub>CH<sub>2</sub>CH<sub>2</sub>N), 49.8 (NCH<sub>2</sub>CH<sub>2</sub>CH<sub>2</sub>N), 54.7 (NCH<sub>2</sub>CHOHCH<sub>2</sub>N), 69.4 (CHOH), 126.9 (CH), 129.9 (CH), 135.4 (C), 143.2 (C). Elemental analysis found: C, 55.0; H, 5.9; N, 6.4. Calc. for C<sub>20</sub>H<sub>26</sub>N<sub>2</sub>O<sub>5</sub>S<sub>2</sub>: C, 54.8; H, 6.0; N, 6.4%. HRMS (ES): Found 461.1194. Calcd. for C<sub>20</sub>H<sub>26</sub>N<sub>2</sub>O<sub>5</sub>S<sub>2</sub>Na, 461.1181.

4.2.13 3-Hydroxy-1,5-diazocane-1,5-dium bromide **127**

HBr (33%) in acetic acid (4.4 cm<sup>3</sup>) was added to a mixture of 1,3-bis-(toluene-4-sulfonyl)-1[1,5]diazocan-3-ol (0.47g 1.1 mmol) and phenol (0.43g 4.5 mmol) at RT. The reaction was heated to 90 °C and stirred for 15 h, after which it was cooled to 50 °C and further HBr (33%) in acetic acid (1.0 cm<sup>3</sup>) added. The reaction was re-heated to 90 °C and monitored by LC-MS. After 24 h another aliquot of HBr (33%) in acetic acid (1.0 cm<sup>3</sup>) was added. The reaction was cooled after 28 h and acetic acid removed under reduced pressure. The crude salt was partitioned between water (100 cm<sup>3</sup>) and DCM (100 cm<sup>3</sup>) and aqueous phase separated. The water was removed under reduced pressure and heat to yield an orange solid of the hydrobromide **127** (0.30 g, 97%).

The hydrochloride salt was also obtained by use of an ion-exchange column. Dowex 1x8-200, 8% cross linking, 100-200 mesh resin was washed with NaOH (2M) followed by water to give water at pH 7. A portion of the HBr salt was dissolved in water and ran through the column. Fractions were collected and those showing a positive ninhydrin stain were collected and combined under reduced pressure and heat. HCl in ether (1M) was added and a yellow solid was provided. Excess HCl / ether was removed under reduced pressure and the solid obtained was dried under vacuum at 40 °C overnight.

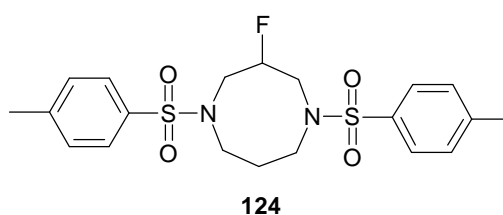
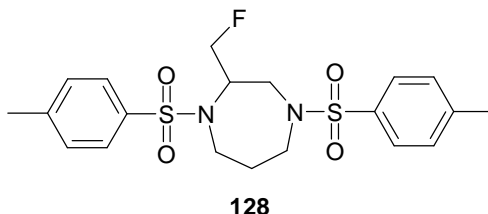
Crystals of both the hydrobromide and hydrochloride salts were provided from DMF and ether. White crystals were obtained in both cases and the hydrobromide was subjected to X-ray crystallography studies.

**4.2.14 3-Hydroxy-1,5-diazocane-1,5-dium chloride**

Mp 194–196 °C.  $\delta_{\text{H}}$  ( $\text{D}_2\text{O}$ , 400.13 MHz): 2.17–2.27 (1 H, m,  $\text{NCH}_2\text{CH}_2\text{CH}_2\text{N}$ ), 2.34–2.45 (1 H, m,  $\text{NCH}_2\text{CH}_2\text{CH}_2\text{N}$ ), 3.30 (2 H, ddd,  $J$  2.6,  $J$  7.4,  $J$  14.5,  $\text{NCH}_2\text{CH}_2\text{CH}_2\text{N}$ ), 3.39 (2 H, dd,  $J$  1.4,  $J$  15.0,  $\text{NCH}_2\text{CHCH}_2\text{N}$ ), 3.46–3.54 (2 H, m,  $\text{NCH}_2\text{CH}_2\text{CH}_2\text{N}$ ), 3.60 (2 H, dd,  $J$  6.5,  $J$  15.0,  $\text{NCH}_2\text{CHCH}_2\text{N}$ ), 4.48 (1 H, m,  $\text{CHOH}$ ).  $\delta_{\text{C}}$  ( $\text{D}_2\text{O}$ , 100.62 MHz): 19.7 ( $\text{NCH}_2\text{CH}_2\text{CH}_2\text{N}$ ), 44.9 ( $\text{NCH}_2\text{CH}_2\text{CH}_2\text{N}$ ), 47.8 ( $\text{NCH}_2\text{CHCH}_2\text{N}$ ), 59.4 ( $\text{CHOH}$ ). HRMS ( $\text{Cl}^+$ ): Found 131.1188. Calcd. for  $\text{C}_6\text{H}_{15}\text{N}_2\text{O}$ , 131.1184.



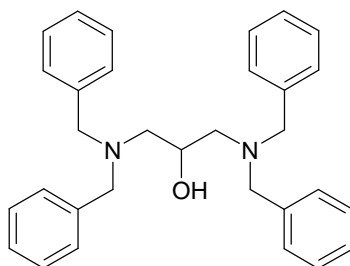
**4.2.15 2-(Fluoromethyl)-1,4-ditosyl-1,4-diazepane 128 and  
3-fluoro-1,5-ditosyl-1,5-diazocane 124**



DAST (0.12 cm<sup>3</sup>, 0.9 mmol) was added to a solution of 1,3-bis-(toluene-4-sulfonyl)-[1,5]diazocan-3-ol (240 mg, 0.6 mmol) in DCM (10 cm<sup>3</sup>) at -78 °C and the reaction was stirred at RT for 18 h and then quenched with NaHCO<sub>3</sub> (aq) solution. The product was partitioned between water and DCM and the latter was separated and dried (MgSO<sub>4</sub>). After filtration and DCM removal under reduced pressure, the product was obtained as a yellow solid. <sup>19</sup>F NMR analysis indicated a **128** : **124** ratio of 7:1. Chromatography over silica gel (hexane: ethyl acetate, 2:1) partially separated the isomers. Preparative plate chromatography (four times sequentially), (hexane: ethyl acetate 3:1) allowed an analytical sample of each isomer to be prepared. Both isomers **128** and **124** were amenable to crystallisation.

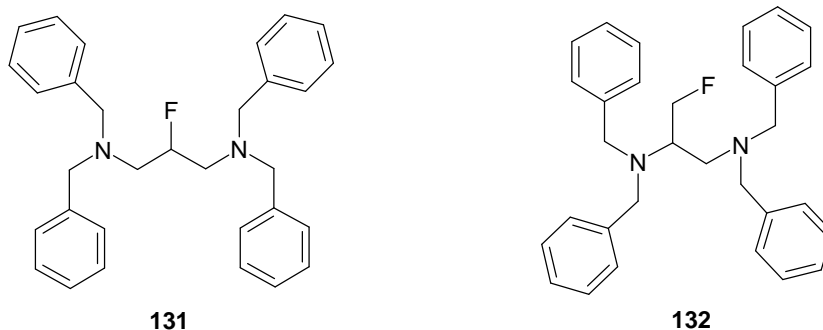
**128**

Mp 136–140 °C (from ethanol).  $\delta_{\text{H}}$  ( $\text{CDCl}_3$ , 400.13 MHz): 1.66–1.88 (2 H, m,  $\text{NCH}_2\text{CH}_2\text{CH}_2\text{N}$ ), 2.42 (6 H, s,  $\text{PhCH}_3$ ), 3.04–3.12 (1 H, m,  $\text{NCH}_2\text{CH}_2\text{CH}_2\text{N}$ ), 3.14–3.23 (1 H, m,  $\text{NCH}_2\text{CH}_2\text{CH}_2\text{N}$ ), 3.26–3.32 (1 H, m,  $\text{NCH}_2\text{CH}_2\text{CH}_2\text{N}$ ), 3.33–3.40 (1 H, m,  $\text{NCH}_2\text{CHN}$ ), 3.44–3.50 (1 H, m,  $\text{NCH}_2\text{CHN}$ ), 3.90 (1 H, dt,  $J$  16.0,  $\text{NCH}_2\text{CH}_2\text{CH}_2\text{N}$ ), 4.36–4.68 (3 H, m,  $\text{CHCH}_2\text{F}$ ,  $\text{CHCH}_2\text{F}$ ), 7.28–7.33 (4 H, m,  $\text{CHCCH}_3$ ), 7.61–7.64 (2 H, m, Ts-H), 7.73–7.77 (2 H, m, Ts-H).  $\delta_{\text{C}}$  ( $\text{CDCl}_3$ , 75.48 MHz): 21.6 ( $\text{CH}_3$ ), 21.7 ( $\text{CH}_3$ ), 29.4 ( $\text{NCH}_2\text{CH}_2\text{CH}_2\text{N}$ ), 42.3 ( $\text{NCH}_2\text{CH}_2\text{CH}_2\text{N}$ ), 49.5 ( $\text{NCH}_2\text{CH}_2\text{CH}_2\text{N}$ ), 51.0 ( $\text{NCH}_2\text{CHN}$ ), 51.1 ( $\text{NCH}_2\text{CHN}$ ), 57.0 (d,  $J$  19.9,  $\text{CHCH}_2\text{F}$ ), 82.7 (d,  $J$  173.4,  $\text{CHCH}_2\text{F}$ ), 127.0 (CH), 127.4 (CH), 129.9 (CH), 130.1 (CH), 137.7 (C), 143.7 (C), 143.8 (C).  $\delta_{\text{F}}$  ( $\text{CDCl}_3$ , 282.29 MHz): -229.8 (dt,  $J$  18.8,  $J$  47.0,  $\text{CH}_2\text{F}$ ).  $\nu_{\text{max}}/\text{cm}^{-1}$  (film): 2920, 1337, 1210, 1152. HRMS (ES): Found 463.1129. Calcd. for  $\text{C}_{20}\text{H}_{25}\text{N}_2\text{O}_4\text{S}_2\text{FNa}$ , 463.1137.

4.2.16 1,3-Bisdibenzylaminopropan-2-ol **130** <sup>10</sup>

Benzyl bromide (5.6 cm<sup>3</sup>, 46.7 mmol) was added to a refluxing solution of 1,3-diamino-2-propanol (1.04 g, 11.5 mmol) and Na<sub>2</sub>CO<sub>3</sub> (5.63 g, 53.1 mmol) in water (50 cm<sup>3</sup>). The reaction was heated under reflux for 3 h and was then cooled to RT. Diethyl ether and water were added and the diethyl ether phase was separated, dried (MgSO<sub>4</sub>) and filtered. The solvent was then removed under reduced pressure and the product purified over silica gel (hexane : ethyl acetate, 8:1) to give **130** as a clear yellow oil (3.86 g, 75%).

$\delta_{\text{H}}$  (CDCl<sub>3</sub>, 300.06 MHz): 2.42 (2 H, d, *J* 6.0, CH<sub>2</sub>CH), 3.55 (8 H, dd, *J* 13.6, *J* 50.3, CH<sub>2</sub>Ph), 3.80 (1 H, q, *J* 6.2, CHOH), 7.19–7.33 (20 H, m, Ph-H).  $\delta_{\text{C}}$  (CDCl<sub>3</sub>, 75.46 MHz): 57.8 (CH<sub>2</sub>CH), 59.0 (CH<sub>2</sub>Ph), 65.8 (CHOH), 127.2 (CH), 128.4 (CH), 129.1 (CH), 139.1 (C).  $\nu_{\text{max}}$ /cm<sup>-1</sup> (film): 3024, 2792, 1492, 1451, 1203, 1148.

4.2.17  $N^1, N^1, N^3, N^3$ -Tetrabenzyl-2-fluoropropane-1,3-diamine **131**

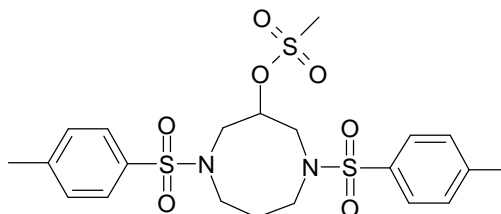
Deoxofluor (0.16 cm<sup>3</sup>, 0.9 mmol) was added to 1,3-bisdibenzylaminopropan-2-ol **130** (330 mg, 0.7 mmol) in DCM (5 cm<sup>3</sup>) at 0 °C. The reaction was stirred at RT for 23 h and was then quenched with Na<sub>2</sub>CO<sub>3</sub> (aq) solution. The crude product was extracted into DCM and dried (MgSO<sub>4</sub>) and removed under reduced pressure to give an orange liquid. <sup>19</sup>F NMR analysis indicated an isomer **131** : **132** ratio of 5:1. Column chromatography over silica gel (hexane : ethyl acetate, 5:1) provided a yellow oil (235 mg, 71%) also as a mixture of isomers. Further purification was accomplished by preparative HPLC, carried out by Helen Weston at GSK. A Zorbax SB-phenyl 150x4.6 mm column and solvents A (H<sub>2</sub>O, 0.2% TFA) and B (MeCN, 5% H<sub>2</sub>O, 0.1% TFA) with a gradient program of 0–100% B over 30 minutes followed by 100% B for 10 minutes was employed. The solvents were removed under reduced pressure and the product was dissolved in a small amount of MeCN. This was applied to a pre-packed SCX-2 column and washed with water followed by methanol / ammonia (7N) solution. The fractions were combined and the solvents were removed under reduced pressure. The product was obtained as an orange viscous liquid, which upon further drying *in vacuo* solidified. The hydrochloride salt was prepared by addition of HCl in ether and crystals of **131** suitable for X-ray crystallography analysis were obtained by dissolving in DMF and slowly migrating ether.

**131**

Mp 58–60 °C.  $\delta_{\text{H}}$  ( $\text{CDCl}_3$ , 300.06 MHz): 2.48–2.70 (4 H, m,  $\text{CH}_2\text{CH}$ ), 3.57 (8 H, dd,  $J$  13.7,  $J$  47.9,  $\text{CH}_2\text{Ph}$ ), 4.80 (1 H, dm,  $J$  49.8, CHF), 7.18–7.34 (20 H, m, Ph-H).  $\delta_{\text{C}}$  ( $\text{CDCl}_3$ , 75.46 MHz): 55.8 (d,  $J$  22.0,  $\text{CH}_2\text{CH}$ ), 59.1 ( $\text{CH}_2\text{Ph}$ ), 92.6 (d,  $J$  169.6, CHF), 127.1 (CH), 128.4 (CH), 129.0 (CH), 139.5 (C).  $\delta_{\text{F}}$  ( $\text{CDCl}_3$ , 282.29 MHz): -182.3 (m, CHF).  $\nu_{\text{max}}/\text{cm}^{-1}$  (film): 3025, 2794, 1493, 1452, 1203, 1148. HRMS (CI<sup>+</sup>): Found 453.2706. Calcd. for  $\text{C}_{31}\text{H}_{34}\text{N}_2\text{F}$ , 453.2706.

**132**

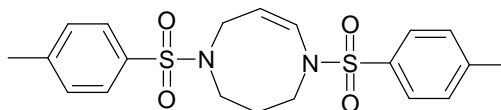
Mp 94–96 °C.  $\delta_{\text{H}}$  ( $\text{CDCl}_3$ , 300.06 MHz): 2.50–2.59 (2 H, m,  $\text{CH}_2\text{CH}$ ), 2.97–3.14 (1 H,  $\text{CH}_2\text{CH}$ ), 3.30 (2 H, d,  $J$  13.7,  $\text{CH}_2\text{Ph}$ ), 3.45 (2 H, d,  $J$  13.4,  $\text{CH}_2\text{Ph}$ ), 3.55 (2 H, d,  $J$  14.0,  $\text{CH}_2\text{Ph}$ ), 3.60 (2 H, d,  $J$  13.7,  $\text{CH}_2\text{Ph}$ ), 4.35–4.63 (2 H, m,  $\text{CH}_2\text{F}$ ), 7.09–7.32 (20 H, m, Ph-H).  $\delta_{\text{C}}$  ( $\text{CDCl}_3$ , 75.46 MHz): 29.9 ( $\text{CH}_2\text{CH}$ ), 54.8 ( $\text{CH}_2\text{Ph}$ ), 55.5 (d,  $J$  17.5,  $\text{CHCH}_2\text{F}$ ), 59.1 ( $\text{CH}_2\text{Ph}$ ), 83.9 (d,  $J$  172.0,  $\text{CHCH}_2\text{F}$ ), 127.0 (CH), 127.1 (CH), 128.3 (CH), 128.7 (CH), 129.1 (CH), 139.2 (C), 140.3 (C).  $\delta_{\text{F}}$  ( $\text{CDCl}_3$ , 376.45 MHz): -225.8 (ddt,  $J$  2.6,  $J$  22.5,  $J$  48.1,  $\text{CH}_2\text{F}$ ). HRMS (ES): Found 453.2704. Calcd. for  $\text{C}_{31}\text{H}_{34}\text{N}_2\text{F}$ , 453.2706.

**4.2.18 Methanesulfonic acid 1,5-bis(toluene-4-sulfonyl)-[1,5]diazocan-3-yl ester 133**

Methylsulfonyl chloride (0.05 cm<sup>3</sup>, 0.7 mmol) was added to a solution of 1,3-bis-(toluene-4-sulfonyl)-[1,5]diazocan-3-ol (112 mg, 0.3 mmol) in DCM (10 cm<sup>3</sup>) and pyridine (0.3 cm<sup>3</sup>) at 0 °C and the reaction was stirred for 18 h at RT. The product was obtained by removal of DCM under reduced pressure and the material was purified by over silica gel (hexane : ethyl acetate, 1:2) to give **133** as a white amorphous solid (107 mg, 81%).

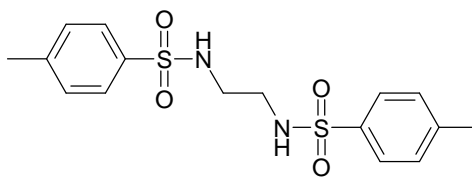
Mp 174–176 °C (from ethanol).  $\delta_{\text{H}}$  (CDCl<sub>3</sub>, 300.06 MHz): 2.01–2.11 (2 H, m, NCH<sub>2</sub>CH<sub>2</sub>CH<sub>2</sub>N), 2.44 (6 H, s, PhCH<sub>3</sub>), 3.20 (3 H, s, SO<sub>2</sub>CH<sub>3</sub>), 3.21–3.30 (4 H, m, NCH<sub>2</sub>CH<sub>2</sub>CH<sub>2</sub>N), 3.52 (4 H, d, *J* 5.7, NCH<sub>2</sub>CHCH<sub>2</sub>N), 5.10 (1 H, q, *J* 5.8, NCH<sub>2</sub>CHCH<sub>2</sub>N), 7.31–7.36 (4 H, m, Ts-H), 7.66–7.71 (4 H, m, Ts-H).  $\delta_{\text{C}}$  (CDCl<sub>3</sub>, 75.48 MHz): 21.7 (PhCH<sub>3</sub>), 29.6 (NCH<sub>2</sub>CH<sub>2</sub>CH<sub>2</sub>N), 38.4 (SO<sub>2</sub>CH<sub>3</sub>), 48.3 (NCH<sub>2</sub>CH<sub>2</sub>CH<sub>2</sub>N), 50.5 (NCH<sub>2</sub>CHCH<sub>2</sub>N), 77.0 (NCH<sub>2</sub>CHCH<sub>2</sub>N), 127.4 (CH), 130.1 (CH), 144.2 (C).  $\nu_{\text{max}}$  /cm<sup>-1</sup> (film): 2952, 1214, 1153. HRMS (ES): Found 539.0938. Calcd. for C<sub>21</sub>H<sub>28</sub>N<sub>2</sub>O<sub>7</sub>S<sub>3</sub>Na, 539.0956.

## 4.2.19 (Z)-1,5-ditosyl-1,2,3,4,5,6-hexahydro-1,5-diazocine 134



A solution of TBAF • 3 H<sub>2</sub>O (101 mg, 0.3 mmol) in MeCN (3 cm<sup>3</sup>) was added to a solution of methanesulfonic acid 1,5-bis(toluene-4-sulfonyl)-[1,5]diazocan-3-yl ester (65 mg, 0.1 mmol) in MeCN (5 cm<sup>3</sup>) at RT. The reaction was then heated under reflux for 17 h and the solvent was then removed under reduced pressure. The product was partitioned between water and DCM, and the organic phase was separated and dried (MgSO<sub>4</sub>). DCM removal under reduced pressure afforded an orange viscous liquid (55 mg, 95%).

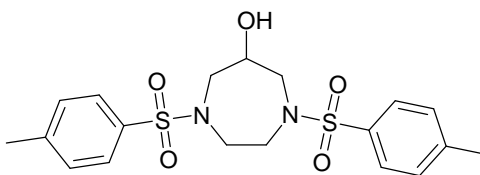
$\delta_{\text{H}}$  (CDCl<sub>3</sub>, 400.13 MHz): 1.84–1.90 (2 H, m, NCH<sub>2</sub>CH<sub>2</sub>CH<sub>2</sub>N), 2.43 (6 H, s, CH<sub>3</sub>), 3.31–3.33 (2 H, m, NCH<sub>2</sub>CH<sub>2</sub>CH<sub>2</sub>N), 3.57–3.61 (2 H, m, NCH<sub>2</sub>CH<sub>2</sub>CH<sub>2</sub>N), 3.96 (2 H, dd, *J* 0.9, *J* 7.5, NCH<sub>2</sub>CH=CHN), 4.76 (1 H, dt, *J* 9.8, *J* 7.5, NCH<sub>2</sub>CH=CHN), 6.51 (1 H, br d, *J* 9.8, NCH<sub>2</sub>CH=CHN), 7.27–7.32 (4 H, m, Ts-H), 7.62–7.67 (4 H, m, Ts-H).  $\delta_{\text{C}}$  (CDCl<sub>3</sub>, 100.62 MHz): 21.5 (CH<sub>3</sub>), 29.5 (NCH<sub>2</sub>CH<sub>2</sub>CH<sub>2</sub>N), 43.6 (NCH<sub>2</sub>CH=CHN), 43.9 (NCH<sub>2</sub>CH<sub>2</sub>CH<sub>2</sub>N), 46.1 (NCH<sub>2</sub>CH<sub>2</sub>CH<sub>2</sub>N), 106.2 (NCH<sub>2</sub>CH=CHN), 127.0 (CH), 129.8 (CH), 130.5 (NCH<sub>2</sub>CH=CHN). LRMS (ES): Found 442.9 (C<sub>20</sub>H<sub>24</sub>N<sub>2</sub>O<sub>4</sub>S<sub>2</sub>+Na). Calcd. for C<sub>20</sub>H<sub>24</sub>N<sub>2</sub>O<sub>4</sub>S<sub>2</sub>Na, 443.11.

**4.2.20 1,2-(Toluene-4-sulfonylamino)-ethane 136**<sup>11</sup>

Toluene-4-sulfonyl chloride (13.84 g, 72.6 mmol) in ether (100 cm<sup>3</sup>) was added to a solution of 1,2-diaminoethane (2.07 g, 34.5 mmol) in water (80 cm<sup>3</sup>) and NaOH (2.84 g, 71.0 mmol) at RT. The reaction was stirred at RT for 17 h and ether (50 cm<sup>3</sup>) was added and then the mixture was filtered. The filtrate was washed with water followed by ether. The product was dried at 80 °C to afford the title compound as a white solid (11.24 g, 88%).

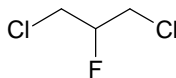
Mp 160–162 °C (from ethanol), (Lit.,<sup>11</sup> 162–164 °C), (Lit.,<sup>12</sup> 156–161 °C).  $\delta_{\text{H}}$  (CDCl<sub>3</sub>, 300.06 MHz): 2.43 (6 H, s, CH<sub>3</sub>), 3.04–3.08 (4 H, m, CH<sub>2</sub>), 4.91 (2 H, br s, NH), 7.28–7.33 (4 H, m, Ts-H), 7.68–7.74 (4 H, m, Ts-H).



4.2.21 1,4-ditosyl-1,4-diazepan-6-ol <sup>13</sup>

Sodium (443 mg, 19.3 mmol) in EtOH (20 cm<sup>3</sup>) was added to a solution of 1,2-(toluene-4-sulfonylamino)-ethane (640 mg, 1.7 mmol) in EtOH (50 cm<sup>3</sup>). The reaction was then stirred under reflux for 1.5 h then 1,3-dichloro-2-propanol (359 mg, 2.7 mmol) was added and the reaction was stirred for a further 20 h under reflux. After cooling to RT the reaction was filtered and the filtrate was concentrated under reduced pressure. Purification over silica gel (toluene: ethyl acetate 4:1) afforded a white solid which was crystallised from hot ethanol (53 mg, 7%).

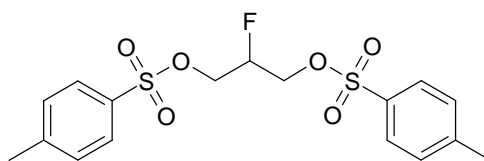
Mp 174–176 °C (from ethanol), (Lit., <sup>13</sup> 175–177 °C).  $\delta_{\text{H}}$  (CDCl<sub>3</sub>, 300.06 MHz): 2.44 (6 H, s, CH<sub>3</sub>), 3.23 (2 H, dd, *J* 5.1, *J* 15.2, CH<sub>2</sub>CHCH<sub>2</sub>), 3.39–3.55 (4 H, m, CH<sub>2</sub>CH<sub>2</sub>), 3.64 (2 H, dd, *J* 5.5, *J* 15.2, CH<sub>2</sub>CHCH<sub>2</sub>), 4.19 (1 H, m, CHOH), 7.29–7.35 (4 H, m, Ts-H), 7.63–7.68 (4 H, m, Ts-H).  $\delta_{\text{C}}$  (CDCl<sub>3</sub>, 75.46 MHz): 21.7 (CH<sub>3</sub>), 53.0 (CH<sub>2</sub>CH<sub>2</sub>), 55.0 (CH<sub>2</sub>CHCH<sub>2</sub>), 70.1 (CHOH), 127.0 (CH), 130.1 (CH), 136.0 (C), 144.1 (C).  $\nu_{\text{max}}$ /cm<sup>-1</sup> (film): 3503, 1347, 1207, 1150.

**4.2.22 1,3-Dichloro-2-fluoropropane **140****<sup>14</sup>

Deoxofluor (3.2 cm<sup>3</sup>, 17.4 mmol) was added to a solution of 1,3-dichloro-2-propanol (2.03 g, 15.8 mmol) in DCM (10 cm<sup>3</sup>) at 0 °C and the reaction was stirred at RT for 19 h. The DCM was removed by distillation and the product, **140** was obtained after further distillation (0.82 g, 40%).

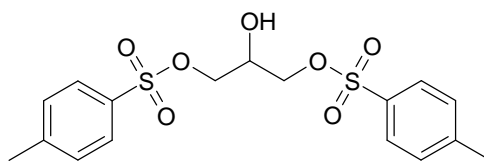
$\delta_{\text{H}}$  (CDCl<sub>3</sub>, 400.13 MHz): 3.73 (2 H, dd,  $J$  4.6,  $J$  5.1, CH<sub>2</sub>), 3.79 (2 H, dd,  $J$  1.8,  $J$  5.0, CH<sub>2</sub>), 4.84 (1 H, dm,  $J$  45.8, CHF).  $\delta_{\text{C}}$  (CDCl<sub>3</sub>, 75.46 MHz): 42.3 (d,  $J$  26.0, CH<sub>2</sub>), 90.0 (d,  $J$  181.7, CHF).  $\delta_{\text{F}}$  (CDCl<sub>3</sub>, 282.29 MHz): -182.7 (m, CHF).  $\delta_{\text{F}}$  (CD<sub>2</sub>Cl<sub>2</sub>, 282.29 MHz): -184.0 (m, CHF).  $J$  from NMR simulation:  $^2J_{\text{HF}} = 45.8$ ,  $^3J_{\text{HF}} = 19.0$ ,  $^3J_{\text{HF}} = 16.4$ .

## 4.2.23 2-Fluoro-1,3-bis-(toluene-4-sulfonyloxy)-propane 142



Deoxofluor (2.4 cm<sup>3</sup>, 13.0 mmol) was added to a solution of 2-hydroxy-1,3-bis-(toluene-4-sulfonyloxy)-propan (3.69 g, 9.2 mmol) in DCM (10 cm<sup>3</sup>) at 0 °C and the reaction was stirred for 18 h at RT. A further aliquot of Deoxofluor (0.5 cm<sup>3</sup>, 2.7 mmol) was then added and the reaction was stirred for an additional 16 h at RT and was then quenched with NaHCO<sub>3</sub> (aq). The mixture was separated with DCM and the solvent was removed under reduced pressure. The crude product was applied to a RediSep® pre-packed column (120 g) and chromatography was carried out on a Teledyne Isco Combiflash Companion® purification system using a gradient program of 20–30% ethyl acetate in cyclohexane. The product was collected by automation. After eluent removal under reduced pressure a white amorphous solid was obtained (2.48 g, 67%).

Mp 110–111 °C (from ethanol), (Lit.,<sup>15</sup> 111–112 °C).  $\delta_{\text{H}}$  (CDCl<sub>3</sub>, 300.06 MHz): 2.47 (6 H, s, CH<sub>3</sub>), 4.16 (2 H, m, CHHO) 4.18 (2 H, d, *J* 20.3, CHHO), 4.81 (1 H, dm, *J* 46.4, CHF), 7.34–7.39 (4 H, m, Ts-H), 7.74–7.79 (4 H, m, Ts-H).  $\delta_{\text{C}}$  (CDCl<sub>3</sub>, 75.48 MHz): 21.8 (CH<sub>3</sub>), 67.0 (d, *J* 25.0, CH<sub>2</sub>O), 87.1 (d, *J* 182.1, CHF), 128.2 (CH), 130.3 (CH), 132.2 (C), 145.7 (C).  $\delta_{\text{F}}$  (CDCl<sub>3</sub>, 282.29 MHz): -195.4 (m, CHF).  $\nu_{\text{max}}$ /cm<sup>-1</sup> (film): 2956, 1595, 1356, 1211. *m/z* (EI): 402 [M]<sup>+</sup> (7%), 231 [OSO<sub>2</sub>C<sub>6</sub>H<sub>4</sub>CH<sub>3</sub>](24), 155 [OSO<sub>2</sub>C<sub>6</sub>H<sub>4</sub>CH<sub>3</sub>] (69), 91 [C<sub>6</sub>H<sub>4</sub>CH<sub>3</sub>]<sup>+</sup> (100). HRMS (ES): Found 425.0507. Calcd. for C<sub>17</sub>H<sub>19</sub>O<sub>6</sub>FS<sub>2</sub>Na, 425.0505.

**4.2.24 2-Hydroxy-1,3-bis-(toluene-4-sulfonyloxy)-propan 144****Method 1**

A suspension of palladium hydroxide on carbon (20 wt%), (565 mg, 0.8 mmol) and 2-[(phenylmethyl)oxy]-1,3-propanediyl bis(4-methylbenzenesulfonate) (5.52 g, 11.3 mmol) in ethanol (225 cm<sup>3</sup>) was prepared. This was stirred under hydrogen gas at atmospheric pressure for 17 h at RT. The catalyst was filtered and washed with ethanol and then the solvent was removed under reduced pressure to give the product as a white amorphous solid (4.50 g, 100%).

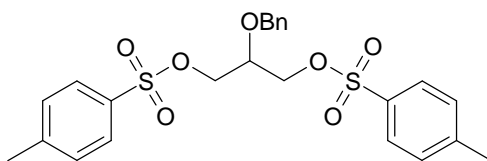
Mp 62–64 °C (Lit.,<sup>8, 16</sup> 45–46 °C).  $\delta_{\text{H}}$  (CDCl<sub>3</sub>, 300.13 MHz): 2.46 (6 H, s, CH<sub>3</sub>), 4.01–4.11 (5 H, m, CH<sub>2</sub>, CH), 7.33–7.39 (4 H, m, Ts-H), 7.74–7.79 (4 H, m, Ts-H).  $\delta_{\text{C}}$  (CDCl<sub>3</sub>, 100.62 MHz): 21.65 (CH<sub>3</sub>), 67.1 (CHOH), 69.5 (CH<sub>2</sub>), 128.0 (CH), 130.1 (CH), 132.1 (C), 145.4 (C).  $\nu_{\text{max}}$ /cm<sup>-1</sup> (film): 1359, 1190, 1150, 1175. HRMS (ES): Found 423.0536. Calcd. for C<sub>17</sub>H<sub>20</sub>O<sub>7</sub>S<sub>2</sub>Na, 423.0548.

**Method 2**

Toluene-4-sulfonyl chloride (8.67 g, 45.5 mmol) was added slowly to a solution of propane-1,2,3-triol (2.10 g, 22.7 mmol) in DCM (50 cm<sup>3</sup>) and pyridine (5 cm<sup>3</sup>) at 0 °C and the reaction was stirred at RT for 23 h. Water was then added (50 cm<sup>3</sup>) and the reaction

mixture was partitioned between the water and DCM. The DCM was separated and dried ( $\text{MgSO}_4$ ). The solvent and any remaining pyridine was removed under reduced pressure. Column chromatography over silica gel (hexane : ethyl acetate, 1:1) was carried out and the product was separated from the mono-tosylate and tri-tosylate by-products to give the desired product as a white amorphous solid (2.01 g, 22%).

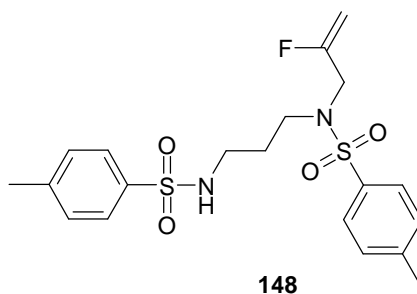
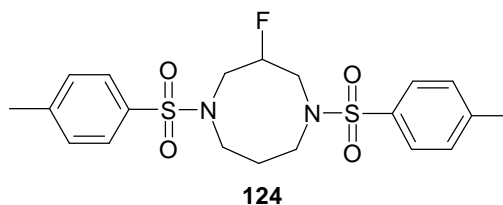
Analytical data were found to be identical to that obtained from **Method 1**.

4.2.25 2-[(Phenylmethyl)oxy]-1,3-propanediyl bis(4-methylbenzenesulfonate) 147<sup>17</sup>

Toluene-4-sulfonyl chloride (6.62 g, 34.7 mmol) was added at 0 °C to a solution of 2-[(phenylmethyl)oxy]-1,3-propanediol (2.11 g, 11.6 mmol) in DCM (50 cm<sup>3</sup>) and triethylamine (7 cm<sup>3</sup>) and then stirred at RT for 23 h. The reaction was then quenched with aqueous NaHCO<sub>3</sub> and passed through a hydrophobic frit. The DCM phase was collected and the solvent was removed under reduced pressure. The crude product was applied to a RediSep® pre-packed column (330 g) and chromatography was carried out on a Teledyne Isco Combiflash Companion® purification system using a gradient program of 20–30% ethyl acetate in cyclohexane. The product was detected by UV and collected by automation. After eluent removal under reduced pressure a white amorphous solid was obtained (5.52 g, 97%).

Mp 106–107 °C (Lit.,<sup>17</sup> 110–111 °C).  $\delta_{\text{H}}$  (CDCl<sub>3</sub>, 300.13 MHz): 2.45 (6 H, s, CH<sub>3</sub>), 3.80 (1 H, q, *J* 5.1, CHOBn) 3.99–4.08 (4 H, m, CH<sub>2</sub>CH), 4.48 (2 H, s, BnOCH<sub>2</sub>), 7.15–7.20 (2 H, m, Bn-H), 7.27–7.34 (7 H, m, Bn-H, Ts-H), 7.71–7.75 (4 H, m, Ts-H).  $\delta_{\text{C}}$  (CDCl<sub>3</sub>, 75.48 MHz): 21.8 (CH<sub>3</sub>), 67.8 (CH<sub>2</sub>CH), 72.7 (BnOCH<sub>2</sub>), 74.0 (CHOBn), 127.9 (CH), 128.1 (CH), 128.2 (CH), 128.6 (CH), 130.1 (CH), 132.5 (C), 137.1 (C), 145.3 (C).  $\nu_{\text{max}}$  /cm<sup>-1</sup> (film): 2867, 1596, 1360, 1149. HRMS (ES): Found 513.1021 Calcd. for C<sub>24</sub>H<sub>26</sub>O<sub>7</sub>S<sub>2</sub>Na, 513.1018.

**4.2.26 3-Fluoro-1,5-ditosyl-1,5-diazocane 124**  
**and *N*-(2-fluoroallyl)-4-methyl-*N*-(3-(4-methylphenylsulfonamido)propyl)benzenesulfonamide 148**



*N, N'*-1,3-Propanediylbis(4-methylbenzenesulfonamide) **142** (969 mg, 2.5 mmol) was added to a slurry of sodium hydride (131 mg, 5.5 mmol) in DMF (20 cm<sup>3</sup>) at RT. The reaction was stirred for 1 h then 2-fluoro-1,3-bis-(toluene-4-sulfonyloxy)-propane (1.01 g, 2.5 mmol) in DMF (5 cm<sup>3</sup>) was added. The reaction was heated at 100 °C for 40 h and was then cooled to RT. Water (5 cm<sup>3</sup>) was added and the DMF and water were removed under reduced pressure with heating. The product was partitioned between water and DCM and separated with use of a hydrophobic frit. On removal of the DCM under reduced pressure a yellow solid was obtained. This was applied in DCM (8 cm<sup>3</sup>) to a RediSep® pre-packed column (120 g) and chromatography was carried out on a Teledyne Isco Combiflash Companion® purification system using a gradient program of 10–70% ethyl acetate in cyclohexane. The product was collected by automation. After eluent removal under reduced pressure both the product **124** (394 mg, 36%) and by-product **148** (126 mg, 11%) were provided as a white amorphous solid and viscous liquid respectively.

**124**

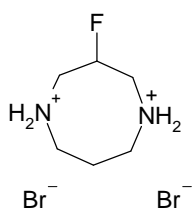
Mp 192–194 °C (from ethanol).  $\delta_{\text{H}}$  (CDCl<sub>3</sub>, 400.13 MHz): 2.00–2.06 (2 H, m, CH<sub>2</sub>CH<sub>2</sub>CH<sub>2</sub>), 2.44 (6 H, s, CH<sub>3</sub>), 3.25–3.29 (4 H, m, CH<sub>2</sub>CH<sub>2</sub>CH<sub>2</sub>), 3.42–3.57 (4 H, m, CH<sub>2</sub>CHFCH<sub>2</sub>), 4.98 (1 H, dm, *J* 45.8, CHF), 7.31–7.35 (4 H, m, Ts-H), 7.68–7.72 (4 H, m, Ts-H).  $\delta_{\text{C}}$  (CDCl<sub>3</sub>, 100.62 MHz): 21.6 (CH<sub>3</sub>), 29.4 (CH<sub>2</sub>CH<sub>2</sub>CH<sub>2</sub>), 48.3 (CH<sub>2</sub>CH<sub>2</sub>CH<sub>2</sub>), 50.1 (CH<sub>2</sub>CHFCH<sub>2</sub>), 89.9 (d, *J* 161.7, CHF), 127.5 (CH), 129.9 (CH).  $\delta_{\text{F}}$  (CDCl<sub>3</sub>, 376.42 MHz): -182.9 (m, CHF). HRMS (ES): Found 463.1139. Calcd. for C<sub>20</sub>H<sub>25</sub>N<sub>2</sub>O<sub>4</sub>FS<sub>2</sub>Na, 463.1137.

**148**

$\delta_{\text{H}}$  (CDCl<sub>3</sub>, 400.13 MHz): 1.76 (2 H, m, NHCH<sub>2</sub>CH<sub>2</sub>CH<sub>2</sub>N), 2.43 (6 H, s, CH<sub>3</sub>), 3.00 (2 H, t, *J* 6.0, NHCH<sub>2</sub>CH<sub>2</sub>CH<sub>2</sub>N), 3.22 (2 H, t, *J* 6.4, NHCH<sub>2</sub>CH<sub>2</sub>CH<sub>2</sub>N), 3.84 (1 H, d, *J* 15.8, NCHHCF), 3.92 (1 H, d, *J* 15.3, NCHHCF), 4.47 (1 H, ddd, *J* 3.3, *J* 23.0, *J* 47.5, CHH=CF), 4.67 (1 H, ddd, *J* 3.3, *J* 8.9, *J* 15.9, CHH=CF), 5.20 (1 H, t, *J* 7.0, NH), 7.25–7.33 (4 H, m, Ts-H), 7.64–7.69 (2 H, m, Ts-H), 7.72–7.75 (2 H, m, Ts-H).  $\delta_{\text{C}}$  (CDCl<sub>3</sub>, 100.62 MHz): 21.7 (CH<sub>3</sub>), 28.4 (NHCH<sub>2</sub>CH<sub>2</sub>CH<sub>2</sub>N), 39.5 (NHCH<sub>2</sub>CH<sub>2</sub>CH<sub>2</sub>N), 44.7 (NHCH<sub>2</sub>CH<sub>2</sub>CH<sub>2</sub>N), 48.3 (d, *J* 30.2, NCH<sub>2</sub>CF), 95.0 (d, *J* 17.3, CH<sub>2</sub>=CF), 127.1 (CH), 127.4 (CH), 129.9 (CH), 135.9 (C), 137.3 (C), 143.5 (C), 144.0 (C), 160.4 (d, *J* 262.2, CF=CH<sub>2</sub>).  $\delta_{\text{F}}$  (CDCl<sub>3</sub>, 376.42 MHz): -101.5 (m, CH<sub>2</sub>=CF).  $\nu_{\text{max}}$  /cm<sup>-1</sup> (film): 3266, 2922, 1674, 1596, 1329, 1204, 1149. HRMS (ES): Found 463.1150. Calcd. for C<sub>20</sub>H<sub>25</sub>N<sub>2</sub>O<sub>4</sub>FS<sub>2</sub>Na, 463.1137.

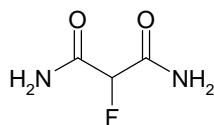


## 4.2.27 3-Fluoro-1,5-diazocane-1,5-dium bromide 149



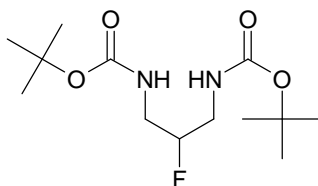
Phenol (537 mg, 5.7 mmol) and HBr (33%) in acetic acid (4.8 cm<sup>3</sup>, 26.6 mmol) were added to a solution of 3-fluoro-1,5-bis[(4-methylphenyl)sulfonyl]octahydro-1,5-diazocine (391 mg, 0.9 mmol) in acetic acid (5 cm<sup>3</sup>) and the reaction was then heated to 90 °C. After 19 h, a further aliquot of HBr (33%) in acetic acid (2.0 cm<sup>3</sup>, 11.0 mmol) was added and the reaction was stirred at 90 °C for an additional 29 h. The reaction was cooled to RT and partitioned between DCM and water. The DCM phase was separated and water was removed under reduced pressure with heating. The product as a salt was obtained as an orange solid (262 mg, 100%) and clear white crystals were obtained after recrystallisation from DMF and ether.

Mp 218–220 °C (from DMF / ether).  $\delta_{\text{H}}$  (D<sub>2</sub>O, 300.13 MHz): 2.18–2.48 (2 H, m, NCH<sub>2</sub>CH<sub>2</sub>CH<sub>2</sub>N), 3.35–3.55 (4 H, m, NCH<sub>2</sub>CH<sub>2</sub>CH<sub>2</sub>N), 3.61 (2 H, ddd, *J* 1.7, *J* 15.7, *J* 33.9, NCH<sub>2</sub>CHFCH<sub>2</sub>N), 3.86–3.97 (2 H, m, NCH<sub>2</sub>CHFCH<sub>2</sub>N), 5.39 (1 H, dm, *J* 39.0, CHF).  $\delta_{\text{C}}$  (D<sub>2</sub>O, 75.48 MHz): 19.0 (NCH<sub>2</sub>CH<sub>2</sub>CH<sub>2</sub>N), 44.6 (NCH<sub>2</sub>CH<sub>2</sub>CH<sub>2</sub>N), 44.8 (NCH<sub>2</sub>CHFCH<sub>2</sub>N), 45.1 (NCH<sub>2</sub>CHFCH<sub>2</sub>N), 83.9 (d, *J* 173.8, CHF).  $\delta_{\text{F}}$  (D<sub>2</sub>O, 282.29 MHz): -189.9 (m, CHF). Elemental analysis found: C, 24.8; H, 4.9; N, 9.5. Calc. for C<sub>6</sub>H<sub>15</sub>N<sub>2</sub>FBr<sub>2</sub>: C, 24.5; H, 5.1; N, 9.53%. HRMS (ES): Found 133.1137. Calcd. for C<sub>6</sub>H<sub>14</sub>N<sub>2</sub>F, 133.1141.

**4.2.28 2-Fluoropropanediamide 153**<sup>18</sup>

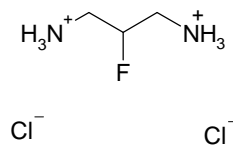
A solution of ammonia in MeOH (7M), (40 cm<sup>3</sup>, 280.0 mmol) was added slowly to diethyl fluoropropanedioate (9.92 g, 55.7 mmol) over 30 min at 0 °C and the reaction was stirred at RT for 20 h then filtered. The product was washed with methanol and dried at 40 °C to afford the product as an amorphous white solid (6.43 g, 96%).

Mp 202–203 °C (from MeCN), (Lit.,<sup>18</sup> 199–201 °C).  $\delta_{\text{H}}$  ((CD<sub>3</sub>)<sub>2</sub>SO, 300.06 MHz): 5.15 (1 H, d, *J* 49.0, CHF), 7.61 (2 H, br s, *NHH*), 7.66 (2 H, br s, *NHH*).  $\delta_{\text{C}}$  ((CD<sub>3</sub>)<sub>2</sub>SO, 75.46 MHz): 87.5 (d, *J* 192.7, CHF), 166.7 (d, *J* 21.2, C=O).  $\delta_{\text{F}}$  (CDCl<sub>3</sub>, 282.29 MHz): -185.4 (ddd, *J* 4.1, *J* 4.1, *J* 48.9, CHF).

4.2.29 1,3-Bis-*N*-*t*-butyloxycarbonyl-2-fluoropropane **155**<sup>18</sup>

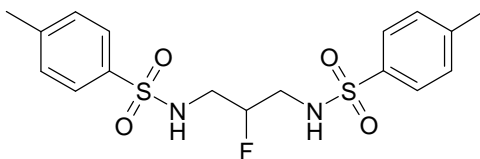
2-Fluoropropanediamide **153** (1.30g, 10.8 mmol) was suspended in THF (20 cm<sup>3</sup>) at RT and diborane / THF (1M, 62 cm<sup>3</sup>, 62 mmol) was added slowly over 45 min. The reaction was heated to 45 °C for 24 h. The reaction was then cooled to 0 °C and HCl (2N, 20 cm<sup>3</sup>) was added slowly over 15 min, this was then stirred for 30 min. THF and water were removed under reduced pressure and the boric acid was co-evaporated with methanol (5 x 20 cm<sup>3</sup>). The white residue was dissolved in water (20 cm<sup>3</sup>) and applied to a Dowex column (1 x 8, 200-400 mesh Cl<sup>-</sup>) which had been pre-washed with water and the 2-fluoro-1,3-propanediamine hydrochloride product **154** was eluted with water. The fractions which showed a positive ninhydrin test were pooled together and water removed under reduced pressure at 30 °C. A yellow sticky solid was recovered (1.86 g). The crude was dissolved in water (10 cm<sup>3</sup>) and di-*t*-butyldicarbonate (5.96 g, 27.3 mmol) in 1,4-dioxane (40 cm<sup>3</sup>) was added at RT, followed by sodium carbonate (3.0 g, 28.3 mmol) in water (20 cm<sup>3</sup>). The reaction was stirred for 13 h at RT and was then concentrated under reduced pressure and the reduced volume (~10 cm<sup>3</sup>) was extracted into ethyl acetate (4 x 25 cm<sup>3</sup>), dried (MgSO<sub>4</sub>) and filtered. Solvent removal under reduced pressure gave a yellow oil which was titrated with hexane to provide a white cloudy mixture. Upon removal of hexane a white solid was obtained and this was crystallised using hexane with heating to give the product as a crystalline white solid **155** (1.48 g, 47%).

Mp 86–88 °C (from hexane), (Lit., <sup>18</sup> 88–90 °C).  $\delta_{\text{H}}$  (CDCl<sub>3</sub>, 300.06 MHz): 1.44 (18 H, s, C(CH<sub>3</sub>)<sub>3</sub>), 3.20–3.51 (4 H, m, CH<sub>2</sub>), 4.56 (1 H, dm, *J* 47.4, CHF), 5.00 (2 H, br s, NH<sub>2</sub>).  $\delta_{\text{C}}$  (CDCl<sub>3</sub>, 75.46 MHz): 28.5 (C(CH<sub>3</sub>)<sub>3</sub>), 41.2 (d, *J* 21.6, CH<sub>2</sub>), 79.8 (C(CH<sub>3</sub>)<sub>3</sub>), 91.0 (d, *J* 174.8, CHF), 156.4 (C=O).  $\delta_{\text{F}}$  (CDCl<sub>3</sub>, 282.30 MHz): -192.8 (m, CHF).

**4.2.30 2-Fluoro-1,3-propanediamine hydrochloride 154**<sup>18</sup>

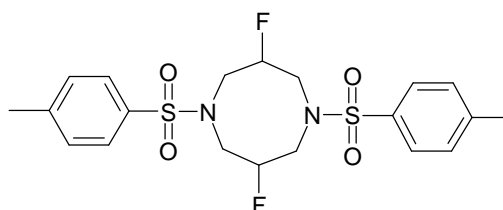
A solution of 1,3-bis-*N-t*-butyloxycarbonyl-2-fluoropropane **155** (1.44 g, 4.9 mmol) in MeOH (5 cm<sup>3</sup>) was added to a solution of acetyl chloride (5 cm<sup>3</sup>, 70.1 mmol) in MeOH (50 cm<sup>3</sup>) at 0 °C. The reaction was stirred at RT for 13 h then the solvent was removed under reduced pressure to give a white amorphous solid (807 mg, 100%).

Mp 246–248 °C (from ethanol / ether), (Lit.,<sup>18</sup> 238–240 °C).  $\delta_{\text{H}}$  (D<sub>2</sub>O, 300.06 MHz): 3.31–3.50 (m, CH<sub>2</sub>), 5.17 (dm, *J* 51.4, CHF).  $\delta_{\text{C}}$  (D<sub>2</sub>O, 75.47 MHz): 40.4 (d, *J* 19.5, CH<sub>2</sub>), 87.1 (d, *J* 174.3, CHF).  $\delta_{\text{F}}$  (D<sub>2</sub>O, 282.29 MHz): -196.6 (m, CHF). Elemental analysis found: C, 22.2; H, 6.9; N, 16.8. Calc. for C<sub>3</sub>H<sub>9</sub>N<sub>2</sub>F : 2HCl: C, 21.8; H, 6.7; N, 17.0%.

4.2.31 *N,N'*-(2-Fluoropropane-1,3-diyl)bis(4-methylbenzenesulfonamide) **157**

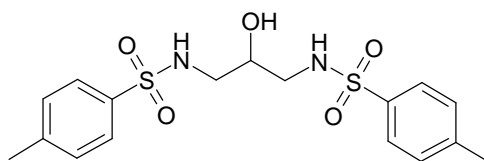
Pyridine (20 cm<sup>3</sup>) and then p-toluenesulfonyl chloride (565 mg, 3.0 mmol) was added to 2-fluoro-1,3-propanediamine hydrochloride (197 mg, 1.2 mmol) was added followed by at RT. The reaction was heated to 80 °C for 10 h and then cooled to 40 °C, DCM (20 cm<sup>3</sup>) was then added to aid in the work-up. The pyridine and DCM were removed under reduced pressure, then the residue was partitioned between DCM and water, the DCM phase was separated, dried with MgSO<sub>4</sub> and filtered. The DCM was removed under reduced pressure to provide **157** as a cream coloured solid (265 mg, 56%).

Mp 176–178 °C (from ethanol).  $\delta_{\text{H}}$  (CDCl<sub>3</sub>, 400.13 MHz): 2.44 (6 H, s, CH<sub>3</sub>), 3.20–3.29 (4 H, m, CH<sub>2</sub>), 4.47 (1 H, dm, *J* 46.0, CHF), 4.92 (2 H, t, *J* 6.9, NH), 7.31–7.35 (4 H, m, Ts-H), 7.71–7.75 (4 H, m, Ts-H).  $\delta_{\text{C}}$  (CDCl<sub>3</sub>, 100.62 MHz): 21.7 (CH<sub>3</sub>), 43.0 (d, *J* 24.6, CH<sub>2</sub>), 90.3 (d, *J* 173.8, CHF), 127.0 (CH), 130.1 (CH), 144.1 (C).  $\delta_{\text{F}}$  (CDCl<sub>3</sub>, 376.45 MHz): -192.2 (m, CHF).  $\nu_{\text{max}}$  /cm<sup>-1</sup> (film): 3284, 2958, 1445, 1329, 1213, 1156. HRMS (Cl<sup>+</sup>): Found 401.1004. Calcd. for C<sub>17</sub>H<sub>22</sub>N<sub>2</sub>O<sub>4</sub>S<sub>2</sub>F, 401.1005.

4.2.32 3,7-Difluoro-1,5-ditosyl-1,5-diazocane **150**

A solution of *N,N'*-(2-fluoropropane-1,3-diyl)bis(4-methylbenzenesulfonamide) **154** (56 mg, 0.14 mmol) in DMF (2 cm<sup>3</sup>) was added to a slurry of sodium hydride (6 mg, 0.26 mmol) in DMF (0.5 cm<sup>3</sup>) at RT and the reaction was stirred at RT for 1 h then 2-fluoro-1,3-bis-(toluene-4-sulfonyloxy)-propane **157** (56 mg, 0.14 mmol) in DMF (1 cm<sup>3</sup>) was added. The reaction was heated at 100 °C for 25 h and was then cooled to RT. The DMF was then removed under reduced pressure with heating. The product was partitioned between water and DCM and the DCM phase was dried (MgSO<sub>4</sub>) and filtered. The solvent was removed under reduced pressure to give a yellow solid. Repetitive chromatography over silica gel (hexane : ethyl acetate, 3:1) and preparative plate purification gave **150** as a white solid (4 mg, 7%). **150** is a mixture of *cis* and *trans* isomers.

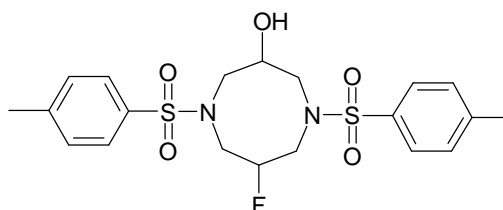
$\delta_{\text{H}}$  (CDCl<sub>3</sub>, 300.13 MHz): 2.45 (6 H, s, CH<sub>3</sub>), 3.31–3.77 (8 H, m, CH<sub>2</sub>CH<sub>2</sub>CH<sub>2</sub>), 4.79–5.09 (2 H, dm, *J* 46.4, CHF, dm *J* 44.8, CHF), 7.33–7.38 (4 H, m, Ts-H), 7.70–7.75 (4 H, m, Ts-H).  $\delta_{\text{C}}$  (CDCl<sub>3</sub>, 75.48 MHz): 21.7 (CH<sub>3</sub>), 51.5 (CH<sub>2</sub>CHFCH<sub>2</sub>), 51.9 (CH<sub>2</sub>CHFCH<sub>2</sub>), 89.8 (d, *J* 178.4, CHF), 127.5 (CH), 127.6 (CH), 130.1 (CH), 130.2 (CH).  $\delta_{\text{F}}$  (CDCl<sub>3</sub>, 376.44 MHz): -182.0 and -182.5 (ratio 1 : 2.5). HRMS (ES): Found 481.1052. Calcd. for C<sub>20</sub>H<sub>24</sub>N<sub>2</sub>O<sub>4</sub>F<sub>2</sub>S<sub>2</sub>Na, 481.1043.

4.2.33 *N,N'*-(2-Hydroxytrimethylene)bis-toluene-4-sulfonamide 161 <sup>19</sup>

p-Toluenesulfonyl chloride (5.26 g, 27.6 mmol) in THF (20 cm<sup>3</sup>) was added to a solution of 1,3-diamino-2-propanol (821 mg, 9.1 mmol) and K<sub>2</sub>CO<sub>3</sub> (4.69 g, 33.9 mmol) in water (20 cm<sup>3</sup>) at RT and the reaction was stirred for 24 h. The water and THF were removed under reduced pressure with heating. The product was partitioned between water and DCM and the DCM phase was separated. After solvent removal under reduced pressure the product was purified over silica gel (hexane : ethyl acetate, 1:1), yielding a white amorphous solid (2.97 g, 82%).

Mp 143–144 °C (from ethanol), (Lit.,<sup>19</sup> 144–145 °C).  $\delta_{\text{H}}$  (CD<sub>3</sub>OD, 300.13 MHz): 2.42 (6 H, s, CH<sub>3</sub>), 2.84 (4 H, ddd, *J* 5.2, *J* 13.5, *J* 40.6, CH<sub>2</sub>), 3.65 (1 H, q, *J* 11.6, CHOH), 7.33–7.39 (4 H, m, Ts-H), 7.69–7.74 (4 H, m, Ts-H).  $\delta_{\text{C}}$  (CD<sub>3</sub>OD, 75.48 MHz): 21.5 (CH<sub>3</sub>), 47.3 (CH<sub>2</sub>), 70.3 (CHOH), 128.0 (CH), 130.8 (CH), 138.6 (C), 144.7 (C). Elemental analysis found: C, 51.51; H, 5.4; N, 6.9. Calc. for C<sub>17</sub>H<sub>22</sub>N<sub>2</sub>O<sub>5</sub>S<sub>2</sub>: C, 51.2; H, 5.56; N, 7.03%.  $\nu_{\text{max}}$  /cm<sup>-1</sup> (film): 3494, 3274, 2924, 1597, 1425, 1322, 1212, 1154.



4.2.34 7-Fluoro-1,5-ditosyl-1,5-diazocan-3-ol **162**

A slurry of sodium hydride (218 mg, 9.1 mmol) in DMF (30 cm<sup>3</sup>) was added to a solution of *N, N'*-(2-hydroxytrimethylene)bis-toluene-4-sulfonamide **161** (1.62 g, 4.1 mmol) in DMF (20 cm<sup>3</sup>) at RT and the reaction was stirred for 40 min. A solution of 2-fluoro-1,3-bis-(toluene-4-sulfonyloxy)-propane (1.64 g, 4.1 mmol) in DMF (20 cm<sup>3</sup>) was then added and the reaction was heated at 100 °C for 28 h and then cooled to RT. Water (5 cm<sup>3</sup>) was added and the DMF and water were removed under reduced pressure with heating. The product was purified over silica gel (hexane : ethyl acetate, 2:1) and a mixture of the isomers was obtained as a white solid (950 mg, 51%). Crystallisation was carried out from ethanol to provide white needles, which were used for X-ray crystallography analysis.

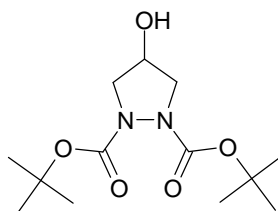
In a separate experiment the isomers were separated successfully by careful silica gel chromatography and the analyses of these isomers is given.

***Cis or trans isomer***

Mp 218–220 °C (from ethanol).  $\delta_{\text{H}}$  ( $\text{CDCl}_3$ , 300.06 MHz): 2.47 (6 H, s,  $\text{CH}_3$ ), 3.27 (2 H, dd,  $J$  5.6,  $J$  15.3,  $\text{NCH}_2\text{CH}(\text{OH})\text{CH}_2\text{N}$ ), 3.43–3.73 (6 H, m,  $\text{NCH}_2\text{CH}(\text{OH})\text{CH}_2\text{N}$ ,  $\text{NCH}_2\text{CH}(\text{F})\text{CH}_2$ ), 4.21 (1 H, m,  $\text{CHOH}$ ), 4.97 (1 H, dm,  $J$  46.0, CHF), 7.35–7.4 (4 H, m, Ts-H), 7.69–7.74 (4 H, m, Ts-H).  $\delta_{\text{C}}$  ( $\text{CDCl}_3$ , 75.47 MHz): 21.7 ( $\text{CH}_3$ ), 52.5 (d,  $J$  29.2,  $\text{CHFCH}_2$ ), 53.5 ( $\text{NCH}_2\text{CH}(\text{OH})\text{CH}_2\text{N}$ ), 53.6 ( $\text{NCH}_2\text{CH}(\text{OH})\text{CH}_2\text{N}$ ), 69.3 ( $\text{CHOH}$ ), 90.1 (d,  $J$  178.6, CHF), 90.1 (d,  $J$  177.9, CHF), 127.5 (CH), 130.2 (CH), 144.6 (C).  $\delta_{\text{F}}$  ( $\text{CDCl}_3$ , 282.29 MHz): -181.4 (CHF).  $\nu_{\text{max}}/\text{cm}^{-1}$  (film): 3487, 1596, 1449, 1348, 1153. HRMS (ES): Found 479.1097. Calcd. for  $\text{C}_{20}\text{H}_{25}\text{N}_2\text{O}_5\text{S}_2\text{F}$ , 479.1087.

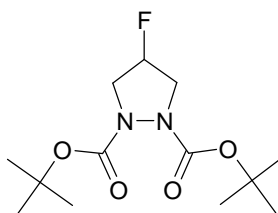
***Cis or trans isomer***

$\delta_{\text{H}}$  ( $\text{CDCl}_3$ , 300.06 MHz): 2.45 (6 H, s,  $\text{CH}_3$ ), 3.18 (2 H, dd,  $J$  5.8,  $J$  15.3,  $\text{NCH}_2\text{CH}(\text{OH})\text{CH}_2\text{N}$ ), 3.43–3.66 (6 H, m,  $\text{NCH}_2\text{CH}(\text{OH})\text{CH}_2\text{N}$ ,  $\text{NCH}_2\text{CH}(\text{F})\text{CH}_2$ ), 4.22 (1 H, m,  $\text{CHOH}$ ), 4.95 (1 H, dm,  $J$  45.7, CHF), 7.32–7.39 (4 H, m, Ts-H), 7.67–7.73 (4 H, m, Ts-H).  $\delta_{\text{F}}$  ( $\text{CDCl}_3$ , 282.29 MHz): -180.7 (CHF). HRMS (ES): Found 479.1092. Calcd. for  $\text{C}_{20}\text{H}_{25}\text{N}_2\text{O}_5\text{S}_2\text{F}$ , 479.1087.

4.2.35 1,2-Di(tert-butyloxycarbonyl)-4-hydroxypyrazolidine **167**<sup>20</sup>

A slurry of NaH (1.57 g, 65.4 mmol) in DMF (20 cm<sup>3</sup>) was added to a solution of di-tert-butyl-hydrazodiformate (5.84 g, 25.1 mmol) in DMF (30 cm<sup>3</sup>) at 0 °C. The reaction was stirred for 45 min and then 1,3-dichloropropanol (2.2 cm<sup>3</sup>, 22.6 mmol) was added at RT over 40 min. A further volume of DMF (20 cm<sup>3</sup>) was added to aid stirring the viscous mixture. The reaction was then stirred at RT for 69 h and was then quenched with ammonium chloride solution. Water and DMF were removed under reduced pressure with heating and the product was purified over silica gel (hexane : ethyl acetate, 1:1). **167** was obtained as a clear viscous oil (1.59 g, 24%).

$\delta_{\text{H}}$  (CDCl<sub>3</sub>, 300.06 MHz): 1.41 (18 H, s, CH<sub>3</sub>), 3.06 (1 H, dd, *J* 3.2, *J* 12.4, CH<sub>2</sub>), 3.29 (1 H, d, *J* 11.6, CH<sub>2</sub>), 3.77 (1 H, dd, *J* 5.2, *J* 11.6, CH<sub>2</sub>), 3.95 (1 H, d, *J* 12.4, CH<sub>2</sub>), 4.53 (1 H, m, CHOH).  $\delta_{\text{C}}$  (CDCl<sub>3</sub>, 75.48 MHz): 28.5 (CH<sub>3</sub>), 28.6 (CH<sub>3</sub>), 55.2 (CH<sub>2</sub>), 56.5 (CH<sub>2</sub>), 71.5 (COH), 81.5 (C(CH<sub>3</sub>)<sub>3</sub>), 81.9 (C(CH<sub>3</sub>)<sub>3</sub>), 155.5 (C=O), 158.1 (C=O).  $\nu_{\text{max}}$  /cm<sup>-1</sup> (film): 3373, 2922, 1698, 1211, 1152. HRMS (ES): found 311.1592. Calcd. for C<sub>13</sub>H<sub>24</sub>N<sub>2</sub>O<sub>5</sub>Na, 311.1583.

4.2.36 Bis(1,1-dimethylethyl)-4-fluoro-1,2-pyrazolidinedicarboxylate **168****Method 1:****Via 1,2-di(tert-butyloxycarbonyl)-4-hydroxypyrazolidine **167****

Deoxofluor (3.6 cm<sup>3</sup>, 19.5 mmol) was added to a solution of 1,2-di(tert-butyloxycarbonyl)-4-hydroxypyrazolidine **167** (0.47 g, 1.7 mmol) in DCM (20 cm<sup>3</sup>) at -78 °C and the reaction was stirred for 18 h at RT. This was then cooled to 0 °C and slowly quenched with aqueous NaHCO<sub>3</sub> solution. The product was partitioned between water and DCM and the organic phase was separated and DCM removed under reduced pressure. Purification over silica gel (hexane : ethyl acetate, 2:1), gave **168** as a clear viscous liquid (0.31 g, 65%).

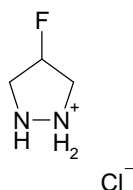
$\delta_{\text{H}}$  (CDCl<sub>3</sub>, 300.06 MHz): 1.47 (18 H, s, CH<sub>3</sub>), 3.14 (1 H, ddd, *J* 2.6, *J* 13.3, *J* 36.5, CH<sub>2</sub>), 3.60 (1 H, dd, *J* 13.3, *J* 29.2, CH<sub>2</sub>), 3.96 (1 H, ddd, *J* 5.0, *J* 13.3, *J* 32.6, CH<sub>2</sub>), 4.31 (1 H, dd, *J* 13.7, *J* 18.6, CH<sub>2</sub>), 5.33 (1 H, dm, *J* 53.9, CHF). VT <sup>1</sup>H NMR (DMSO, 105 °C): NMR signals coalesce at 105 °C owing to more rapid *cis* / *trans* isomerism about the carbamates.  $\delta_{\text{C}}$  (CDCl<sub>3</sub>, 75.46 MHz): 28.5 (CH<sub>3</sub>), 28.6 (CH<sub>3</sub>), 53.3 (CH<sub>2</sub>), 53.6 (CH<sub>2</sub>), 81.9 (C(CH<sub>3</sub>)<sub>3</sub>), 82.3 (C(CH<sub>3</sub>)<sub>3</sub>), 93.0 (d, *J* 180.3, CHF).  $\delta_{\text{F}}$  (CDCl<sub>3</sub>, 282.29 MHz): -178.0 (m, CHF).

$\nu_{\text{max}}$  /cm<sup>-1</sup> (film): 3446, 2979, 1702, 1367, 1142. HRMS (ES): found 313.1545. Calcd. for C<sub>13</sub>H<sub>23</sub>N<sub>2</sub>O<sub>4</sub>FNa, 313.1540.

**Method 2:****Via 2-fluoro-1,3-bis(toluene-4-sulfonyloxy)-propane 142**

A slurry of NaH (0.31 g, 12.9 mmol) in DMF (10 cm<sup>3</sup>) was added to a solution of di-tert-butyl-hydrazodiformate (1.48 g, 6.4 mmol) in DMF (15 cm<sup>3</sup>) at 0 °C and the reaction was stirred for 1 h. Then 2-fluoro-1,3-bis(toluene-4-sulfonyloxy)-propane **142** (2.33 g, 5.8 mmol) was added at 0 °C and the reaction was stirred at RT for 21 h. This was then heated to 100 °C for 22 h before further NaH (0.08 g, 3.7 mmol) was added at 0 °C. The reaction was then re-heated to 100 °C and stirred for 16 h, after which it was quenched with NH<sub>4</sub>Cl solution at RT. Water and DMF were removed under reduced pressure. The product was extracted into ethyl acetate and the organic phase was dried (MgSO<sub>4</sub>) and the solvent removed under reduced pressure. The crude product was purified over silica gel (hexane: ethyl acetate, 2:1) followed by (chloroform: ethyl acetate, 20:1) to give **168** as a clear viscous liquid (0.64 g, 38%).

The <sup>1</sup>H, <sup>13</sup>C and <sup>19</sup>F NMR analysis was found to be identical to **Method 1**.

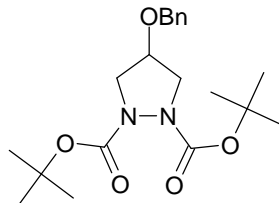
4.2.37 4-Fluoro-pyrazolidine hydrochloride **169**

Acetyl chloride (2 cm<sup>3</sup>, 25.5 mmol) was added to bis(1,1-dimethylethyl)-4-fluoro-1,2-pyrazolidinedicarboxylate **168** (0.94 g, 3.2 mmol) in MeOH (30 cm<sup>3</sup>) at 0 °C and the reaction was stirred at RT for 21 h. The MeOH was removed under reduced pressure and product **169** was obtained a white solid (0.41 g, 100%). Crystals suitable for X-ray crystallography were obtained after recrystallisation from EtOH and ether at 4 °C.

$\delta_{\text{H}}$  (D<sub>2</sub>O, 300.06 MHz): 3.21–3.39 (2 H, m, CH<sub>2</sub>), 3.49–3.61 (2 H, m, CH<sub>2</sub>), 5.52 (1H, dm, *J* 53.2, CHF).  $\delta_{\text{C}}$  (D<sub>2</sub>O, 75.48 MHz): 52.9 (CH<sub>2</sub>), 53.2 (CH<sub>2</sub>), 92.5 (d, *J* 177.7, CHF).  $\delta_{\text{F}}$  (D<sub>2</sub>O, 282.29 MHz): -179.2 (m, CHF).  $\delta_{\text{F}}$  (D<sub>2</sub>O, 282.29 MHz): -174.9 (m, CHF), free base (after treatment with NaOH).

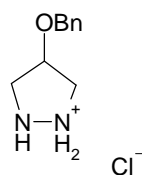
$\delta_{\text{H}}$  (CDCl<sub>3</sub>, 300.06 MHz): 2.95–3.13 (2 H, m, CH<sub>2</sub>), 3.17–3.33 (2 H, m, CH<sub>2</sub>), 5.42 (1H, dm, *J* 56.5, CHF). free base (after treatment with SCX-2 column).  $\delta_{\text{F}}$  (CDCl<sub>3</sub>, 282.29 MHz): -175.1 (m, CHF), free base (after treatment with SCX-2 column). Elemental analysis: found C, 28.7; H, 6.2; N, 21.8. Calc. for C<sub>3</sub>H<sub>8</sub>N<sub>2</sub>F · Cl : C, 28.5; H, 6.4; N, 22.1%.

**4.2.38 Bis(1,1-dimethylethyl)-4-[(phenylmethyl)oxy]-1,2-pyrazolidinedicarboxylate **173****



NaH (0.35 g, 8.7 mmol) in DMF (2 cm<sup>3</sup>) was added to a solution of di-tert-butylhydrazodiformate (1.0 g, 4.3 mmol) in DMF (10 cm<sup>3</sup>) at 0 °C. The reaction was stirred for 30 min then 2-[phenylmethyl]oxy]-1,3-propanediyl bis(4-methylbenzenesulfonate) **147** (2.11 g, 4.3 mmol) in DMF (10 cm<sup>3</sup>) and TBAI (0.1 g, 0.3 mmol) were added at RT and stirred for 23 h. The reaction was then heated at 100 °C for 24 h, after which unreacted NaH was quenched with saturated aqueous NH<sub>4</sub>Cl solution. Water and DMF were then removed under reduced pressure and the product was extracted into chloroform. The organic phase was separated and the solvent was removed under reduced pressure purified over silica gel (chloroform : ethyl acetate, 20:1) to give **173** as an off white solid (1.09 g, 67%). Crystallisation from hot cyclohexane gave colourless crystals.

Mp 92–94 °C (cyclohexane).  $\delta_{\text{H}}$  (CDCl<sub>3</sub>, 400.13 MHz): 1.45 (9 H, s, CH<sub>3</sub>), 1.48 (9 H, s, CH<sub>3</sub>), 3.05 (1 H, d, *J* 11.0, CH<sub>2</sub>), 3.45 (1 H, d, *J* 12.4, CH<sub>2</sub>), 3.86 (1 H, dd, *J* 5.7, *J* 11.8, CH<sub>2</sub>), 4.29–4.32 (1 H, m, CH<sub>2</sub>), 4.29–4.32 (1 H, m, CHO), 4.45 (1 H, d, *J* 11.5, CH<sub>2</sub>O), 4.58 (1 H, d, *J* 11.5, CH<sub>2</sub>O), 7.30–7.38 (5 H, m, Ph-H). VT <sup>1</sup>H NMR (DMSO, 140 °C): coalescence of the rotamers occurred at 140 °C.  $\delta_{\text{C}}$  (CDCl<sub>3</sub>, 100.62 MHz): 28.1 (CH<sub>3</sub>), 28.3 (CH<sub>3</sub>), 52.6 (CH<sub>2</sub>), 70.8 (CH<sub>2</sub>Ph), 78.1 (CHO), 81.0 (C(CH<sub>3</sub>)<sub>3</sub>), 81.4 (C(CH<sub>3</sub>)<sub>3</sub>), 127.7 (CH), 127.8 (CH), 128.4 (CH), 137.3 (C).  $\nu_{\text{max}}$ /cm<sup>-1</sup> (film): 2926, 1697, 1365, 1210, 1152. HRMS (ES): Found 401.2058. Calcd. for C<sub>20</sub>H<sub>30</sub>N<sub>2</sub>O<sub>5</sub>Na, 401.2052.

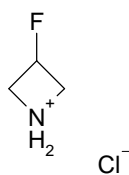
4.2.39 4-[(Phenylmethyl)oxy]pyrazolidine chloride **174**

Acetyl chloride (5 cm<sup>3</sup>, 63.7 mmol) and MeOH (20 cm<sup>3</sup>) was added to bis(1,1-dimethylethyl)-4-[(phenylmethyl)oxy]-1,2-pyrazolidinedicarboxylate **173** (0.84 g, 2.21 mmol) in MeOH (30 cm<sup>3</sup>) at 0 °C and the reaction was then stirred at RT for 24 h. The MeOH was removed under reduced pressure to give the salt **174** as a viscous liquid (0.47 g, 100%).

$\delta_{\text{H}}$  (D<sub>2</sub>O, 300.13 MHz): 3.17–3.23 (2 H, m, CH<sub>2</sub>), 3.35–3.41 (2 H, m, CH<sub>2</sub>), 4.45 (2 H, s, CH<sub>2</sub>O), 4.46–4.51 (1 H, m, CHO), 7.24–7.34 (5 H, m, Ph-H).  $\delta_{\text{C}}$  (MeOH, 75.46 MHz): 53.7 (NCH<sub>2</sub>), 72.5 (CH<sub>2</sub>Ph), 80.7 (CHO), 129.0 (CH), 129.2 (CH), 129.5 (CH), 138.8 (C). HRMS (ES): found 179.1187. Calcd. for C<sub>10</sub>H<sub>15</sub>N<sub>2</sub>O, 179.1184.

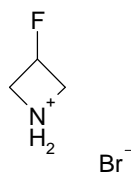


## 4.2.40 3-Fluoroazetidinium hydrochloride 182



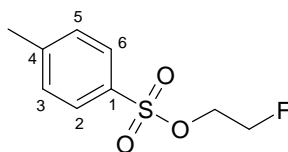
This product was kindly provided by Steve Sollis at GlaxoSmithKline after preparation of an in-house GSK project. Prior to our crystallographic study the compound was subjected to analysis at St Andrews.

Mp 126–128 °C.  $\delta_{\text{H}}$  ( $\text{D}_2\text{O}$ , 300.13 MHz): 4.12–4.26 (2 H, m,  $\text{CH}_2$ ), 4.32–4.46 (2 H, m,  $\text{CH}_2$ ), 5.34 (1 H, dm,  $J$  56.4, CHF).  $\delta_{\text{C}}$  ( $\text{D}_2\text{O}$ , 75.48 MHz): 53.6 ( $\text{CH}_2$ ), 54.0 ( $\text{CH}_2$ ), 83.8 (d,  $J$  200.8, CHF).  $\delta_{\text{F}}$  ( $\text{D}_2\text{O}$ , 282.29 MHz): -178.9 (m, CHF).  $\delta_{\text{F}}$  ( $\text{D}_2\text{O}$ , 282.29 MHz): -173.7 (m, CHF), free base (after treatment with NaOH). Elemental analysis found: C, 32.54; H, 6.3; N, 12.4. Calc. for  $\text{C}_3\text{H}_6\text{NF} : \text{HCl}$ : C, 32.3; H, 6.3; N, 12.56%.

4.2.41 3-Fluoroazetidinium hydrobromide **183**

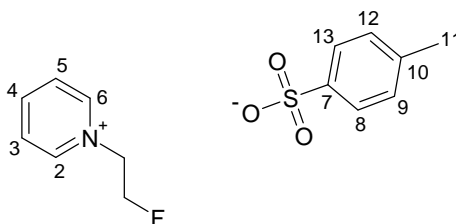
3-Fluoroazetidinium hydrochloride **182** (0.0135 g, 0.12 mmol) was dissolved in deionised water (~3 cm<sup>3</sup>) and HBr in water (1.8 cm<sup>3</sup>, 15.9 mmol) was added. The water was removed under reduced pressure with heating to provide a light brown solid. White needle like crystals were obtained after recrystallisation from ethanol and ether at 4 °C.

Mp 127–128 °C.  $\delta_{\text{H}}$  (D<sub>2</sub>O, 300.06 MHz): 4.09–4.23 (2 H, m, CH<sub>2</sub>), 4.29–4.43 (2 H, m, CH<sub>2</sub>), 5.31 (1 H, dm, *J* 56.5, CHF).  $\delta_{\text{F}}$  (D<sub>2</sub>O, 282.29 MHz): -178.9 (m, CHF). Elemental analysis found C, 23.4; H, 4.4; N, 9.0. Calc. for C<sub>3</sub>H<sub>6</sub>NF : HBr: C, 23.1; H, 4.52; N, 9.0%.

4.2.42 2-Fluoroethyltosylate 206<sup>21</sup>

p-Toluenesulfonyl chloride (6.40 g, 33.6 mmol) and 2-fluoroethanol (0.95 cm<sup>3</sup>, 16.3 mmol) were added to pyridine (15 cm<sup>3</sup>) at 0 °C and stirred for 4 h. The reaction was quenched with water (20 cm<sup>3</sup>) and then the product was extracted into ethyl acetate. This organic layer was washed sequentially with 1M HCl, water and saturated Na<sub>2</sub>CO<sub>3</sub> solution. The ethyl acetate was dried (MgSO<sub>4</sub>) and then removed under reduced pressure giving the product as a light yellow liquid (3.44 g, 97%).

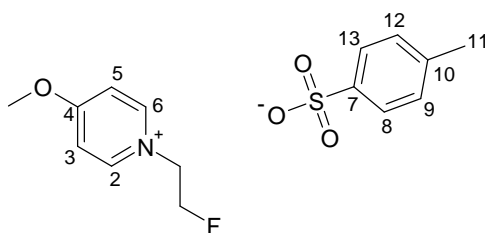
$\delta_{\text{H}}$  (CDCl<sub>3</sub>, 300.06 MHz): 2.45 (3 H, s, CH<sub>3</sub>), 4.26 (2 H, dm, *J* 27.3, CH<sub>2</sub>N), 4.56 (2 H, dm, *J* 47.1, CH<sub>2</sub>F), 7.33–7.38 (2 H, m, H-3, H-5), 7.78–7.83 (2 H, m, H-2, H-6).  $\delta_{\text{C}}$  (CDCl<sub>3</sub>, 75.48 MHz): 21.8 (CH<sub>3</sub>), 68.6 (d, *J* 20.9, OCH<sub>2</sub>), 80.7 (d, *J* 174.0, CH<sub>2</sub>F), 128.1 (C-2, C-6), 130.1 (C-3, C-5), 132.7 (C-1), 145.3 (C-4).  $\delta_{\text{F}}$  (CDCl<sub>3</sub>, 282.28 MHz): -225.1 (dt, *J* 27.0, *J* 47.3, CH<sub>2</sub>F). HRMS (ES): found 241.0311. Calcd. for C<sub>9</sub>H<sub>11</sub>O<sub>3</sub>FSNa, 241.0311.

4.2.43 1-(2-Fluoro-ethyl)-pyridinium 4-methylbenzenesulfonate **198**

A solution of 2-fluoroethyltosylate **206** (100 mg, 0.46 mmol) in pyridine (59 mg, 0.74 mmol) was heated to 110 °C for 20 h. Residual pyridine was removed under vacuum and the residue was freeze dried. HCl in ether was added and then the volatiles were removed *en vacuo*. The resultant solid was re-crystallised from EtOH and ether at 4 °C to give the product **198** as colourless needles (51 mg, 37%).

Mp 207–210 °C (ether / ethanol).  $\delta_{\text{H}}$  ( $\text{D}_2\text{O}$ , 300.06 MHz): 2.35 (3 H, s,  $\text{CH}_3$ ), 4.82–5.02 (2 H, m,  $\text{NCH}_2$ ), 4.82–5.02 (2 H, m,  $\text{CH}_2\text{F}$ ), 7.28–7.34 (2 H, m, H-9, H-12), 7.62–7.66 (2 H, m, H-8, H-13), 8.02–8.08 (2 H, m, H-3, H-5), 8.51–8.58 (1 H, m, H-4), 8.80–8.84 (2 H, m, H-2, H-6).  $\delta_{\text{C}}$  ( $\text{D}_2\text{O}$ , 75.48 MHz): 20.4 ( $\text{CH}_3$ ), 61.4 (d,  $J$  18.1,  $\text{NCH}_2$ ), 81.8 (d,  $J$  169.8,  $\text{CH}_2\text{F}$ ), 125.3 (C-8, C-13), 128.3 (C-3, C-5), 129.4 (C-9, C-12), 139.4 (C-7), 142.4 (C-10), 144.7 (C-2, C-6), 146.3 (C-4).  $\delta_{\text{F}}$  ( $\text{D}_2\text{O}$ , 282.28 MHz): -224.2 (ddd,  $J$  47.1,  $J$  26.4,  $J$  4.3 (by simulation, Bruker-Topspin),  $\text{CH}_2\text{F}$ ). HRMS (ES): found 126.0714. Calcd. for  $\text{C}_7\text{H}_9\text{NF}$ , 126.0719.

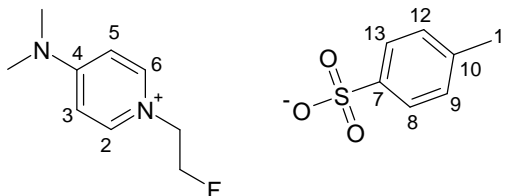
## 4.2.44 1-(2-Fluoroethyl)-4-methoxypyridinium 4-methylbenzenesulfonate 199



4-Methoxypyridine (233 mg, 2.14 mmol) and 2-fluoroethyltosylate (445 mg, 2.0 mmol) were heated to 100 °C for 9 h. The salt was then cooled and to room temperature to give an orange viscous liquid (683 mg).

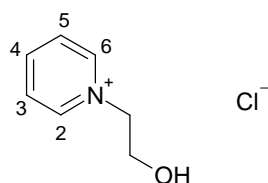
$\delta_{\text{H}}$  (CD<sub>3</sub>OD, 400.13 MHz): 2.36 (3 H, s, TsCH<sub>3</sub>), 4.12 (3 H, s, OCH<sub>3</sub>), 4.74–4.84 (3 H, m, NCH<sub>2</sub>, CH<sub>2</sub>F), 4.90–4.92 (1 H, m, CH<sub>2</sub>F), 7.21–7.25 (2 H, m, H-9, H-12), 7.54–7.57 (2 H, m, H-2, H-6), 7.68–7.71 (2 H, m, H-8, H-13), 8.71–8.74 (2 H, m, H-3, H-5).  $\delta_{\text{C}}$  (CD<sub>3</sub>OD, 100.62 MHz): 21.3 (PhCH<sub>3</sub>), 58.8 (OCH<sub>3</sub>), 60.7 (d, *J* 18.8, NCH<sub>2</sub>), 83.1 (d, *J* 170.7, CH<sub>2</sub>F), 114.7 (C-2 C-6), 126.9 (C-8, C-13), 129.9 (C-9, C-12), 141.7 (C-10), 143.7 (C-7), 147.6 (C-3, C-5), 173.2 (C-4).  $\delta_{\text{F}}$  (D<sub>2</sub>O, 282.28 MHz): -224.4 (tt, *J* 46.7, *J* 27.6, CH<sub>2</sub>F). HRMS (ES): found 156.0822. Calcd. for C<sub>8</sub>H<sub>11</sub>NFO, 156.0825.

**4.2.45 4-(Dimethylamino)-1-(2-fluoroethyl) pyridinium 4-methylbenzenesulfonate 200**



A solution of 4-dimethylaminopyridine (44 mg, 0.36 mmol) and 2-fluoroethyltosylate **206** (76 mg, 0.35 mmol) in MeCN (1 cm<sup>3</sup>) was heated to 90 °C for 16 h. The solvent was then removed under vacuum and the product was recrystallised from EtOH and ether at 4 °C to give a white crystalline solid (90 mg, 76%).

Mp 118–120 °C (ether / ethanol).  $\delta_{\text{H}}$  (D<sub>2</sub>O, 300.06 MHz): 2.37 (3 H, s, PhCH<sub>3</sub>), 3.18 (6 H, s, N(CH<sub>3</sub>)<sub>2</sub>), 4.42 (2 H, dm, *J* 27.8, NCH<sub>2</sub>), 4.79 (2 H, dm, *J* 46.6, CH<sub>2</sub>F), 6.84–6.89 (2 H, m, H-3, H-5), 7.32–7.36 (2 H, m, H-9, H-12), 7.64–7.68 (2 H, m, H-8, H-13), 7.97–8.01 (2 H, m, H-2, H-6).  $\delta_{\text{C}}$  (D<sub>2</sub>O, 75.48 MHz): 20.4 (CH<sub>3</sub>), 39.3 (N(CH<sub>3</sub>)<sub>2</sub>), 57.2 (d, *J* 19.1, NCH<sub>2</sub>), 81.4 (d, *J* 167.6, CH<sub>2</sub>F), 107.5 (C-3, C-5), 125.3 (C-8, C-13), 129.4 (C-9, C-12), 139.3 (C-7), 141.5 (C-2, C-6), 142.5 (C-10), 156.4 (CN(CH<sub>3</sub>)<sub>2</sub>).  $\delta_{\text{F}}$  (D<sub>2</sub>O, 282.28 MHz): -224.5 (dt, *J* 27.4, *J* 46.8, CH<sub>2</sub>F). HRMS (ES): found 169.1135. Calcd. for C<sub>9</sub>H<sub>14</sub>N<sub>2</sub>F, 169.1141. Elemental analysis: found C, 56.2; H, 6.3; N, 7.9. Calc. for C<sub>9</sub>H<sub>14</sub>N<sub>2</sub>F : C<sub>7</sub>H<sub>7</sub>O<sub>3</sub>S: C, 56.5; H, 6.2; N, 8.2%.

**4.2.46 1-(2-Hydroxyethyl)-pyridinium chloride 201**

A solution of 2-chloroethanol (0.95 cm<sup>3</sup>, 14.2 mmol) in pyridine (1.3 cm<sup>3</sup>, 15.9 mmol) was heated to 110 °C for 16 h. The residual pyridine was removed under vacuum, to give a light brown solid. Colourless crystalline needles were obtained after re-crystallisation from EtOH and ether at 4 °C (2.22 g, 98%).

$\delta_{\text{H}}$  (CD<sub>3</sub>OD, 300.06 MHz): 4.02 (2 H, t, *J* 5.1, OCH<sub>2</sub>), 4.76 (2 H, t, *J* 5.1, NCH<sub>2</sub>), 8.10–8.19 (2 H, m, H-3, H-5), 8.61–8.68 (1 H, m, H-4), 8.98–9.0 (2 H, m, H-2, H-6).  $\delta_{\text{C}}$  (CD<sub>3</sub>OD, 75.46 MHz): 61.7 (OCH<sub>2</sub>), 65.1 (NCH<sub>2</sub>), 129.1 (C-3, C-5), 146.4 (C-2, C-6), 147.0 (C-4). HRMS (ES): found 124.0763. Calcd. for C<sub>7</sub>H<sub>10</sub>NO, 124.0762.

**4.2.47**      **1-(2-Chloroethyl)pyridinium chloride 202**<sup>22</sup>  
**and 1,1'-(ethane-1,2-diyl)dipyridinium chloride 210**<sup>23</sup>



A solution of 1,2-dichloroethane (1.0 cm<sup>3</sup>, 12.7 mmol) in pyridine (1.0 cm<sup>3</sup>, 12.6 mmol) were heated to 90 °C for 16 h. Any residual pyridine was removed under vacuum to generate an off white solid. Crystals suitable for X-ray structure analysis were obtained by recrystallisation from EtOH and ether 4 °C. X-ray analysis showed these to be 1,1'-(ethane-1,2-diyl)dipyridinium chloride **210** however. <sup>1</sup>H NMR indicated a ratio of 1-(2-chloroethyl)pyridinium chloride **202** and 1,1'-(ethane-1,2-diyl)dipyridinium chloride **210** at 1:7 was provided from the reaction. The principle product **202** was obtained from the crystallisation residue and after solvent removal under reduced pressure gave **202** as a clear liquid.

**1-(2-chloroethyl)pyridinium chloride 202**

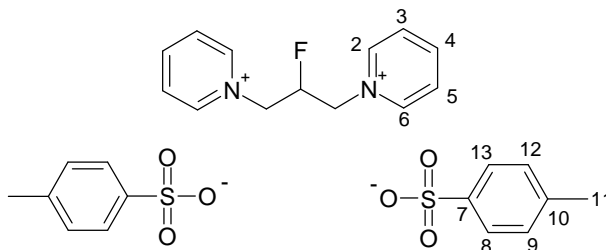
$\delta_{\text{H}}$  (D<sub>2</sub>O, 300.06 MHz): 4.16 (2 H, t, *J* 5.6, CH<sub>2</sub>Cl), 5.00 (2 H, t, *J* 5.6, NCH<sub>2</sub>), 8.10–8.18 (2 H, m, H-3, H-5), 8.60–8.69 (1 H, m, H-4), 8.91–8.96 (2 H, m, H-2, H-6).  $\delta_{\text{C}}$  (D<sub>2</sub>O, 75.46 MHz): 43.3 (CH<sub>2</sub>Cl), 62.7 (NCH<sub>2</sub>), 128.6 (C-3, C-5), 145.2 (C-2, C-6), 146.9 (C-4). HRMS (ES): found 142.0425. Calcd. for C<sub>7</sub>H<sub>9</sub>NCl, 142.0424.

**1,1'-(ethane-1,2-diyl)dipyridinium chloride 210**

Mp >250°C.  $\delta_{\text{H}}$  (D<sub>2</sub>O, 300.06 MHz): 5.34 (4 H, s, CH<sub>2</sub>), 8.10–8.16 (4 H, m, H-3, H-5), 8.64–8.71 (2 H, m, H-4), 8.82–8.86 (4 H, m, H-2, H-6).  $\delta_{\text{C}}$  (D<sub>2</sub>O, 75.46 MHz): 60.5 (CH<sub>2</sub>), 129.5 (C-3, C-5), 145.1 (C-2, C-6), 147.9 (C-4).



**4.2.48 1,1'-(2-Fluoropropane-1,3-diyl)dipyridinium 4-methylbenzenesulfonate**  
**203**



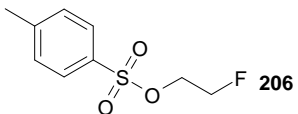
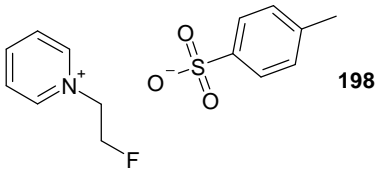
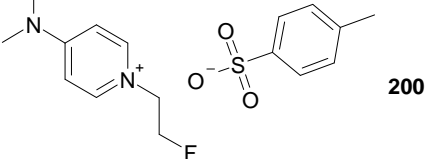
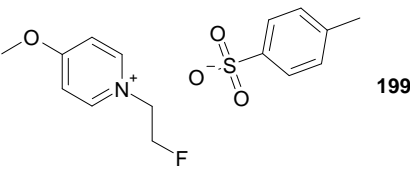
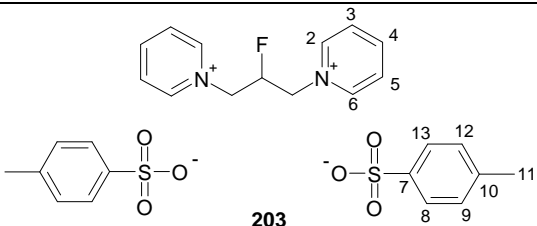
A solution of 2-fluoro-1,3-propanediol, bis-4-(methylbenzenesulfonate) (19 mg, 0.047 mmol) in anhydrous pyridine (386 mg, 4.8 mmol) was heated to 100 °C for 12 h. The reaction was then cooled and the excess pyridine was removed under vacuum to leave a brown semi-solid (25 mg, 95%). After treatment with aqueous HBr and water removal under reduced pressure, followed by freeze drying a crystal suitable for X-ray studies was obtained from ethanol and ether.

$\delta_{\text{H}}$  (CD<sub>3</sub>OD, 400.13 MHz): 2.37 (6 H, s, CH<sub>3</sub>), 5.07–5.17 (2 H, m, CH<sub>2</sub>), 5.37 (2 H, ddd,  $J$  1.8,  $J$  14.4,  $J$  32.4, CH<sub>2</sub>), 5.67 (1 H, dm,  $J$  51.2, CHF), 7.23–7.26 (4 H, m, H-9, H-12), 7.69–7.73 (4 H, m, H-8, H-13), 8.13–8.19 (4 H, m, H-2, H-6), 8.64–8.70 (2 H, m, H-4), 9.08–9.11 (4 H, m, H-3, H-5).  $\delta_{\text{C}}$  (CD<sub>3</sub>OD, 100.62 MHz): 21.3 (CH<sub>3</sub>), 62.3 (d,  $J$  17.8, CH<sub>2</sub>), 92.2 (d,  $J$  182.5, CHF), 126.9 (C-8, C-13), 129.7 (C-2, C-6), 129.9 (C-9, C-12), 141.8 (C-10), 143.5 (C-7), 147.0 (C-3, C-5), 148.1 (C-4).  $\delta_{\text{F}}$  (CD<sub>3</sub>OD, 376.45 MHz): -193.2 (dt,  $J$  48.9,  $J$  33.0,  $J$  16.2, CHF). HRMS (ES): found 389.1335. Calcd. for C<sub>13</sub>H<sub>15</sub>N<sub>2</sub>F · C<sub>7</sub>H<sub>7</sub>O<sub>3</sub>S, 389.1333.

## 4.2.49 An interesting effect with quaternary carbon shifts in the tosylates

 $^{13}\text{C}$  NMR of 206, 198, 199, 200 and 203.

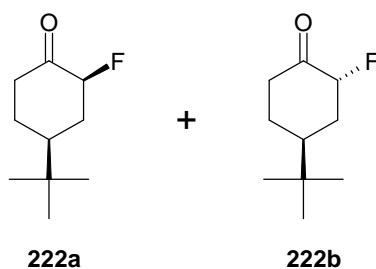
Upon analysis of the  $^{13}\text{C}$  NMR data from compounds containing a tosylate or tosyl ether counter ion, an interesting effect was noted. It appears that the quaternary carbon (SCCH and  $\text{CCH}_3$ ) shift differs between compounds. One may expect the shifts to be similar and given in the same order for similar compounds but this is not the case. **Table 4.1** shows the carbon shifts for the two quaternary carbons in five synthesised molecules. Assignment was provided by use of  $^1\text{H}$ ,  $^{13}\text{C}$  and HMBC NMR analysis.

	S-C (ppm)	CH <sub>3</sub> -C (ppm)
	132.6	145.2
	139.4	142.4
	139.3	142.5
	142.4	140.3
	142.1	140.3

**Table 4.1** Differences in quaternary carbon  $^{13}\text{C}$  NMR shifts.

Perhaps there is a variation in the contact between the <sup>+</sup>ve and <sup>-</sup>ve ions changing the electron withdrawing power and also alter the shielding properties of the tosyl group.

When this occurs it can be said to have a 'contact ion pair'.<sup>24</sup>

4.2.50 2-Fluoro-4-(1,1-dimethylethyl)cyclohexanone **222a** and **222b**<sup>25, 26</sup>**Method 1**

A suspension of Accufluor® 50% on silica (10.2 g, 15.9 mmol) was added to a solution of 4-*tert*-butylcyclohexanone **221** (2.45 g, 15.9 mmol) in acetonitrile (20 cm<sup>3</sup>) at RT. The reaction was then heated to 80 °C and stirred for 1.5 h. The solvent was removed under reduced pressure and crude analysed by <sup>19</sup>F NMR, this showed a 1.7 : 1 ratio of **222a** : **222b** isomers. Separation of the two isomers could be achieved by chromatography over silica gel (hexane : ethyl acetate 10:1) affording yellow solids.

**222a**

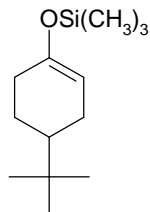
Mp 40–42 °C, (Lit.,<sup>27</sup> 40–42 °C).  $\delta_{\text{H}}$  (CDCl<sub>3</sub>, 300.06 MHz): 0.95 (9 H, s, C(CH<sub>3</sub>)<sub>3</sub>), 1.37–1.55 (1 H, m, C=OCH<sub>2</sub>CH<sub>2</sub>), 1.57–1.71 (2 H, m, CHFCH<sub>2</sub>, CHC(CH<sub>3</sub>)<sub>3</sub>), 2.04–2.14 (1 H, m, C=OCH<sub>2</sub>CH<sub>2</sub>), 2.25–2.38 (1 H, m, C=OCH<sub>2</sub>), 2.47–2.58 (2 H, m, CHFCH<sub>2</sub>, C=OCH<sub>2</sub>), 4.95 (1 H, dm, *J* 48.8, CHF).  $\delta_{\text{C}}$  (CDCl<sub>3</sub>, 75.46 MHz): 27.7 (C(CH<sub>3</sub>)<sub>3</sub>), 27.9 (C=OCH<sub>2</sub>CH<sub>2</sub>), 32.8 (C(CH<sub>3</sub>)<sub>3</sub>), 35.5 (d, *J* 17.3, CHFCH<sub>2</sub>), 39.2 (C=OCH<sub>2</sub>CH<sub>2</sub>), 45.5 (d, *J* 8.4, CHC(CH<sub>3</sub>)<sub>3</sub>), 92.6 (d, *J* 191.8, CHF), 206.2 (C=O).  $\delta_{\text{F}}$  (CDCl<sub>3</sub>, 282.29 MHz): -188.5 (m, CHF). HRMS (ES): found 195.1158. Calcd. for C<sub>10</sub>H<sub>17</sub>OFNa, 195.1161. *m/z* (EI): 172 (16%), 116 (53), 57 [C(CH<sub>3</sub>)<sub>3</sub>]<sup>+</sup> (100), 41 (29).

**222b**

Mp 73–75 °C (from hexane), (Lit.,<sup>27</sup> 75–77 °C).  $\delta_{\text{H}}$  ( $\text{CDCl}_3$ , 400.13 MHz): 0.91 (9 H, s,  $\text{C}(\text{CH}_3)_3$ ), 1.40–1.80 (2 H, m,  $\text{CHFCH}_2$ ,  $\text{C}=\text{OCH}_2\text{CH}_2$ ), 1.88 (1 H, m,  $\text{CHC}(\text{CH}_3)_3$ ), 2.12 (1 H, m,  $\text{C}=\text{OCH}_2\text{CH}_2$ ), 2.33–2.47 (2 H, m,  $\text{CHFCH}_2$ ,  $\text{C}=\text{OCH}_2\text{CH}_2$ ), 2.80 (1 H, m,  $\text{C}=\text{OCH}_2\text{CH}_2$ ), 4.67 (1 H, dm,  $J$  51.0, CHF).  $\delta_{\text{C}}$  ( $\text{CDCl}_3$ , 75.46 MHz): 27.6 ( $\text{C}(\text{CH}_3)_3$ ), 28.1 ( $\text{C}=\text{OCH}_2\text{CH}_2$ ), 32.0 ( $\text{C}(\text{CH}_3)_3$ ), 34.6 (d,  $J$  22.1,  $\text{CHFCH}_2$ ), 37.9 ( $\text{C}=\text{OCH}_2\text{CH}_2$ ), 40.6 ( $\text{CHC}(\text{CH}_3)_3$ ), 92.8 (d,  $J$  177.2, CHF).  $\delta_{\text{F}}$  ( $\text{CDCl}_3$ , 282.29 MHz): -186.0 (m, CHF). m/z (EI): 172 (18%), 116 (50), 57 [ $\text{C}(\text{CH}_3)_3$ ]<sup>+</sup> (100), 41 (28).

## Method 2

Via 4-*tert*-butyl-1-trimethylsilyloxycyclohexene **243** <sup>28</sup>



4-*tert*-Butylcyclohexanone **221** (9.95 g, 64.5 mmol) in DMF (10 cm<sup>3</sup>) was added to a solution of TMSCl (10 cm<sup>3</sup>, 76.7 mmol), Et<sub>3</sub>N (22 cm<sup>3</sup>, 157.8 mmol) in DMF (20 cm<sup>3</sup>) at RT. The reaction was heated at 160 °C for 24 h and was then cooled to RT and hexane was added (50 cm<sup>3</sup>), followed by aqueous NaHCO<sub>3</sub> (50 cm<sup>3</sup>). The phases were separated and each washed with hexane (100cm<sup>3</sup>) and aqueous NaHCO<sub>3</sub> (100 cm<sup>3</sup>). The hexane phases were combined and the solvent was removed under reduced pressure to provide **243** as an orange viscous liquid (14.0 g, 96%).

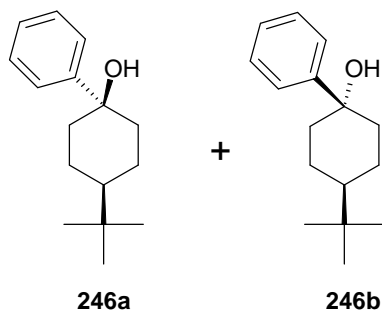
$\delta_{\text{H}}$  (CDCl<sub>3</sub>, 300.13 MHz): 0.17 (9 H, m, Si(CH<sub>3</sub>)<sub>3</sub>), 0.86 (9 H, s, C(CH<sub>3</sub>)<sub>3</sub>), 1.18–1.32 (2 H, m, CH), 1.73–1.86 (2 H, m, CH), 1.94–2.13 (3 H, m, CH), 4.84 (1 H, m, C=CH).  $\delta_{\text{C}}$  (CDCl<sub>3</sub>, 75.48 MHz): 0.5 (Si(CH<sub>3</sub>)<sub>3</sub>), 24.5 (CH<sub>2</sub>), 25.2 (CH<sub>2</sub>), 27.5 (C(CH<sub>3</sub>)<sub>3</sub>), 31.1 (CH<sub>2</sub>), 32.3 (C(CH<sub>3</sub>)<sub>3</sub>), 44.1 (CHC(CH<sub>3</sub>)<sub>3</sub>), 104.2 (C=CH), 150.4 (COSi(CH<sub>3</sub>)<sub>3</sub>).  $m/z$  (EI): 226 (22%), 211 (100), 169 (40), 142 (46), 127 (100), 75 (52), 73 (54), 57 [C(CH<sub>3</sub>)<sub>3</sub>]<sup>+</sup> (100).

Selectfluor® (20.61 g, 58.2 mmol) in DMF (100 cm<sup>3</sup>) was added to a solution of 4-*tert*-butyl-1-trimethylsilyloxycyclohexene **243** (10.49 g, 46.4 mmol) in DMF (100 cm<sup>3</sup>) at 0 °C. The reaction was stirred for 21 h at RT then partitioned between water (100 cm<sup>3</sup>) and ether (200 cm<sup>3</sup>). The ether phase was separated and the water / DMF phase was re-washed with further ether (100 cm<sup>3</sup>). The ether phases were combined and dried with MgSO<sub>4</sub>, this was filtered off and ether removed under reduced pressure. The product was analysed by <sup>19</sup>F NMR and a ratio of equatorial : axial isomers was found to be 1 : 1. This was then purified over silica gel (hexane : ethyl acetate, 10:1) to afford fractions of **222a**, **222b** and a mix of **222a** and **222b** isomers (36%).

**Method 2** appeared to be a more suitable method owing to the even ratio of isomers (**222a** : **222b**, 1:1), thus the axial could be more easily obtained by chromatography and used in subsequent reactions.

NMR and GCMS data matched that as found with **222a** and **222b** from **Method 1**.

**4.2.51 (1S, 4S)-4-Tert-butyl-1-phenylcyclohexanol 246a**  
**and (1R, 4R)-4-tert-butyl-1-phenylcyclohexanol 246b**<sup>29</sup>



A mixture of magnesium filings (453 mg, 18.6 mmol), 2 pellets I<sub>2</sub> and ether (10 cm<sup>3</sup>) was prepared and to this bromobenzene (2.2 cm<sup>3</sup>, 20.9 mmol) was slowly added at 0 °C over 20 minutes. On completion of the addition the reaction was stirred at RT for 30 minutes, after which no magnesium metal was visible.

To a solution of 4-*tert*-butylcyclohexanone **221** (288 mg, 1.85 mmol) in ether (2 cm<sup>3</sup>) at RT was added phenylmagnesium bromide (1 cm<sup>3</sup>, 1.86 mmol). The reaction was stirred for 16 h at RT and then quenched with aqueous ammonium chloride. The product was extracted into ether and the solvent was then removed under reduced pressure. Purification over silica gel (hexane : ethyl acetate, 5:1) afforded both isomers **246a** and **246b** as white solids. **246a** = 138 mg, 32% and **246b** = 179 mg, 42%.

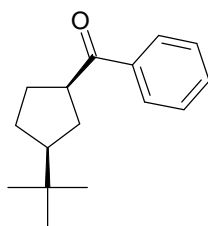
**246a**

Mp 113–114 °C (from pentane), (Lit.,<sup>29</sup> 116–117 °C).  $\delta_{\text{H}}$  (CDCl<sub>3</sub>, 300.13 MHz): 0.84 (9 H, s, C(CH<sub>3</sub>)<sub>3</sub>), 0.96–1.07 (1 H, m, CHC(CH<sub>3</sub>)<sub>3</sub>), 1.38–1.81 (9 H, m, CH<sub>2</sub>, OH), 7.13–7.29 (3 H, m, Ph-H), 7.40–7.45 (2 H, m, Ph-H). *m/z* (EI): 232 (14%), 133 (100), 105 (17), 57 (9).



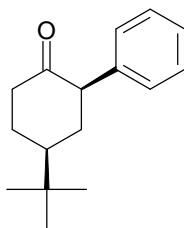
**246b**

Mp 149–151 °C (from hexane), (Lit.,<sup>29</sup> 158–160 °C).  $\delta_{\text{H}}$  (CDCl<sub>3</sub>, 300.13 MHz): 0.77 (9 H, s, C(CH<sub>3</sub>)<sub>3</sub>), 0.93–1.08 (2 H, m, CH<sub>2</sub>), 1.11–1.21 (1 H, m, *CHC*(CH<sub>3</sub>)<sub>3</sub>), 1.52–1.80 (5 H, m, CH<sub>2</sub>, OH), 2.50–2.59 (2 H, m, CH<sub>2</sub>), 7.27–7.41 (3 H, m, Ph-H), 7.53–7.58 (2 H, m, Ph-H). m/z (EI): 232 (9%), 133 (100), 105 (17), 57 (11).

4.2.52 (3-*Tert*-butylcyclopentyl)(phenyl)methanone **249a**

Phenylmagnesium bromide (1 cm<sup>3</sup>, 1.86 mmol), freshly prepared, was added to a solution of equatorial ketone **222a** (247 mg, 1.4 mmol) in ether (5 cm<sup>3</sup>) at -78 °C. The reaction was then stirred for 19 h at RT, after which it was quenched with aqueous ammonium chloride and the crude was extracted into ether. This was dried with MgSO<sub>4</sub> and filtered. The ether was removed under reduced pressure and the crude was purified over silica gel (hexane : ethyl acetate, 5:1). **249a** was obtained as a yellow liquid (162 mg, 49%).

$\delta_{\text{H}}$  (CDCl<sub>3</sub>, 300.06 MHz): 0.88 (9 H, s, C(CH<sub>3</sub>)<sub>3</sub>), 1.37–2.03 (7 H, m, CHC(CH<sub>3</sub>)<sub>3</sub>, CH<sub>2</sub>), 3.65–3.78 (1 H, m, CHC=O), 7.41–7.61 (3 H, m, Ph-H), 7.95–8.0 (2 H, m, Ph-H).  $\delta_{\text{C}}$  (CDCl<sub>3</sub>, 75.46 MHz): 26.8 (C=OCH<sub>2</sub>CH<sub>2</sub>CH), 27.8 (C(CH<sub>3</sub>)<sub>3</sub>), 29.2 (C=OCH<sub>2</sub>CH<sub>2</sub>CH), 31.9 (C=OCH<sub>2</sub>CH), 32.0 (C(CH<sub>3</sub>)<sub>3</sub>), 46.4 (CHC=O), 52.0 (CHC(CH<sub>3</sub>)<sub>3</sub>), 128.5 (Ph-C), 128.6 (Ph-C), 132.8 (Ph-C), 137.0 (CC=O), 202.7 (C=O).  $\nu_{\text{max}}$  /cm<sup>-1</sup> (film): 2953, 2865, 1678, 1595, 1579, 1447, 1362. m/z (EI): 230 (20%), 133 (56), 105 (100), 77 (27). HRMS (ES): found 253.1572. Calcd. for C<sub>16</sub>H<sub>22</sub>ONa, 253.1568.

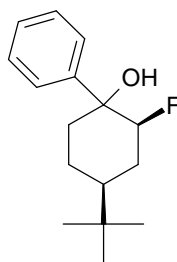
4.2.53 (2S, 4S)-4-*Tert*-butyl-2-phenylcyclohexanone **250a**

The isomer **250a** was obtained as a minor by-product from the reaction of **222a** as described above.

**250a** was obtained as a white solid (22 mg, 7%) and was crystallised from hexane. This was analysed by X-ray diffraction and a crystal structure was obtained. This showed **250a** was the equatorial (*cis*) isomer.

$\delta_{\text{H}}$  ( $\text{CDCl}_3$ , 300.06 MHz): 0.94 (9 H, s,  $\text{C}(\text{CH}_3)_3$ ), 1.58–2.61 (7 H, m,  $\text{CHC}(\text{CH}_3)_3$ ,  $\text{CH}_2$ ), 3.56–3.64 (1 H, m,  $\text{CHPh}$ ), 7.11–7.16 (2 H, m, Ph-H), 7.23–7.38 (3 H, m, Ph-H).  $\delta_{\text{C}}$  ( $\text{CDCl}_3$ , 75.48 MHz): 27.8 ( $\text{C}(\text{CH}_3)_3$ ), 28.7 ( $\text{C}=\text{OCH}_2\text{CH}_2$ ), 37.0 ( $\text{CH}_2\text{CHPh}$ ), 41.9 ( $\text{C}=\text{OCH}_2\text{CH}_2$ ), 47.6 ( $\text{CHC}(\text{CH}_3)_3$ ), 57.1 ( $\text{CHPh}$ ), 127.1 (Ph-C), 128.5 (Ph-C), 128.9 (Ph-C).  $m/z$  (EI): 230 (56%), 173 (83), 155 (62), 130 (100), 117 (28), 104 (30), 91 (75), 57 (75).

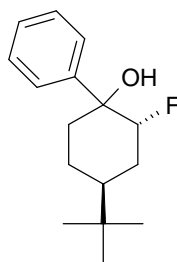
## 4.2.54 (2S, 4S)-4-Tert-butyl-2-fluoro-1-phenylcyclohexanol 238a/c



Equatorial **222a** (159 mg, 0.9 mmol) in THF (2 cm<sup>3</sup>) was added to phenyllithium (0.6 cm<sup>3</sup>, 1.1 mmol) and cerium trichloride (384 mg, 1.6 mmol) in THF (1 cm<sup>3</sup>) at -78 °C. The reaction was stirred for 16 h and then quenched with ammonium chloride. The crude was extracted into ether and dried with MgSO<sub>4</sub>. After filtration and solvent removal under reduced pressure, purification over silica gel (hexane : ethyl acetate, 2 : 1) afforded **238a/c** as partially purified yellow solid (6 mg, 3%).

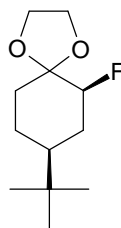
$\delta_{\text{H}}$  (CDCl<sub>3</sub>, 300.06 MHz): 0.83 (9 H, s, C(CH<sub>3</sub>)<sub>3</sub>), 0.84–2.52 (8 H, m, CHC(CH<sub>3</sub>)<sub>3</sub>, CH<sub>2</sub>, OH), 4.78 (1 H, dm, *J* 49.4, CHF), 7.24–7.71 (5 H, m, Ph-H).  $\delta_{\text{C}}$  (CDCl<sub>3</sub>, 100.62 MHz): 24.1 (CH<sub>2</sub>), 27.6 (C(CH<sub>3</sub>)<sub>3</sub>), 29.8 (CH<sub>2</sub>), 37.6 (CH<sub>2</sub>), 47.1 (CHC(CH<sub>3</sub>)<sub>3</sub>), 100.6 (d, *J* 183.5, CHF), 127.9 (Ph-C), 128.2 (Ph-C), 128.9 (Ph-C).  $\delta_{\text{F}}$  (CDCl<sub>3</sub>, 282.29 MHz): -185.4 (m, CHF). *m/z* (EI): 250 (12%), 133 (100), 105 (16). HRMS (ES): found 273.1639. Calcd. for C<sub>16</sub>H<sub>23</sub>OFNa, 273.1631.

## 4.2.55 (2R, 4S)-4-Tert-butyl-2-fluoro-1-phenylcyclohexanol 238b/d



Axial **222b** (157 mg, 0.9 mmol) in THF (2 cm<sup>3</sup>) was added to phenyllithium (0.6 cm<sup>3</sup>, 1.1 mmol) and cerium trichloride (388 mg, 1.6 mmol) in THF (1 cm<sup>3</sup>) at -78 °C. The reaction was stirred for 16 h and then quenched with ammonium chloride. The crude was extracted into ether and dried with MgSO<sub>4</sub>. After filtration and solvent removal under reduced pressure, the product was purified over silica gel (hexane : ethyl acetate, 2 : 1) affording **238b/d** as a white solid (78 mg, 9%).

$\delta_{\text{H}}$  (CDCl<sub>3</sub>, 300.06 MHz): 0.73 (9 H, s, C(CH<sub>3</sub>)<sub>3</sub>), 0.98–2.07 (6 H, m, CHC(CH<sub>3</sub>)<sub>3</sub>, CH<sub>2</sub>, OH), 2.36–2.44 (2 H, m, CH<sub>2</sub>), 5.10 (1 H, dm, *J* 49.8, CHF), 7.18–7.47 (5 H, m, Ph-H).  $\delta_{\text{C}}$  (CDCl<sub>3</sub>, 100.62 MHz): 24.6 (CH<sub>2</sub>), 27.5 (C(CH<sub>3</sub>)<sub>3</sub>), 29.5 (d, *J* 21.1, CHFCH<sub>2</sub>), 33.6 (CH<sub>2</sub>), 40.2 (CHC(CH<sub>3</sub>)<sub>3</sub>), 95.5 (d, *J* 172.1, CHF), 127.0 (Ph-C), 128.2 (Ph-C), 128.8 (Ph-C).  $\delta_{\text{F}}$  (CDCl<sub>3</sub>, 282.29 MHz): -191.8 (m, CHF). *m/z* (EI): 250 (11%), 133 (100), 105 (14). HRMS (ES): found 273.1635. Calcd. for C<sub>16</sub>H<sub>23</sub>OFNa, 273.1631.

4.2.56 (6S, 8S)-8-*Tert*-butyl-6-fluoro-1,4-dioxaspiro[4.5]decane **237a****Method 1**

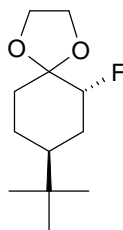
To a solution of equatorial **222a** (171 mg, 0.99 mmol) in toluene (10 cm<sup>3</sup>) was added ethylene glycol (73 mg, 1.18 mmol) and *p*-TsOH (4.5 mg, 0.02 mmol). The mixture was heated to 110 °C for 24 h then the solvent was removed under reduced pressure. Column chromatography (hexane : ethyl acetate, 5 :1) afforded **237a** as a yellow liquid (200 mg, 93%).

$\delta_{\text{H}}$  (CDCl<sub>3</sub>, 300.13 MHz): 0.88 (9 H, s, C(CH<sub>3</sub>)<sub>3</sub>), 1.09–1.83 (6 H, m, CHC(CH<sub>3</sub>)<sub>3</sub>, CH<sub>2</sub>), 2.0–2.10 (1 H, m, CHFCH<sub>2</sub>), 3.93–4.13 (4 H, m, CH<sub>2</sub>O), 4.43 (1 H, dm, *J* 48.8, CHF).  $\delta_{\text{C}}$  (CDCl<sub>3</sub>, 75.48 MHz): 24.1 (CH<sub>2</sub>), 27.7 (C(CH<sub>3</sub>)<sub>3</sub>), 31.2 (d, *J* 17.5, CHFCH<sub>2</sub>), 32.4 (C(CH<sub>3</sub>)<sub>3</sub>), 34.2 (CH<sub>2</sub>), 45.7 (d, *J* 9.7, CHC(CH<sub>3</sub>)<sub>3</sub>), 65.9 (CH<sub>2</sub>O), 66.2 (CH<sub>2</sub>O), 95.1 (d, *J* 185.7, CHF), 107.9 (d, *J* 15.4, COCH<sub>2</sub>).  $\delta_{\text{F}}$  (CDCl<sub>3</sub>, 282.29 MHz): -191.3 (m, CHF). *m/z* (EI): 216 (4%), 181 (17), 159 (13), 127 (27), 99 (100), 86 (77), 55 (28), 41 (25). HRMS (ES): found 239.1432. Calcd. for C<sub>12</sub>H<sub>21</sub>O<sub>2</sub>FNa, 239.1423.

**Method 2**

Ethylene glycol (41 mg, 0.7 mmol) in THF (2 cm<sup>3</sup>) was added to a solution of equatorial **222a** (92 mg, 0.5 mmol) in THF (5 cm<sup>3</sup>) followed by a pellet of I<sub>2</sub> at RT. The mixture was stirred for 23 h and then the solvent was removed under reduced pressure. Chromatography over silica gel (hexane : ethyl acetate, 5 :1) afforded **237a** as a yellow liquid (67 mg, 58%).

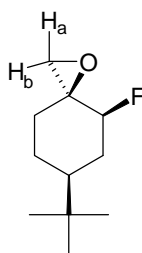
The NMR and GCMS analysis were found to be identical to that from **Method 1**.

4.2.57 (6R, 8S)-8-*Tert*-butyl-6-fluoro-1,4-dioxaspiro[4.5]decane **237b**

Iodine pellets (~ 40 mg) were added to a solution of ethylene glycol (39 mg, 0.6 mmol) and axial **222b** (99 mg, 0.6 mmol) in THF (10 cm<sup>3</sup>) at RT. The mixture was stirred at RT for 20 h then the solvent was removed under reduced pressure. Purification over silica gel (hexane : ethyl acetate, 5 :1) afforded **237b** as a yellow liquid (56 mg, 46%).

$\delta_{\text{H}}$  (CDCl<sub>3</sub>, 300.06 MHz): 0.87 (9 H, s, C(CH<sub>3</sub>)<sub>3</sub>), 1.21–2.15 (7 H, m, CHC(CH<sub>3</sub>)<sub>3</sub>, CH<sub>2</sub>), 3.88–4.09 (4 H, m, CH<sub>2</sub>O), 4.41 (1 H, dm, *J* 49.9, CHF).  $\delta_{\text{F}}$  (CDCl<sub>3</sub>, 282.29 MHz): -189.7 (m, CHF). HRMS (ES): found 239.1418. Calcd. for C<sub>12</sub>H<sub>21</sub>O<sub>2</sub>FNa, 239.1423.



4.2.58 (3S, 4S, 6S)-6-*Tert*-butyl-4-fluoro-1-oxaspiro[2.5]octane **239a****Method 1**

Firstly diazomethane was synthesised according to the method described in Vogel's Textbook of Practical Organic Chemistry.<sup>30</sup>

A mixture of KOH (6.07 g, 108.4 mmol) in water (10 cm<sup>3</sup>) and 2-(2-ethoxyethoxy)ethanol (35.03 g, 261.1 mmol) in water (10 cm<sup>3</sup>) was prepared with ether (35 cm<sup>3</sup>). This was heated to 75 °C and the diazomethane receiver was cooled to -78 °C. Upon distillation of ether, diazald (21.32 g, 99.5 mmol) in ether (125 cm<sup>3</sup>) was added over 30 minutes followed by ether (40 cm<sup>3</sup>). The diazomethane was distilled over with ether and the distillation was stopped when the ether became colourless. 140 cm<sup>3</sup> diazomethane solution was obtained which according to the textbook would contain ~ 3.4 g diazomethane.

Equatorial ketone **222a** (113 mg, 0.7 mmol) was added to diazomethane in ether (70 cm<sup>3</sup>) at RT and stirred for 17 h. A further portion of diazomethane in ether (40 cm<sup>3</sup>) was added as the <sup>1</sup>H NMR showed unreacted starting material. The reaction was then stirred for 16 h and the remaining diazomethane in ether (30 cm<sup>3</sup>) was added owing to starting material still being present. After a further 3 h the ether was removed under reduced pressure and the product was purified over silica gel (hexane : ethyl acetate, 10 : 1). **239a** was provided as a yellow oil (31 mg, 26%).

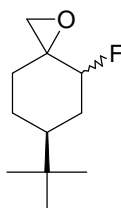
$\delta_{\text{H}}$  ( $\text{CDCl}_3$ , 300.06 MHz): 0.91 (9 H, s,  $\text{C}(\text{CH}_3)_3$ ), 1.17–1.89 (6 H, m,  $\text{CHC}(\text{CH}_3)_3$ ,  $\text{CH}_2$ ), 2.12–2.22 (1 H, m,  $\text{CHFCH}_2$ ), 2.63–2.67 (1 H, m,  $\text{CH}_b\text{O}$ ), 3.09–3.12 (1 H, m,  $\text{CH}_a\text{O}$ ), 4.67 (1 H, dm,  $J$  47.9, CHF).  $\delta_{\text{C}}$  ( $\text{CDCl}_3$ , 75.46 MHz): 24.0 ( $\text{CH}_2\text{CH}_2\text{CO}$ ), 27.7 ( $\text{C}(\text{CH}_3)_3$ ), 31.4 ( $\text{CH}_2\text{CH}_2\text{CO}$ ), 31.7 (d,  $J$  15.4,  $\text{CHFCH}_2$ ), 32.6 ( $\text{C}(\text{CH}_3)_3$ ), 46.2 (d,  $J$  9.1,  $\text{CHC}(\text{CH}_3)_3$ ), 50.0 (d,  $J$  6.3,  $\text{CH}_2\text{O}$ ), 59.2 (d,  $J$  15.6,  $\text{CCH}_2\text{O}$ ), 88.6 (d,  $J$  185.5, CHF).  $\delta_{\text{F}}$  ( $\text{CDCl}_3$ , 282.29 MHz): -193.4 (m, CHF).  $m/z$  (EI): 171 (25%), 129 (9), 97 (24), 81 (25), 57 [ $\text{C}(\text{CH}_3)_3$ ]<sup>+</sup> (100), 41 (25). HRMS (ES): found 209.1320. Calcd. for  $\text{C}_{11}\text{H}_{19}\text{OFNa}$ , 209.1318.

## Method 2

A mixture of equatorial **222a** (1.58 g, 9.2 mmol), trimethyloxosulfonium iodide (3.42 g, 15.5 mmol) and ground KOH (1.20 g, 21.5 mmol) was prepared and rotated together for 24 h at RT. The solid was then taken up into water and ether and the ether phase was separated off and dried with  $\text{MgSO}_4$ . The ether phase was filtered and solvent removed under reduced pressure. Chromatography over silica gel (hexane : ethyl acetate, 10 : 1) was carried out and this afforded **239a** as a yellow oil (275 mg, 16%).

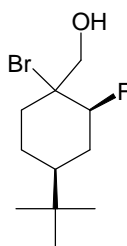
The NMR and GCMS analysis were found to be identical to that of the **239a** isomer obtained from **Method 1**.

## 4.2.59 (4R, 6S)-6-Tert-butyl-4-fluoro-1-oxaspiro[2.5]octane 239b/d



A mixture of axial **222b** (1.45 g, 8.4 mmol), trimethylsulfonium iodide (2.82 g, 13.8 mmol), ground KOH (1.52 g, 27.1 mmol) and water (1 cm<sup>3</sup>) in acetonitrile (20 cm<sup>3</sup>) was stirred at 60 °C for 3 hours. The acetonitrile and water was then removed under reduced pressure and the crude was purified over silica gel (hexane : ethyl acetate, 10 : 1) followed by further purification (hexane : ethyl acetate, 20 : 1). <sup>1</sup>H NMR analysis showed that 4-*t*-butylcyclohexanone was present, contaminated the epoxide product, purification using preparative plate chromatography was successful however in obtaining a clean sample (<10% yield).

$\delta_{\text{H}}$  (CDCl<sub>3</sub>, 300.06 MHz): 0.89 (9 H, s, C(CH<sub>3</sub>)<sub>3</sub>), 1.01–1.12 (1 H, m, CHC(CH<sub>3</sub>)<sub>3</sub>), 1.24–2.44 (6 H, m, CH), 3.32–3.45 (2 H, m, CH<sub>2</sub>O), 4.66 (1 H, dm, *J* 47.9, CHF).  $\delta_{\text{C}}$  (CDCl<sub>3</sub>, 100.62 MHz): 15.7 (CH<sub>2</sub>O), 21.6 (COCH<sub>2</sub>CH<sub>2</sub>), 27.7 (C(CH<sub>3</sub>)<sub>3</sub>), 29.1 (d, *J* 17.7, CH<sub>2</sub>CHF), 34.9 (COCH<sub>2</sub>CH<sub>2</sub>), 46.2 (d, *J* 9.5, CHC(CH<sub>3</sub>)<sub>3</sub>), 93.8 (d, *J* 178.5, CHF).  $\delta_{\text{F}}$  (CDCl<sub>3</sub>, 282.29 MHz): -188.8 (m, CHF). HRMS (ES): found 209.1321. Calcd. for C<sub>11</sub>H<sub>19</sub>OFNa, 209.1318.

**4.2.60 (2S,4S)-1-Bromo-4-tert-butyl-2-fluorocyclohexylmethanol 241a**

HBr (30%) in acetic acid (2 cm<sup>3</sup>) was added to the equatorial epoxide **239a** (40.8 mg, 0.2 mmol) at RT. The solution was stirred for 30 minutes and then excess HBr and acetic acid was removed under reduced pressure. The residual material was purified over silica gel (hexane : ethyl acetate, 20 : 1) to yield **241a** as a yellow oil (9 mg, 15%).

$\delta_{\text{H}}$  (CDCl<sub>3</sub>, 400.13 MHz): 0.89 (9 H, s, C(CH<sub>3</sub>)<sub>3</sub>), 1.05–1.13 (1 H, m, CHC(CH<sub>3</sub>)<sub>3</sub>), 1.21–1.66 (4 H, m, CH<sub>2</sub>CBr, CH<sub>2</sub>CH<sub>2</sub>CH, CH<sub>2</sub>CHF), 1.84–1.92 (1 H, m, CH<sub>2</sub>CBr), 1.94–2.02 (1 H, m, CH<sub>2</sub>CHF), 3.45–3.52 (2 H, m, CH<sub>2</sub>OH), 4.67 (1 H, dm, *J* 47.9, CHF).  $\delta_{\text{C}}$  (CDCl<sub>3</sub>, 100.62 MHz): 21.3 (CH<sub>2</sub>CH<sub>2</sub>CH), 27.6 (C(CH<sub>3</sub>)<sub>3</sub>), 28.7 (d, *J* 17.3, CH<sub>2</sub>CHF), 33.0 (CH<sub>2</sub>CBr), 39.0 (CH<sub>2</sub>OH), 46.0 (d, *J* 9.5, CHC(CH<sub>3</sub>)<sub>3</sub>), 93.4 (d, *J* 178.2, CHF).  $\delta_{\text{F}}$  (CDCl<sub>3</sub>, 282.29 MHz): -189.4 (m, CHF). HRMS (Cl<sup>+</sup>): found 247.0697. Calcd. for C<sub>11</sub>H<sub>20</sub>O<sub>79</sub>Br, 247.0698. HRMS (Cl<sup>+</sup>): found 249.0683. Calcd. for C<sub>11</sub>H<sub>20</sub>O<sub>81</sub>Br, 249.0677.

### 4.3 References for chapter four

1. H. E. Gottlieb, V. Kotlyar and A. Nudelman, *J. Org. Chem.*, 1997, **62**, 7512-7515.
2. H. J. Veith, A. Guggisberg and M. Hesse, *Helv. Chim. Acta*, 1971, **54**, 653-680.
3. J. Nosek, *Chem. Listy*, 1953, **47**, 1236-1238.
4. G. Cirrincione, W. Hinz and R. A. Jones, *J. Chem. Soc., Perkin Trans. 2*, 1984, 1089-1091.
5. M. A. Korshunov, F. N. Bodnaryuk and V. S. Mikhlin, *Zh. Org. Khim.*, 1969, **5**, 1947-1952.
6. D. F. Harvey and D. M. Sigano, *J. Org. Chem.*, 1996, **61**, 2268-2272.
7. G. I. Ostroumova, *Plast. Massy*, 1968, 59.
8. J. R. Piper, L. M. Rose, T. P. Johnston and M. M. Grenan, *J. Med. Chem.*, 1975, **18**, 803-812.
9. M. Wu, G. Cheng, Y. He and C. Wu, *Synth. Commun.*, 1995, **25**, 1427-1431.
10. J. Huskens and M. T. Reetz, *Eur. J. Org. Chem.*, 1999, 1775-1786.
11. G. H. Searle and R. J. Geue, *Aust. J. Chem.*, 1984, **37**, 959-970.
12. J. Dale and T. Sigvartsen, *Acta Chem. Scand.*, 1991, **45**, 1064-1070.
13. W. Saari, A. W. Raab and S. W. King, *J. Org. Chem.*, 1971, **36**, 1711-1714.
14. N. N. Chuvatkin, I. Y. Panteleeva and L. S. Boguslavskaya, *Zh. Org. Khim.*, 1982, **18**, 946-953.
15. W. J. Lloyd and R. Harrison, *Carbohydr. Res.*, 1971, **20**, 133-139.
16. M. Benbouzid, A. Bhati and R. J. Hamilton, *Fett Wiss. Technol.*, 1988, **90**, 292-295.
17. G. J. F. Chittenden, *Carbohydr. Res.*, 1981, **91**, 85-88.
18. P. Najappan, N. Raju, K. Ramalingam and D. P. Nowotnik, *Tetrahedron*, 1994, **50**, 8617-8632.

19. W. W. Paudler, G. R. Gapski and J. M. Barton, *J. Org. Chem.*, 1966, **31**, 277-280.
20. K. J. Wildonger and R. W. Ratcliffe, *J. Antibiot.*, 1993, **46**, 1866-1882.
21. A. D. C. Parenty, L. V. Smith and L. Cronin, *Tetrahedron*, 2005, **61**, 8410-8418.
22. A. Nudelman and R. J. McCaully, *J. Org. Chem.*, 1977, **42**, 2887-2890.
23. S. J. Loeb, J. Tiburcio, S. J. Vella and J. A. Wisner, *Org. Biomol. Chem.*, 2006, **4**, 667-680.
24. H. Mayr, A. R. Ofial, E.-U. Wurthwein and N. C. Aust, *J. Am. Chem. Soc.*, 1997, **119**, 12727-12733.
25. S. Stavber and M. Zupan, *Tetrahedron Lett.*, 1996, **37**, 3591-3594.
26. S. E. Denmark, Z. Wu, C. M. Crudden and H. Matsuhashi, *J. Org. Chem.*, 1997, **62**, 8288-8289.
27. N. L. Allinger and H. M. Blatter, *J. Org. Chem.*, 1962, **27**, 1523-1526.
28. H. O. House, L. J. Czuba, M. Gall and H. D. Olmstead, *J. Org. Chem.*, 1969, **34**, 2324-2336.
29. G. Berti, B. Macchia and F. Macchia, *Tetrahedron*, 1968, **24**, 1755-1764.
30. A. I. Vogel, *Vogels Textbook of Practical Organic Chemistry*, 1989, 430-433.

## Appendix 1

### X-ray crystallographic data

#### General experimental

X-ray diffraction studies were conducted by Professor Alexandra M Z Slawin at the University of St Andrews. The X-ray data was collected at 93K from a Rigaku MM007 / Saturn 70 / Mercury diffractometer (confocal optics Mo-K $\alpha$  radiation) or at 173K from a Rigaku MM007 / Saturn 92 diffractometer (confocal optics Cu-K $\alpha$  radiation). The intensity data was gathered using narrow frames accumulating area detector frames spanning at least a hemisphere of reciprocal space for all structures. The data was corrected for Lorentz, polarisation and long-term intensity fluctuations. Absorption effects were also adjusted on the basis of multiple equivalent reflections or by semi-empirical methods. Crystal structures were solved using direct methods and were refined by full-matrix least-squares against  $F^2$  (SHELXTL). O-H and N-H hydrogen atoms were isotropically refined subject to a distance constraint (E-H = 0.98Å). The remaining hydrogen atoms were assigned riding isotropic displacement parameters and constrained to idealised geometries.

#### Interpretation of data

X-ray crystal structures were obtained from Professor Alexandra M Z Slawin as a CIF or MRY file which were viewed on 'Mercury 1.4.2' - a crystal structure visualisation program. From there torsion angles, bond angles and distances were measured and structures evaluated.

### 3-Hydroxy-1,5-diazocane-1,5-dium bromide 127

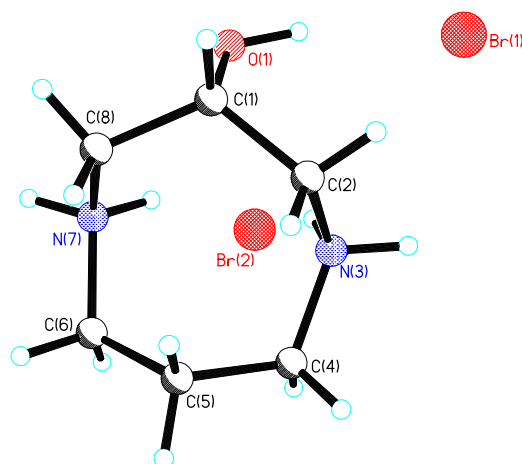


Table 1. Crystal data and structure refinement for ngdh13.

Identification code	ngdh13	
Empirical formula	C <sub>6</sub> H <sub>16</sub> Br <sub>2</sub> N <sub>2</sub> O	
Formula weight	292.03	
Temperature	93(2) K	
Wavelength	0.71073 Å	
Crystal system	Monoclinic	
Space group	Cc	
Unit cell dimensions	a = 9.775(3) Å	α = 90°.
	b = 10.556(3) Å	β = 104.422(9)°.
	c = 10.007(3) Å	γ = 90°.
Volume	1000.0(5) Å <sup>3</sup>	
Z	4	
Density (calculated)	1.940 Mg/m <sup>3</sup>	
Absorption coefficient	8.061 mm <sup>-1</sup>	
F(000)	576	
Crystal size	0.060 x 0.060 x 0.060 mm <sup>3</sup>	
Theta range for data collection	2.89 to 25.34°.	
Index ranges	-10 ≤ h ≤ 11, -12 ≤ k ≤ 11, -9 ≤ l ≤ 12	
Reflections collected	2668	
Independent reflections	1364 [R(int) = 0.0217]	
Completeness to theta = 25.00°	96.6 %	
Absorption correction	Multiscan	
Max. and min. transmission	1.0000 and 0.7069	



Refinement method	Full-matrix least-squares on F <sup>2</sup>
Data / restraints / parameters	1364 / 7 / 121
Goodness-of-fit on F <sup>2</sup>	1.054
Final R indices [I>2sigma(I)]	R1 = 0.0232, wR2 = 0.0552
R indices (all data)	R1 = 0.0237, wR2 = 0.0555
Absolute structure parameter	0.086(15)
Largest diff. peak and hole	0.504 and -1.205 e.Å <sup>-3</sup>

Table 2. Torsion angles [°] for ngdh13.

---

O(1)-C(1)-C(2)-N(3)	-53.9(5)
C(8)-C(1)-C(2)-N(3)	68.6(5)
C(1)-C(2)-N(3)-C(4)	-100.7(4)
C(2)-N(3)-C(4)-C(5)	41.8(5)
N(3)-C(4)-C(5)-C(6)	68.7(5)
C(4)-C(5)-C(6)-N(7)	-65.1(5)
C(5)-C(6)-N(7)-C(8)	-48.2(5)
C(6)-N(7)-C(8)-C(1)	104.1(4)
O(1)-C(1)-C(8)-N(7)	57.6(4)
C(2)-C(1)-C(8)-N(7)	-68.1(5)

---

## 2-(Fluoromethyl)-1,4-ditosyl-1,4-diazepane 128

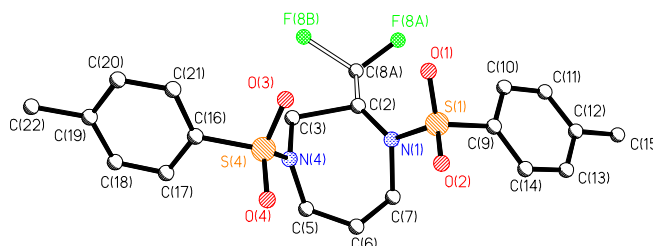


Table 1. Crystal data and structure refinement for ngdh1.

Identification code	ngdh1	
Empirical formula	C <sub>20</sub> H <sub>25</sub> F N <sub>2</sub> O <sub>4</sub> S <sub>2</sub>	
Formula weight	440.54	
Temperature	93(2) K	
Wavelength	0.71073 Å	
Crystal system	Monoclinic	
Space group	C2/c	
Unit cell dimensions	a = 23.528(2) Å	α = 90°.
	b = 11.7875(9) Å	β = 92.578(4)°.
	c = 14.9958(12) Å	γ = 90°.
Volume	4154.7(6) Å <sup>3</sup>	
Z	8	
Density (calculated)	1.409 Mg/m <sup>3</sup>	
Absorption coefficient	0.295 mm <sup>-1</sup>	
F(000)	1856	
Crystal size	0.05 x 0.1 x 0.1 mm <sup>3</sup>	
Theta range for data collection	2.34 to 25.39°.	
Index ranges	-27 ≤ h ≤ 19, -13 ≤ k ≤ 13, -12 ≤ l ≤ 17	
Reflections collected	14163	
Independent reflections	3396 [R(int) = 0.0793]	
Completeness to theta = 25.00°	90.2 %	
Absorption correction	Multiscan	
Max. and min. transmission	1.0000 and 0.9706	
Refinement method	Full-matrix least-squares on F <sup>2</sup>	
Data / restraints / parameters	3396 / 0 / 274	
Goodness-of-fit on F <sup>2</sup>	2.309	
Final R indices [I > 2σ(I)]	R1 = 0.1495, wR2 = 0.4636	
R indices (all data)	R1 = 0.1524, wR2 = 0.4705	
Extinction coefficient	0.13(3)	
Largest diff. peak and hole	1.454 and -0.869 e.Å <sup>-3</sup>	

### 3-Fluoro-1,5-ditosyl-1,5-diazocane 124

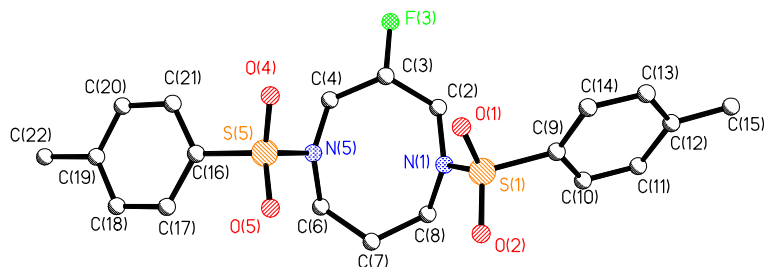


Table 1. Crystal data and structure refinement for ngdh2.

Identification code	ngdh2	
Empirical formula	C <sub>20</sub> H <sub>25</sub> F N <sub>2</sub> O <sub>4</sub> S <sub>2</sub>	
Formula weight	440.54	
Temperature	93(2) K	
Wavelength	0.71073 Å	
Crystal system	Triclinic	
Space group	P-1	
Unit cell dimensions	a = 11.5794(19) Å	α = 91.637(13)°.
	b = 13.104(2) Å	β = 91.215(11)°.
	c = 14.953(2) Å	γ = 112.825(9)°.
Volume	2089.1(6) Å <sup>3</sup>	
Z	4	
Density (calculated)	1.401 Mg/m <sup>3</sup>	
Absorption coefficient	0.293 mm <sup>-1</sup>	
F(000)	928	
Crystal size	0.300 x 0.200 x 0.010 mm <sup>3</sup>	
Theta range for data collection	3.17 to 25.34°.	
Index ranges	-13 ≤ h ≤ 13, -15 ≤ k ≤ 15, -18 ≤ l ≤ 9	
Reflections collected	11991	
Independent reflections	6294 [R(int) = 0.0657]	
Completeness to theta = 25.00°	83.8 %	
Absorption correction	Multiscan	
Max. and min. transmission	1.0000 and 0.9144	
Refinement method	Full-matrix least-squares on F <sup>2</sup>	
Data / restraints / parameters	6294 / 0 / 528	
Goodness-of-fit on F <sup>2</sup>	1.164	
Final R indices [I > 2σ(I)]	R1 = 0.1093, wR2 = 0.2644	
R indices (all data)	R1 = 0.1289, wR2 = 0.2794	
Largest diff. peak and hole	0.670 and -0.397 e.Å <sup>-3</sup>	

Table 2. Selected torsion angles [°] for ngdh2.

---

N(1)-C(2)-C(3)-F(3)	171.5(6)
F(3)-C(3)-C(4)-N(5)	-167.9(6)

---

## Methanesulfonic acid 1,5-bis(toluene-4-sulfonyl)-[1,5]diazocan-3-yl ester 133

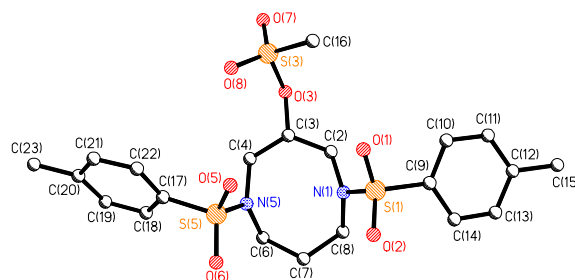


Table 1. Crystal data and structure refinement for ngdh4.

Identification code	ngdh4	
Empirical formula	C <sub>21</sub> H <sub>28</sub> N <sub>2</sub> O <sub>7</sub> S <sub>3</sub>	
Formula weight	516.63	
Temperature	173(2) K	
Wavelength	1.54178 Å	
Crystal system	Monoclinic	
Space group	C2/c	
Unit cell dimensions	a = 25.5174(12) Å	α = 90°.
	b = 18.5467(9) Å	β = 100.351(2)°.
	c = 11.7629(6) Å	γ = 90°.
Volume	5476.4(5) Å <sup>3</sup>	
Z	8	
Density (calculated)	1.253 Mg/m <sup>3</sup>	
Absorption coefficient	2.818 mm <sup>-1</sup>	
F(000)	2176	
Crystal size	0.300 x 0.020 x 0.010 mm <sup>3</sup>	
Theta range for data collection	4.58 to 67.86°.	
Index ranges	-29 ≤ h ≤ 30, -21 ≤ k ≤ 22, -12 ≤ l ≤ 12	
Reflections collected	35271	
Independent reflections	4645 [R(int) = 0.0515]	
Completeness to theta = 25.00°	95.2 %	
Absorption correction	Multiscan	
Max. and min. transmission	1.0000 and 0.4257	
Refinement method	Full-matrix least-squares on F <sup>2</sup>	
Data / restraints / parameters	4645 / 0 / 302	
Goodness-of-fit on F <sup>2</sup>	1.101	
Final R indices [I > 2σ(I)]	R1 = 0.0440, wR2 = 0.1150	
R indices (all data)	R1 = 0.0496, wR2 = 0.1190	
Largest diff. peak and hole	0.555 and -0.310 e.Å <sup>-3</sup>	

## 2-Fluoro-1,3-bis-(toluene-4-sulfonyloxy)-propane 142

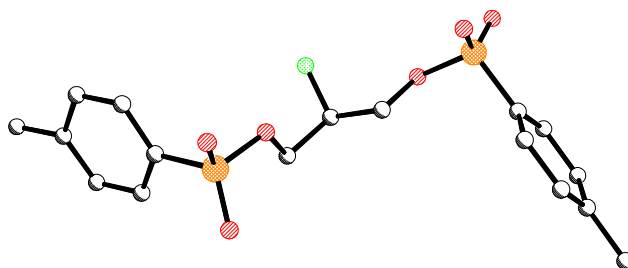


Table 1. Crystal data and structure refinement for ngdh7.

Identification code	ngdh7	
Empirical formula	C <sub>17</sub> H <sub>19</sub> F O <sub>6</sub> S <sub>2</sub>	
Formula weight	402.44	
Temperature	93(2) K	
Wavelength	0.71073 Å	
Crystal system	Triclinic	
Space group	P-1	
Unit cell dimensions	a = 7.7837(18) Å	$\alpha = 68.202(19)^\circ$ .
	b = 10.2663(17) Å	$\beta = 75.30(3)^\circ$ .
	c = 12.684(19) Å	$\gamma = 82.15(3)^\circ$ .
Volume	909.3(14) Å <sup>3</sup>	
Z	2	
Density (calculated)	1.470 Mg/m <sup>3</sup>	
Absorption coefficient	0.334 mm <sup>-1</sup>	
F(000)	420	
Crystal size	0.1500 x 0.0300 x 0.0300 mm <sup>3</sup>	
Theta range for data collection	2.14 to 25.34°.	
Index ranges	-9 ≤ h ≤ 7, -12 ≤ k ≤ 10, -15 ≤ l ≤ 15	
Reflections collected	5907	
Independent reflections	3180 [R(int) = 0.0558]	
Completeness to theta = 25.34°	95.6 %	
Absorption correction	Multiscan	
Max. and min. transmission	1.0000 and 0.3966	
Refinement method	Full-matrix least-squares on F <sup>2</sup>	
Data / restraints / parameters	3180 / 0 / 239	
Goodness-of-fit on F <sup>2</sup>	0.993	
Final R indices [I > 2σ(I)]	R <sub>1</sub> = 0.0682, wR <sub>2</sub> = 0.1496	
R indices (all data)	R <sub>1</sub> = 0.0956, wR <sub>2</sub> = 0.1704	
Extinction coefficient	0.0010(19)	
Largest diff. peak and hole	0.644 and -0.582 e.Å <sup>-3</sup>	

Table 2. Selected torsion angles [°] for ngdh7.

---

O(1)-C(1)-C(2)-F(2)	-58.4(5)
F(2)-C(2)-C(3)-O(2)	-66.0(4)

---

### 3-Fluoro-1,5-diazocane-1,5-dium bromide 149

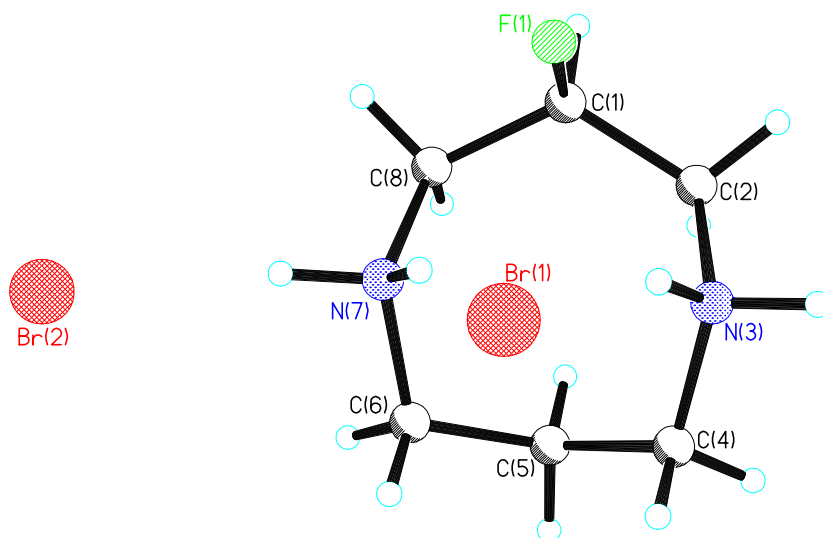


Table 1. Crystal data and structure refinement for NGDH8.

Identification code	ngdh8	
Empirical formula	C <sub>6</sub> H <sub>15</sub> Br <sub>2</sub> F N <sub>2</sub>	
Formula weight	294.02	
Temperature	93(2) K	
Wavelength	0.71073 Å	
Crystal system	Monoclinic	
Space group	P2(1)/c	
Unit cell dimensions	a = 7.0901(16) Å	α = 90°.
	b = 12.250(3) Å	β = 106.266(6)°.
	c = 12.581(3) Å	γ = 90°.
Volume	1049.0(4) Å <sup>3</sup>	
Z	4	
Density (calculated)	1.862 Mg/m <sup>3</sup>	
Absorption coefficient	7.691 mm <sup>-1</sup>	
F(000)	576	
Crystal size	0.1000 x 0.0300 x 0.0300 mm <sup>3</sup>	
Theta range for data collection	2.37 to 25.37°.	
Index ranges	-8 ≤ h ≤ 8, -14 ≤ k ≤ 10, -15 ≤ l ≤ 14	
Reflections collected	6572	
Independent reflections	1887 [R(int) = 0.0333]	
Completeness to theta = 25.37°	97.6 %	
Absorption correction	Multiscan	



Max. and min. transmission	1.0000 and 0.4862
Refinement method	Full-matrix least-squares on F <sup>2</sup>
Data / restraints / parameters	1887 / 4 / 117
Goodness-of-fit on F <sup>2</sup>	1.026
Final R indices [I>2sigma(I)]	R1 = 0.0248, wR2 = 0.0568
R indices (all data)	R1 = 0.0293, wR2 = 0.0589
Largest diff. peak and hole	0.646 and -0.685 e.Å <sup>-3</sup>

Table 2. Torsion angles [°] for NGDH8.

---

F(1)-C(1)-C(2)-N(3)	55.4(3)
C(8)-C(1)-C(2)-N(3)	-67.2(3)
C(1)-C(2)-N(3)-C(4)	99.7(3)
C(2)-N(3)-C(4)-C(5)	-40.8(3)
N(3)-C(4)-C(5)-C(6)	-69.5(3)
C(4)-C(5)-C(6)-N(7)	66.2(3)
C(5)-C(6)-N(7)-C(8)	47.1(3)
C(6)-N(7)-C(8)-C(1)	-100.1(3)
F(1)-C(1)-C(8)-N(7)	-57.7(3)
C(2)-C(1)-C(8)-N(7)	64.9(4)

---

## 2-Fluoro-1,3-propanediamine hydrochloride 154

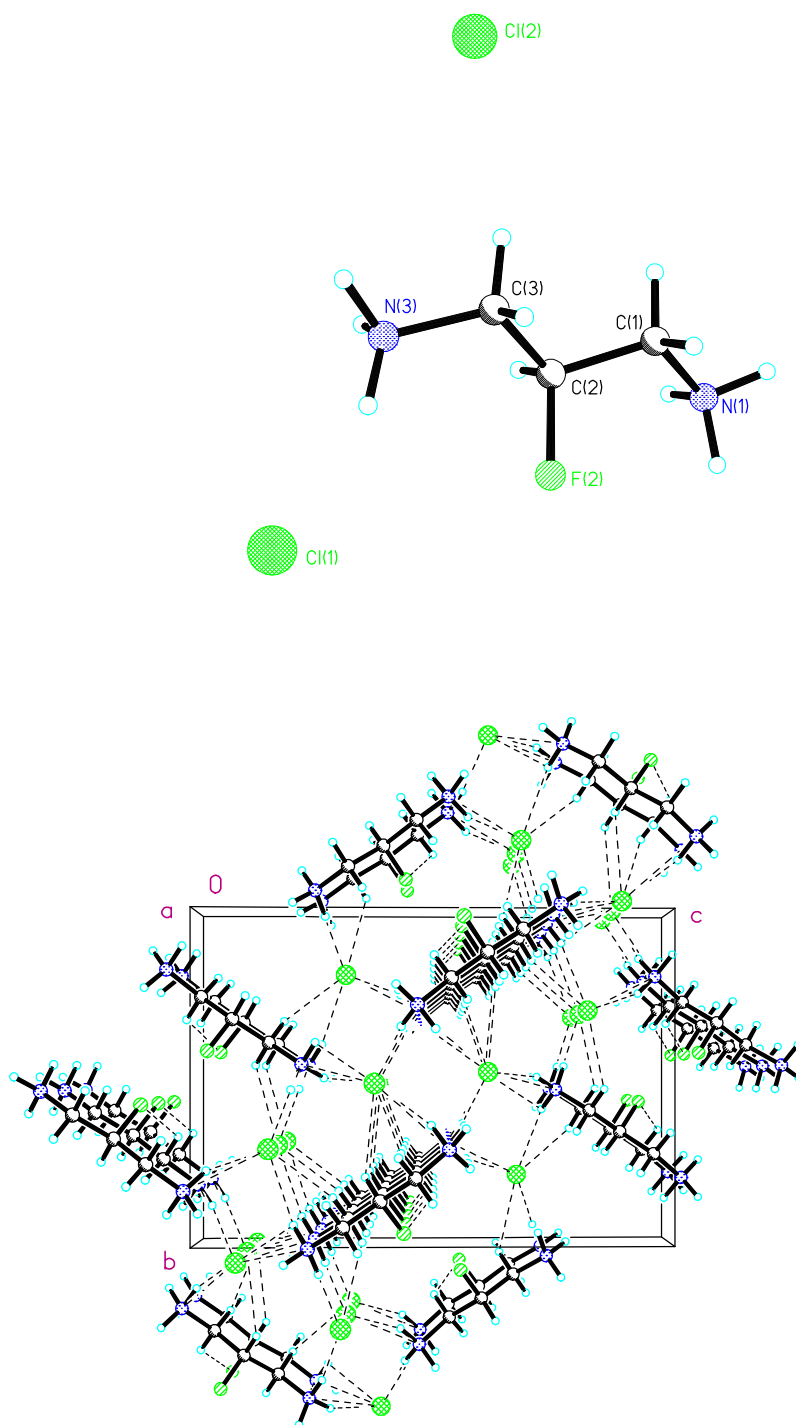


Table 1. Crystal data and structure refinement for ngdh47.

Identification code	ngdh47	
Empirical formula	C <sub>3</sub> H <sub>11</sub> Cl <sub>2</sub> F N <sub>2</sub>	
Formula weight	165.04	
Temperature	93(2) K	
Wavelength	0.71073 Å	
Crystal system	Monoclinic	
Space group	P2(1)/c	
Unit cell dimensions	a = 4.3955(6) Å	α = 90°.
	b = 10.5924(14) Å	β = 92.559(7)°.
	c = 15.170(2) Å	γ = 90°.
Volume	705.61(16) Å <sup>3</sup>	
Z	4	
Density (calculated)	1.554 Mg/m <sup>3</sup>	
Absorption coefficient	0.844 mm <sup>-1</sup>	
F(000)	344	
Crystal size	0.100 x 0.050 x 0.010 mm <sup>3</sup>	
Theta range for data collection	3.31 to 25.35°.	
Index ranges	-5 ≤ h ≤ 5, -12 ≤ k ≤ 11, -15 ≤ l ≤ 18	
Reflections collected	6464	
Independent reflections	1273 [R(int) = 0.0929]	
Completeness to theta = 25.00°	98.2 %	
Absorption correction	Multiscan	
Max. and min. transmission	1.0000 and 0.9402	
Refinement method	Full-matrix least-squares on F <sup>2</sup>	
Data / restraints / parameters	1273 / 6 / 98	
Goodness-of-fit on F <sup>2</sup>	1.237	
Final R indices [I > 2σ(I)]	R1 = 0.0765, wR2 = 0.1760	
R indices (all data)	R1 = 0.0826, wR2 = 0.1800	
Largest diff. peak and hole	0.433 and -0.509 e.Å <sup>-3</sup>	

Table 2. Selected torsion angles [°] for ngdh47.

N(1)-C(1)-C(2)-F(2)	62.4(5)
F(2)-C(2)-C(3)-N(3)	-65.8(5)

## 2-Fluoropropanediamide 153

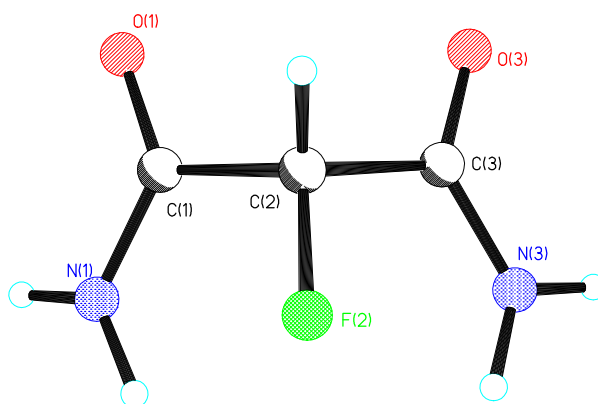


Table 1. Crystal data and structure refinement for ngdh12.

Identification code	ngdh12	
Empirical formula	C <sub>3</sub> H <sub>5</sub> F N <sub>2</sub> O <sub>2</sub>	
Formula weight	120.09	
Temperature	173(2) K	
Wavelength	1.54178 Å	
Crystal system	Monoclinic	
Space group	P2(1)/n	
Unit cell dimensions	a = 5.0882(6) Å	$\alpha = 90^\circ$ .
	b = 11.6000(14) Å	$\beta = 105.099(4)^\circ$ .
	c = 8.3420(11) Å	$\gamma = 90^\circ$ .
Volume	475.37(10) Å <sup>3</sup>	
Z	4	
Density (calculated)	1.678 Mg/m <sup>3</sup>	
Absorption coefficient	1.451 mm <sup>-1</sup>	
F(000)	248	
Crystal size	0.100 x 0.010 x 0.010 mm <sup>3</sup>	
Theta range for data collection	6.69 to 67.92°.	
Index ranges	-5 ≤ h ≤ 5, -13 ≤ k ≤ 13, -9 ≤ l ≤ 9	
Reflections collected	5931	
Independent reflections	786 [R(int) = 0.0483]	
Completeness to theta = 66.50°	92.5 %	
Absorption correction	Multiscan	
Max. and min. transmission	1.0000 and 0.8635	
Refinement method	Full-matrix least-squares on F <sup>2</sup>	

Data / restraints / parameters	786 / 4 / 90
Goodness-of-fit on F <sup>2</sup>	1.120
Final R indices [I>2sigma(I)]	R1 = 0.0375, wR2 = 0.0969
R indices (all data)	R1 = 0.0424, wR2 = 0.1003
Largest diff. peak and hole	0.185 and -0.192 e.Å <sup>-3</sup>

Table 2. Selected torsion angles [°] for ngdh12.

---

N(1)-C(1)-C(2)-F(2)	-19.32(19)
F(2)-C(2)-C(3)-N(3)	15.26(19)
O(1)-C(1)-C(2)-F(2)	162.48(13)
F(2)-C(2)-C(3)-O(3)	-165.75(14)

---

# $N^1, N^1, N^3, N^3$ -Tetrabenzyl-2-fluoropropane-1,3-diamine 156

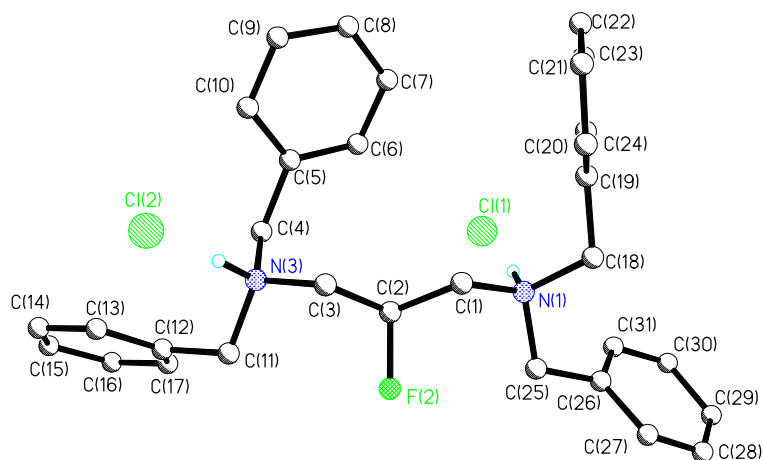


Table 1. Crystal data and structure refinement for ngdh5.

Identification code	ngdh5	
Empirical formula	C <sub>34</sub> H <sub>42</sub> Cl <sub>2</sub> F N <sub>3</sub> O	
Formula weight	598.61	
Temperature	173(2) K	
Wavelength	1.54178 Å	
Crystal system	Orthorhombic	
Space group	Pbcn	
Unit cell dimensions	a = 21.801(2) Å	$\alpha = 90^\circ$ .
	b = 12.1112(13) Å	$\beta = 90^\circ$ .
	c = 24.478(3) Å	$\gamma = 90^\circ$ .
Volume	6463.1(12) Å <sup>3</sup>	
Z	8	
Density (calculated)	1.230 Mg/m <sup>3</sup>	
Absorption coefficient	2.090 mm <sup>-1</sup>	
F(000)	2544	
Crystal size	0.110 x 0.010 x 0.010 mm <sup>3</sup>	
Theta range for data collection	3.61 to 68.02°.	
Index ranges	-25 ≤ h ≤ 26, -14 ≤ k ≤ 14, -27 ≤ l ≤ 28	
Reflections collected	80245	
Independent reflections	5675 [R(int) = 0.4057]	
Completeness to theta = 66.50°	97.3 %	
Absorption correction	Multiscan	
Max. and min. transmission	1.0000 and 0.9439	
Refinement method	Full-matrix least-squares on F <sup>2</sup>	

Data / restraints / parameters	5675 / 2 / 381
Goodness-of-fit on F <sup>2</sup>	1.140
Final R indices [I>2sigma(I)]	R1 = 0.1396, wR2 = 0.2042
R indices (all data)	R1 = 0.2396, wR2 = 0.2418
Largest diff. peak and hole	0.496 and -0.494 e.Å <sup>-3</sup>

Table 2. Selected torsion angles [°] for ngdh5.

---

N(1)-C(1)-C(2)-F(2)	77.0(7)
F(2)-C(2)-C(3)-N(3)	-88.1(7)

---

7-Fluoro-1,5-ditosyl-1,5-diazo-octan-3-ol 162

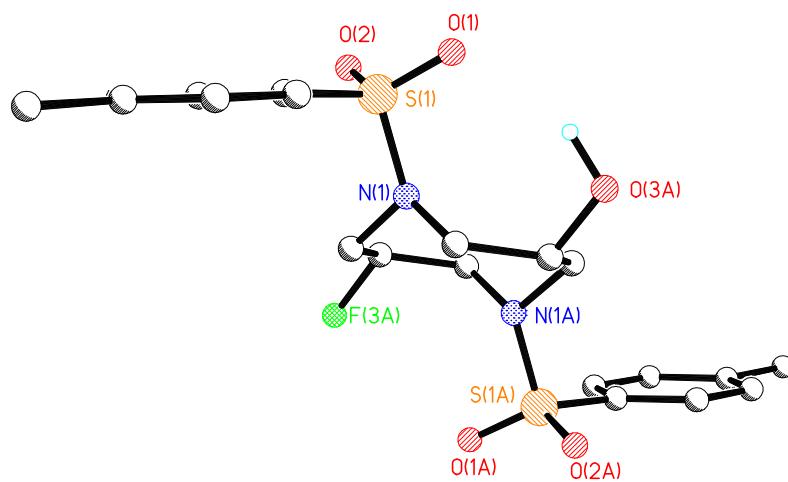
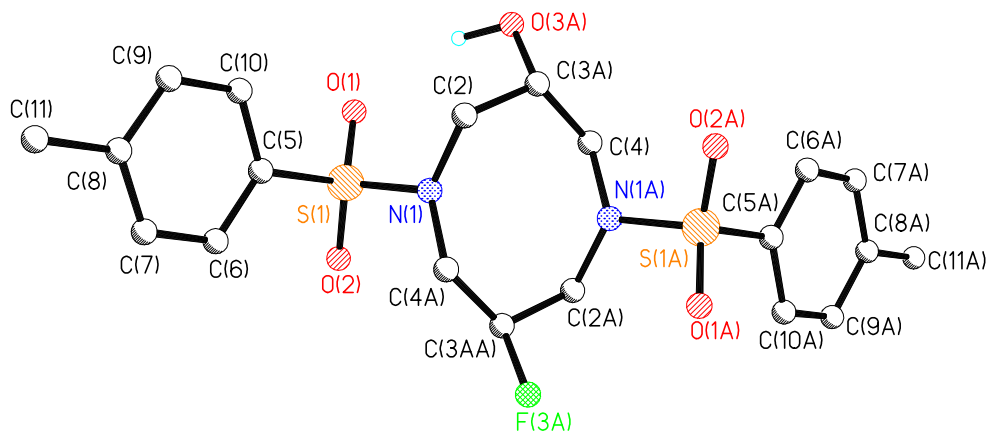




Table 1. Crystal data and structure refinement for NGDH46.

Identification code	ngdh46	
Empirical formula	C <sub>20</sub> H <sub>25</sub> F N <sub>2</sub> O <sub>5</sub> S <sub>2</sub>	
Formula weight	456.54	
Temperature	93(2) K	
Wavelength	0.71073 Å	
Crystal system	Triclinic	
Space group	P-1	
Unit cell dimensions	a = 5.1351(16) Å	α = 68.00(2)°.
	b = 9.736(3) Å	β = 83.97(3)°.
	c = 11.130(3) Å	γ = 85.89(3)°.
Volume	512.7(3) Å <sup>3</sup>	
Z	1	
Density (calculated)	1.479 Mg/m <sup>3</sup>	
Absorption coefficient	0.305 mm <sup>-1</sup>	
F(000)	240	
Crystal size	0.1000 x 0.0300 x 0.0300 mm <sup>3</sup>	
Theta range for data collection	1.98 to 25.31°.	
Index ranges	-5 ≤ h ≤ 6, -10 ≤ k ≤ 11, -11 ≤ l ≤ 13	
Reflections collected	3225	
Independent reflections	1755 [R(int) = 0.0225]	
Completeness to theta = 25.00°	94.8 %	
Absorption correction	Multiscan	
Max. and min. transmission	1.0000 and 0.9708	
Refinement method	Full-matrix least-squares on F <sup>2</sup>	
Data / restraints / parameters	1755 / 0 / 147	
Goodness-of-fit on F <sup>2</sup>	1.118	
Final R indices [I > 2σ(I)]	R1 = 0.0773, wR2 = 0.1826	
R indices (all data)	R1 = 0.0839, wR2 = 0.1900	
Extinction coefficient	0.033(10)	
Largest diff. peak and hole	1.176 and -0.490 e.Å <sup>-3</sup>	

## 4-Fluoro-pyrazolidine hydrochloride 169

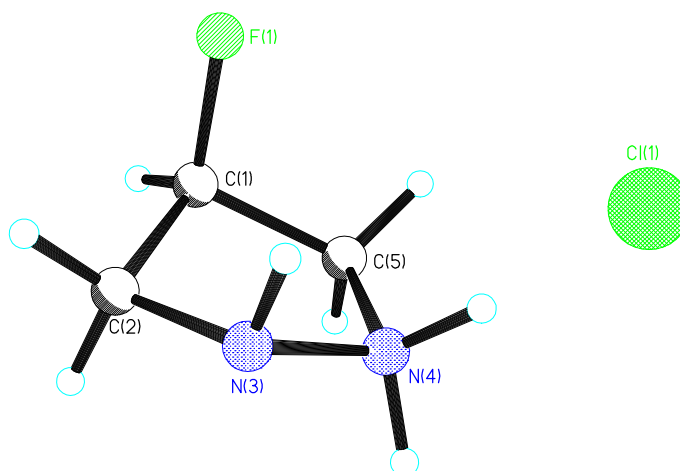


Table 1. Crystal data and structure refinement for ngdh11.

Identification code	ngdh11	
Empirical formula	C <sub>3</sub> H <sub>8</sub> Cl F N <sub>2</sub>	
Formula weight	126.56	
Temperature	93(2) K	
Wavelength	0.71073 Å	
Crystal system	Orthorhombic	
Space group	P2(1)2(1)2(1)	
Unit cell dimensions	a = 5.0061(8) Å	α = 90°.
	b = 7.4977(10) Å	β = 90°.
	c = 15.220(2) Å	γ = 90°.
Volume	571.28(14) Å <sup>3</sup>	
Z	4	
Density (calculated)	1.472 Mg/m <sup>3</sup>	
Absorption coefficient	0.566 mm <sup>-1</sup>	
F(000)	264	
Crystal size	0.100 x 0.080 x 0.010 mm <sup>3</sup>	
Theta range for data collection	3.03 to 25.34°.	
Index ranges	-4 ≤ h ≤ 5, -8 ≤ k ≤ 9, -16 ≤ l ≤ 18	
Reflections collected	3355	
Independent reflections	904 [R(int) = 0.0148]	
Completeness to theta = 25.34°	86.6 %	
Absorption correction	Multiscan	
Max. and min. transmission	1.0000 and 0.8266	
Refinement method	Full-matrix least-squares on F <sup>2</sup>	

Data / restraints / parameters	904 / 3 / 77
Goodness-of-fit on F <sup>2</sup>	1.088
Final R indices [I>2sigma(I)]	R1 = 0.0157, wR2 = 0.0385
R indices (all data)	R1 = 0.0157, wR2 = 0.0385
Absolute structure parameter	0.37(6)
Largest diff. peak and hole	0.131 and -0.114 e.Å <sup>-3</sup>

Table 2. Torsion angles [°] for ngdh11.

---

F(1)-C(1)-C(2)-N(3)	-76.85(11)
C(5)-C(1)-C(2)-N(3)	38.23(13)
C(1)-C(2)-N(3)-N(4)	-34.92(12)
C(2)-N(3)-N(4)-C(5)	18.60(12)
F(1)-C(1)-C(5)-N(4)	89.23(11)
C(2)-C(1)-C(5)-N(4)	-25.69(13)
N(3)-N(4)-C(5)-C(1)	4.96(13)

---

## Azetidiniun hydrobromide 179

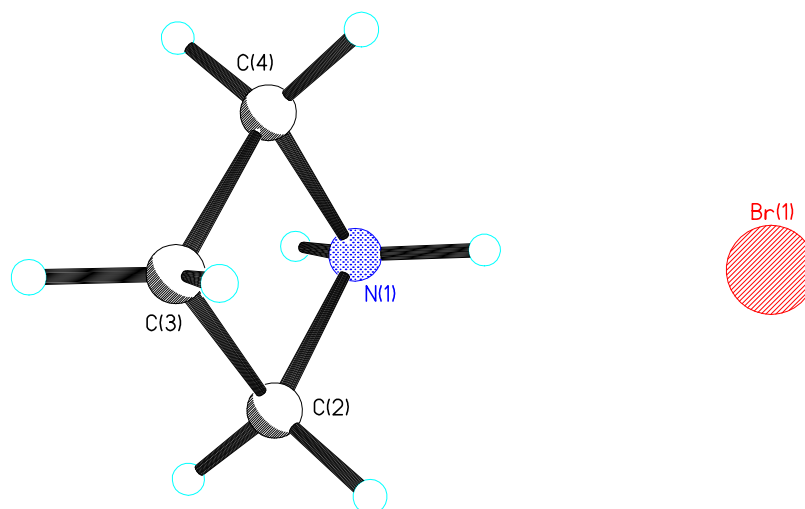


Table 1. Crystal data and structure refinement for ngdh30.

Identification code	ngdh30	
Empirical formula	C <sub>3</sub> H <sub>8</sub> Br N	
Formula weight	138.01	
Temperature	93(2) K	
Wavelength	0.71073 Å	
Crystal system	Orthorhombic	
Space group	Ibam	
Unit cell dimensions	a = 8.724(4) Å	α = 90°.
	b = 17.455(8) Å	β = 90°.
	c = 6.757(3) Å	γ = 90°.
Volume	1029.0(8) Å <sup>3</sup>	
Z	8	
Density (calculated)	1.782 Mg/m <sup>3</sup>	
Absorption coefficient	7.821 mm <sup>-1</sup>	
F(000)	544	
Crystal size	0.1000 x 0.0100 x 0.0100 mm <sup>3</sup>	
Theta range for data collection	2.33 to 25.37°.	
Index ranges	-10 ≤ h ≤ 10, -20 ≤ k ≤ 20, -8 ≤ l ≤ 7	
Reflections collected	4419	
Independent reflections	470 [R(int) = 0.0587]	
Completeness to theta = 25.00°	89.9 %	
Absorption correction	Multiscan	

Max. and min. transmission	1.0000 and 0.6193
Refinement method	Full-matrix least-squares on F <sup>2</sup>
Data / restraints / parameters	470 / 2 / 36
Goodness-of-fit on F <sup>2</sup>	0.880
Final R indices [I>2sigma(I)]	R1 = 0.0300, wR2 = 0.0640
R indices (all data)	R1 = 0.0382, wR2 = 0.0691
Largest diff. peak and hole	0.951 and -0.351 e.Å <sup>-3</sup>

Table 2. Bond lengths [Å] and angles [°] for ngdh30.

N(1)-C(2)	1.495(7)
N(1)-C(4)	1.508(8)
C(2)-C(3)	1.509(10)
C(3)-C(4)	1.528(9)
C(2)-N(1)-C(4)	91.0(4)
N(1)-C(2)-C(3)	90.2(5)
C(2)-C(3)-C(4)	89.7(5)
N(1)-C(4)-C(3)	89.0(5)

Table 3. Torsion angles [°] for ngdh30.

C(4)-N(1)-C(2)-C(3)	0.0
N(1)-C(2)-C(3)-C(4)	0.0
C(2)-N(1)-C(4)-C(3)	0.0
C(2)-C(3)-C(4)-N(1)	0.0

### 3-Fluoroazetidinium hydrochloride 182

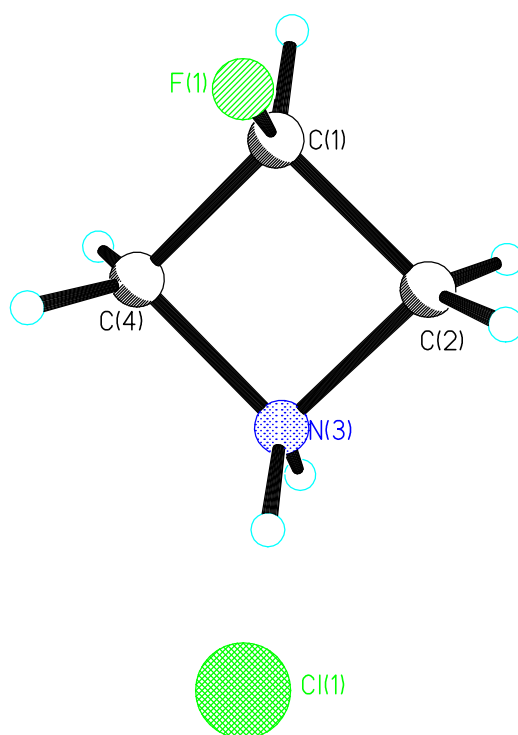


Table 1. Crystal data and structure refinement for ngdh9.

Identification code	ngdh9	
Empirical formula	C <sub>3</sub> H <sub>7</sub> Cl F N	
Formula weight	111.55	
Temperature	93(2) K	
Wavelength	0.71073 Å	
Crystal system	Monoclinic	
Space group	P2(1)/n	
Unit cell dimensions	a = 6.5872(11) Å	$\alpha = 90^\circ$ .
	b = 8.3434(14) Å	$\beta = 97.565(8)^\circ$ .
	c = 9.0693(15) Å	$\gamma = 90^\circ$ .
Volume	494.11(14) Å <sup>3</sup>	
Z	4	
Density (calculated)	1.499 Mg/m <sup>3</sup>	
Absorption coefficient	0.638 mm <sup>-1</sup>	
F(000)	232	
Crystal size	0.030 x 0.030 x 0.010 mm <sup>3</sup>	
Theta range for data collection	3.33 to 25.35°.	

Index ranges	-7<=h<=7, -10<=k<=9, -6<=l<=10
Reflections collected	3221
Independent reflections	856 [R(int) = 0.0127]
Completeness to theta = 25.35°	94.8 %
Absorption correction	Multiscan
Max. and min. transmission	1.0000 and 0.8947
Refinement method	Full-matrix least-squares on F <sup>2</sup>
Data / restraints / parameters	856 / 2 / 64
Goodness-of-fit on F <sup>2</sup>	0.902
Final R indices [I>2sigma(I)]	R1 = 0.0199, wR2 = 0.0502
R indices (all data)	R1 = 0.0219, wR2 = 0.0517
Largest diff. peak and hole	0.273 and -0.192 e.Å <sup>-3</sup>

Table 2. Torsion angles [°] for ngdh9.

---

F(1)-C(1)-C(2)-N(3)	106.91(11)
C(4)-C(1)-C(2)-N(3)	-6.18(10)
C(1)-C(2)-N(3)-C(4)	6.22(10)
C(2)-N(3)-C(4)-C(1)	-6.26(10)
F(1)-C(1)-C(4)-N(3)	-106.51(11)
C(2)-C(1)-C(4)-N(3)	6.17(10)

---

### 3-Fluoroazetidinium hydrobromide 183

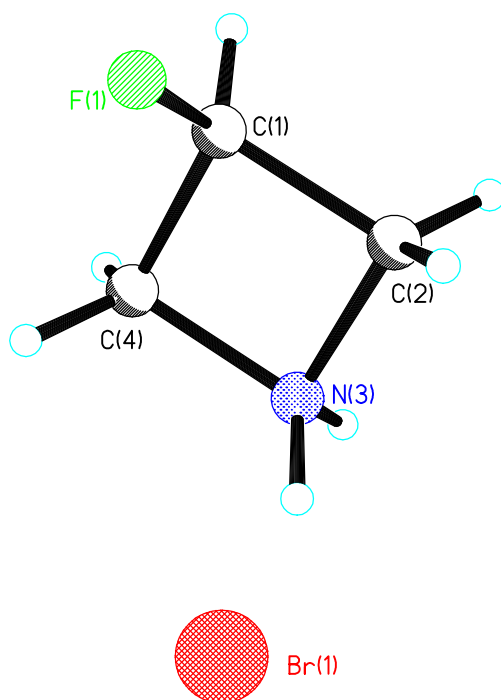


Table 1. Crystal data and structure refinement for NGDH20.

Identification code	ngdh20	
Empirical formula	C <sub>3</sub> H <sub>7</sub> Br F N	
Formula weight	156.01	
Temperature	93(2) K	
Wavelength	0.71073 Å	
Crystal system	Orthorhombic	
Space group	Pbca	
Unit cell dimensions	a = 10.0178(19) Å	α = 90°.
	b = 9.206(2) Å	β = 90°.
	c = 11.847(2) Å	γ = 90°.
Volume	1092.6(4) Å <sup>3</sup>	
Z	8	
Density (calculated)	1.897 Mg/m <sup>3</sup>	
Absorption coefficient	7.403 mm <sup>-1</sup>	
F(000)	608	
Crystal size	0.1000 x 0.0300 x 0.0300 mm <sup>3</sup>	
Theta range for data collection	3.44 to 25.35°.	



Index ranges	-11<=h<=11, -9<=k<=11, -12<=l<=14
Reflections collected	6218
Independent reflections	958 [R(int) = 0.0521]
Completeness to theta = 25.35°	96.3 %
Absorption correction	Multiscan
Max. and min. transmission	1.0000 and 0.2044
Refinement method	Full-matrix least-squares on F <sup>2</sup>
Data / restraints / parameters	958 / 2 / 64
Goodness-of-fit on F <sup>2</sup>	0.889
Final R indices [I>2sigma(I)]	R1 = 0.0222, wR2 = 0.0531
R indices (all data)	R1 = 0.0249, wR2 = 0.0543
Largest diff. peak and hole	0.489 and -0.381 e.Å <sup>-3</sup>

Table 2. Torsion angles [°] for NGDH20.

---

F(1)-C(1)-C(2)-N(3)	113.0(2)
C(4)-C(1)-C(2)-N(3)	-1.38(19)
C(1)-C(2)-N(3)-C(4)	1.40(19)
C(2)-N(3)-C(4)-C(1)	-1.40(19)
F(1)-C(1)-C(4)-N(3)	-112.1(2)
C(2)-C(1)-C(4)-N(3)	1.39(19)

---

**(S)-(+)-3-Fluoropyrrolidine hydrochloride 187**

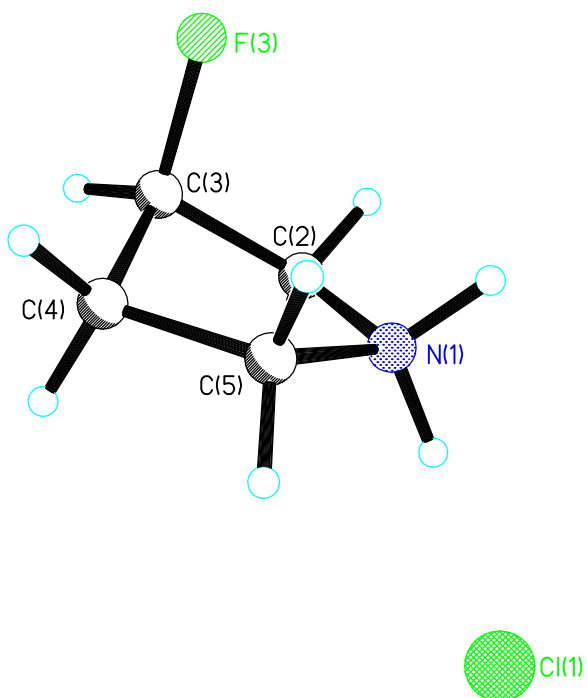


Table 1. Crystal data and structure refinement for ngdh32.

Identification code	ngdh32	
Empirical formula	C <sub>4</sub> H <sub>9</sub> Cl F N	
Formula weight	125.57	
Temperature	93(2) K	
Wavelength	0.71073 Å	
Crystal system	Monoclinic	
Space group	P2(1)	
Unit cell dimensions	a = 5.121(3) Å	$\alpha = 90^\circ$ .
	b = 10.597(5) Å	$\beta = 113.161(10)^\circ$ .
	c = 6.248(3) Å	$\gamma = 90^\circ$ .
Volume	311.7(3) Å <sup>3</sup>	
Z	2	
Density (calculated)	1.338 Mg/m <sup>3</sup>	
Absorption coefficient	0.514 mm <sup>-1</sup>	
F(000)	132	
Crystal size	0.1000 x 0.0500 x 0.0500 mm <sup>3</sup>	
Theta range for data collection	4.04 to 25.33°.	
Index ranges	-5 ≤ h ≤ 6, -12 ≤ k ≤ 9, -7 ≤ l ≤ 7	
Reflections collected	1973	
	283	

Independent reflections	866 [R(int) = 0.0633]
Completeness to theta = 25.00°	93.5 %
Absorption correction	Multiscan
Max. and min. transmission	1.0000 and 0.7060
Refinement method	Full-matrix least-squares on F <sup>2</sup>
Data / restraints / parameters	866 / 3 / 73
Goodness-of-fit on F <sup>2</sup>	0.762
Final R indices [I>2sigma(I)]	R1 = 0.0412, wR2 = 0.0628
R indices (all data)	R1 = 0.0628, wR2 = 0.0711
Absolute structure parameter	-0.03(15)
Largest diff. peak and hole	0.253 and -0.226 e.Å <sup>-3</sup>

Table 2. Torsion angles [°] for ngdh32.

---

C(5)-N(1)-C(2)-C(3)	18.0(4)
N(1)-C(2)-C(3)-F(3)	81.0(4)
N(1)-C(2)-C(3)-C(4)	-35.4(3)
F(3)-C(3)-C(4)-C(5)	-76.6(4)
C(2)-C(3)-C(4)-C(5)	39.3(3)
C(2)-N(1)-C(5)-C(4)	6.5(4)
C(3)-C(4)-C(5)-N(1)	-28.2(3)

---

**(R)-(-)-3-Pyrrolidinol hydrochloride 188**

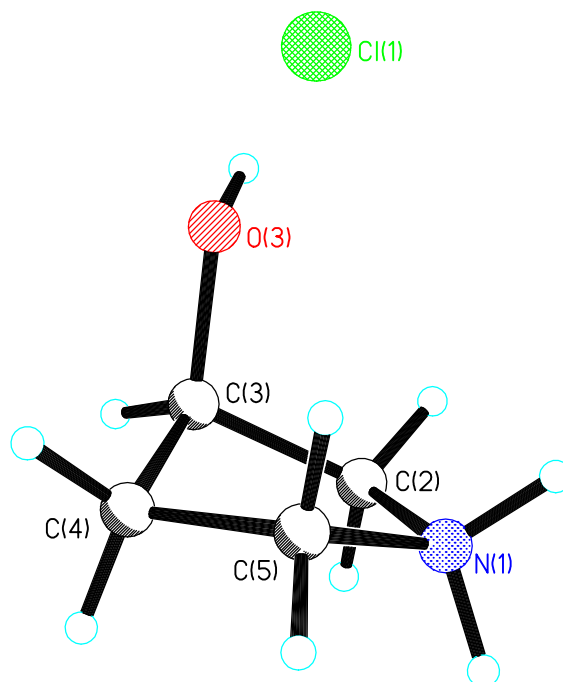


Table 1. Crystal data and structure refinement for NGDH33.

Identification code	ngdh33	
Empirical formula	C <sub>4</sub> H <sub>10</sub> Cl N O	
Formula weight	123.58	
Temperature	93(2) K	
Wavelength	0.71073 Å	
Crystal system	Orthorhombic	
Space group	P2(1)2(1)2(1)	
Unit cell dimensions	a = 5.0923(11) Å	$\alpha = 90^\circ$ .
	b = 6.2896(16) Å	$\beta = 90^\circ$ .
	c = 19.461(5) Å	$\gamma = 90^\circ$ .
Volume	623.3(3) Å <sup>3</sup>	
Z	4	
Density (calculated)	1.317 Mg/m <sup>3</sup>	
Absorption coefficient	0.502 mm <sup>-1</sup>	
F(000)	264	
Crystal size	0.3000 x 0.2000 x 0.1000 mm <sup>3</sup>	
Theta range for data collection	2.09 to 25.30°.	
Index ranges	-6<=h<=4, -7<=k<=6, -22<=l<=23	

Reflections collected	4006
Independent reflections	1112 [R(int) = 0.0303]
Completeness to theta = 25.00°	97.2 %
Absorption correction	Multiscan
Max. and min. transmission	1.0000 and 0.6867
Refinement method	Full-matrix least-squares on F <sup>2</sup>
Data / restraints / parameters	1112 / 3 / 77
Goodness-of-fit on F <sup>2</sup>	1.042
Final R indices [I > 2sigma(I)]	R1 = 0.0361, wR2 = 0.0662
R indices (all data)	R1 = 0.0396, wR2 = 0.0680
Absolute structure parameter	-0.02(10)
Largest diff. peak and hole	0.270 and -0.280 e.Å <sup>-3</sup>

Table 2. Torsion angles [°] for NGDH33.

---

C(5)-N(1)-C(2)-C(3)	10.1(2)
N(1)-C(2)-C(3)-O(3)	82.4(2)
N(1)-C(2)-C(3)-C(4)	-31.9(2)
O(3)-C(3)-C(4)-C(5)	-75.4(2)
C(2)-C(3)-C(4)-C(5)	41.8(2)
C(2)-N(1)-C(5)-C(4)	15.7(2)
C(3)-C(4)-C(5)-N(1)	-35.2(2)

---

## 1-(2-Fluoro-ethyl)-pyridinium 4-methylbenzenesulfonate 198

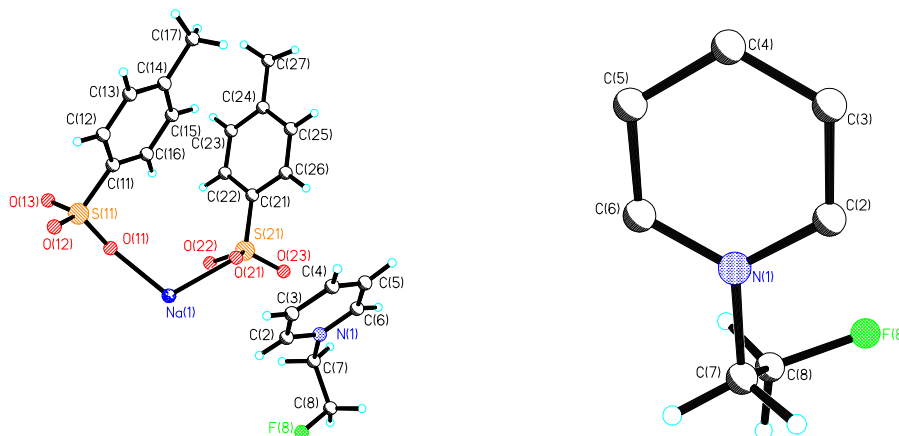


Table 1. Crystal data and structure refinement for ngdh38.

Identification code	ngdh38	
Empirical formula	C <sub>21</sub> H <sub>23</sub> F N Na O <sub>6</sub> S <sub>2</sub>	
Formula weight	491.51	
Temperature	173(2) K	
Wavelength	1.54178 Å	
Crystal system	Triclinic	
Space group	P-1	
Unit cell dimensions	a = 9.7646(17) Å	α = 78.499(8)°.
	b = 9.8148(16) Å	β = 80.851(8)°.
	c = 13.290(2) Å	γ = 66.472(7)°.
Volume	1139.9(3) Å <sup>3</sup>	
Z	2	
Density (calculated)	1.432 Mg/m <sup>3</sup>	
Absorption coefficient	2.716 mm <sup>-1</sup>	
F(000)	512	
Crystal size	0.150 x 0.030 x 0.010 mm <sup>3</sup>	
Theta range for data collection	3.41 to 67.61°.	
Index ranges	-9 ≤ h ≤ 10, -11 ≤ k ≤ 11, -15 ≤ l ≤ 15	
Reflections collected	14680	
Independent reflections	3712 [R(int) = 0.1643]	
Completeness to theta = 25.00°	98.5 %	
Absorption correction	Multiscan	

Max. and min. transmission	1.0000 and 0.0362
Refinement method	Full-matrix least-squares on F <sup>2</sup>
Data / restraints / parameters	3712 / 0 / 292
Goodness-of-fit on F <sup>2</sup>	1.090
Final R indices [I>2sigma(I)]	R1 = 0.0948, wR2 = 0.2167
R indices (all data)	R1 = 0.1305, wR2 = 0.2380
Largest diff. peak and hole	0.525 and -0.434 e.Å <sup>-3</sup>

Table 2. Selected torsion angle [°] for ngdh38.

---

N(1)-C(7)-C(8)-F(8)	68.1(7)
---------------------	---------

---

Table 3. Selected bond length [Å] for ngdh38.

---

F(8)-C(8)	1.400(8)
-----------	----------

---

## 4-(Dimethylamino)-1-(2-fluoroethyl) pyridinium 4-methylbenzenesulfonate 200

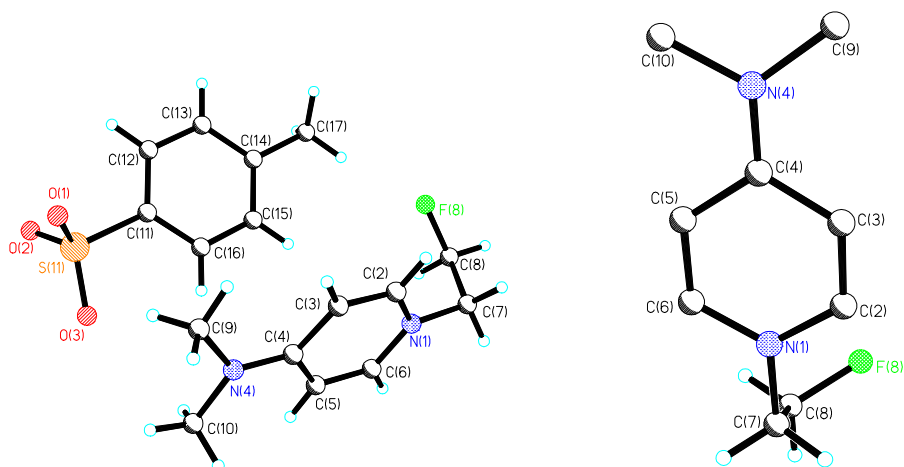


Table 1. Crystal data and structure refinement for ngdh40.

Identification code	ngdh40	
Empirical formula	C <sub>16</sub> H <sub>21</sub> F N <sub>2</sub> O <sub>3</sub> S	
Formula weight	340.41	
Temperature	93(2) K	
Wavelength	0.71073 Å	
Crystal system	Triclinic	
Space group	P-1	
Unit cell dimensions	a = 9.3305(12) Å	α = 78.152(13)°.
	b = 9.4854(13) Å	β = 79.100(15)°.
	c = 9.6604(14) Å	γ = 74.664(14)°.
Volume	798.70(19) Å <sup>3</sup>	
Z	2	
Density (calculated)	1.415 Mg/m <sup>3</sup>	
Absorption coefficient	0.230 mm <sup>-1</sup>	
F(000)	360	
Crystal size	0.1500 x 0.1000 x 0.0100 mm <sup>3</sup>	
Theta range for data collection	2.18 to 25.34°.	
Index ranges	-11 ≤ h ≤ 8, -11 ≤ k ≤ 8, -11 ≤ l ≤ 11	
Reflections collected	5130	
Independent reflections	2727 [R(int) = 0.0429]	
Completeness to theta = 25.00°	93.5 %	
Absorption correction	Multiscan	
Max. and min. transmission	1.0000 and 0.7087	



Refinement method	Full-matrix least-squares on F <sup>2</sup>
Data / restraints / parameters	2727 / 0 / 213
Goodness-of-fit on F <sup>2</sup>	1.048
Final R indices [I>2sigma(I)]	R1 = 0.0617, wR2 = 0.1178
R indices (all data)	R1 = 0.1111, wR2 = 0.1416
Extinction coefficient	0.004(2)
Largest diff. peak and hole	0.320 and -0.319 e.Å <sup>-3</sup>

Table 2. Selected torsion angle [°] for ngdh40.

---

N(1)-C(7)-C(8)-F(8)	59.1(4)
---------------------	---------

---

Table 3. Selected bond length [Å] for ngdh40.

---

C(8)-F(8)	1.413(4)
-----------	----------

---

## 1-(2-Hydroxy-ethyl)-pyridinium chloride 201

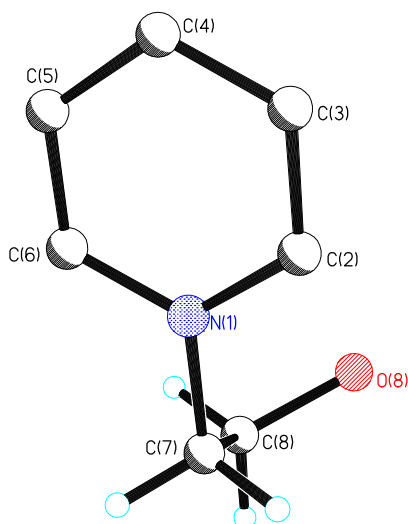


Table 1. Crystal data and structure refinement for ngdh36.

Identification code	ngdh36	
Empirical formula	C7 H10 Cl N O	
Formula weight	159.61	
Temperature	93(2) K	
Wavelength	0.71073 Å	
Crystal system	Orthorhombic	
Space group	Pbca	
Unit cell dimensions	a = 12.023(3) Å	$\alpha = 90^\circ$ .
	b = 7.2111(15) Å	$\beta = 90^\circ$ .
	c = 17.605(4) Å	$\gamma = 90^\circ$ .
Volume	1526.3(6) Å <sup>3</sup>	
Z	8	
Density (calculated)	1.389 Mg/m <sup>3</sup>	
Absorption coefficient	0.428 mm <sup>-1</sup>	
F(000)	672	
Crystal size	0.100 x 0.100 x 0.100 mm <sup>3</sup>	
Theta range for data collection	2.87 to 25.35°.	
Index ranges	-13<=h<=14, -8<=k<=6, -16<=l<=21	
Reflections collected	8307	
Independent reflections	1361 [R(int) = 0.0327]	
Completeness to theta = 25.00°	97.9 %	

Absorption correction	Multiscan
Max. and min. transmission	1.0000 and 0.7271
Refinement method	Full-matrix least-squares on F <sup>2</sup>
Data / restraints / parameters	1361 / 1 / 96
Goodness-of-fit on F <sup>2</sup>	1.108
Final R indices [I>2sigma(I)]	R1 = 0.0297, wR2 = 0.0590
R indices (all data)	R1 = 0.0341, wR2 = 0.0606
Largest diff. peak and hole	0.197 and -0.142 e.Å <sup>-3</sup>

Table 2. Selected torsion angle [°] for ngdh36.

---

N(1)-C(7)-C(8)-O(8)	61.16(16)
---------------------	-----------

---

Table 3. Selected bond length [Å] for ngdh36.

---

C(8)-O(8)	1.4075(18)
-----------	------------

---

# 1,1'-(2-Fluoropropane-1,3-diyl)dipyridinium nickel tetrabromide 203

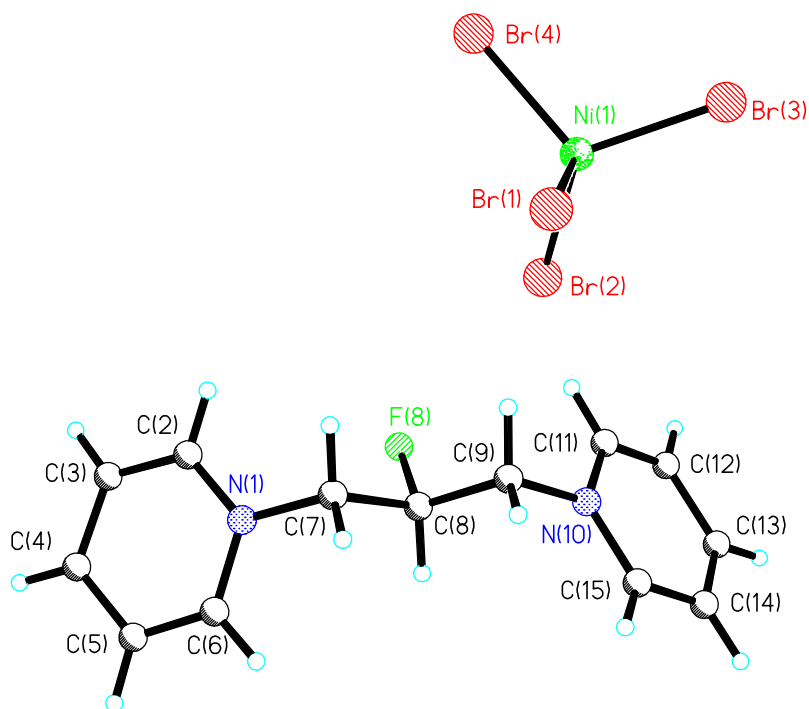


Table 1. Crystal data and structure refinement for ngdh48.

Identification code	ngdh48	
Empirical formula	C <sub>13</sub> H <sub>15</sub> Br <sub>4</sub> F N <sub>2</sub> Ni	
Formula weight	596.62	
Temperature	93(2) K	
Wavelength	0.71073 Å	
Crystal system	Monoclinic	
Space group	P2(1)/c	
Unit cell dimensions	a = 15.760(7) Å	α = 90°.
	b = 8.044(4) Å	β = 107.49(2)°.
	c = 14.667(8) Å	γ = 90°.
Volume	1773.5(15) Å <sup>3</sup>	
Z	4	
Density (calculated)	2.235 Mg/m <sup>3</sup>	
Absorption coefficient	10.109 mm <sup>-1</sup>	
F(000)	1136	
Crystal size	0.100 x 0.080 x 0.010 mm <sup>3</sup>	
Theta range for data collection	2.82 to 25.35°.	
Index ranges	-15 ≤ h ≤ 18, -9 ≤ k ≤ 7, -17 ≤ l ≤ 16	

Reflections collected	9375
Independent reflections	3202 [R(int) = 0.2678]
Completeness to theta = 25.00°	98.8 %
Absorption correction	Multiscan
Max. and min. transmission	1.0000 and 0.8927
Refinement method	Full-matrix least-squares on F <sup>2</sup>
Data / restraints / parameters	3202 / 54 / 191
Goodness-of-fit on F <sup>2</sup>	1.092
Final R indices [I > 2sigma(I)]	R1 = 0.1233, wR2 = 0.2298
R indices (all data)	R1 = 0.2149, wR2 = 0.2671
Largest diff. peak and hole	1.451 and -1.357 e.Å <sup>-3</sup>

Table 2. Selected torsion angles [°] for ngdh48.

---

N(1)-C(7)-C(8)-F(8)	60(2)
F(8)-C(8)-C(9)-N(10)	-72(2)

---

## 1,1'-(ethane-1,2-diyl)dipyridinium chloride 210

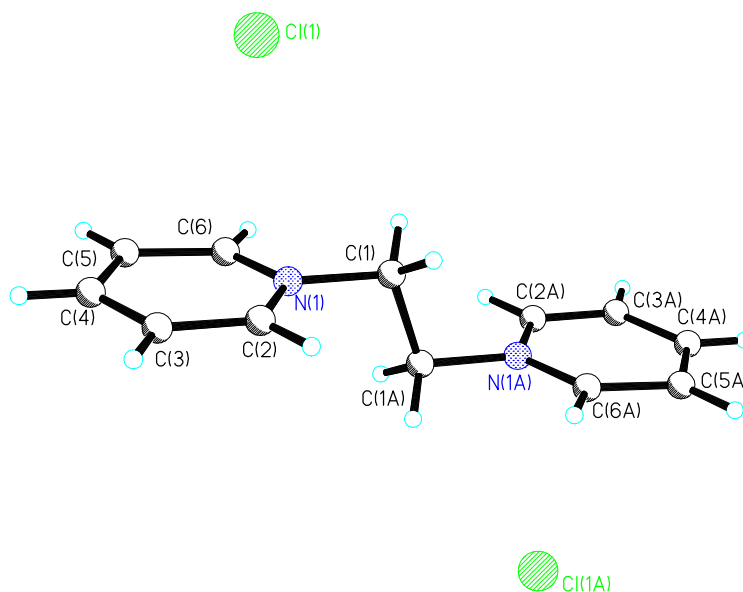


Table 1. Crystal data and structure refinement for NGDH42.

Identification code	ngdh42	
Empirical formula	C <sub>12</sub> H <sub>14</sub> Cl <sub>2</sub> N <sub>2</sub>	
Formula weight	257.15	
Temperature	173(2) K	
Wavelength	1.54178 Å	
Crystal system	Triclinic	
Space group	P-1	
Unit cell dimensions	a = 5.568(3) Å	$\alpha = 82.93(7)^\circ$ .
	b = 6.255(3) Å	$\beta = 81.86(7)^\circ$ .
	c = 9.4304(10) Å	$\gamma = 70.09(6)^\circ$ .
Volume	304.7(2) Å <sup>3</sup>	
Z	1	
Density (calculated)	1.401 Mg/m <sup>3</sup>	
Absorption coefficient	4.566 mm <sup>-1</sup>	
F(000)	134	
Crystal size	0.1000 x 0.1000 x 0.0100 mm <sup>3</sup>	
Theta range for data collection	4.75 to 68.36°.	
Index ranges	-6 ≤ h ≤ 6, -6 ≤ k ≤ 6, -11 ≤ l ≤ 11	
Reflections collected	3323	
Independent reflections	993 [R(int) = 0.3664]	

Completeness to theta = 25.00°	67.6 %
Absorption correction	Multiscan
Max. and min. transmission	1.0000 and 0.0948
Refinement method	Full-matrix least-squares on F <sup>2</sup>
Data / restraints / parameters	993 / 0 / 75
Goodness-of-fit on F <sup>2</sup>	1.561
Final R indices [I>2sigma(I)]	R1 = 0.1876, wR2 = 0.4232
R indices (all data)	R1 = 0.2093, wR2 = 0.4638
Extinction coefficient	0.05(4)
Largest diff. peak and hole	0.906 and -1.006 e.Å <sup>-3</sup>

Table 2. Selected torsion angles [°] for NGDH42.

C(1)#1-C(1)-N(1)-C(6)	-93.0(11)
C(1)#1-C(1)-N(1)-C(2)	85.8(11)
C(6)-N(1)-C(2)-C(3)	-1.9(11)
C(1)-N(1)-C(2)-C(3)	179.2(8)
N(1)-C(2)-C(3)-C(4)	-0.3(13)
C(2)-N(1)-C(6)-C(5)	2.9(11)
C(1)-N(1)-C(6)-C(5)	-178.3(6)
C(4)-C(5)-C(6)-N(1)	-1.5(11)

Table 3. Bond lengths [Å] and angles [°] for NGDH42.

C(1)-N(1)	1.497(9)
C(1)-C(1)#1	1.499(14)
N(1)-C(1)-C(1)#1	108.9(8)
N(1)-C(1)-H(1A)	109.9
C(1)#1-C(1)-H(1A)	109.9
N(1)-C(1)-H(1B)	109.9

## *cis*-4-*tert*-Butyl-2-fluorocyclohexanone 222a

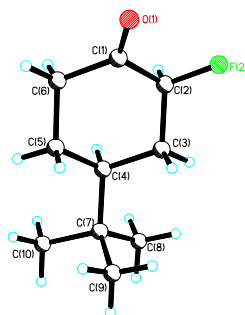


Table 1. Crystal data and structure refinement for NGDH14.

Identification code	ngdh14
Empirical formula	C <sub>10</sub> H <sub>17</sub> F O
Formula weight	172.24
Temperature	93(2) K
Wavelength	0.71073 Å
Crystal system	Monoclinic
Space group	P2(1)/c
Unit cell dimensions	a = 10.866(7) Å                      α = 90°. b = 14.216(9) Å                      β = 93.420(9)°. c = 6.295(4) Å                      γ = 90°.
Volume	970.7(10) Å <sup>3</sup>
Z	4
Density (calculated)	1.179 Mg/m <sup>3</sup>
Absorption coefficient	0.086 mm <sup>-1</sup>
F(000)	376
Crystal size	0.4000 x 0.0300 x 0.0300 mm <sup>3</sup>
Theta range for data collection	2.87 to 25.42°.
Index ranges	-13 ≤ h ≤ 7, -17 ≤ k ≤ 17, -7 ≤ l ≤ 5
Reflections collected	5897
Independent reflections	1594 [R(int) = 0.0440]
Completeness to theta = 25.42°	88.9 %
Absorption correction	Multiscan
Max. and min. transmission	1.0000 and 0.3124
Refinement method	Full-matrix least-squares on F <sup>2</sup>
Data / restraints / parameters	1594 / 0 / 118
Goodness-of-fit on F <sup>2</sup>	0.946
Final R indices [I > 2σ(I)]	R1 = 0.1056, wR2 = 0.2530
R indices (all data)	R1 = 0.1106, wR2 = 0.2583
Largest diff. peak and hole	0.655 and -0.314 e.Å <sup>-3</sup>



## (2*S*, 4*S*)-4-*tert*-butyl-2-phenylcyclohexanone 250a

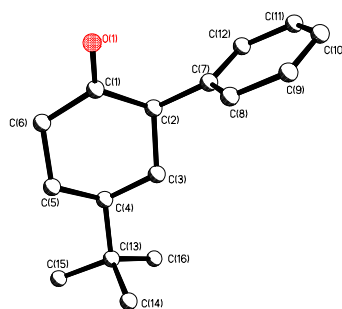


Table 1. Crystal data and structure refinement for NGDH15.

Identification code	ngdh15	
Empirical formula	C <sub>16</sub> H <sub>22.08</sub> O <sub>1.04</sub>	
Formula weight	231.09	
Temperature	93(2) K	
Wavelength	0.71073 Å	
Crystal system	Rhombohedral	
Space group	R-3	
Unit cell dimensions	a = 34.753(5) Å	α = 90°.
	b = 34.753(5) Å	β = 90°.
	c = 6.0563(8) Å	γ = 120°.
Volume	6334.5(16) Å <sup>3</sup>	
Z	18	
Density (calculated)	1.090 Mg/m <sup>3</sup>	
Absorption coefficient	0.066 mm <sup>-1</sup>	
F(000)	2276	
Crystal size	0.080 x 0.080 x 0.030 mm <sup>3</sup>	
Theta range for data collection	2.03 to 25.35°.	
Index ranges	-41 ≤ h ≤ 39, -41 ≤ k ≤ 41, -7 ≤ l ≤ 6	
Reflections collected	15113	
Independent reflections	2569 [R(int) = 0.0894]	
Completeness to theta = 25.00°	99.6 %	
Absorption correction	Multiscan	
Max. and min. transmission	1.0000 and 0.9942	
Refinement method	Full-matrix least-squares on F <sup>2</sup>	
Data / restraints / parameters	2569 / 0 / 155	
Goodness-of-fit on F <sup>2</sup>	1.862	
Final R indices [I > 2σ(I)]	R1 = 0.1537, wR2 = 0.4375	
R indices (all data)	R1 = 0.1670, wR2 = 0.4457	
Largest diff. peak and hole	1.841 and -0.435 e.Å <sup>-3</sup>	

**(2)-1-((3-*tert* butylcyclopentyl)(phenyl)methylene)-2-(2-4-dinitrophenyl)hydrazine 251**

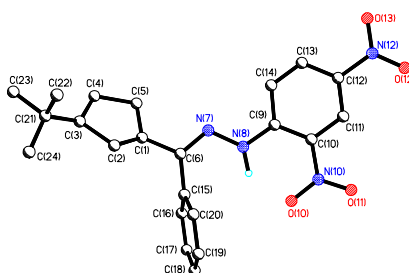


Table 1. Crystal data and structure refinement for ngdh23.

Identification code	ngdh23	
Empirical formula	C <sub>22</sub> H <sub>26</sub> N <sub>4</sub> O <sub>4</sub>	
Formula weight	410.47	
Temperature	173(2) K	
Wavelength	1.54178 Å	
Crystal system	Monoclinic	
Space group	P2(1)/c	
Unit cell dimensions	a = 12.882(7) Å b = 7.282(5) Å c = 23.460(12) Å	α = 90°. β = 99.75(4)°. γ = 90°.
Volume	2169(2) Å <sup>3</sup>	
Z	4	
Density (calculated)	1.257 Mg/m <sup>3</sup>	
Absorption coefficient	0.720 mm <sup>-1</sup>	
F(000)	872	
Crystal size	0.1000 x 0.0300 x 0.0100 mm <sup>3</sup>	
Theta range for data collection	3.48 to 67.95°.	
Index ranges	-15 ≤ h ≤ 15, -8 ≤ k ≤ 8, -28 ≤ l ≤ 28	
Reflections collected	27239	
Independent reflections	3897 [R(int) = 0.1189]	
Completeness to theta = 66.50°	99.1 %	
Absorption correction	Multiscan	
Max. and min. transmission	1.0000 and 0.9290	
Refinement method	Full-matrix least-squares on F <sup>2</sup>	
Data / restraints / parameters	3897 / 1 / 277	
Goodness-of-fit on F <sup>2</sup>	1.180	
Final R indices [I > 2σ(I)]	R1 = 0.1457, wR2 = 0.3512	
R indices (all data)	R1 = 0.1718, wR2 = 0.3715	
Extinction coefficient	0.0019(6)	
Largest diff. peak and hole	0.533 and -0.298 e.Å <sup>-3</sup>	

## Appendix 2

### Publications

- **The intramolecular  $\beta$ -fluorine $\cdots$ ammonium interaction in 4- and 8-membered rings**

Natalie E. J. Gooseman, David O'Hagan, Alexandra M. Z. Slawin, Andrew M. Teale, David J. Tozer and Robert J. Young, *Chem. Commun.*, 2006, 3190–3192.

- **An Electrostatic *Gauche* Effect in  $\beta$ -Fluoro- and  $\beta$ -Hydroxy-*N*-ethylpyridinium Cations**

Natalie E. J. Gooseman, David O'Hagan, Michael J. G. Peach, Alexandra M. Z. Slawin, David J. Tozer, and Robert J. Young, *Angew. Chem. Int. Ed.* 2007, **46**, 5904–5908.

### Conferences attended

- 32<sup>nd</sup> RSC Scottish Organic Division Meeting, University of Edinburgh, December 2003.
- 4<sup>th</sup> RSC Fluorine subject group postgraduate meeting, University of Durham, September 2004.

- 33<sup>rd</sup> RSC Scottish Organic Division Meeting, University of St Andrews, December 2004.
- 5<sup>th</sup> RSC Fluorine Subject Group Postgraduate Meeting, University of Oxford, September 2005.
- 34<sup>th</sup> RSC Scottish Organic Division Meeting, University of Strathclyde, December 2005.
- 17<sup>th</sup> SCI Fine Chemicals Group Post Graduate Meeting, University of Dundee, April 2006.
- 18<sup>th</sup> International Symposium on Fluorine Chemistry, University of Bremen, July 2006 (**poster presented**).
- 6<sup>th</sup> RSC Fluorine Subject Group Postgraduate Meeting, University of Manchester, August 2006 (**poster presented**).
- 35<sup>th</sup> RSC ScotChem Organic Division Meeting, Heriot-Watt University, Edinburgh, December 2006.

# The intramolecular $\beta$ -fluorine . . . ammonium interaction in 4- and 8-membered rings

Natalie E. J. Gooseman, David O'Hagan, Alexandra M. Z. Slawin, Andrew M. Teale, David J. Tozer and Robert J. Young

**Chemical Communications - Royal Society of Chemistry** (ISSN: 1359-7345)  
2006 (pp. 3190-3192)

DOI: 10.1039/b606334a

**(Owing to copyright restrictions, the electronic version of this thesis does not contain the text of this article)**

## An Electrostatic Gauche Effect in $\beta$ -Fluoro- and $\beta$ -Hydroxy-Nethylpyridinium Cations

Natalie E. J. Gooseman, David O'Hagan, Michael J. G. Peach, Alexandra M. Z. Slawin, David J. Tozer, and Robert J. Young

**Angewandte Chemie -International Edition in English-** (ISSN: 1433-7851)  
2007, 46, (pp. 5904-5908)

DOI: 10.1002/anie.200700714

**(Owing to copyright restrictions, the electronic version of this thesis does not contain the text of this article)**